FR-19545-1
MAY 1987

NASA

FINAL REPORT ON SHUTTLE CENTAUR ENGINE COOLDOWN EVALUATION AND EFFECTS OF EXPANDED INLETS ON START TRANSIENT

CONTRACT NAS3-22902

Prepared for
National Aeronautics and Space Administration
Lewis Research Center
21000 Brookpark Road
Cleveland, Ohio 44135

Prepared by
United Technologies Corporation
Pratt & Whitney
Government Products Division
P.O. Box 109600, West Palm Beach, Florida 33410-9600

UNITED TECHNOLOGIES
PRATT & WHITNEY

Printed in the United States of America

FR-19545-1
MAY 1987

NASA

FINAL REPORT ON SHUTTLE CENTAUR ENGINE COOLDOWN EVALUATION AND EFFECTS OF EXPANDED INLETS ON START TRANSIENT

CONTRACT NAS3-22902

Prepared for
National Aeronautics and Space Administration
Lewis Research Center
21000 Brookpark Road
Cleveland, Ohio 44135

Prepared by
United Technologies Corporation
Pratt & Whitney
Government Products Division
P.O. Box 109600, West Palm Beach, Florida 33410-9600

UNITED TECHNOLOGIES PRATT&WHITNEY

FOREWORD

This report presents the results of the cooldown testing and the expanded inlet condition testing of the RL10 engine for the Shuttle/Centaur program. The testing was conducted by Pratt & Whitney, Government Products Division (P&W/GPD) of the United Technologies Corporation (UTC) for the National Aeronautics and Space Administration Lewis Research Center (NASA/LeRC) under contract NAS3-22902.

This testing was conducted during the period from August 1984 to December 1985, with other test programs. The testing effort was conducted under the direction of LeRC Space Flight Systems Directorate with Mr. James A. Burkhart as Contracting Officer Representative. The effort at P&W/GPD was carried out under the direction of Mr. Carl Ring, Assistant Project Engineer, and Mr. Tom Vogel, Senior Test Engineer.

CONTENTS

ILLUSTRATIONS

ILLUSTRATIONS (Continued)

ILLUSTRATIONS (Continued)

ILLUSTRATIONS (Continued)

ILLUSTRATIONS (Continued)

TABLES

INTRODUCTION

As part of the integration of the RL10 engine into the Shuttle Centaur vehicle, a satisfactory method of conditioning the engine to operating temperatures had to be established. This procedure, known as cooldown, is different from the existing Atlas Centaur due to vehicle configuration and mission profile differences. This report describes the program and reports the results of a Shuttle Centaur cooldown program conducted by Pratt & Whitney.

Mission peculiarities cause substantial variation in propellant inlet conditions between the substantiated Atlas Centaur and Shuttle Centaur with the Shuttle Centaur having much larger variation in conditions. A test program was conducted to demonstrate operation of the RL10 engine over the expanded inlet conditions.

As a result of this program the Shuttle Centaur requirements have been proven satisfactory. Minor configuration changes incorporated as a result of this program provide substantial reduction in cooldown propellant consumption.

SECTION 1.0
BACKGROUND

1.1 ATLAS CENTAUR COOLDOWN SEQUENCE

On the Atlas Centaur vehicle, the engine inlet valves are the only ones on the oxidizer and fuel inlet lines. These valves are mounted immediately upstream of the oxidizer and fuel pumps. Because the engine inlet valves are downstream of the inlet lines, these lines are cooled during propellant tanking. Cooldown of the Centaur engines takes place after propellant tanking, and is done in two stages.

Before launch, the fuel turbopump is cooled by flowing liquid helium through the pump, entering at a fitting near the pump inlet and exiting through the interstage and discharge cooldown valves. The oxidizer pump components are cooled by conduction with the fuel pump housing. The turbopump is enclosed in insulating cover to aid this process. Neither the cooldown duration nor the quantity of helium consumed are constraining factors. The only cooldown constraints are that the fuel pump must be maintained below 64°R, and the LOX pump must be below 270°R for the last five minutes before launch. Helium flow is stopped about eight seconds before launch, and no cooling is provided during the boost phase. The period before launch after the helium flow is stopped and the time during the boost phase of the mission amounts to approximately 4.8 minutes, during which time the pumps warm slightly to about 120°R on the fuel side, and 255°R on the oxidizer side.

Immediately after staging, the engine inlet valves are opened (known as prestart), and propellants are allowed to flow through the fuel pump for five seconds and the LOX system for nine seconds before engine start. This prestart flow consumes approximately 22 lb of oxidizer, and six lb of fuel per engine.

On the Atlas Centaur vehicle, the cooldown flow area which determines propellant consumption on the oxidizer side is 0.34 $in.^2$, and on the fuel side the fuel pump interstage and discharge cooldown flow areas are 0.36 and 0.30 $in.^2$ respectively. Large cooldown areas are used to minimize cooldown time because the first Centaur engine burn occurs during the ascent trajectory where velocity losses must be minimized.

1.2 SHUTTLE CENTAUR COOLDOWN SEQUENCE

The Shuttle Centaur vehicle includes prevalves between the propellant tanks and the engine inlet valves. Because of this, the inlet lines remain at the Shuttle cargo bay ambient temperature of approximately 500°R until engine cooldown begins. The Centaur engines do not undergo any cooling flow before liftoff and are not cooled until immediately prior to engine start, after the vehicle has been released from the Shuttle bay. Due to the elevated metal temperatures involved, propellants must be flowed for a much longer period of time than on the Atlas Centaur flights. Because the propellants used to cool the engines and vehicle propellant inlet lines cannot be replenished, it is very important to use the smallest amount possible. The time required is not a significant factor because the vehicle is already in orbit. The goal of the cooldown program is to minimize propellant consumption.

Two Shuttle Centaur launch vehicles have been configured: the G-Prime and the G. The G-Prime vehicle requires one cooldown sequence and engine firing and is intended to boost payloads into high energy interplanetary trajectories. The G vehicle requires two engine cooldowns and firings and is intended to place payloads into a geosynchronous orbit.

With both missions, propellants are maintained at saturated conditions during the initial part of the launch sequence, and are pressurized shortly before initiation of cooldown, after the vehicle has been released from the Shuttle.

At the onset of the cooldown program, three options existed for propellant pressurization techniques. In all three cases, the propellants were maintained at saturated conditions during the boost phase. After the boost phase, the three cases differ:

1. Before cooldown commences, the propellants are pressurized to a predetermined level regardless of tank saturation pressure. Pressure is then maintained within a range around the target pressure. This procedure results in inlet boxes shown in Figures 1-1 and 1-2. These inlet boxes are known as the absolute pressure inlet boxes.

2. Before cooldown commences, the propellants are pressurized to a predetermined amount above saturation pressure. Pressure is then maintained within a range around the target pressure. This procedure results in inlet boxes which are shown in Figures 1-3 and 1-4. These inlet boxes are known as the delta pressure inlet boxes.

3. Before cooldown commences, propellants are pressurized as in case 2, however, the increase above saturation pressure is lower. These inlet boxes appear in Figures 1-5 and 1-6, and are known as the low delta P inlet boxes. In this case pressure is increased to case 2 levels just prior to engine start.

These inlet boxes, along with the ranges of engine and propellant duct temperatures, determine the necessary engine/inlet duct cooldown durations and associated propellant consumptions.

The RL10 Atlas Centaur cooldown deck was originally written to model the cooldown characteristics of the RL10 engine at the Atlas Centaur conditions. The inlet ducts were not included in the cooldown calculations because they were at their respective fluid temperatures at engine prestart. The engine temperatures at start of cooldown are well below ambient because of the ground prechill. The cooldown deck was matched to the cooldown characteristics of the RL10 in the Atlas Centaur configuration, based on existing test data.

To provide accurate predictions of cooldown rates and required cooldown durations for the RL10 Shuttle Centaur configuration, inlet ducts were added to the simulation, along with prevalves which are not present on the Atlas/Centaur vehicle. Two versions of the simulation were prepared: one in the test configuration to compare to ground test data, which was used to verify the analytical formulation of the prediction process, and the other in the flight configuration to predict cooldown times and consumptions. The Atlas Centaur and Shuttle Centaur configurations are shown in Figure 1-7.

The cooldown program was initiated to anchor the cooldown simulation to the Shuttle/Centaur inlet duct/engine cooldown characteristics, to choose which inlet box is the most advantageous for each mission, and to optimize the cooldown sequence and flow areas so as to consume the smallest amount of propellant possible while cooling the engines sufficiently to allow consistent start transient operation.

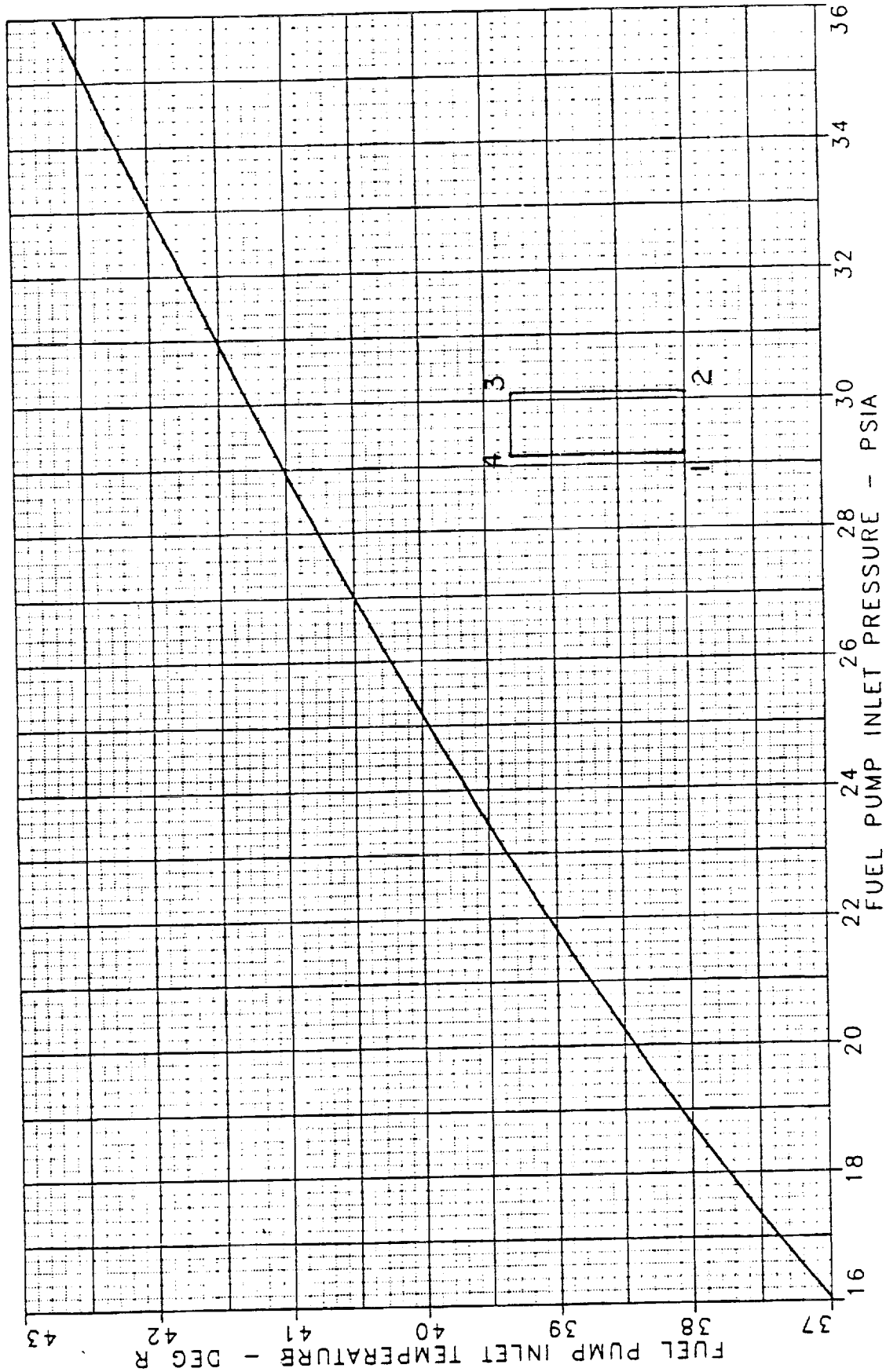

Figure 1-1. G-Prime Fuel — Absolute Pressure Inlet Box

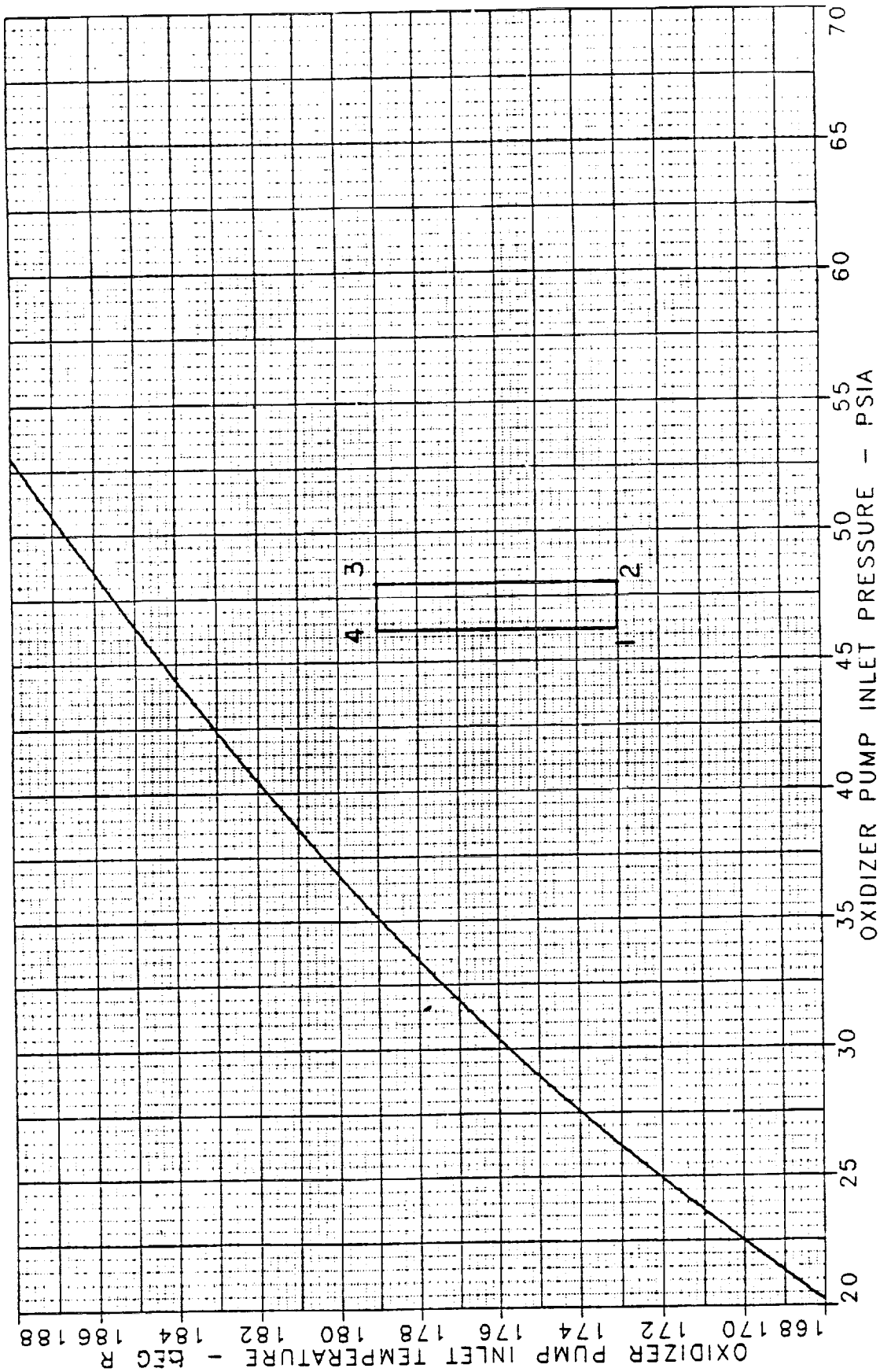

Figure 1-2. G-Prime Oxidizer — Absolute Pressure Inlet Box

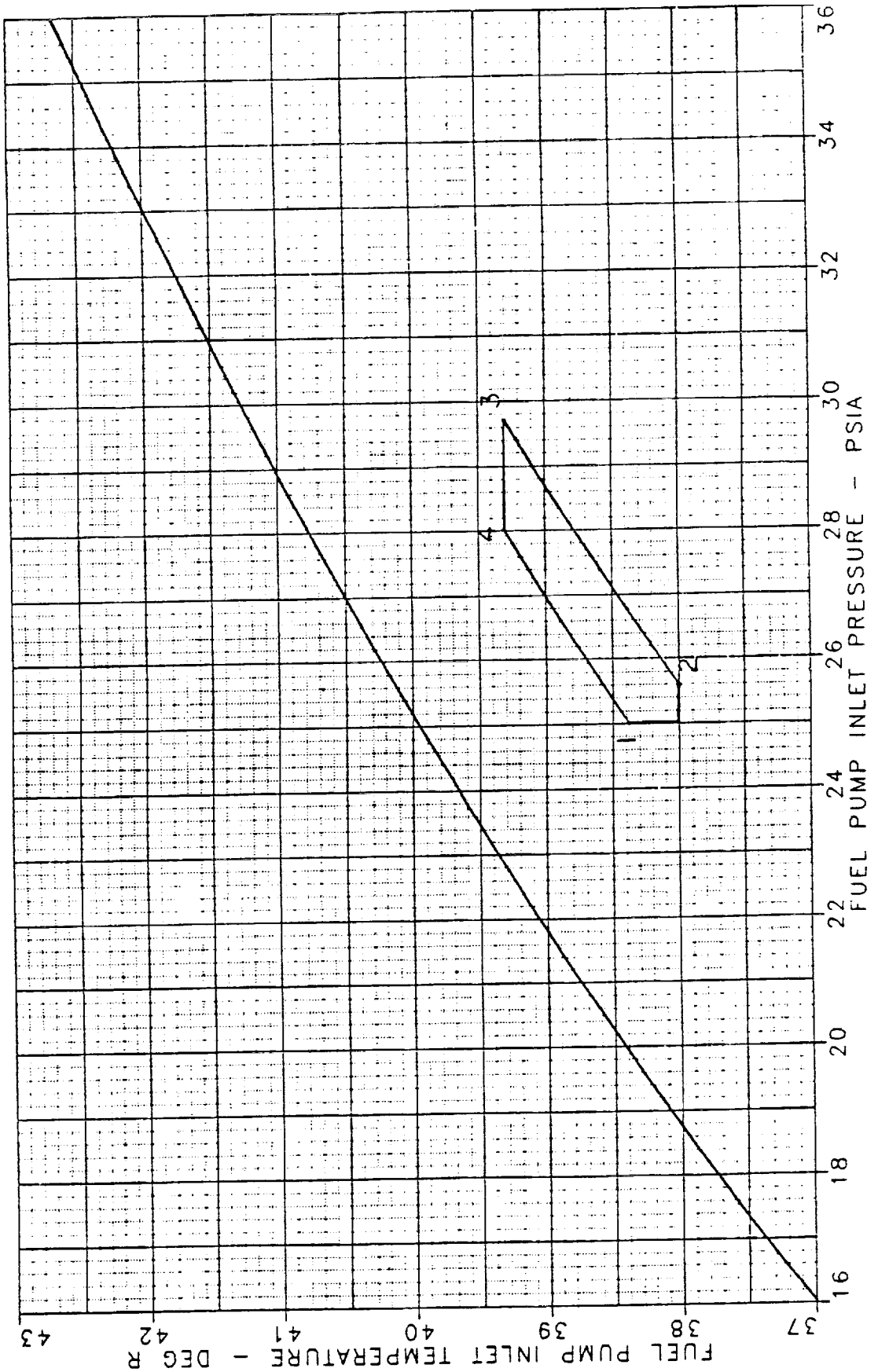

Figure 1-3. G-Prime Fuel — Delta P Inlet Box

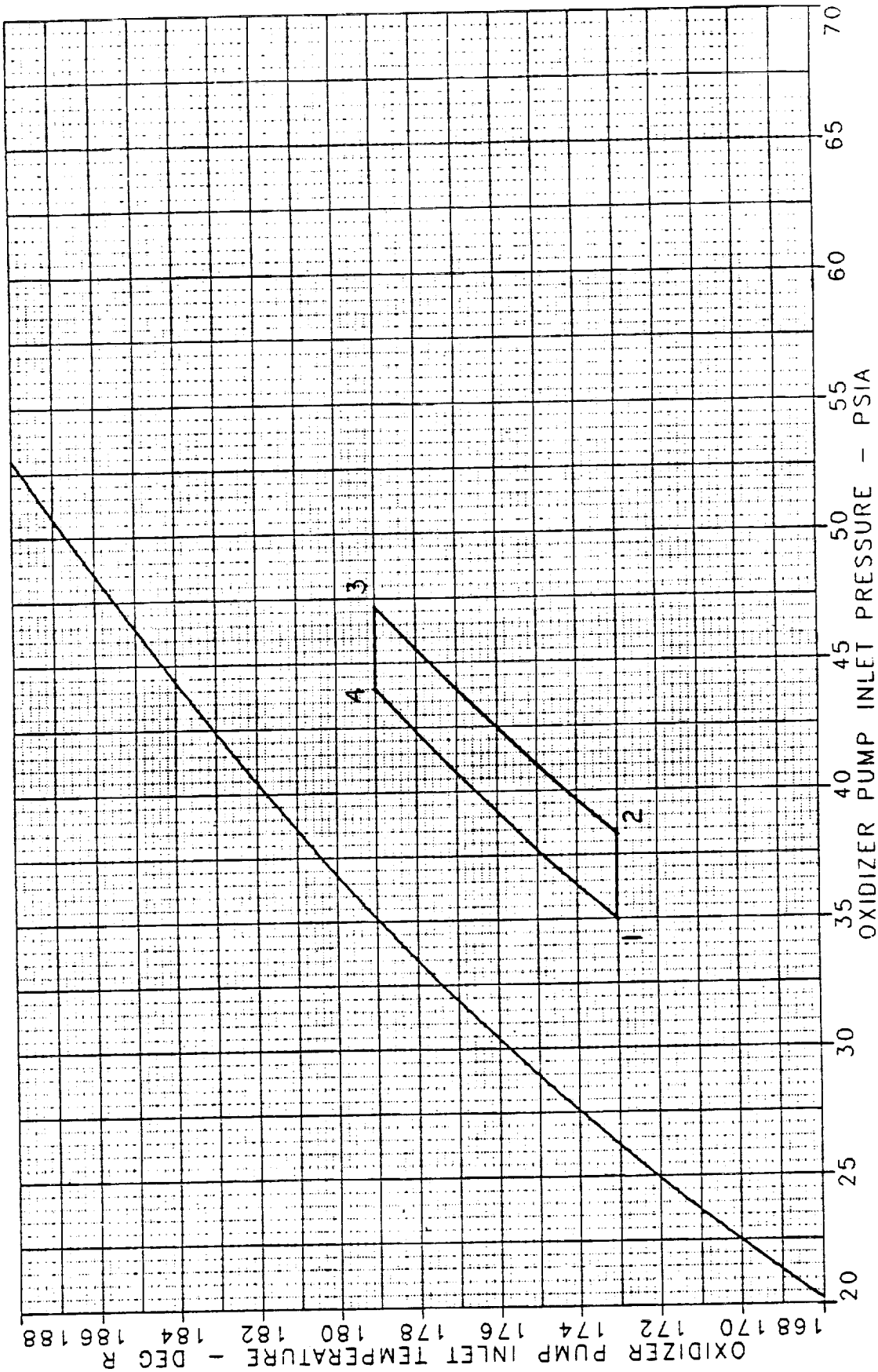

Figure 1-4. G-Prime Oxidizer — Delta P Inlet Box

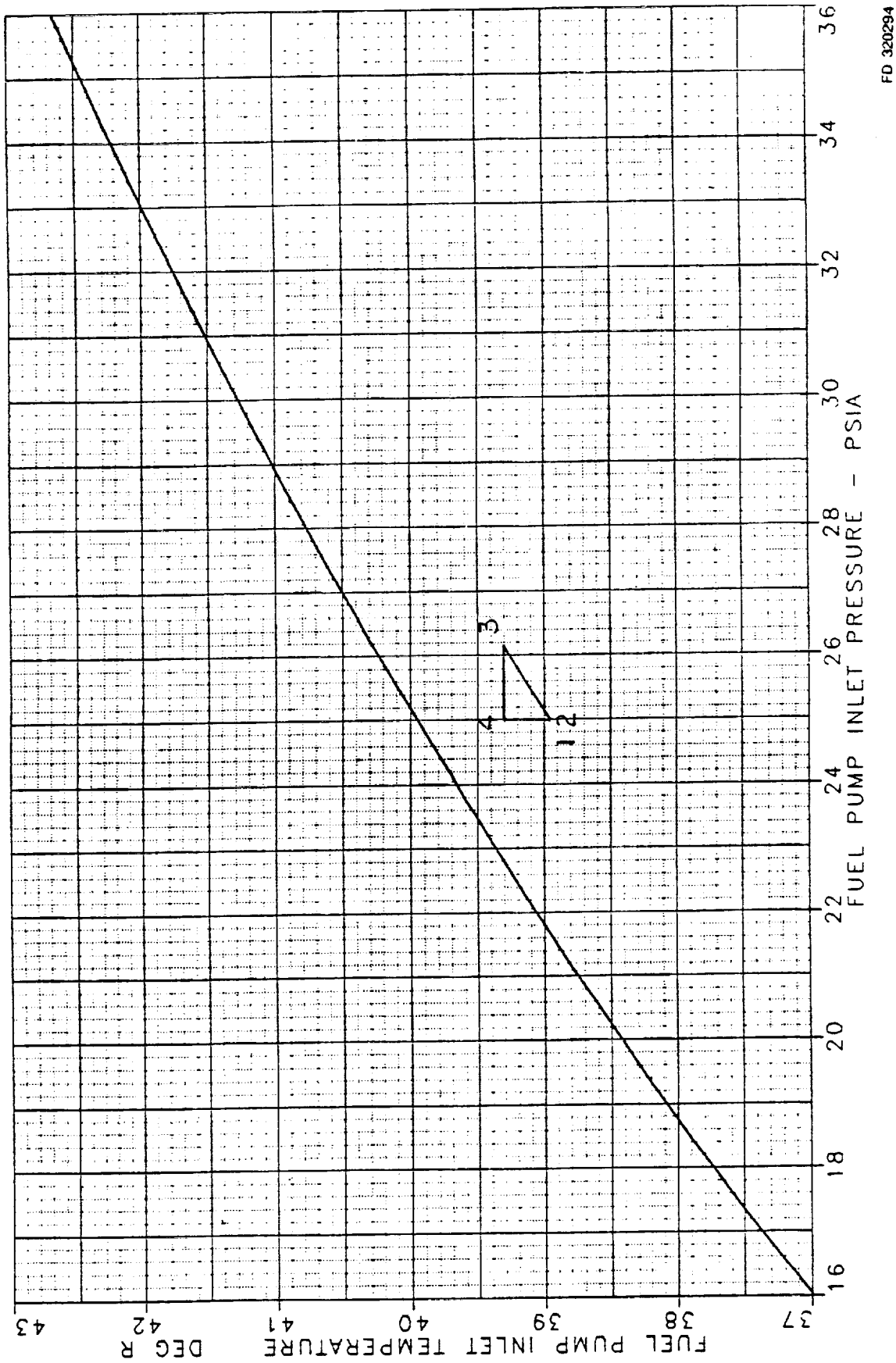

Figure 1-5. G-Prime Fuel — Low Delta P Inlet Box

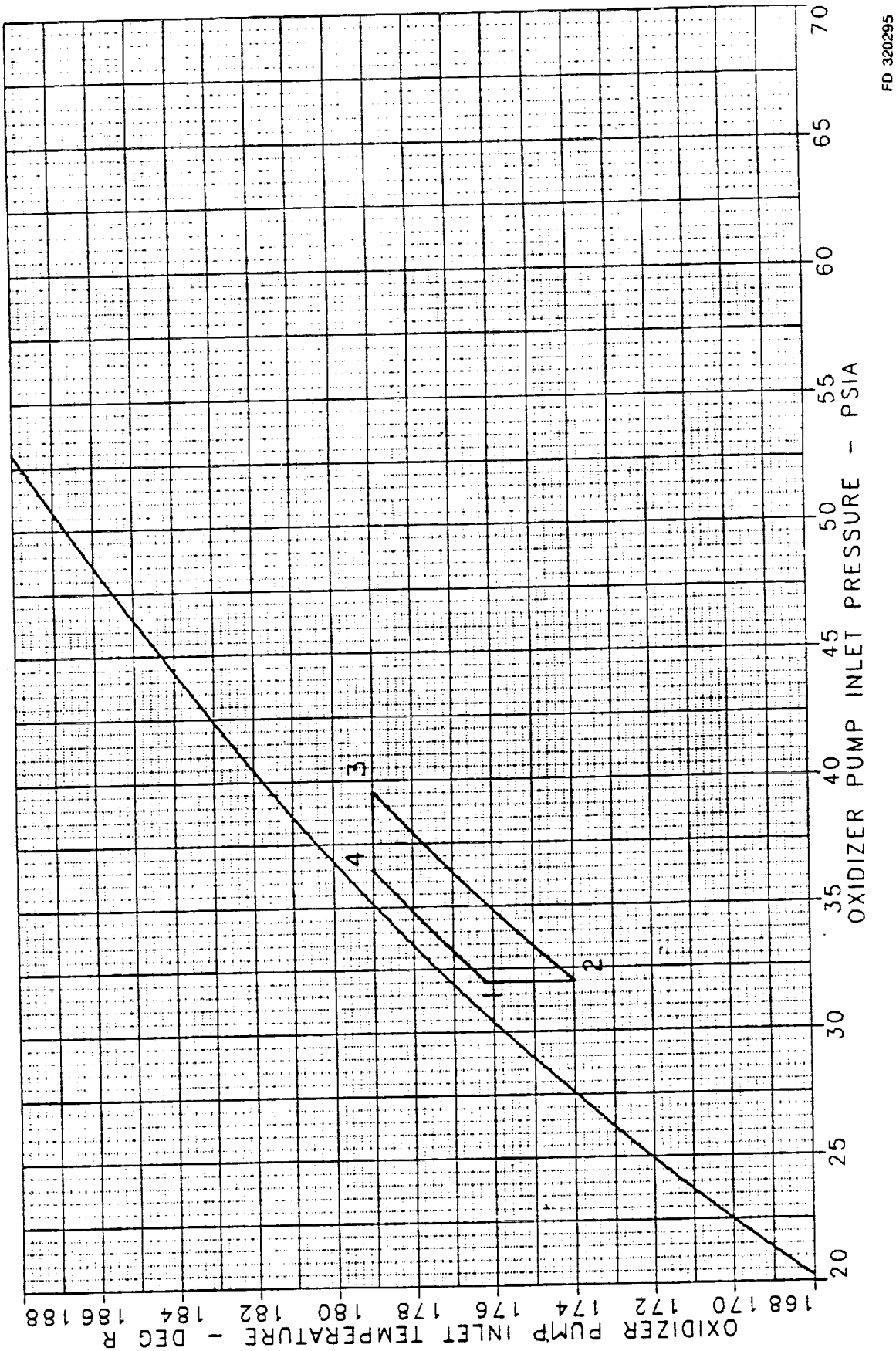

Figure 1-6. G-Prime Oxidizer — Low Delta P Inlet Box

Atlas Centaur

Full ducts (cold)
Prechill, W/LHe
RL10 start at launch + 4.5 min

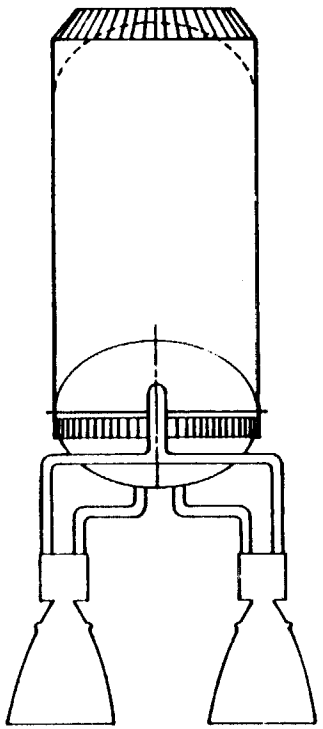

Shuttle Centaur

Empty ducts (warm)
No prechill
RL10 start at launch + 5 hrs to 3 days

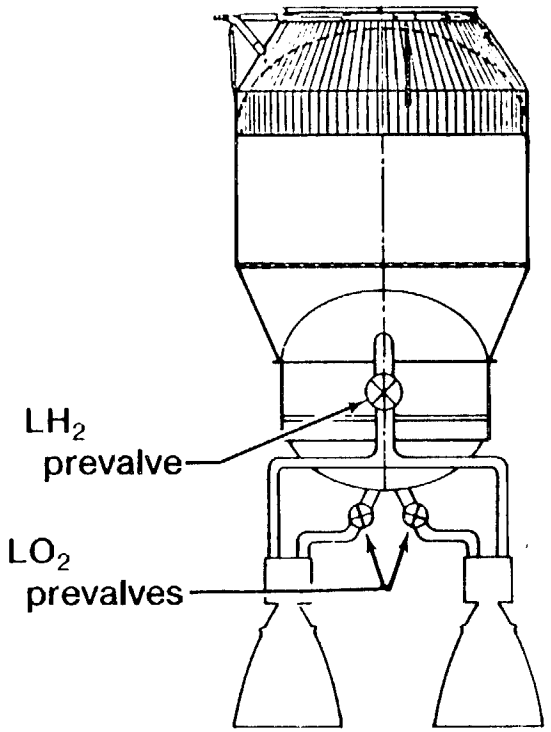

FD 320484

Figure 1-7. Engine and Propellant Duct Cooldown

SECTION 2.0
TEST CONFIGURATION

2.1 CENTAUR G AND G-PRIME TESTING

Flight conditions cannot be accurately represented on the ground due to gravity effects on flow through a previously empty propellant duct.

Engine cooldown and firing tests were conducted to substantiate the analytical cooldown model. The test stand was configured as shown in Figure 2-1. The prevalves were procured from General Dynamics, and were the first set of prototype Centaur flight valves designed and built by Fairchild. Figure 2-2 shows the G/D P/N 65-02400-3 oxidizer prevalve. Figure 2-3 shows the insulated G/D P/N 65-02240-3 fuel prevalve. The propellant ducts were designed by Pratt & Whitney to simulate the flight configuration as close as possible and still be compatible with the E-6 test stand altitude capsule. Both propellant ducts use the same wall thickness, gimbal joints and bellows section as the flight units. To be compatible with the existing oxidizer supply to the capsule and the installed engine orientation, the oxidizer duct was made a mirror image of the flight unit. To best simulate the fuel side Centaur Y-duct with a single engine, a 3-½ in. duct (diameter of individual leg) with a length equal to the common, plus one individual leg, was made. Both ducts were instrumented with skin thermocouples along their lengths as shown in Figures 2-4, 2-5, 2-6 and 2-7. A thermal analysis of the ducts installed in the E-6 altitude capsule (0.6 psia) indicated that the half-inch foam and mylar insulation used on the Atlas Centaur ducts would best simulate the Shuttle Centaur ducts in the hard vacuum of space. The insulated ducts are shown in Figures 2-8, 2-9, 2-10 and 2-11.

The propellant ducts, prevalves and engine were installed in E-6 test stand. The stand plumbing was modified to provide simulated oxidizer and fuel sumps. This was accomplished by flowing propellant from the vacuum jacketed supply line past the closed prevalve and overboard via a dump line. This configuration is shown schematically in Figure 2-1. The actual oxidizer side is shown in Figure 2-12 and the fuel side in Figure 2-13. After initial testing it was determined that the non-vacuum jacketed elbow upstream of the oxidizer prevalve, Figure 2-12, and the short non-vacuum jacketed straight section upstream of the fuel prevalve, Figure 2-13, provided too large a heat leak. This problem was resolved by adding foam insulation to the non-jacketed areas.

The helium supply to the prevalves was configured such that the prevalves and engine inlet valves could be actuated independently. This allowed evacuation of the propellant ducts for "waterhammer" testing. During the cooldown tests, each prevalve was opened simultaneously with its respective inlet valve.

When testing revealed that the cooldown areas should be reduced, plumbing changes were made to close the ISCDV to the first step and to close the OFC bypass during their respective cooldown periods. The plumbing changes consisted of moving the helium supply from the start solenoid valve to the appropriate prestart solenoid valves. The resultant engine changes are shown in Figure 2-14.

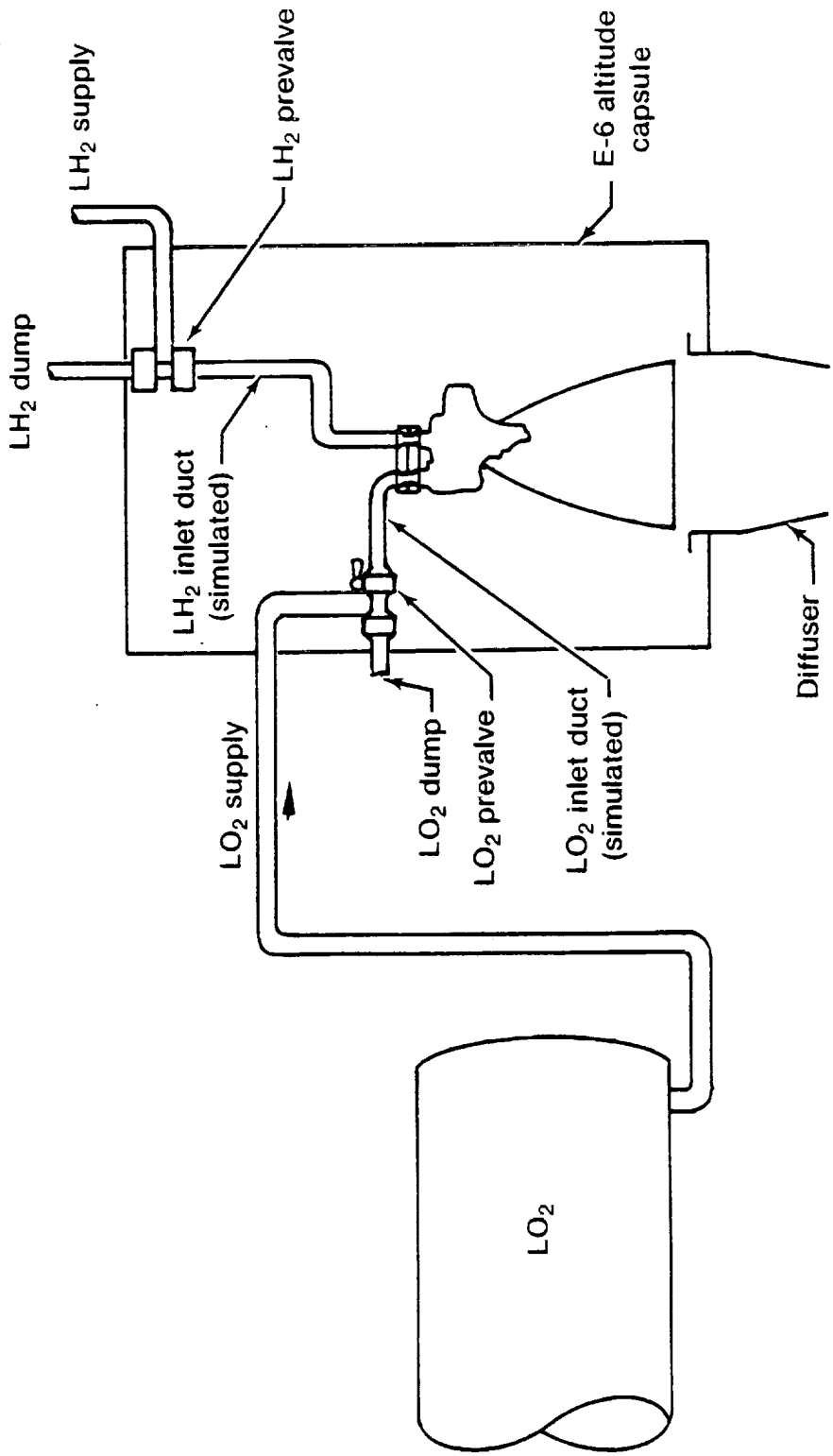

Figure 2-1. Test Stand Configuration

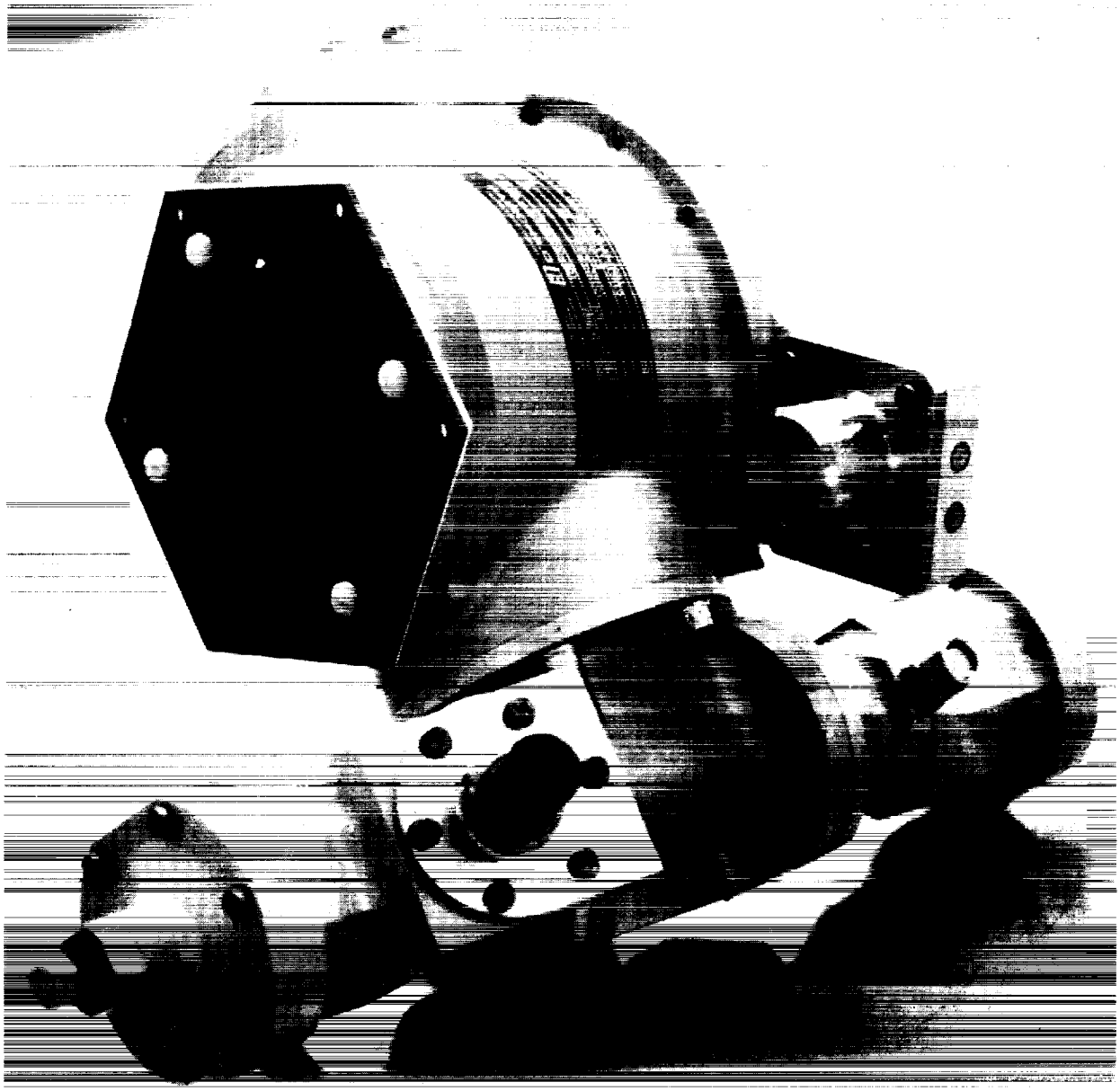

FE 358533-4

Figure 2-2. Oxidizer Prevalve

FE 359559-7

ORIGINAL PAGE
BLACK AND WHITE PHOTOGRAPH

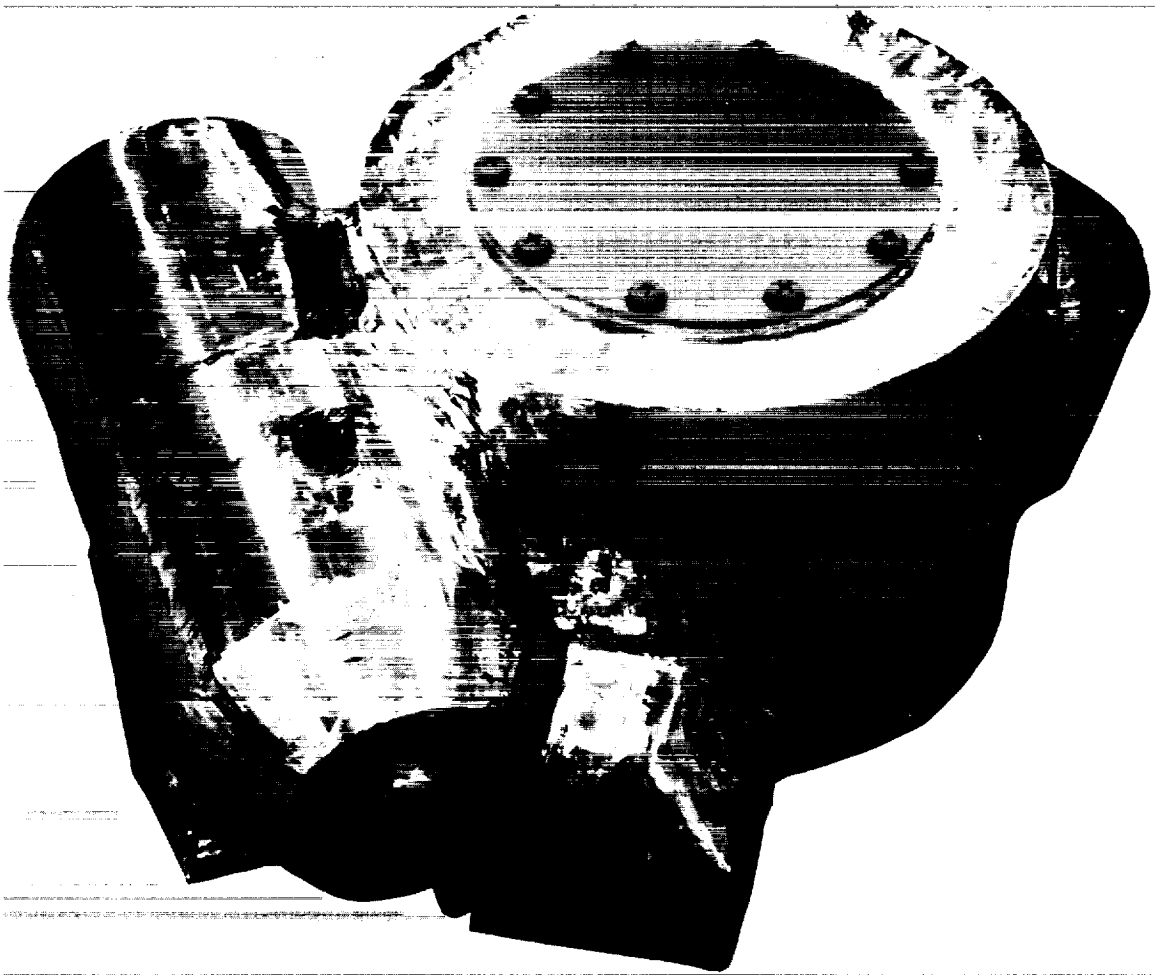

Figure 2-3. Insulated Fuel Prevalve

ORIGINAL PAGE
BLACK AND WHITE PHOTOGRAPH

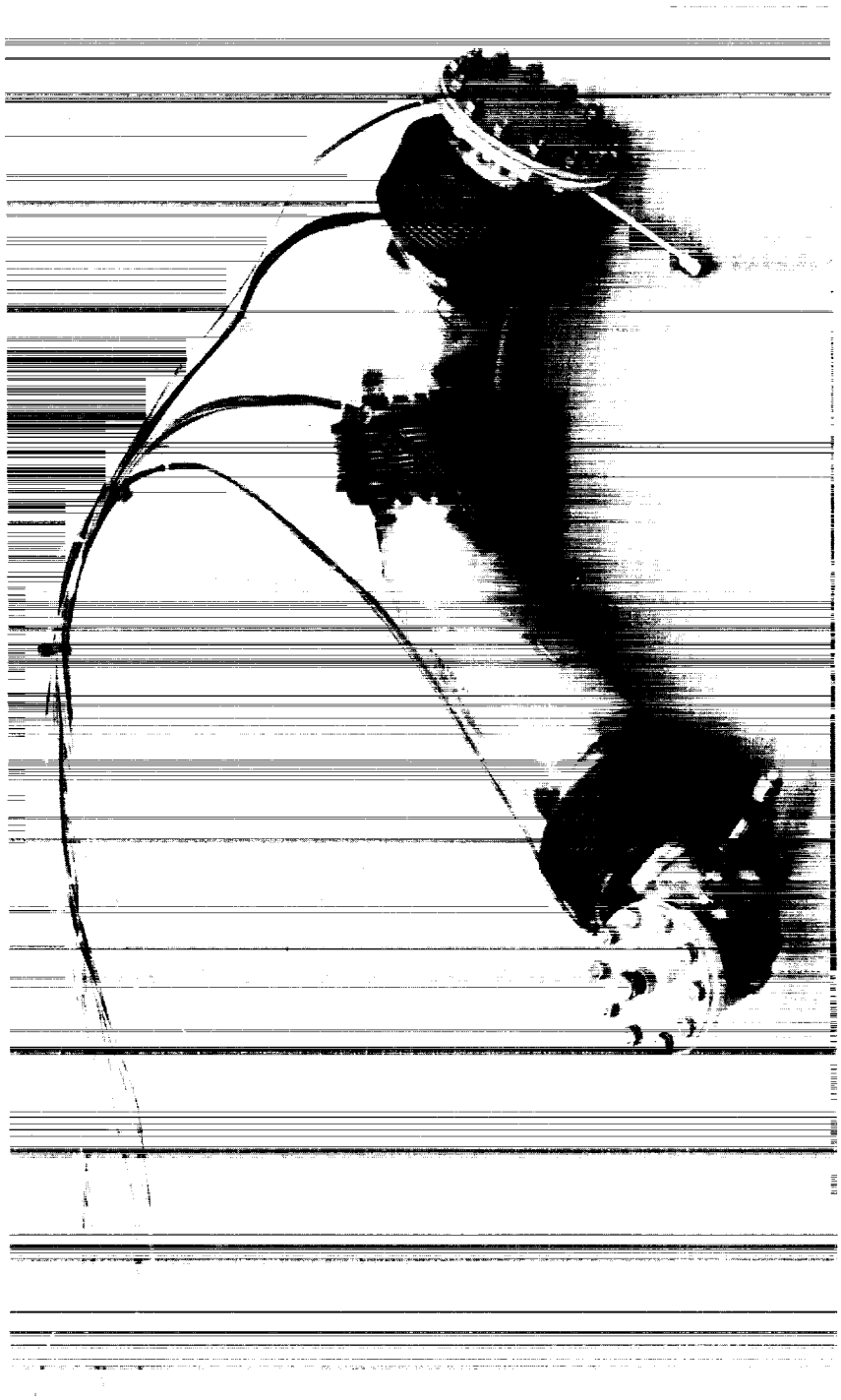

FE 359560-10

Figure 2-4. Duct Instrumented With Skin Thermocouples

ORIGINAL PAGE
BLACK AND WHITE PHOTOGRAPH

FE 359561-3

Figure 2-5. Duct Instrumented With Skin Thermocouples

ORIGINAL PAGE
BLACK AND WHITE PHOTOGRAPH

Figure 2-6. Duct Instrumented With Skin Thermocouples

ORIGINAL PAGE
BLACK AND WHITE PHOTOGRAPH

FE 359560-5

Figure 2-7. Duct Instrumented With Skin Thermocouples

ORIGINAL PAGE
BLACK AND WHITE PHOTOGRAPH

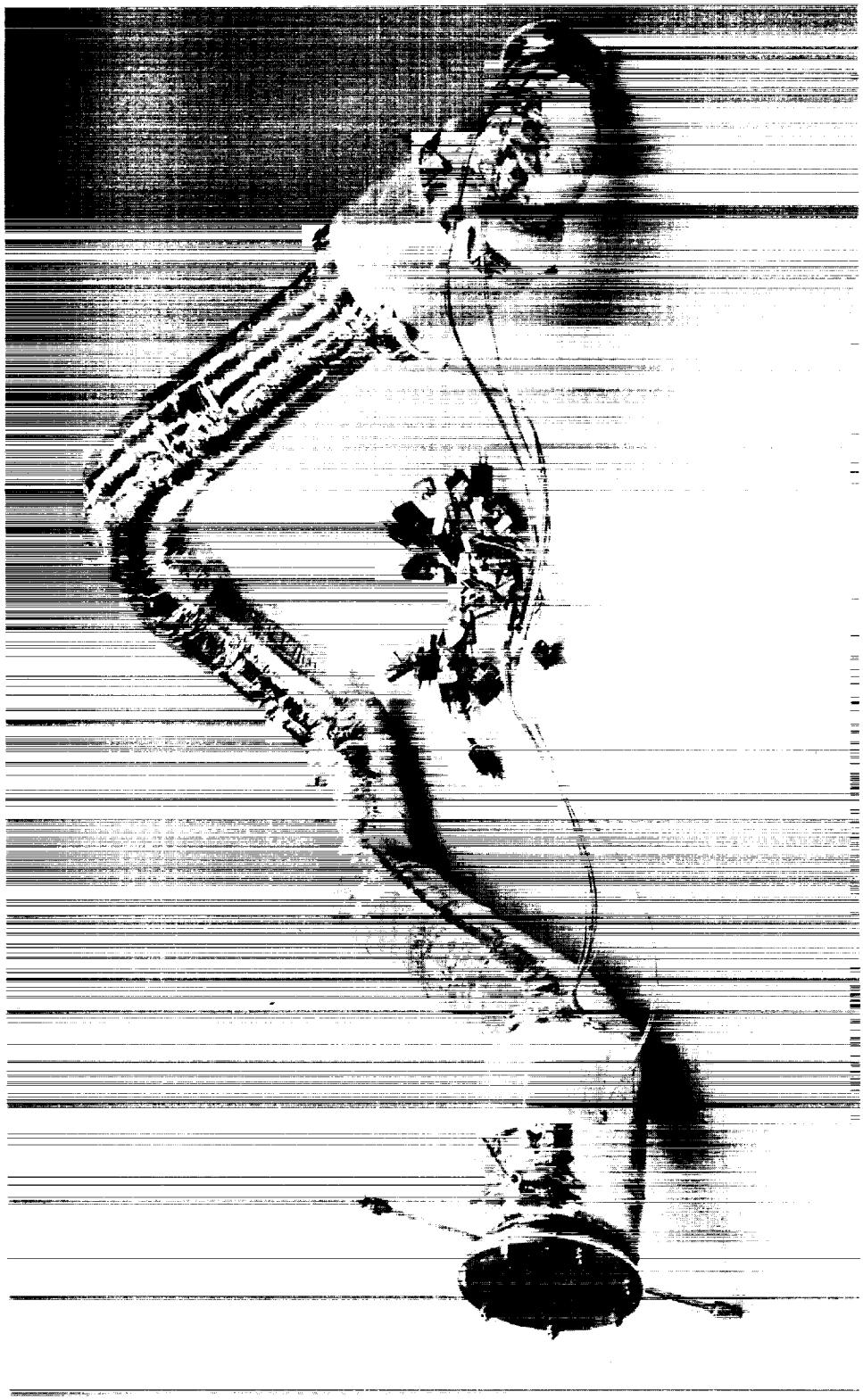

FE 359682-6

Figure 2-8. Insulated Duct

ORIGINAL PAGE
BLACK AND WHITE PHOTOGRAPH

FE 359682-3

Figure 2-9. Insulated Duct

ORIGINAL PAGE
BLACK AND WHITE PHOTOGRAPH

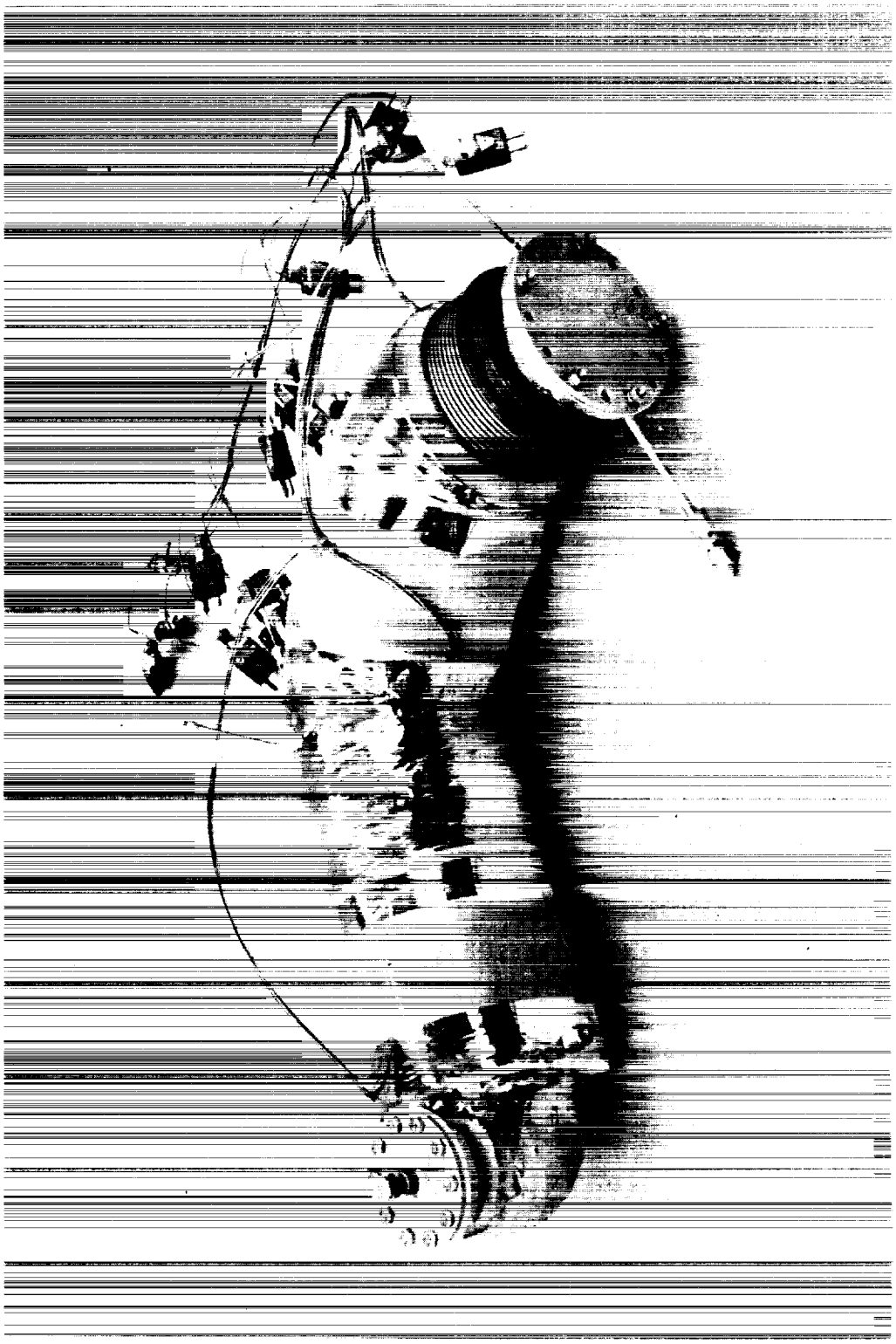

FE 359682-7

Figure 2-10. Insulated Duct

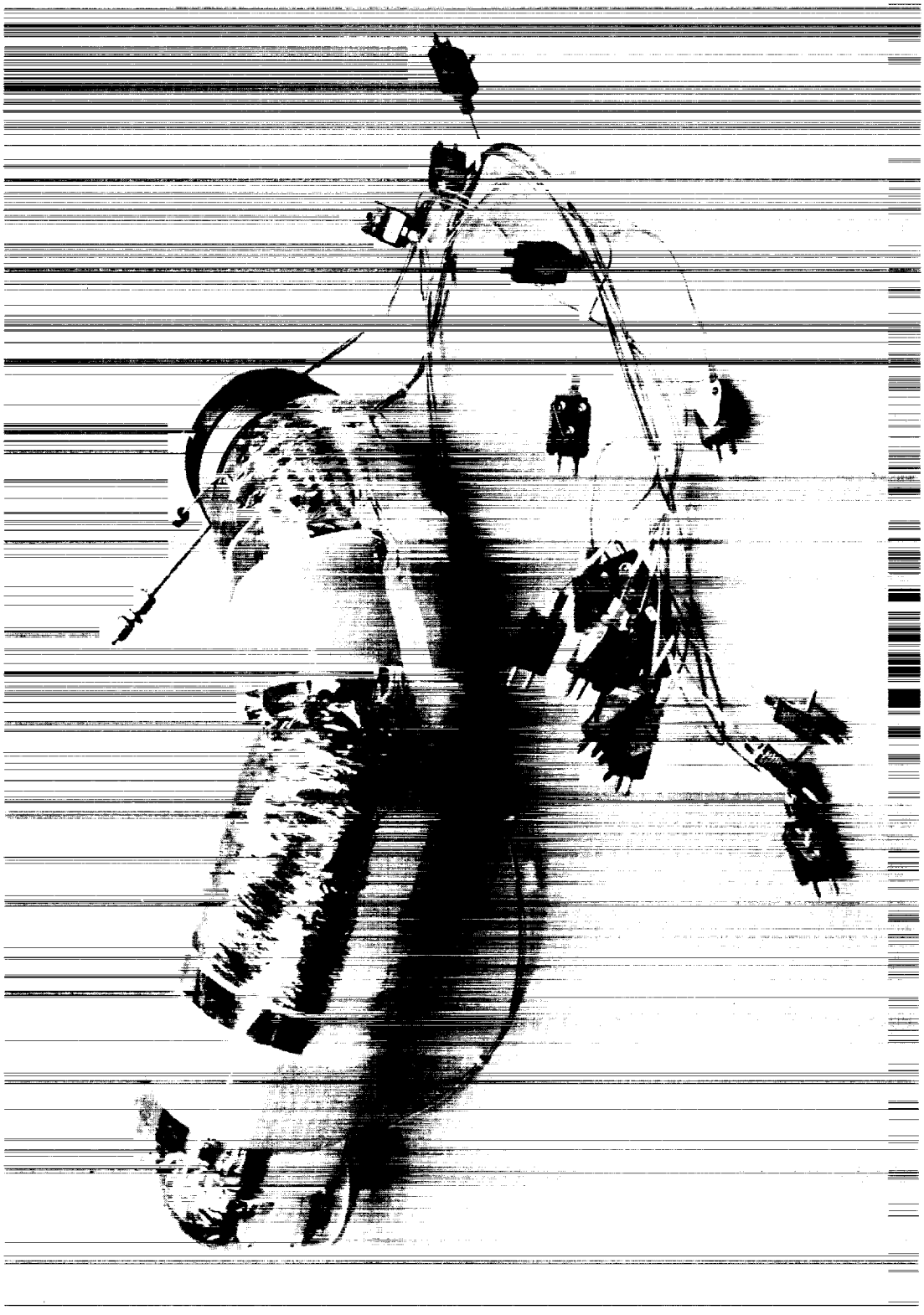

FE 359682-10

Figure 2-11. Insulated Duct

ORIGINAL PAGE
BLACK AND WHITE PHOTOGRAPH

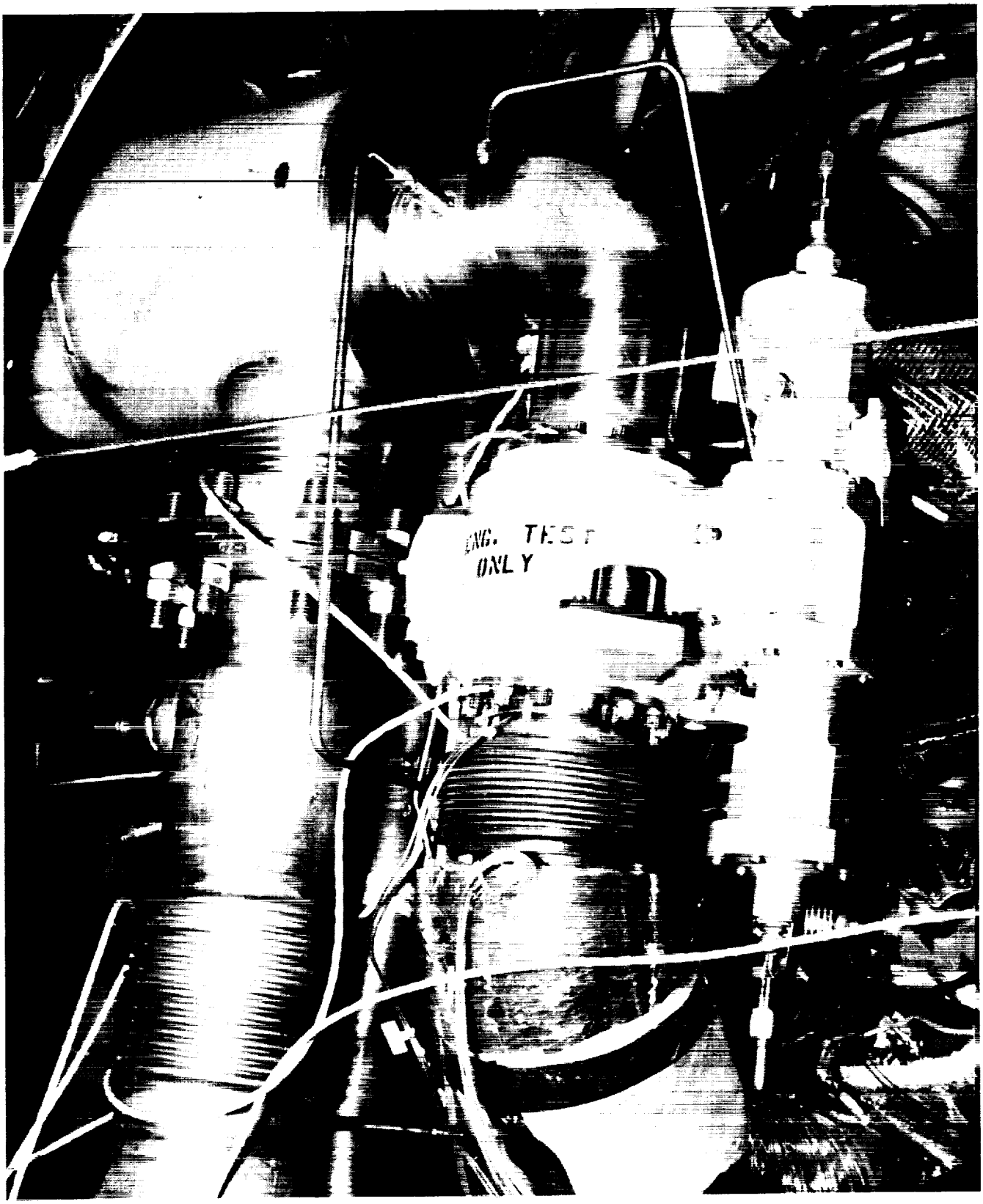

FE 359858-2

Figure 2-12. Oxidizer Side

FE 359858-7

Figure 2-13. Fuel Side

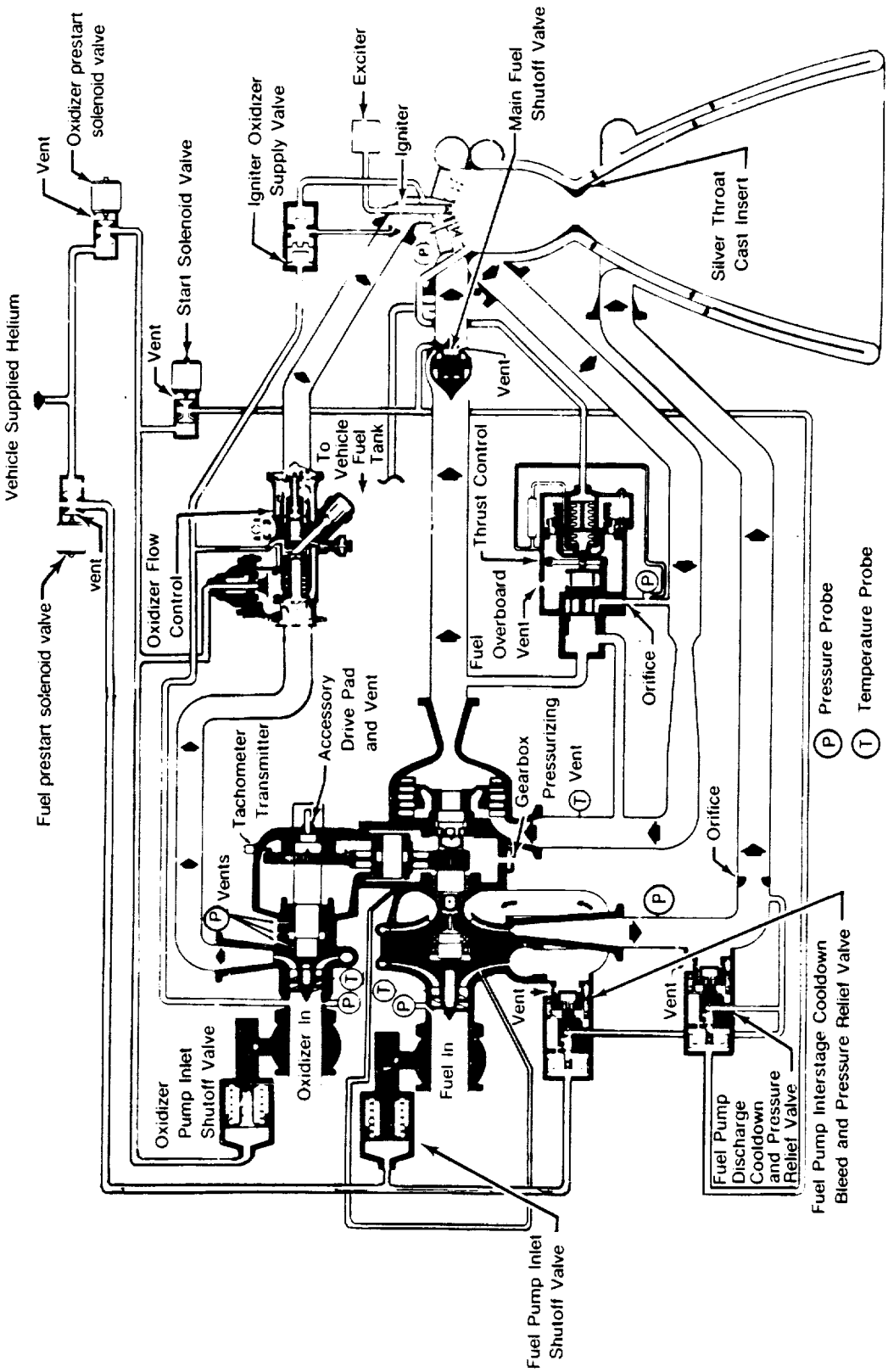

Figure 2-14. Engine Changes

2.2 FUEL PREVALVE FAILURE

The fuel prevalve failed to open fully on test number 50.01 during the XR102 test program. The valve had been subjected to 59 cryogenic and 430 ambient cycles prior to the failure. The valve was returned to Fairchild for analysis and repair. While waiting for the refurbished valve a spool piece was installed in place of the valve so that cooldown testing of the oxidizer side could be continued. Disassembly of the valve showed that the tang on the rotator ring had failed.

2.3 VERTICAL DUCT TESTING

Data from the cooldown testing indicated that propellant was traveling along the bottom side of the horizontal ducts at cooldown flow rates. This gravity effect decreases the duct cooldown efficiency, particularly on the oxidizer side. To help verify the predicted change in cooldown efficiency that would be encountered under zero-G conditions, it was desirable to run tests with the oxidizer supply duct vertical. However, the test capsule/test stand diffuser system precludes the engine from operating in any orientation other than vertical. To run a vertical oxidizer duct with this constraint would require adding an elbow which would cloud the test results. It was decided to build a rig that oriented the oxidizer components in the desired orientation and conduct oxidizer cold flows only. Figures 2-15, 2-16 and 2-17 show the rig installed in the E-6 test capsule.

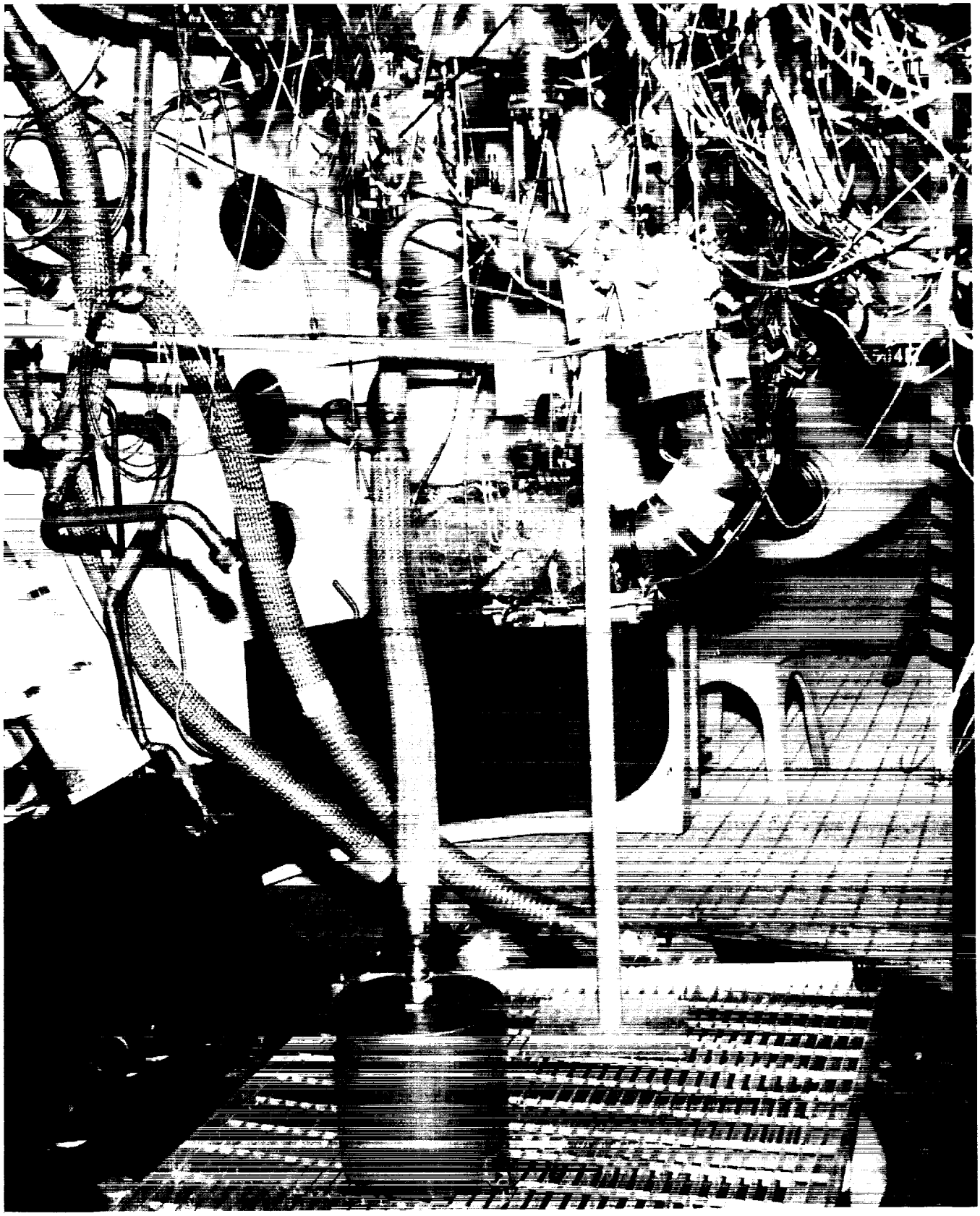

FE 359937-8

Figure 2-15. Rig Installed in E-6 Test Stand

ORIGINAL PAGE
BLACK AND WHITE PHOTOGRAPH

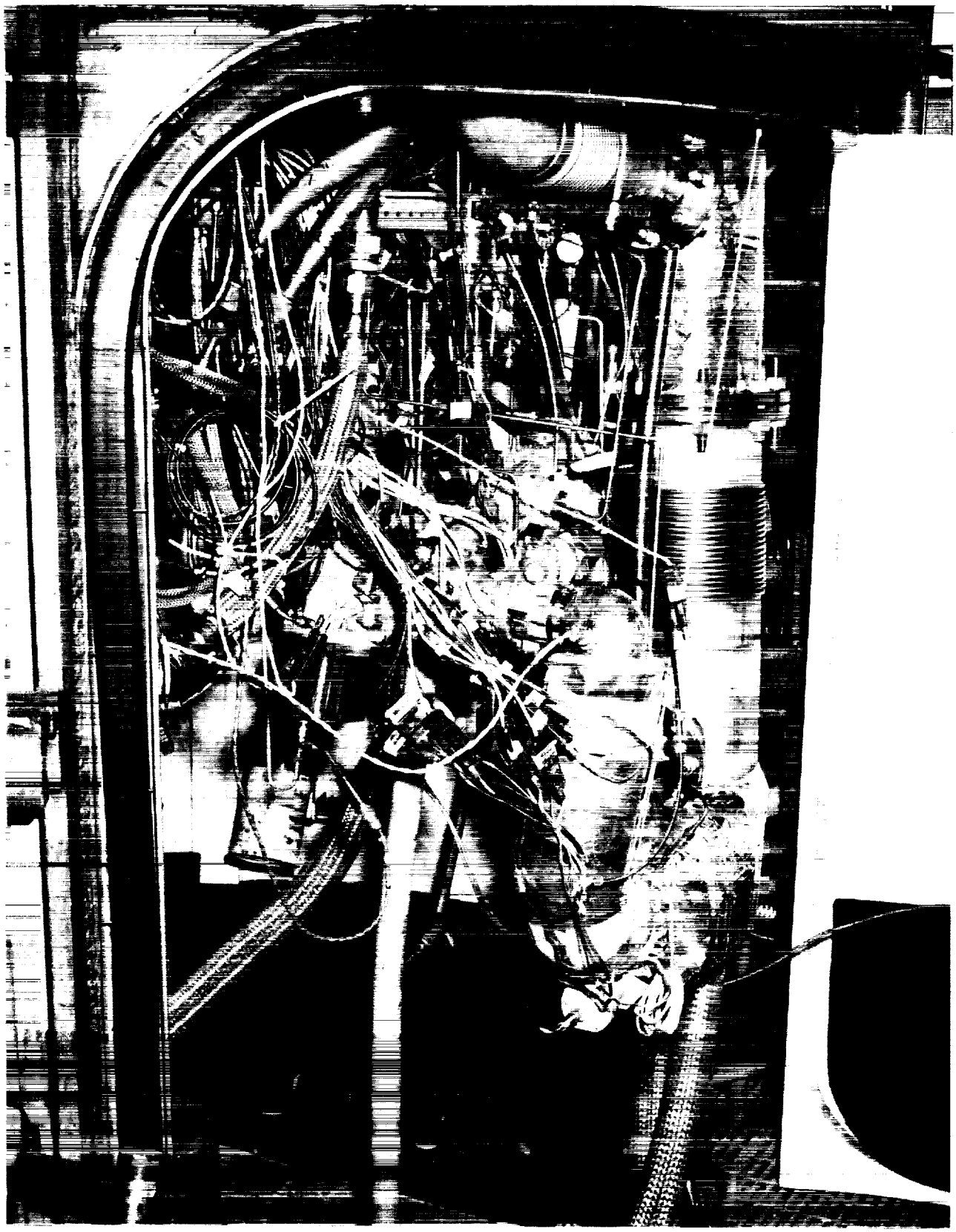

FE 359937-4

Figure 2-16. Rig Installed in E-6 Test Stand

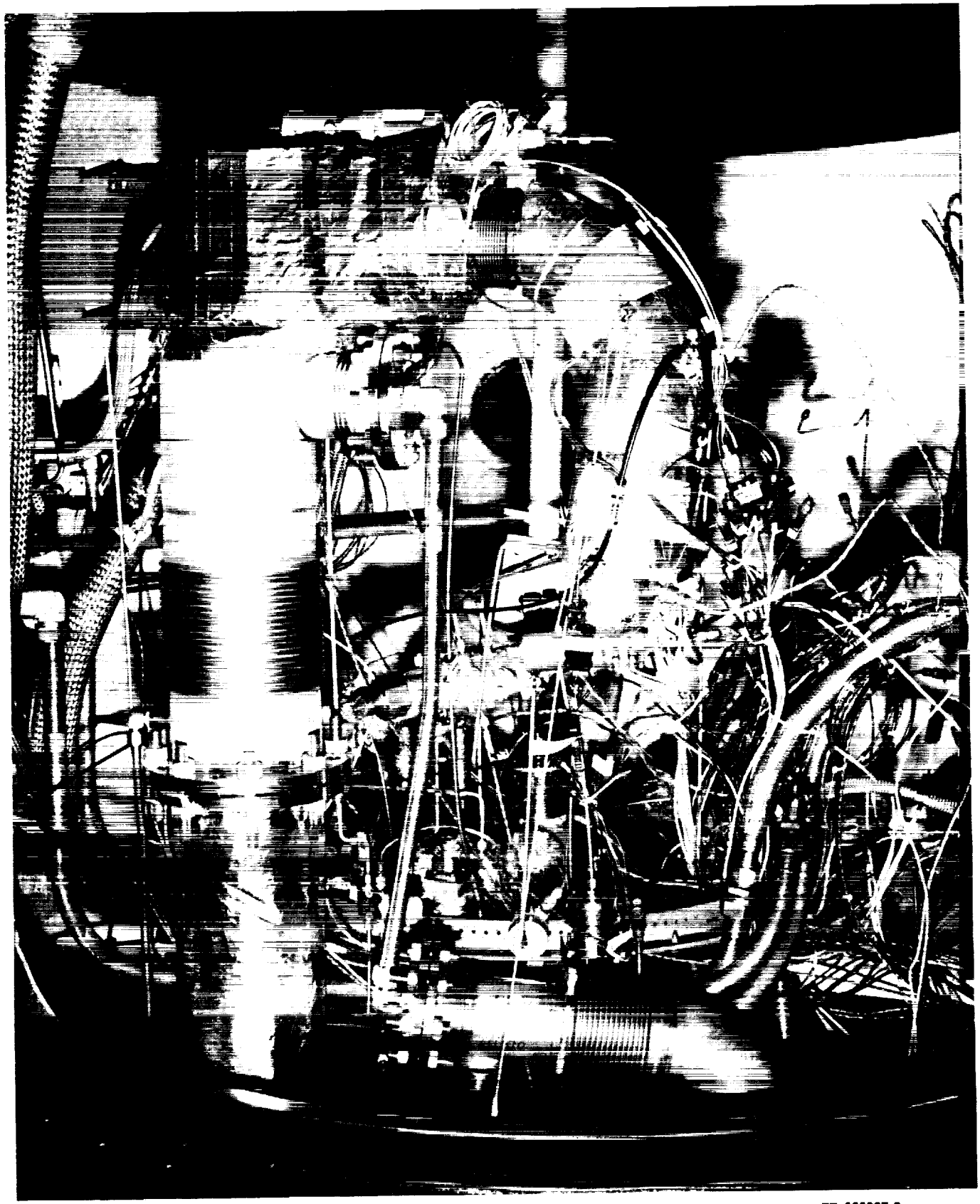

FE 359937-2

Figure 2-17. Rig Installed in E-6 Test Stand

SECTION 3.0
PRELIMINARY COOLDOWN ANALYSIS

3.1 COOLDOWN CONFIGURATION AND PRESSURIZATION SCHEMES

Before testing began, cooldown cases were run using the Shuttle Centaur cooldown deck to predict the best combination of inlet box, cooldown flow area, and inlet pressurization scenario to achieve the lowest possible propellant consumption. The cooldown times and propellant consumptions presented in Figures 3-1 and through 3-10 are preliminary estimates which were used only to determine the relative merit of the various cooldown configurations. Final cooldown durations and resulting consumptions are presented in later sections.

Cooldown testing was done using a development RL10 engine, inlet ducts designed to closely resemble those of the Shuttle Centaur vehicle, and prevalves located at the inlet to each of the ducts. All testing was done with evacuated cooldown valves which allowed engine firing to verify proper engine cooldown.

Figures 3-1, 3-2, 3-3, and 3-4 show the required cooldown time and resulting propellant consumption for simulations run using the delta pressure inlet box. The cases were run with fuel interstage flow areas of 0.36 and 0.18 $in.^2$, and Oxidizer Flow Control areas of 0.34 and 0.05 $in.^2$. These cases show that for both the normal and reduced areas, point 1 on the inlet box, Figures 1-3 and 1-4, yields the longest cooldown time. To determine the maximum amount of propellant use possible, cooldown simulations were run with inlet conditions of point 3 for the period of time from point 1.

When using the absolute pressure inlet box, the maximum consumption resulted from running with the inlet conditions at point 4 for the period of time determined from point 2.

On the oxidizer side, the propellant flowrate is determined by the oxidizer flow control valve effective area. Oxidizer flow control valve areas of 0.34 and 0.05 $in.^2$ were tested. The reduction in the oxidizer valve area is achieved by closing the oxidizer flow control valve cooldown bypass at the beginning of cooldown. A diagram of the flow control valve will be shown later in Figure 3-11. On the Atlas Centaur vehicle, the bypass is kept open until engine start, when it is closed by helium pressure from the start solenoid valve. To close the valve early, the bypass is connected to the oxidizer prestart solenoid valve. This involves a minor helium line plumbing change on the engine.

On the fuel side, the propellant flowrate is determined by the fuel pump interstage and discharge cooldown valve effective areas. Two interstage cooldown valve flow areas of 0.36 and 0.18 $in.^2$ were tested. On the Atlas/Centaur vehicle, the interstage cooldown valve is normally open to a 0.36 $in.^2$ flow area during cooldown, and, at the engine start signal, is closed half way by helium pressure from the start solenoid valve. The valve is then closed completely by fuel pump discharge pressure during the start transient. To achieve the 0.18 $in.^2$ flow area, the interstage valve is connected to the fuel prestart solenoid valve, allowing helium pressure to close the valve half way during cooldown. Comparisons of cooldown consumption for oxidizer flow areas of 0.05 and 0.34 $in.^2$ and fuel interstage valve flow areas of 0.18 and 0.36 $in.^2$ are made in Figures 3-1, 3-2, 3-3, and 3-4.

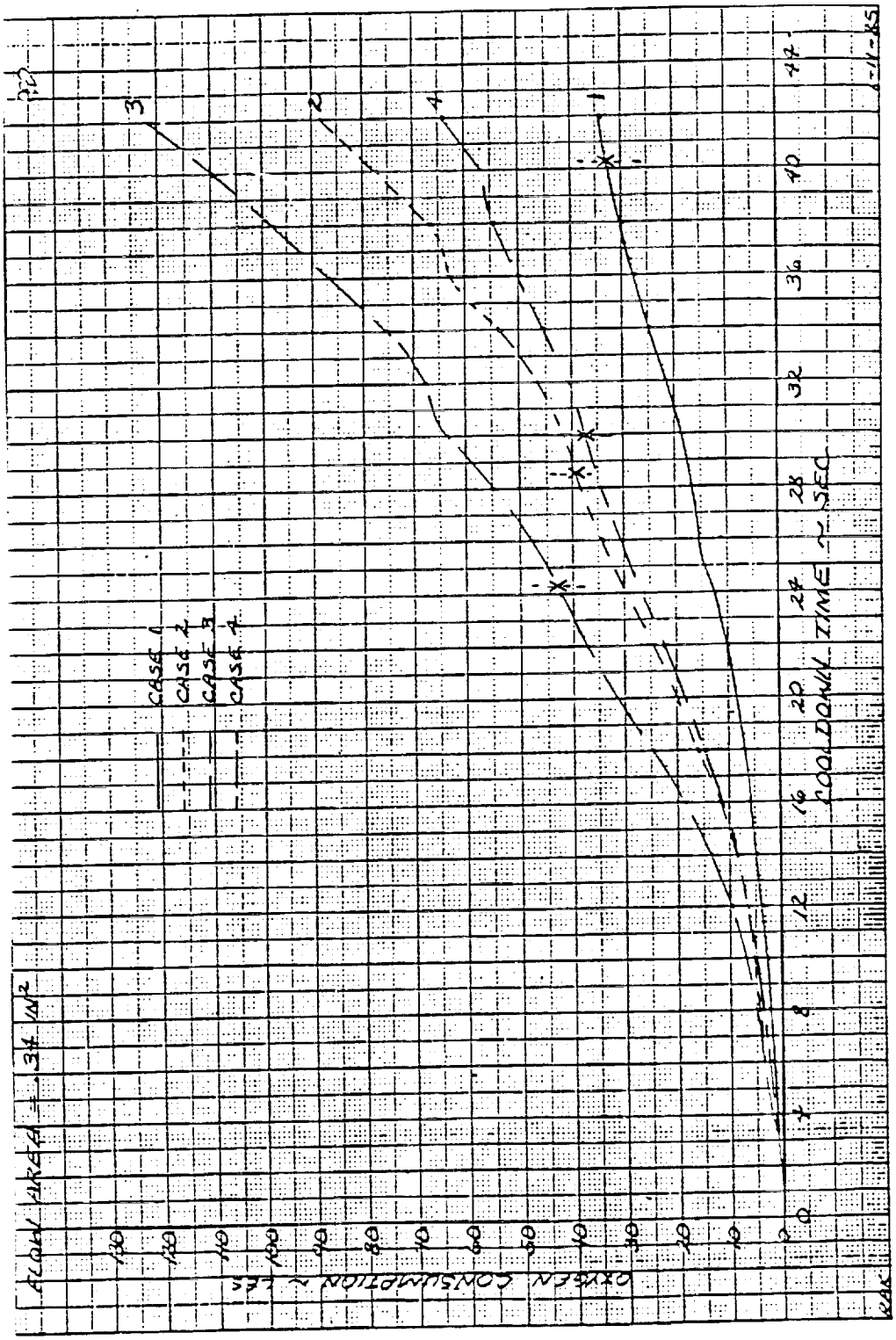

Figure 3-1. Oxygen Consumption vs Cooldown Time-Flow Area 0.34 in.²

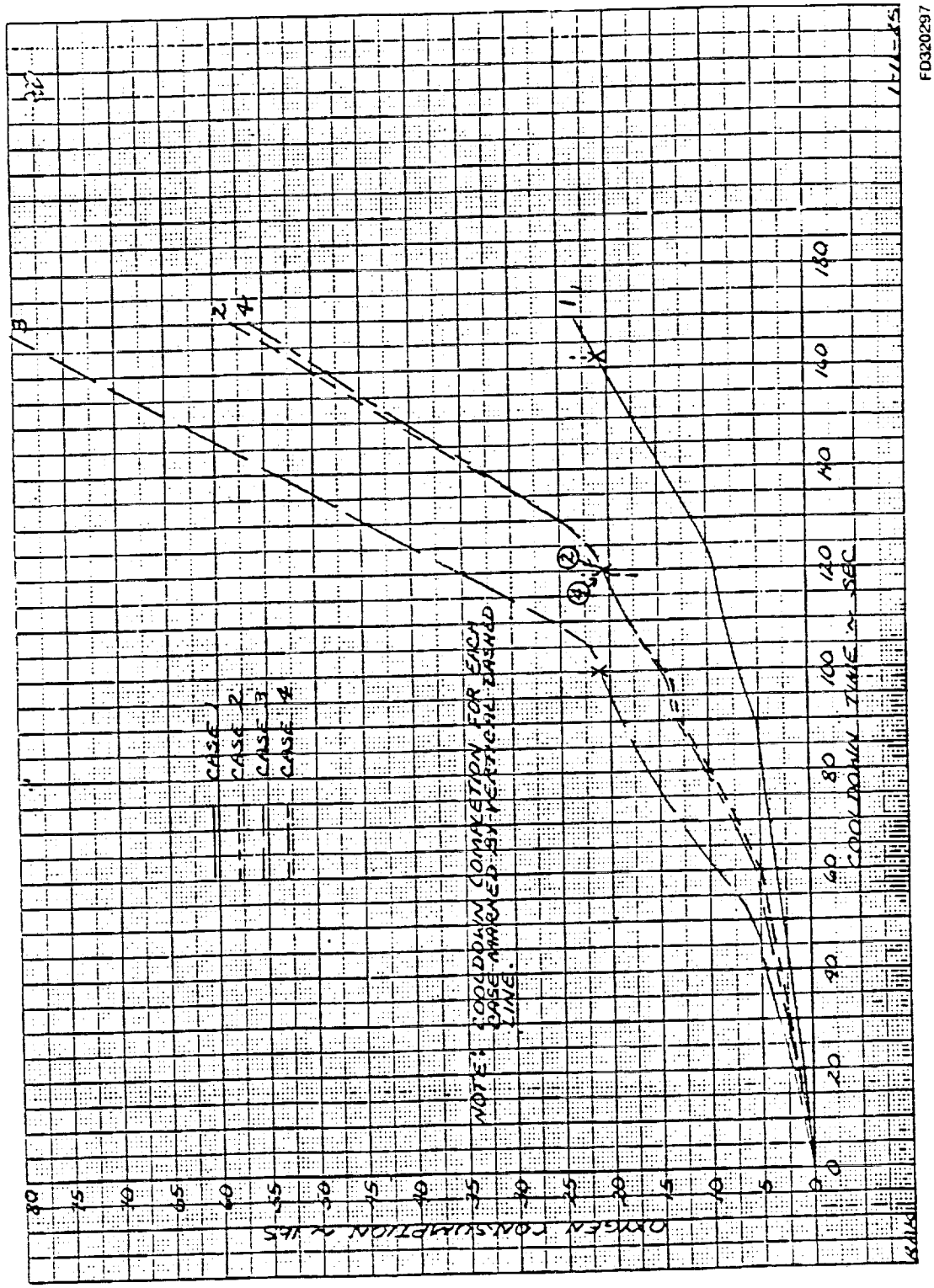

Figure 3-2. Oxygen Consumption vs Cooldown Time-Flow Area 0.05 in.²

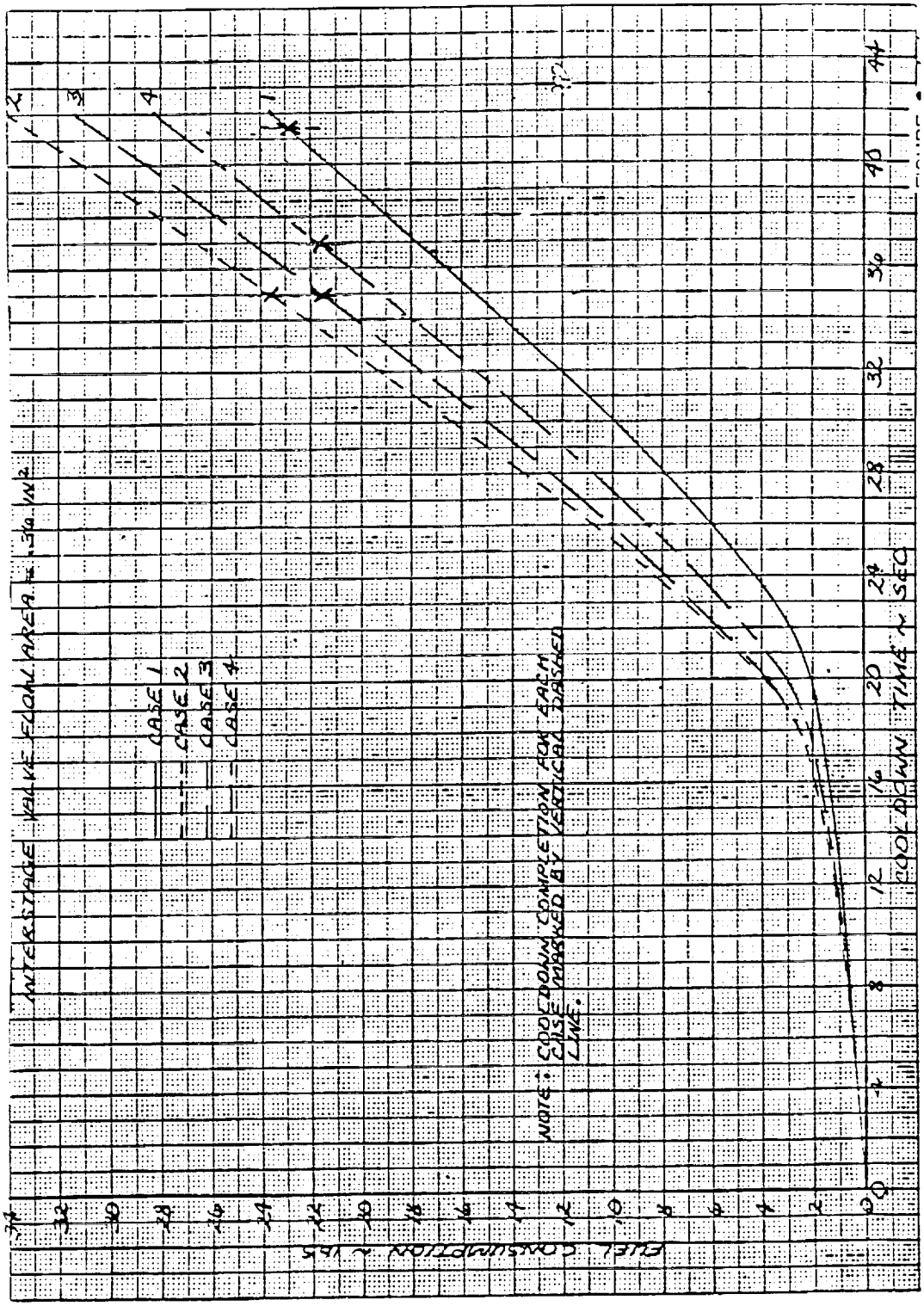

Figure 3-3. Fuel Consumption vs Cooldown Time-Flow Area 0.36 in.²

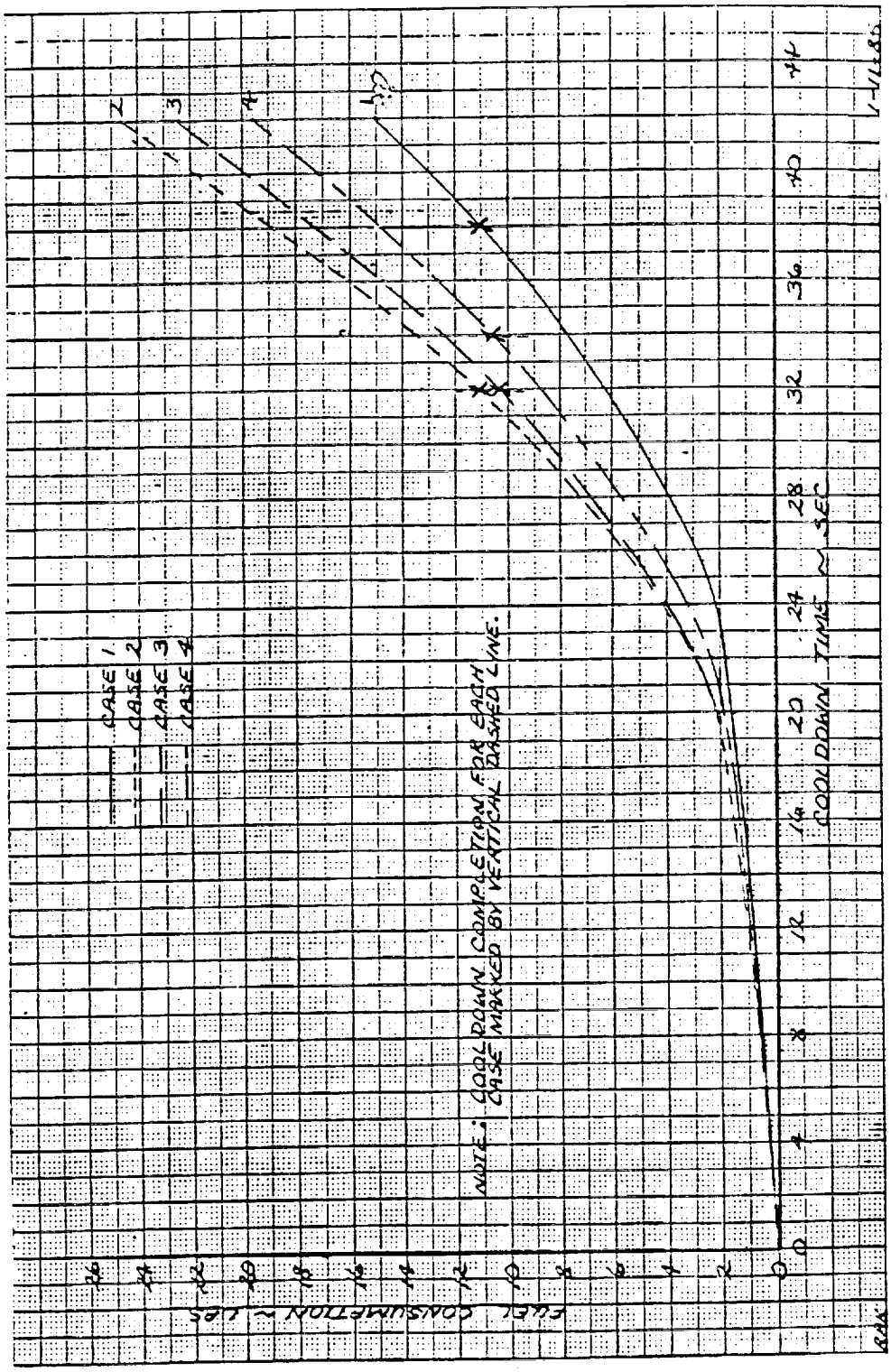

Figure 3-4. Fuel Consumption vs Cooldown Time-Flow Area 0.18 in.²

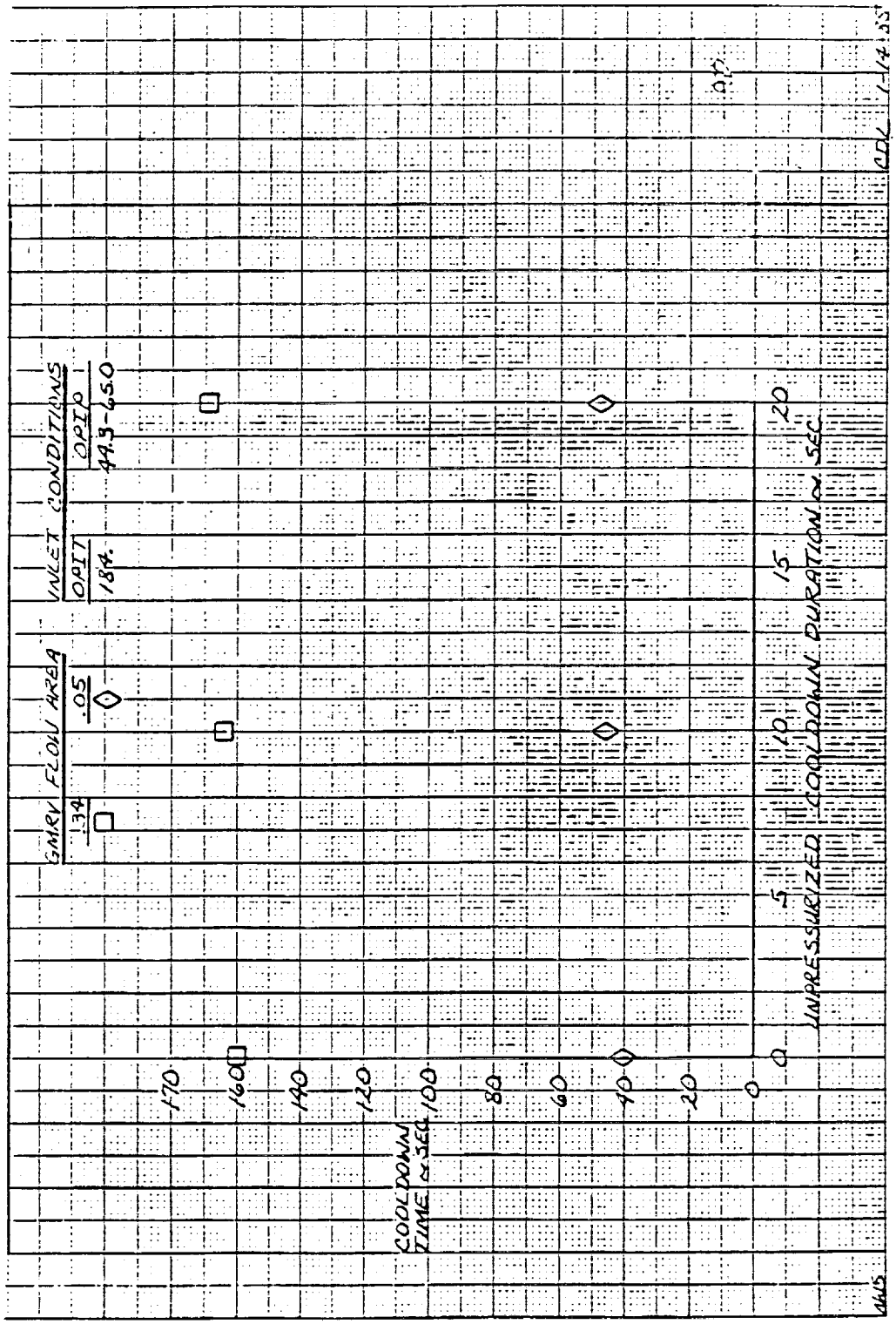

Figure 3-5. Effect of Blowdown on Oxidizer Cooldown Time

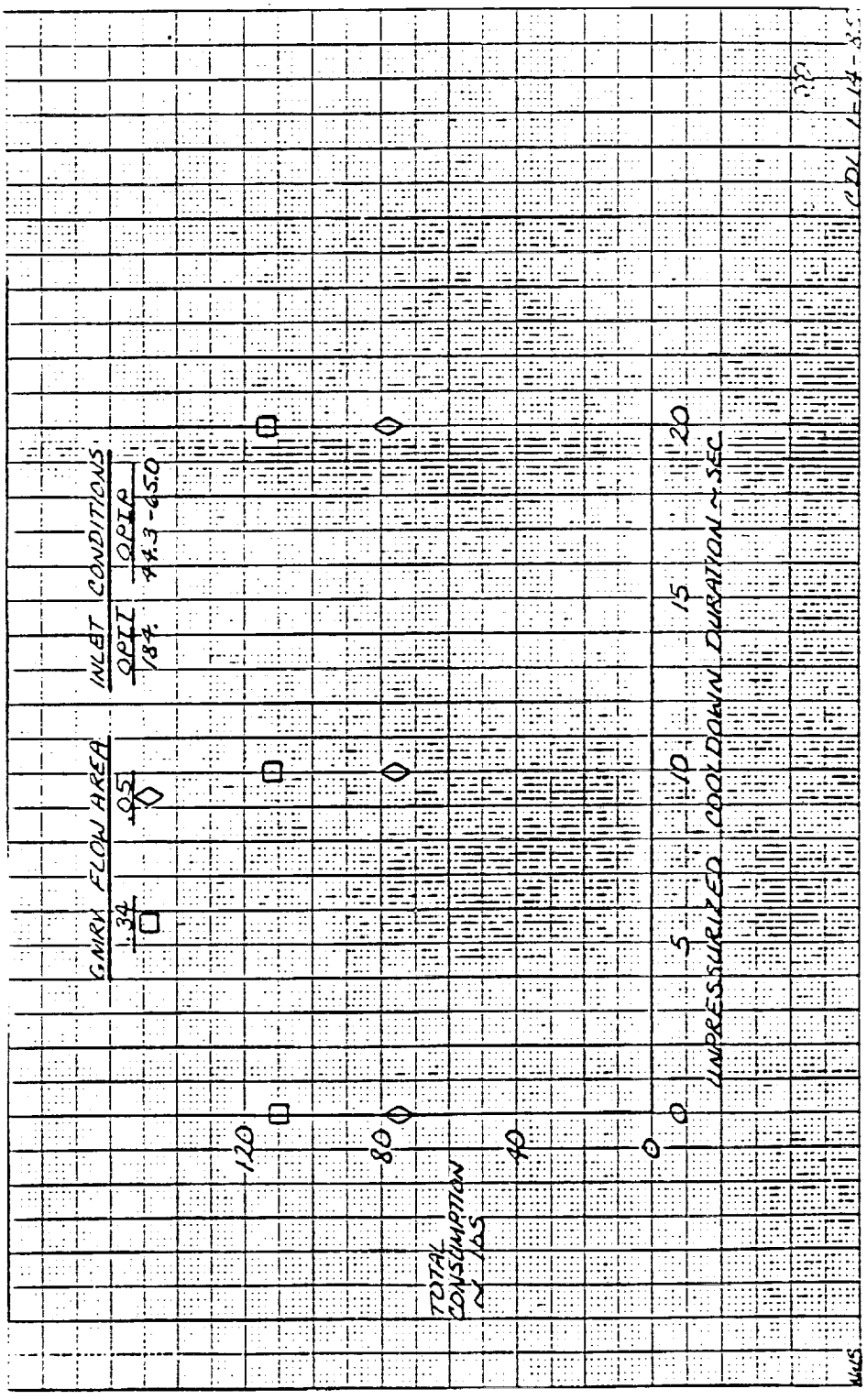

Figure 3-6. Effect of Blowdown on Oxidizer Consumption

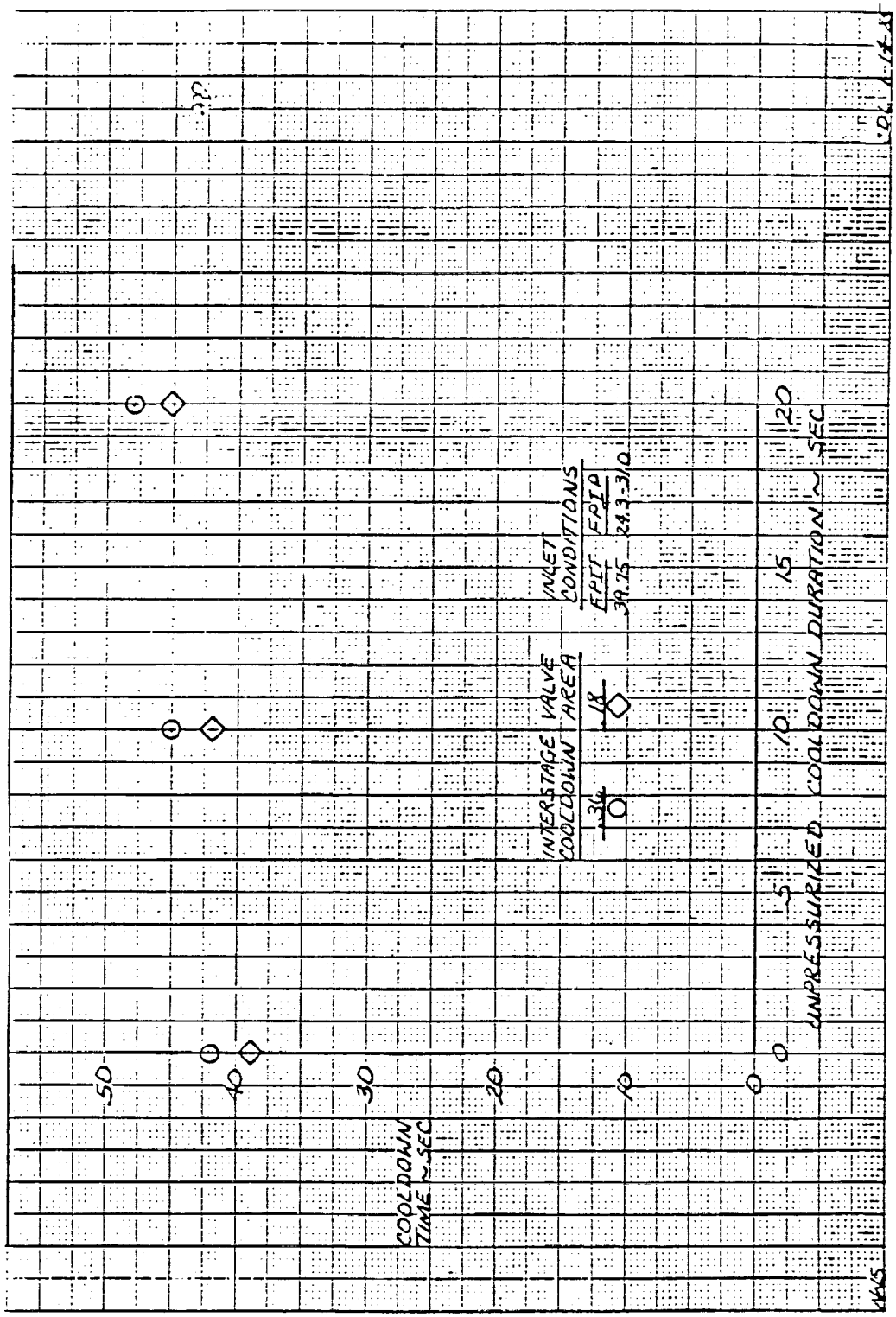

Figure 3-7. Effect of Blowdown on Fuel Cooldown Time

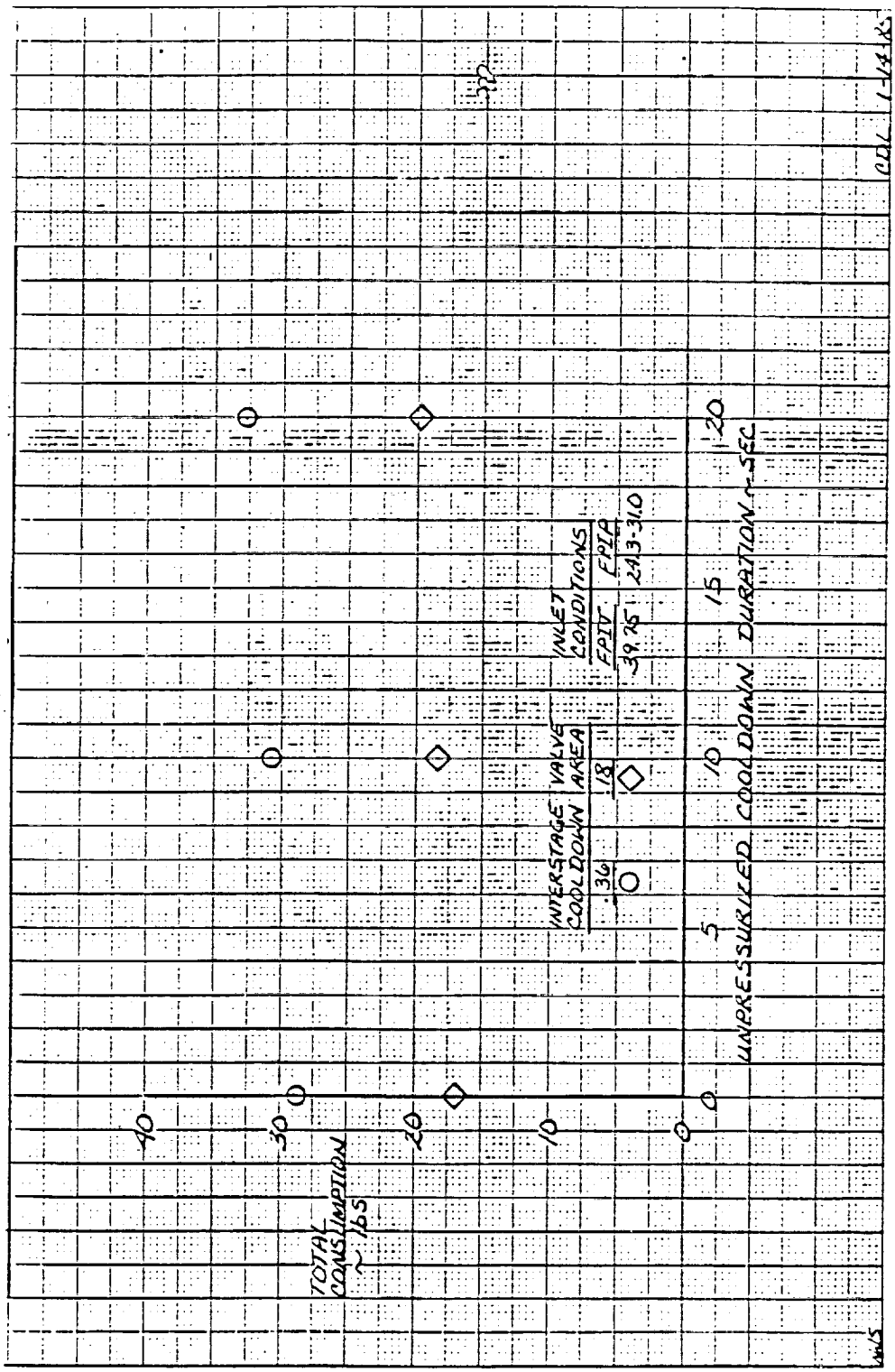

Figure 3-8. Effect of Blowdown on Fuel Consumption

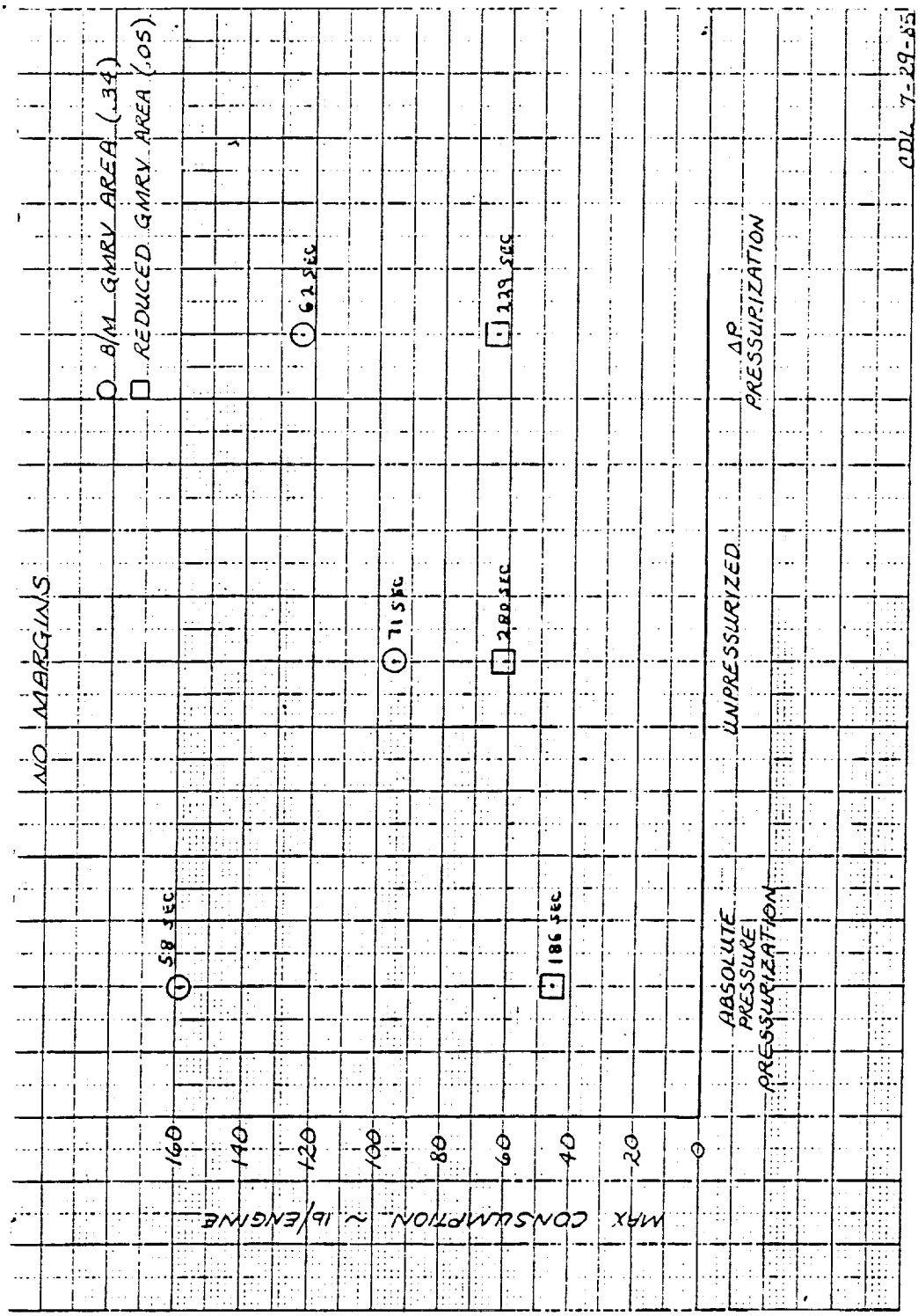

Figure 3-9. G Oxidizer Cooldown Consumption Characteristics

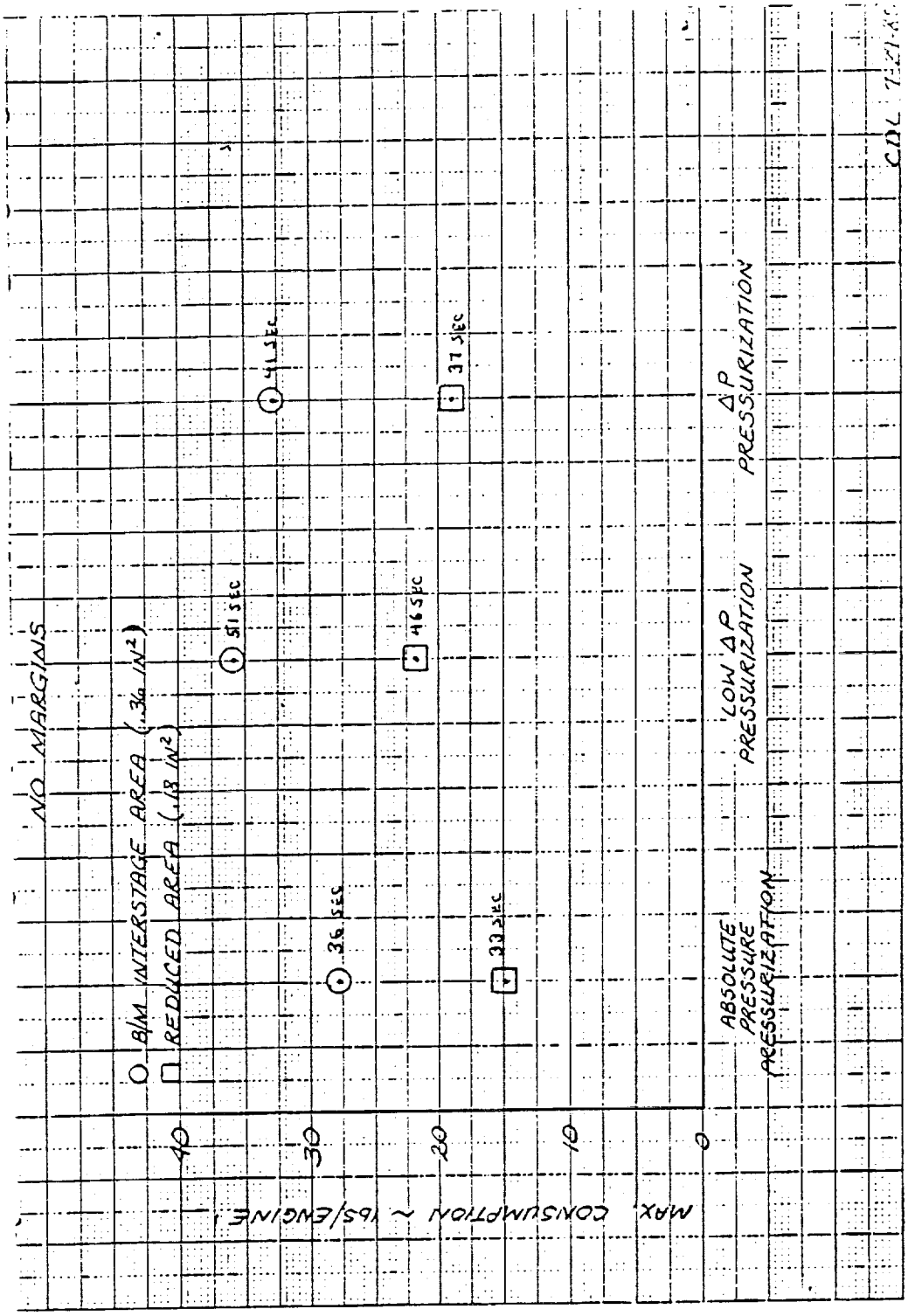

Figure 3-10. G Fuel Cooldown Consumption Characteristics

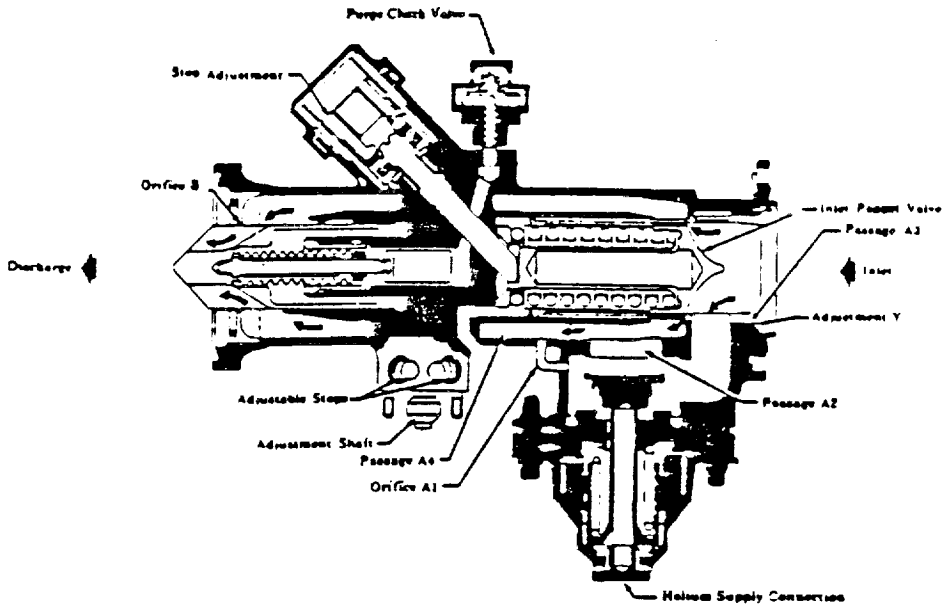

FD 320306

Figure 3-11. Oxidizer Flow Control and Purge Check Valve

In addition to cooldown valve flow area changes, the effect of propellant pressurization was also investigated. Cases were run with the cooldown prediction deck keeping the fuel and oxidizer inlet temperatures constant, but varying inlet pressure from saturation pressure to the level desired. The duration of unpressurized cooldown was varied from zero to twenty seconds. The effect of the unpressurized flow duration was to slightly increase cooldown time and consumption regardless of cooldown flow area. This is shown in Figures 3-5, 3-6, 3-7, and 3-8. Due to the adverse effect of unpressurized cooldown, it was decided that engine cooldown would be accomplished under pressurized conditions.

To determine the pressurization scenario to be used on the G-Prime flights, worst case predictions were made using each of the three inlet boxes. The runs were done both with large and small flow areas. It was found that the smaller flow areas produced universally lower propellant consumptions when compared to the larger areas, and that of the cases run with the smaller areas, the absolute pressure pressurization box yielded the lowest consumption as well as the lowest cooldown time. The worst case consumption and the required cooldown times for the three inlet boxes are shown in Figures 3-9 and 3-10 for both normal and reduced oxidizer and fuel flow areas.

3.2 COOLDOWN DECK MATCHING

The initial series of cooldown tests was run to match the simulation deck to actual cooldown data. Comparisons were made between fuel and oxidizer flowrate, engine oxidizer and fuel inlet duct temperatures, and fuel and oxidizer pump temperatures.

In the tests with the flight weight inlet ducts, it was noticed that inlet temperatures on both the fuel and oxidizer side varied with time, where the prevalve inlet temperature would start at saturated temperature, and approach the desired inlet temperature as the duct cooled. This will be shown later in Figure 3-41. Duct temperature profiles indicated that gas was being trapped along the top of the ducts due to the one-G environment. This allowed hot oxygen and fuel vapor

to travel backward against the flow and warm the incoming propellants. To accurately model this, an inlet temperature profile was included in the simulation deck. After a test was made, the temperature profile from the test was used as input to the simulation deck. In this way, the simulation results could be compared directly to test results.

Fitting of the simulation deck to test data was completed during the first sixteen runs of the cooldown program, which were cold flows done without any attempt to start the engine. Comparisons of calculated and actual propellant flowrates and component temperatures are shown in Figures 3-12 through 3-36. Figure 3-12 shows the comparison between calculated and actual oxidizer flow for a cooldown run, while Figure 3-13 shows the same comparison for the fuel side. The oxidizer plot shows close agreement between predicted and actual flowrate, while the fuel side plot shows a difference during the first 20 seconds of flow. This discrepancy is due to the effects of duct filling and the rising of warm hydrogen up the inlet ducts. Figures 3-14 through 3-36 show comparisons between predicted and actual metal temperatures. In these figures, the square symbols mark prediction data, while the round symbols mark test data. The header names, shown with different line types, refer to Figures 3-37 and 3-38 which show the locations of the cooldown temperature probes.

In all figures, it can be seen that the predictions of duct temperatures agreed well with test data, while the predicted gimbal cooldown rate was slower than test data showed. This discrepancy is due to the thickness of the gimbals and the locations of their thermocouples. The gimbals were modeled as bulk masses with a small surface area available for cooling. The predicted temperatures shown in the figures is the average temperature of the gimbals, while the measured temperatures are taken at the gimbal flange, which cools faster than the body of the gimbal. To get a true indication of the gimbal temperature, the thermocouple would have had to be placed inside the gimbal, which was impractical. It is believed the predicted temperature curves for the gimbals are representative of the actual gimbal average temperature. The tubular portions of the ducts, because of their thin profile, had a skin temperature very close to their average temperature which resulted in close agreement between the predicted and actual data. The temperature probes for duct 4 on the fuel side could not be used, resulting in no test data comparison for the predicted curve in Figure 3-34.

The oxidizer pump temperature probes are located on the skin of the oxidizer pump in locations shown in Figure 3-39. Conduction calculations allowed the prediction of these skin temperatures using the dimensions of the pump and the calculated pump internal temperatures. The oxidizer pump temperatures, shown in Figures 3-21 through 3-24, show close agreement with the test data. The fuel pump first stage temperature probe is imbedded in the pump housing, which allows accurate measurement of the pump bulk metal temperature and close agreement with predicted values. The second stage probe, because it is a surface probe, does not match well with predicted results. The predicted second stage pump temperature is believed to be a good representation of the pump bulk metal temperature.

A description of the cooldown deck is presented in Appendix A.

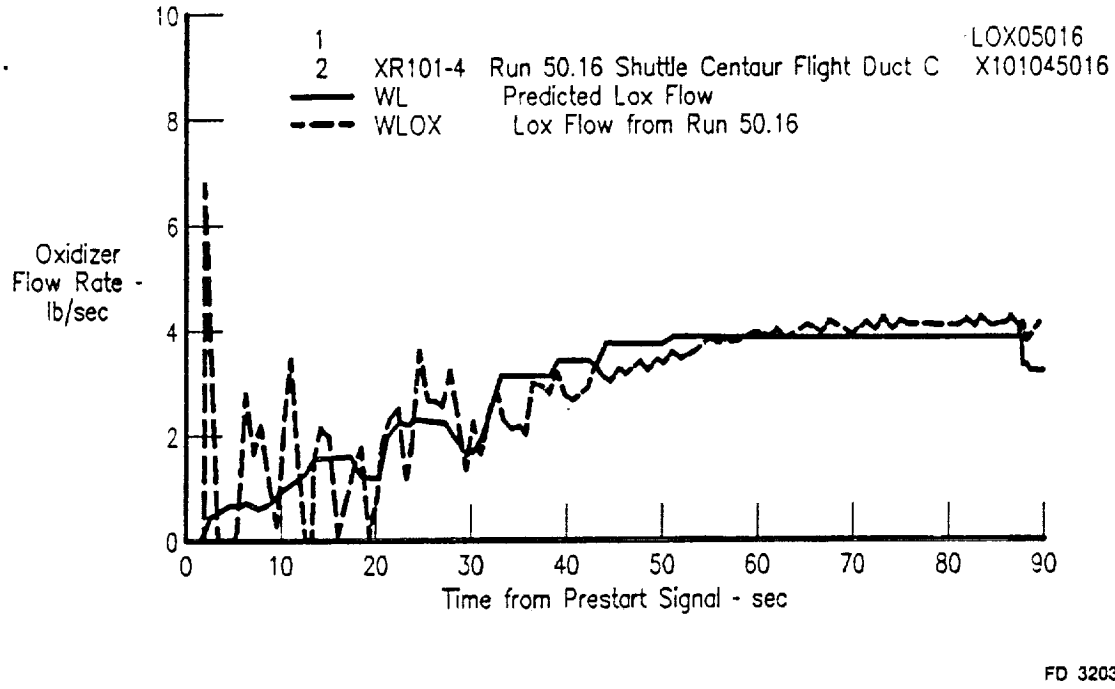

Figure 3-12. Comparison of Predicted and Test Run LOX Flow Rate

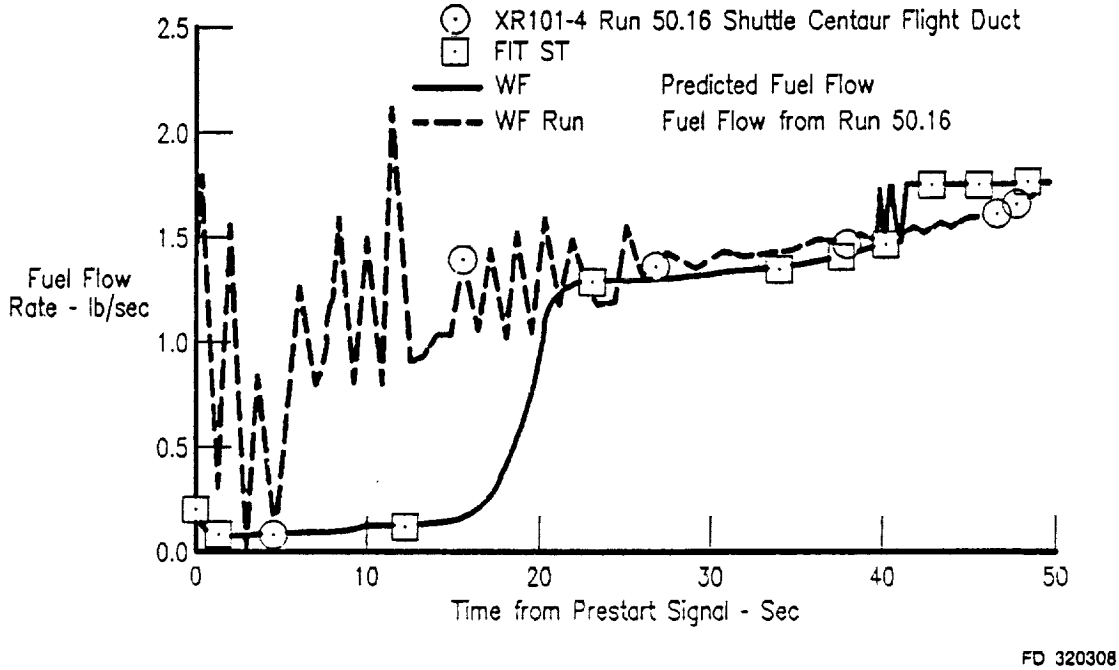

Figure 3-13. Comparison of Predicted and Test Run Fuel Flow Rate

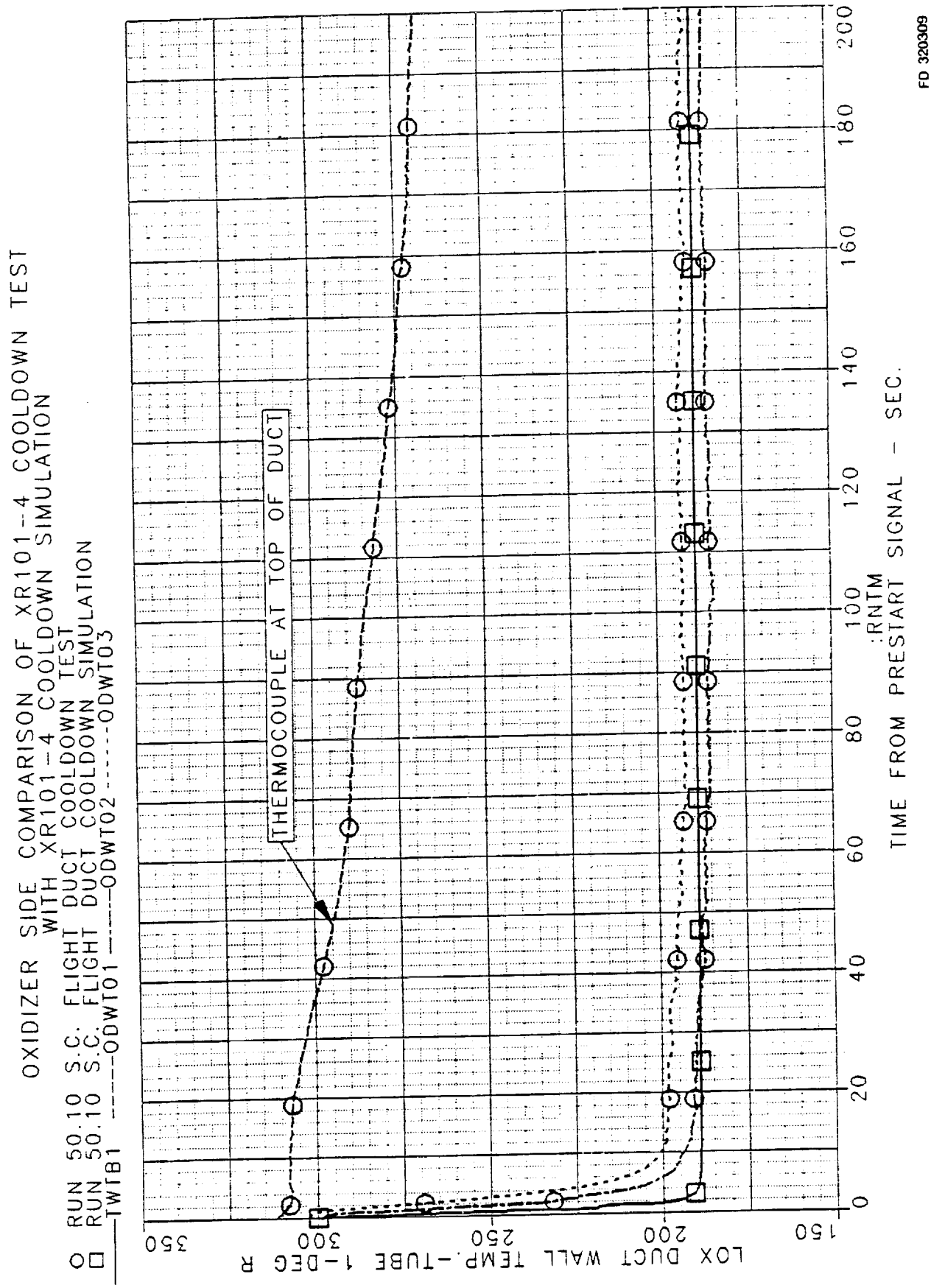

Figure 3-14. LOX Duct Wall Temperature — Tube 1

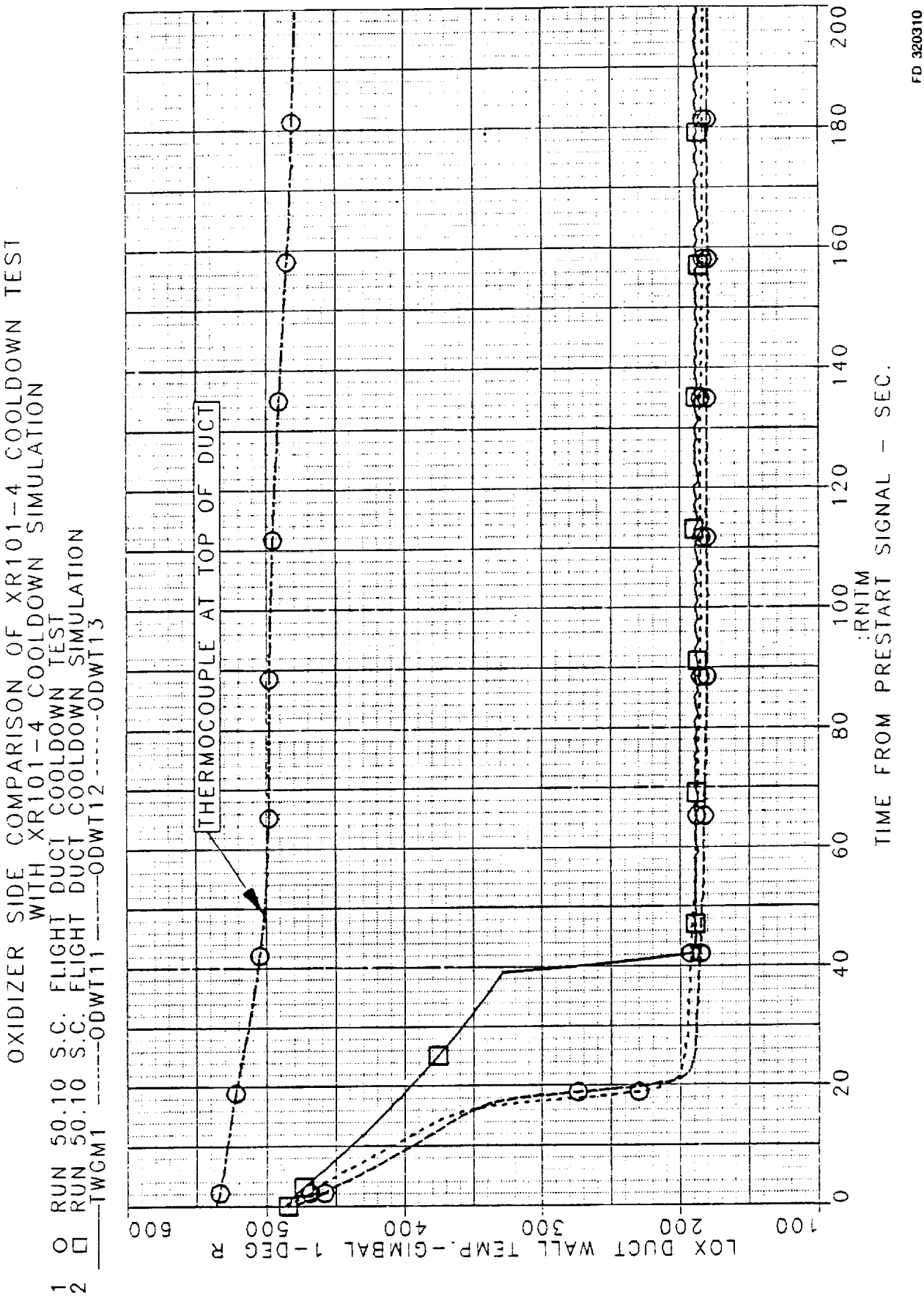

Figure 3-15. LOX Duct Wall Temperature — Gimbal 1

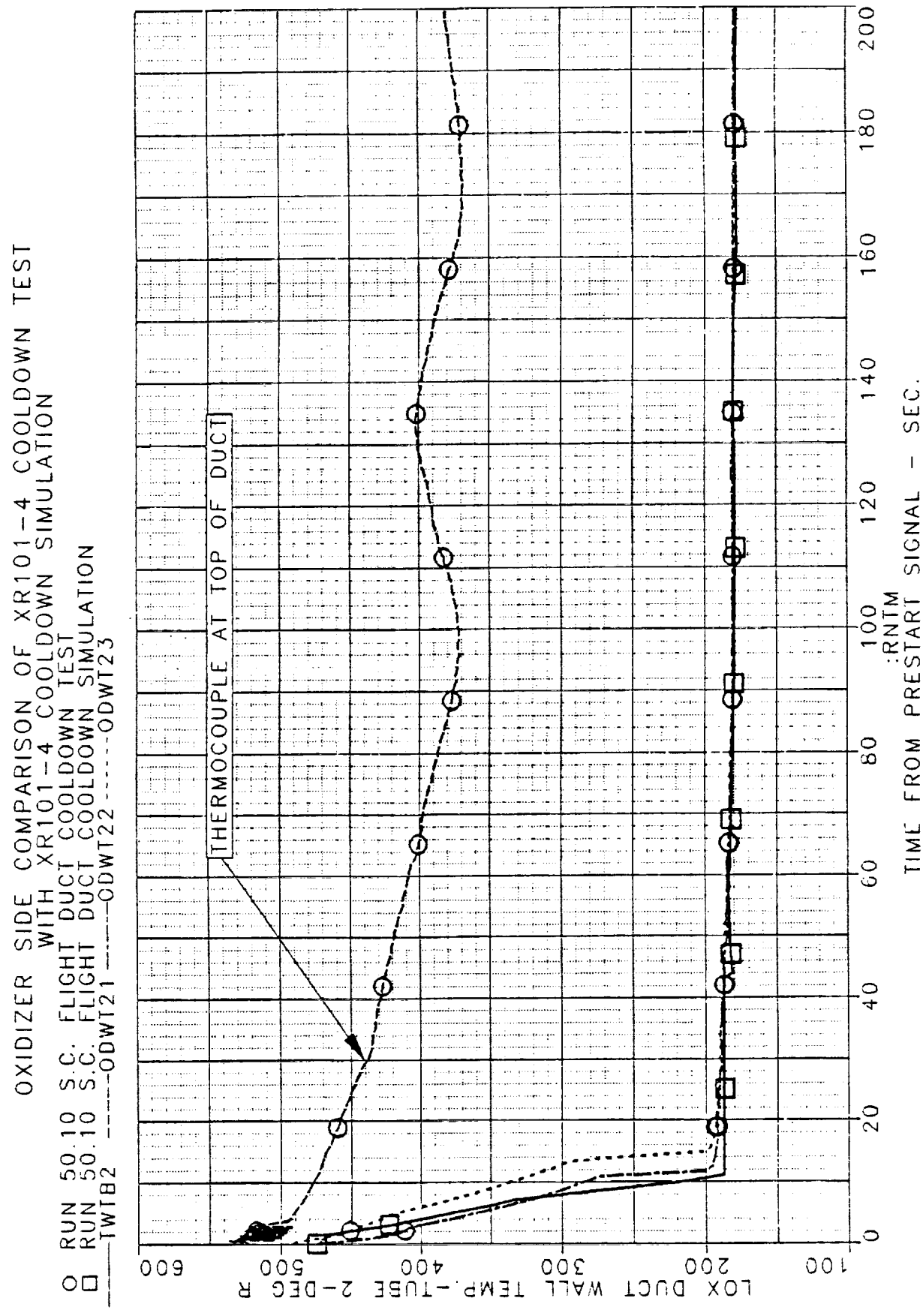

Figure 3-16. LOX Duct Wall Temperature — Tube 2

0632C

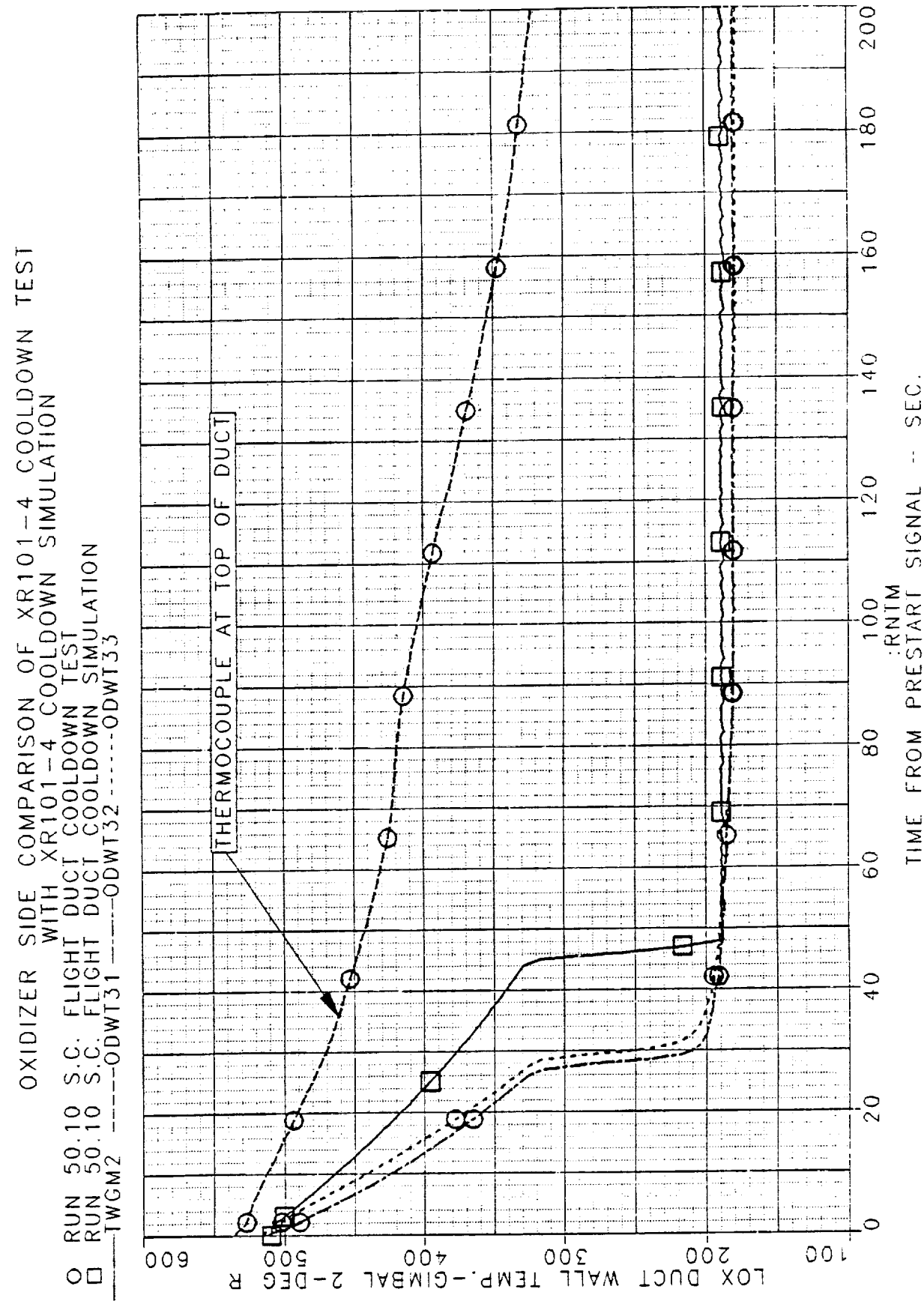

Figure 3-17. LOX Duct Wall Temperature — Gimbal 2

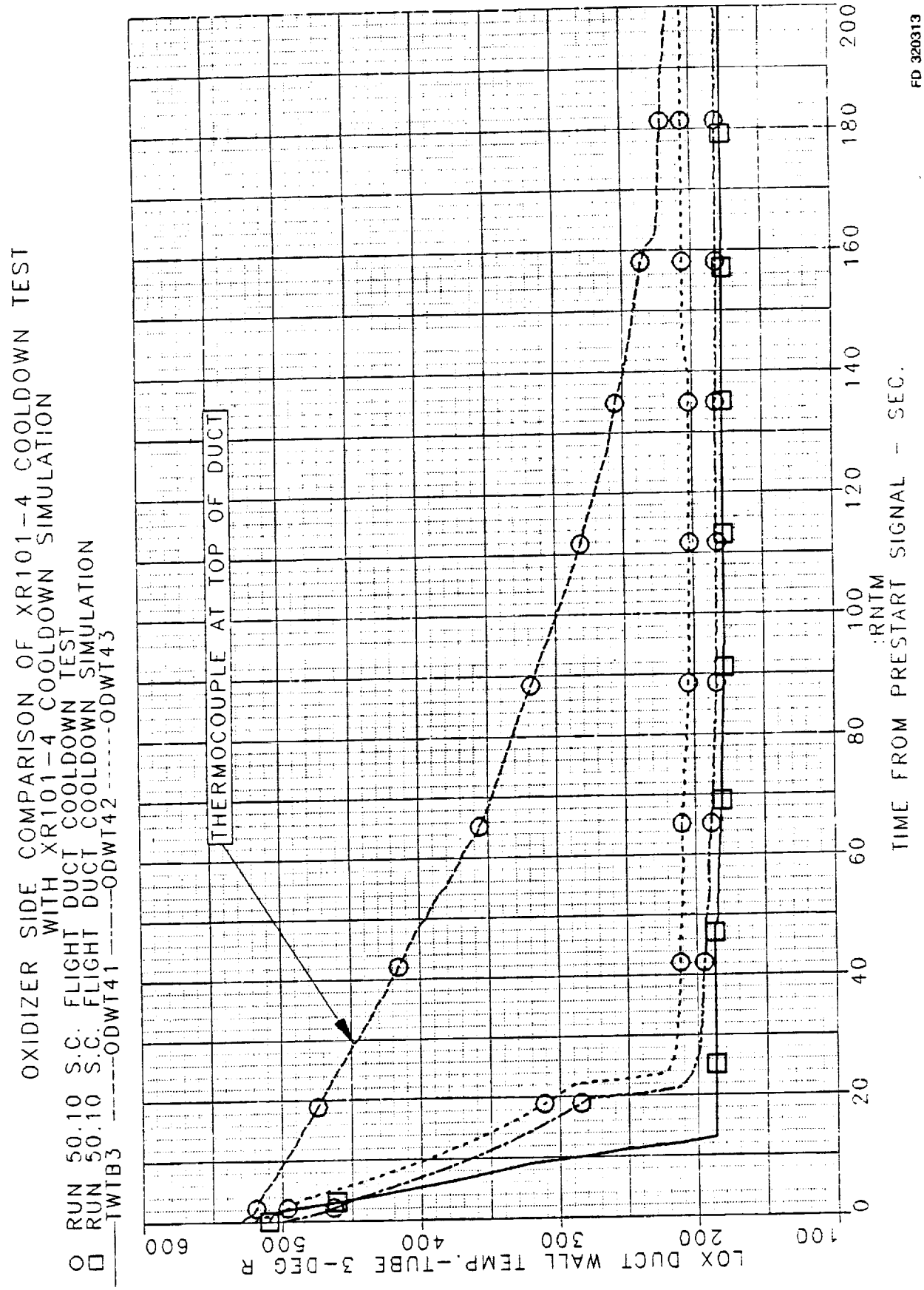

Figure 3-18. LOX Duct Wall Temperature — Tube 3

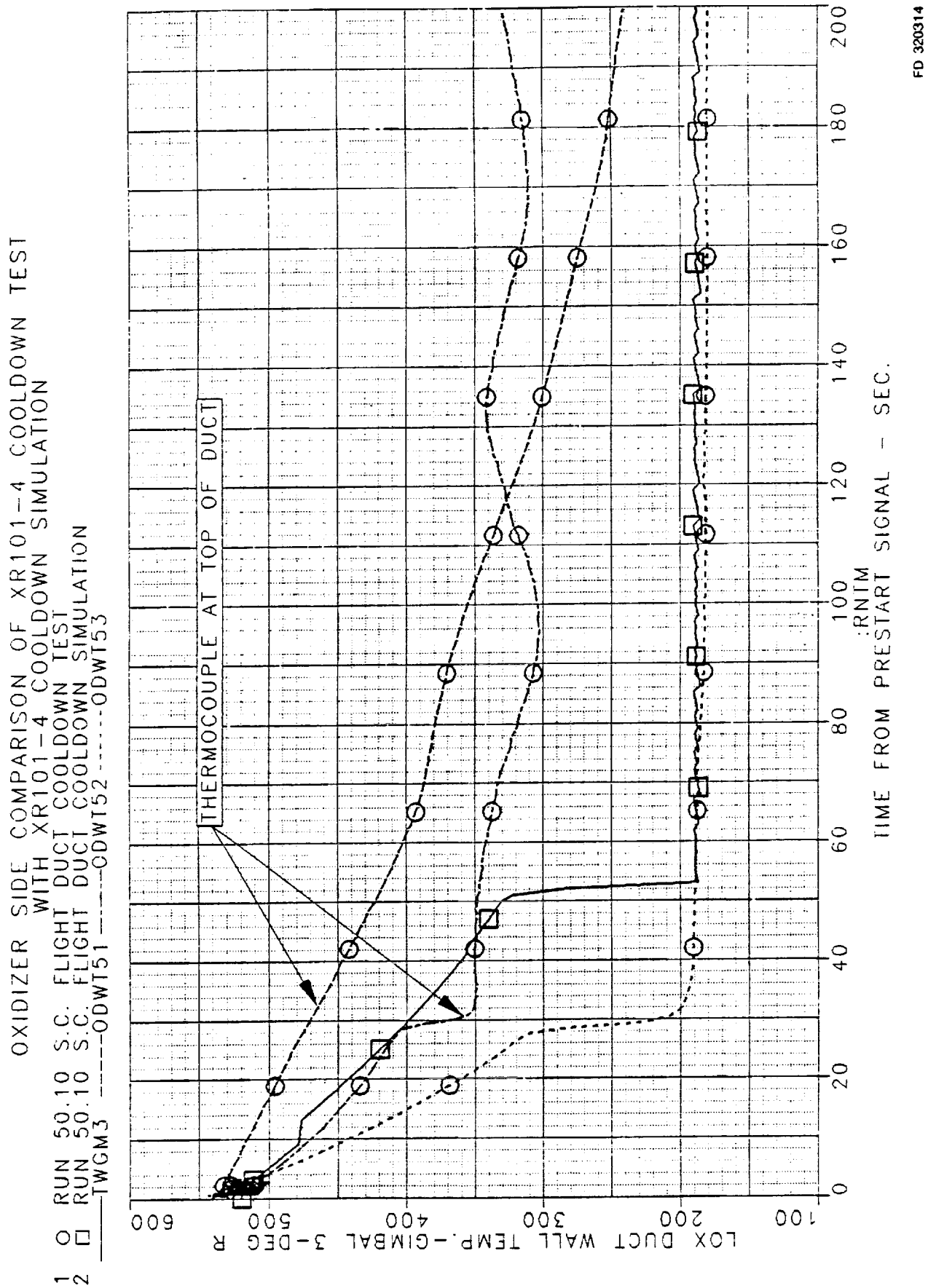

Figure 3-19. LOX Duct Wall Temperature — Gimbal 3

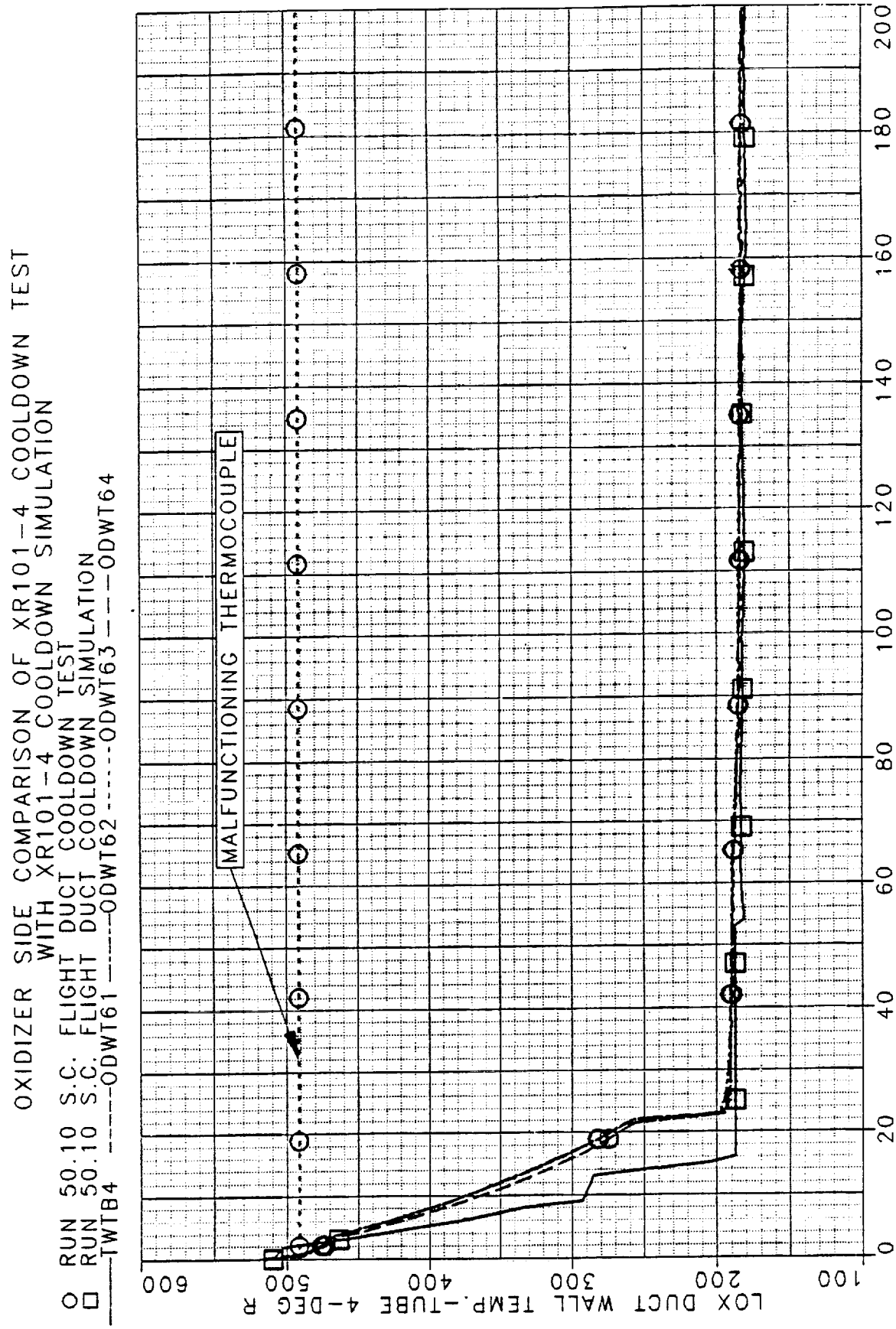

FD 320315

Figure 3-20. LOX Duct Wall Temperature — Tube 4

0632C

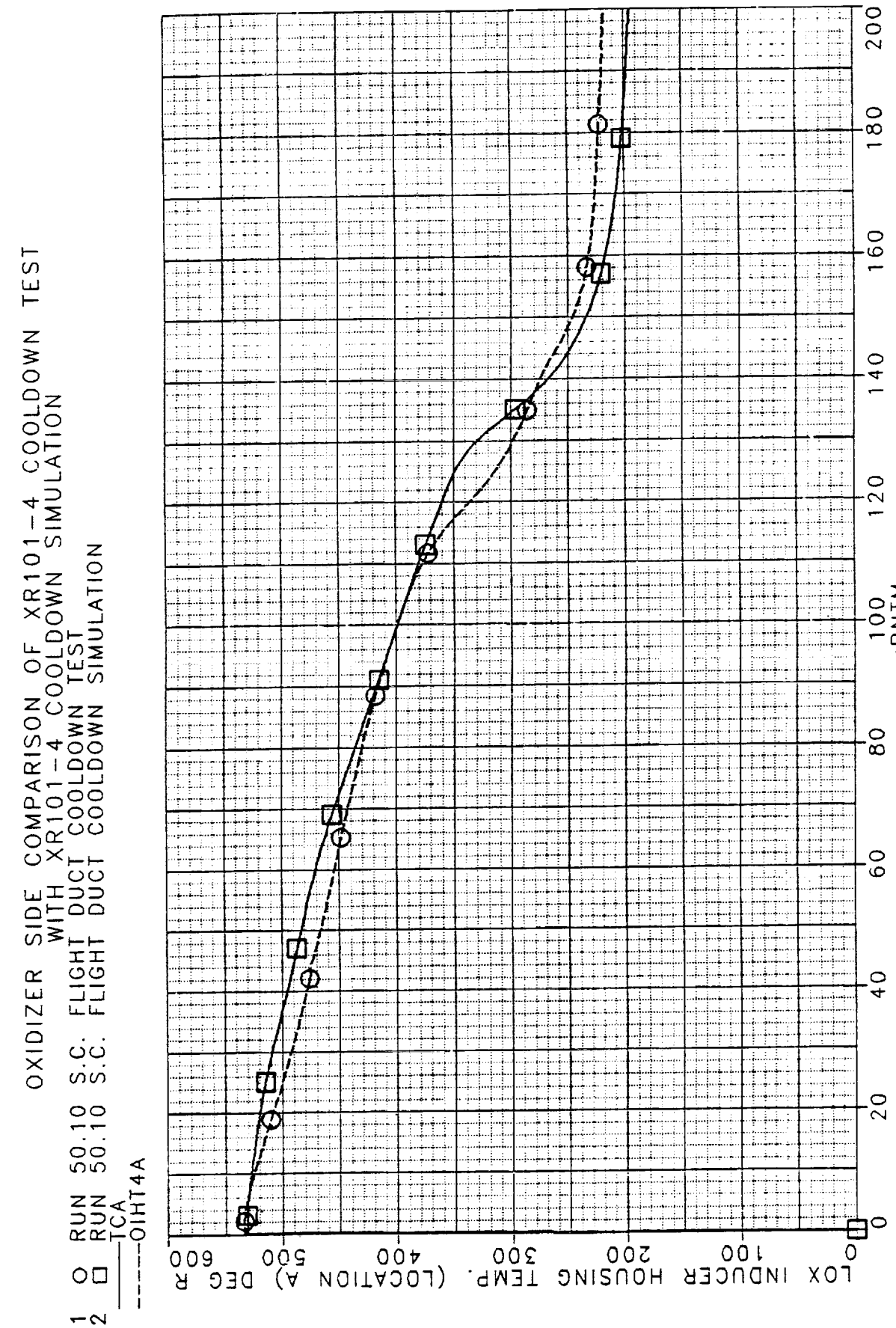

Figure 3-21. LOX Inducer Housing Temperature — Location A

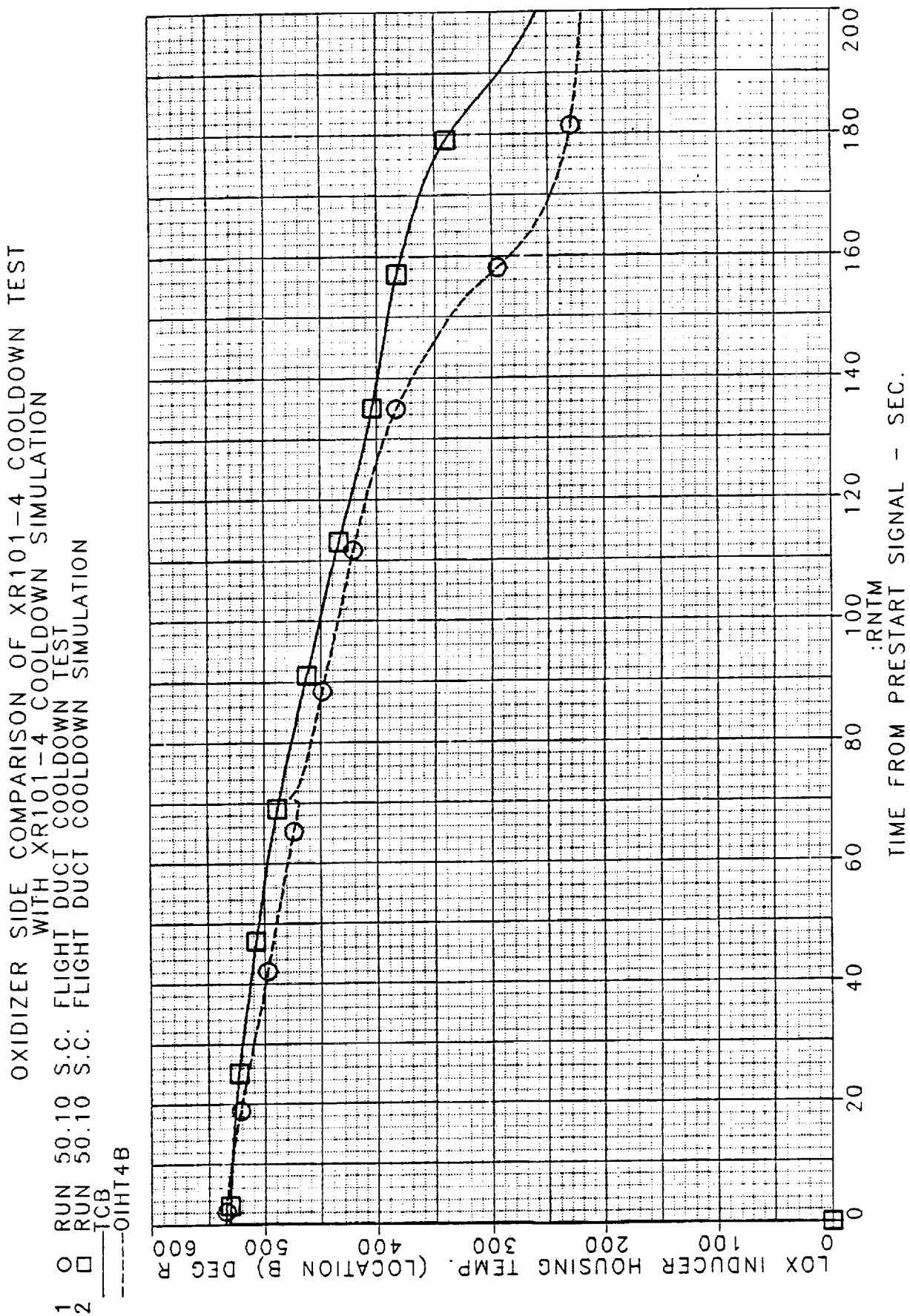

Figure 3-22. LOX Inducer Housing Temperature — Location B

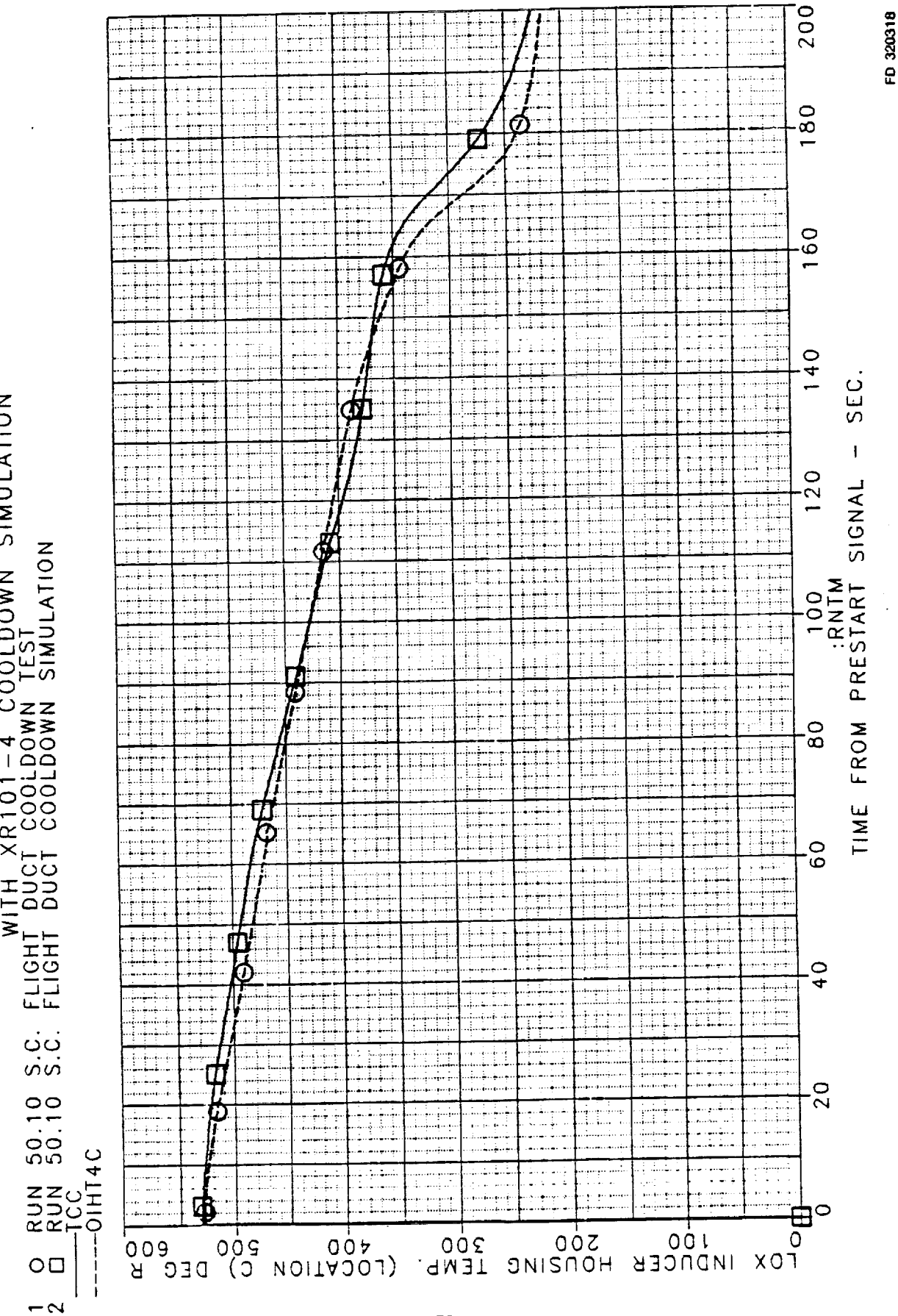

Figure 3-23. LOX Inducer Housing Temperature — Location C

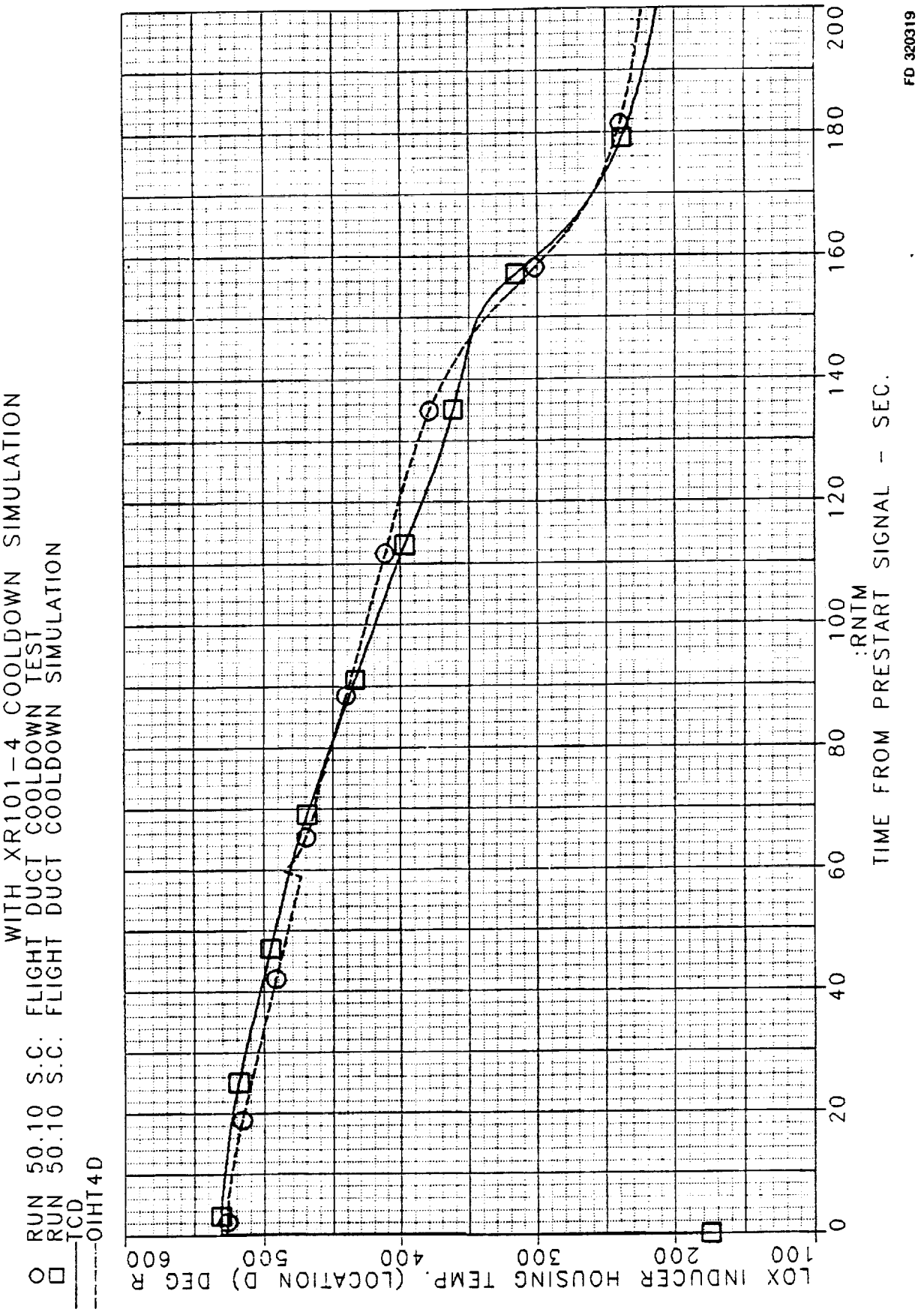

Figure 3-24. LOX Inducer Housing Temperature — Location D

0632C

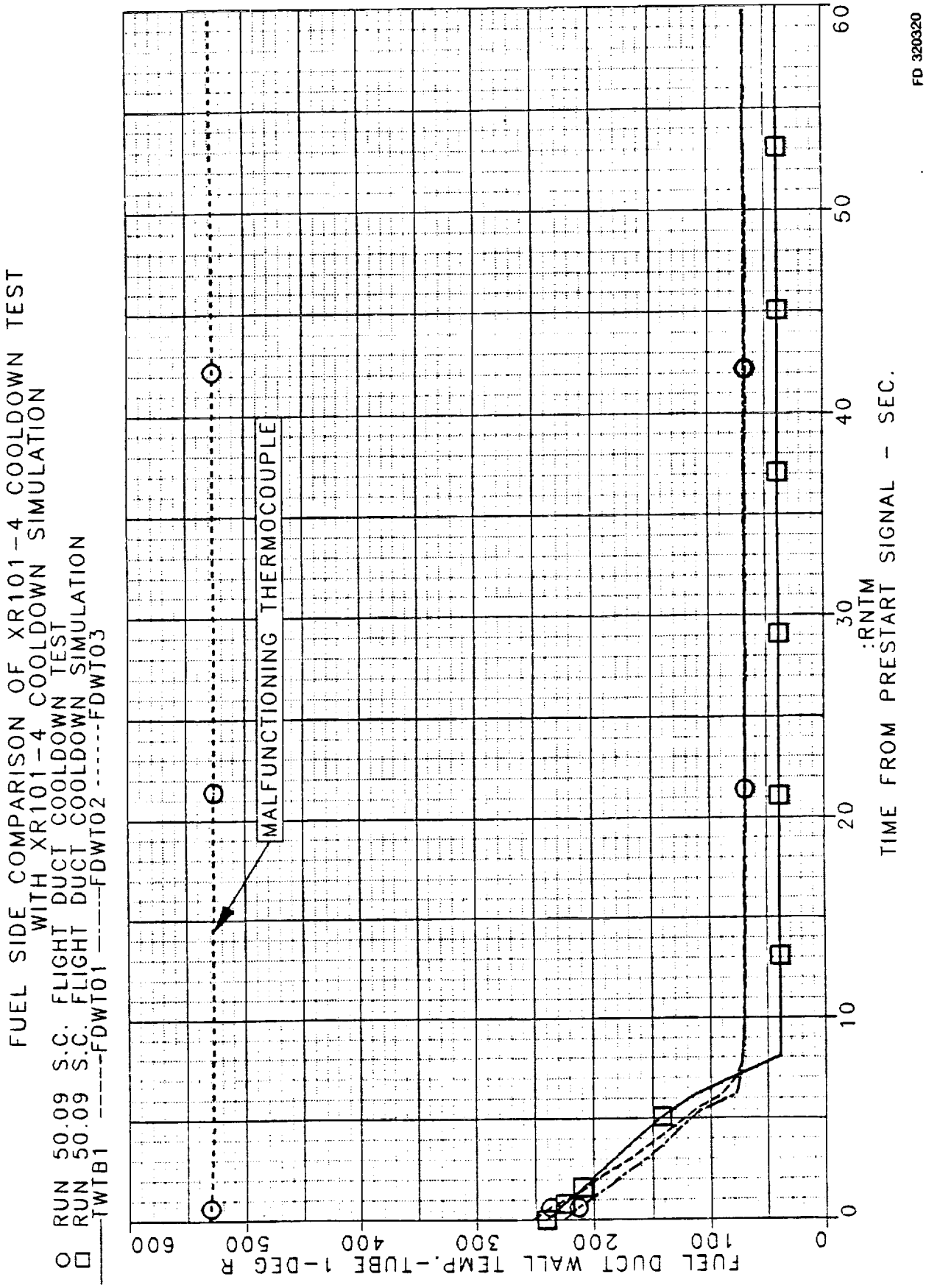

Figure 3-25. Fuel Duct Wall Temperature — Tube 1

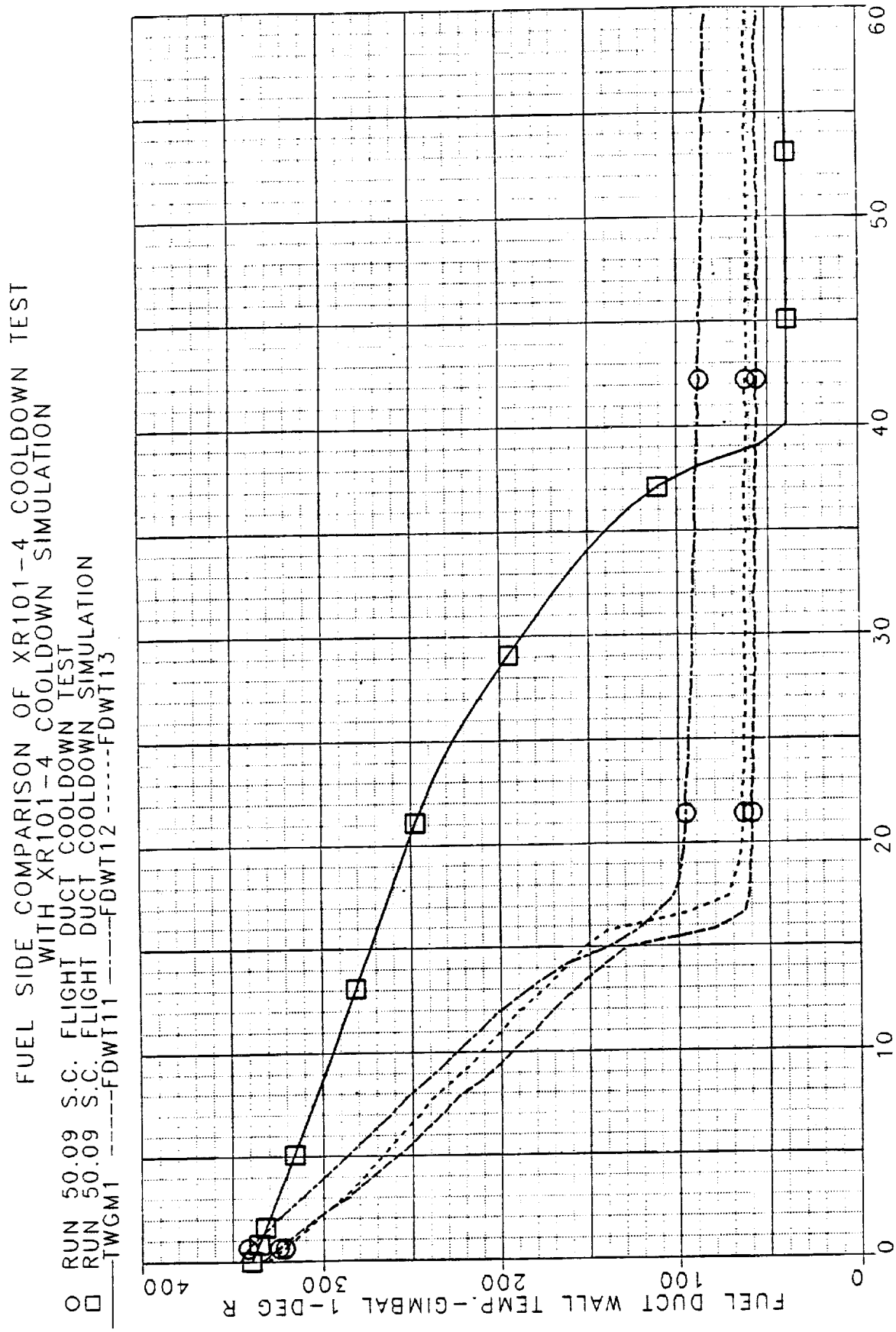

Figure 3-26. Fuel Duct Wall Temperature — Gimbal 1

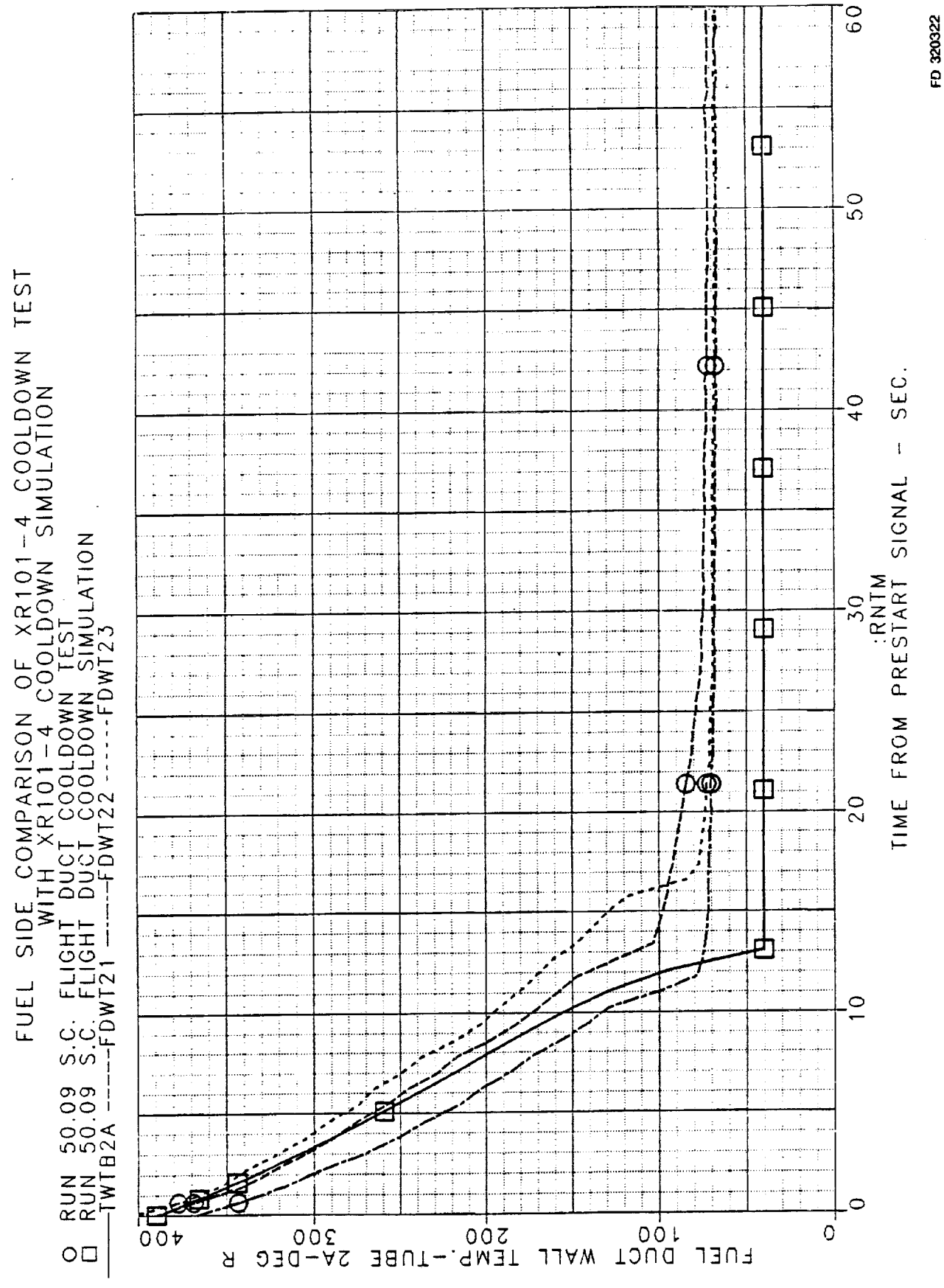

Figure 3-27. Fuel Duct Wall Temperature — Tube 2A

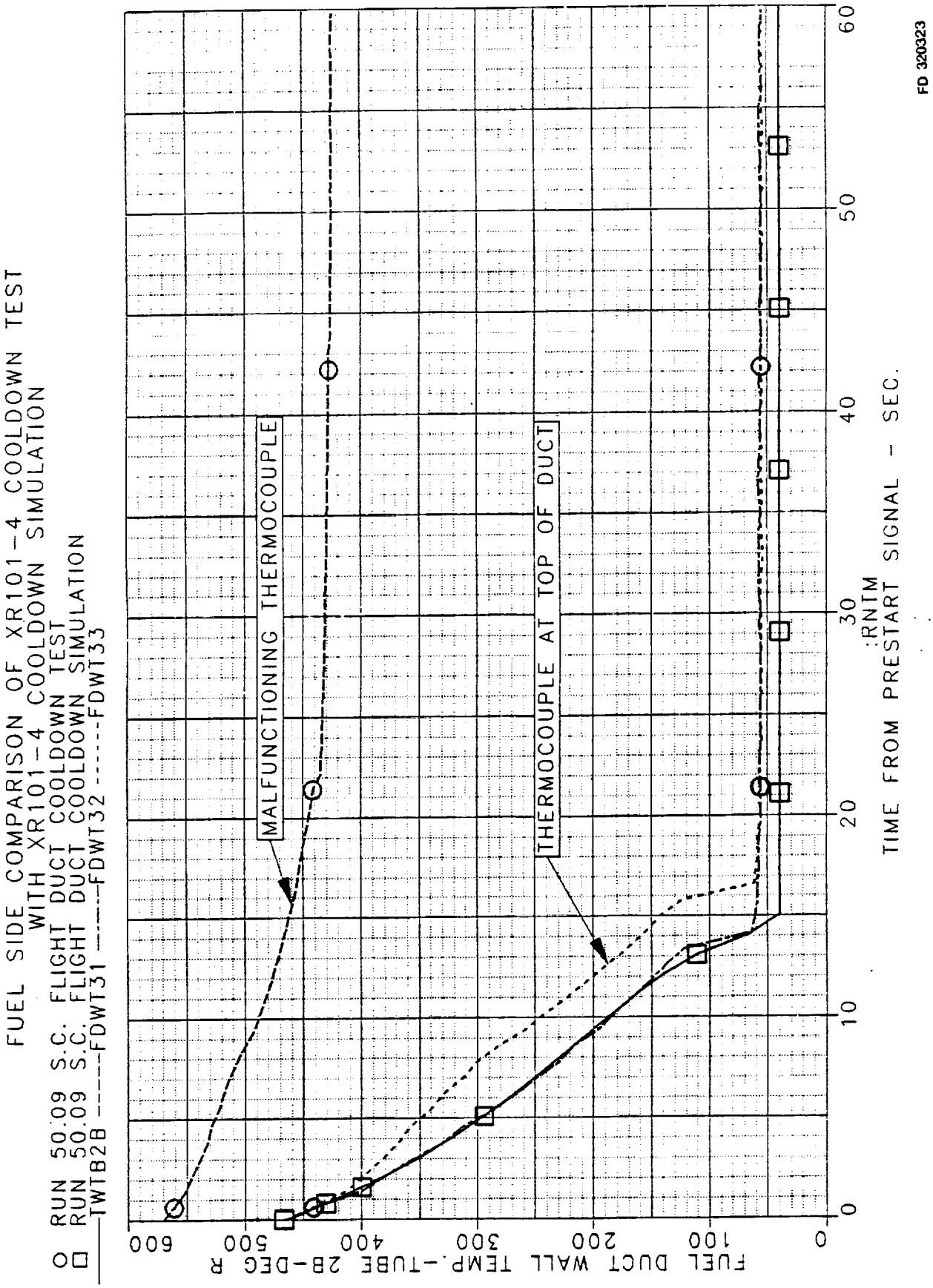

Figure 3-28. Fuel Duct Wall Temperature — Tube 2B

0632C

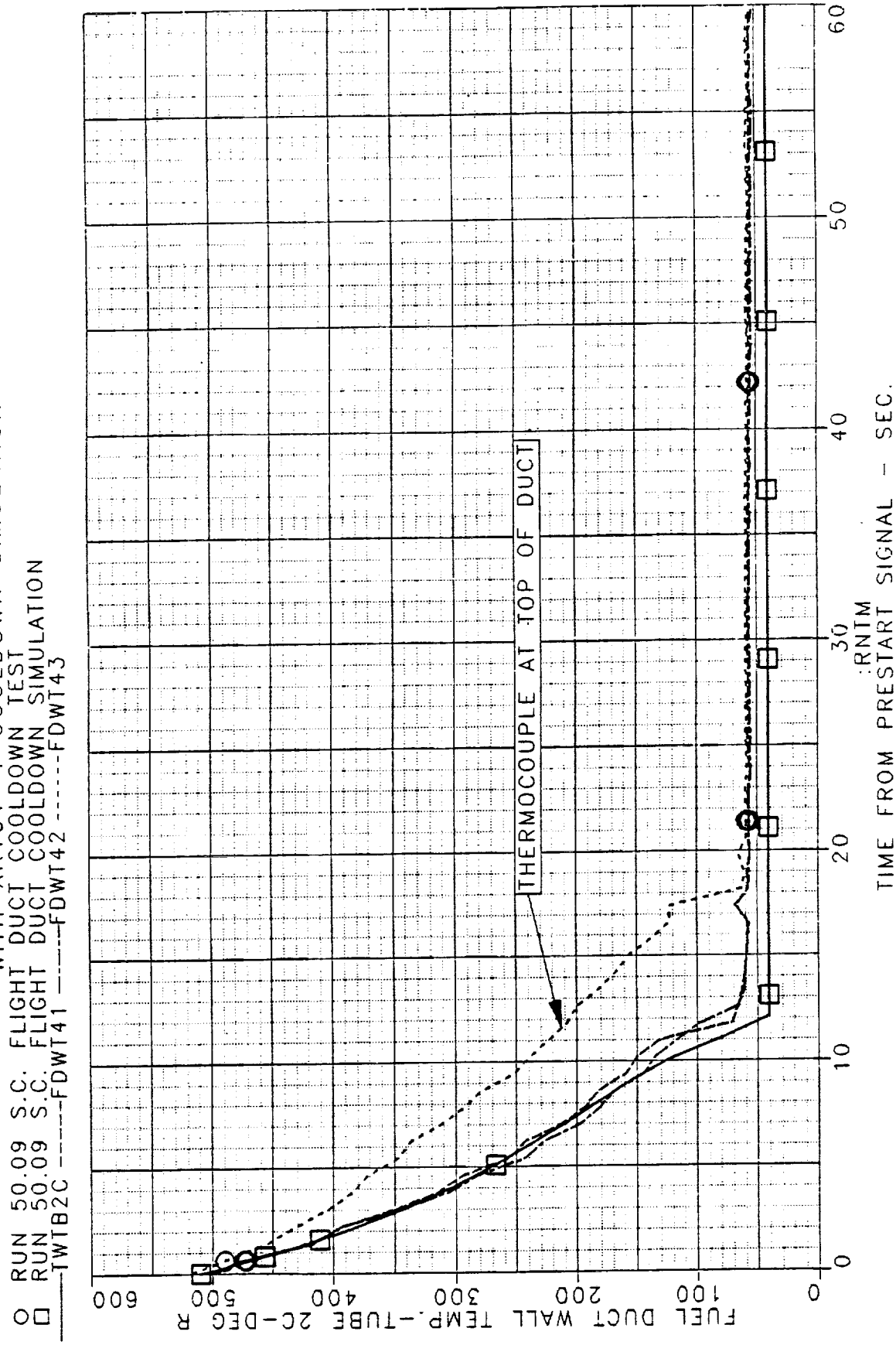

Figure 3-29. Fuel Duct Wall Temperature — Tube 2C

0632C

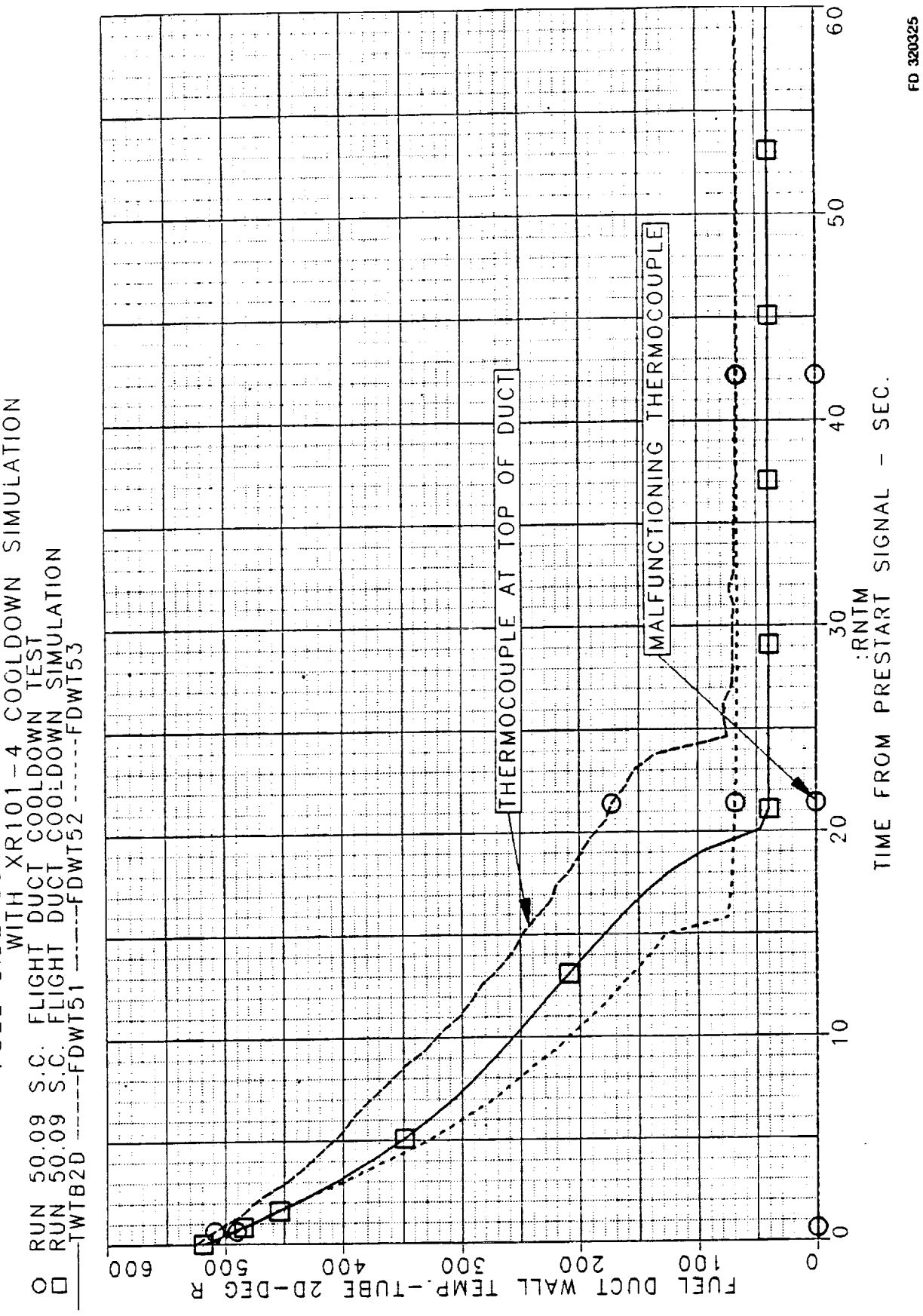

Figure 3-30. Fuel Duct Wall Temperature — Tube 2D

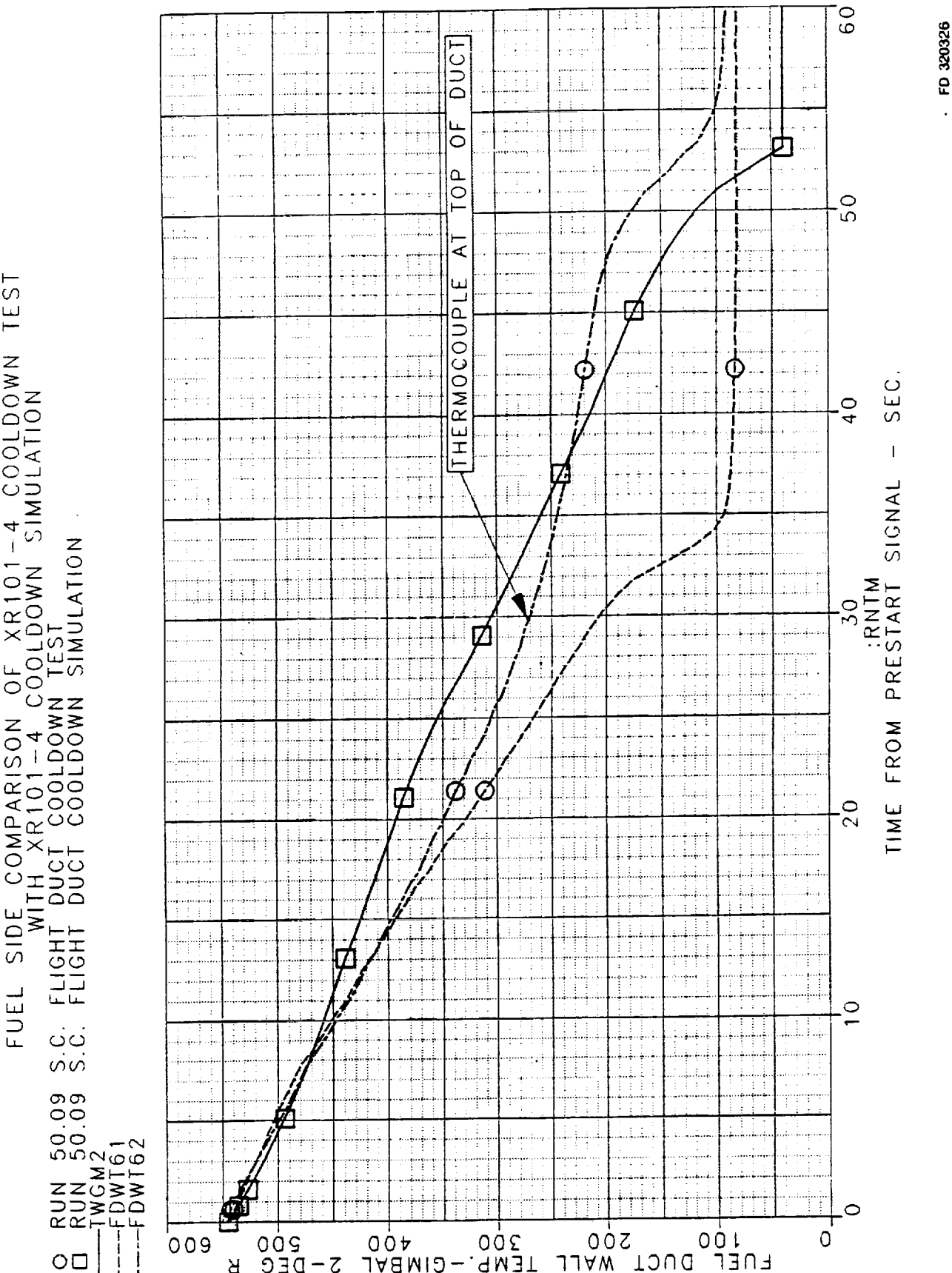

Figure 3-31. Fuel Duct Wall Temperature — Gimbal 2

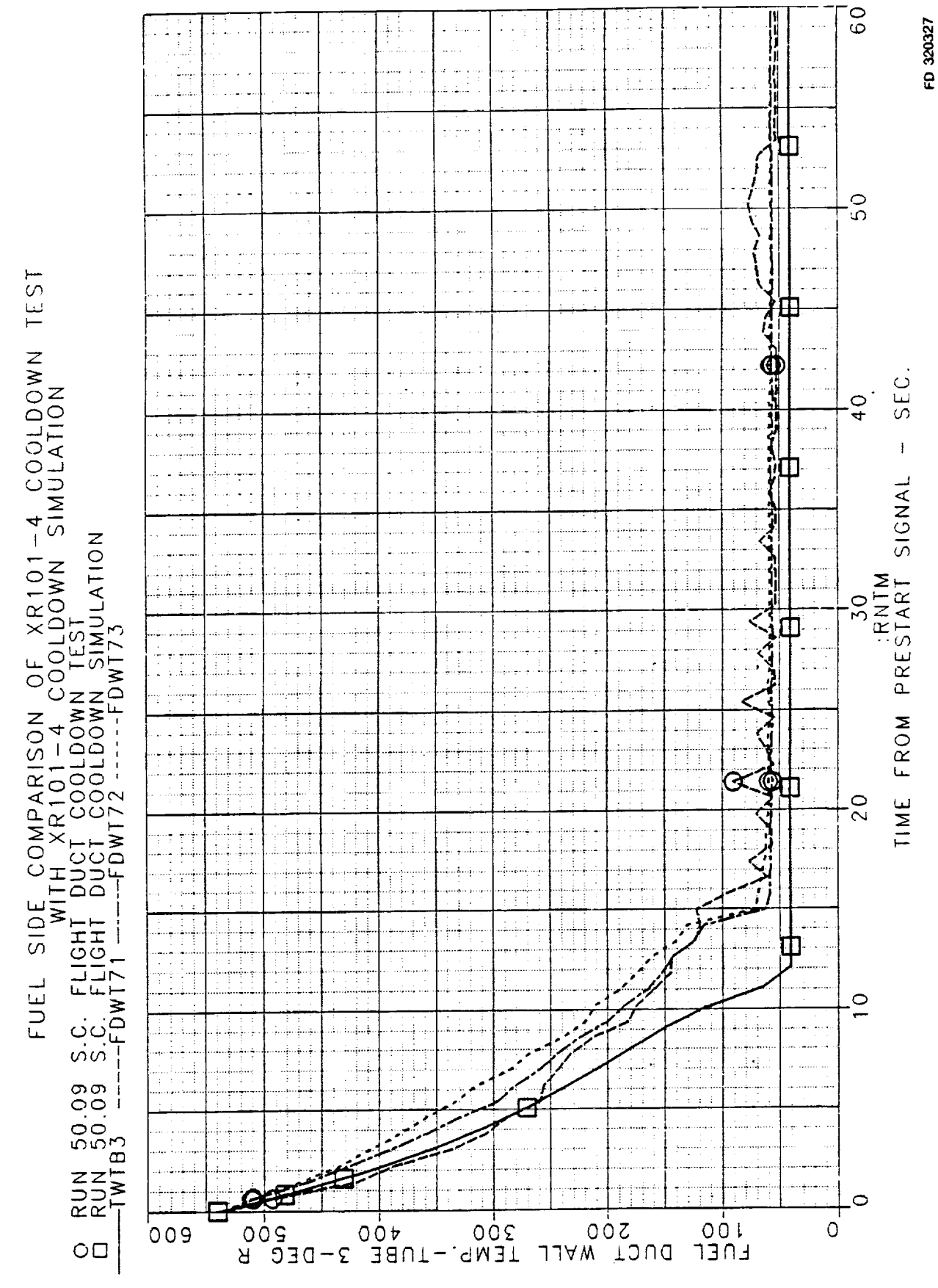

Figure 3-32. Fuel Duct Wall Temperature — Tube 3

0632C

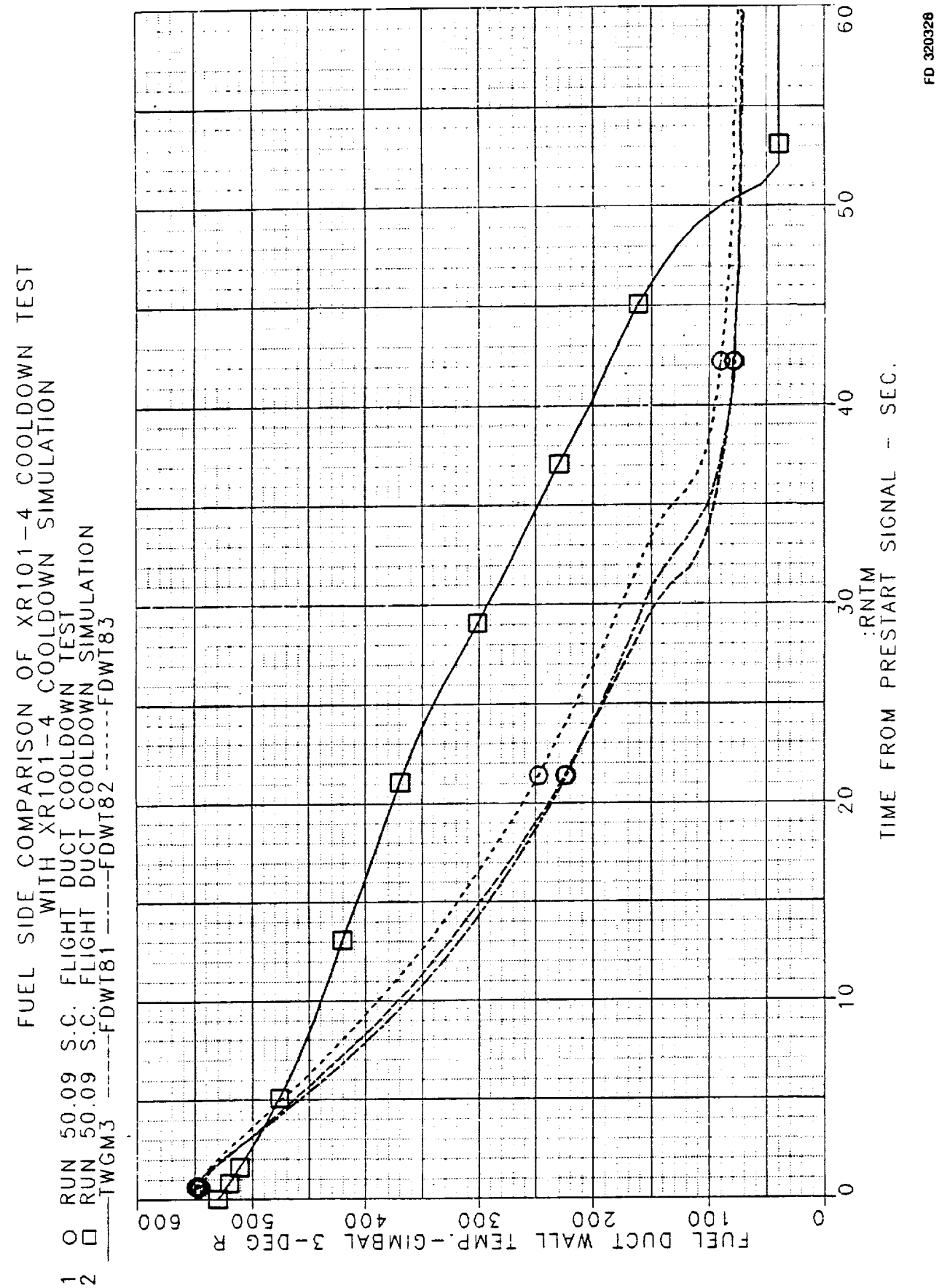

Figure 3-33. Fuel Duct Wall Temperature — Gimbal 3

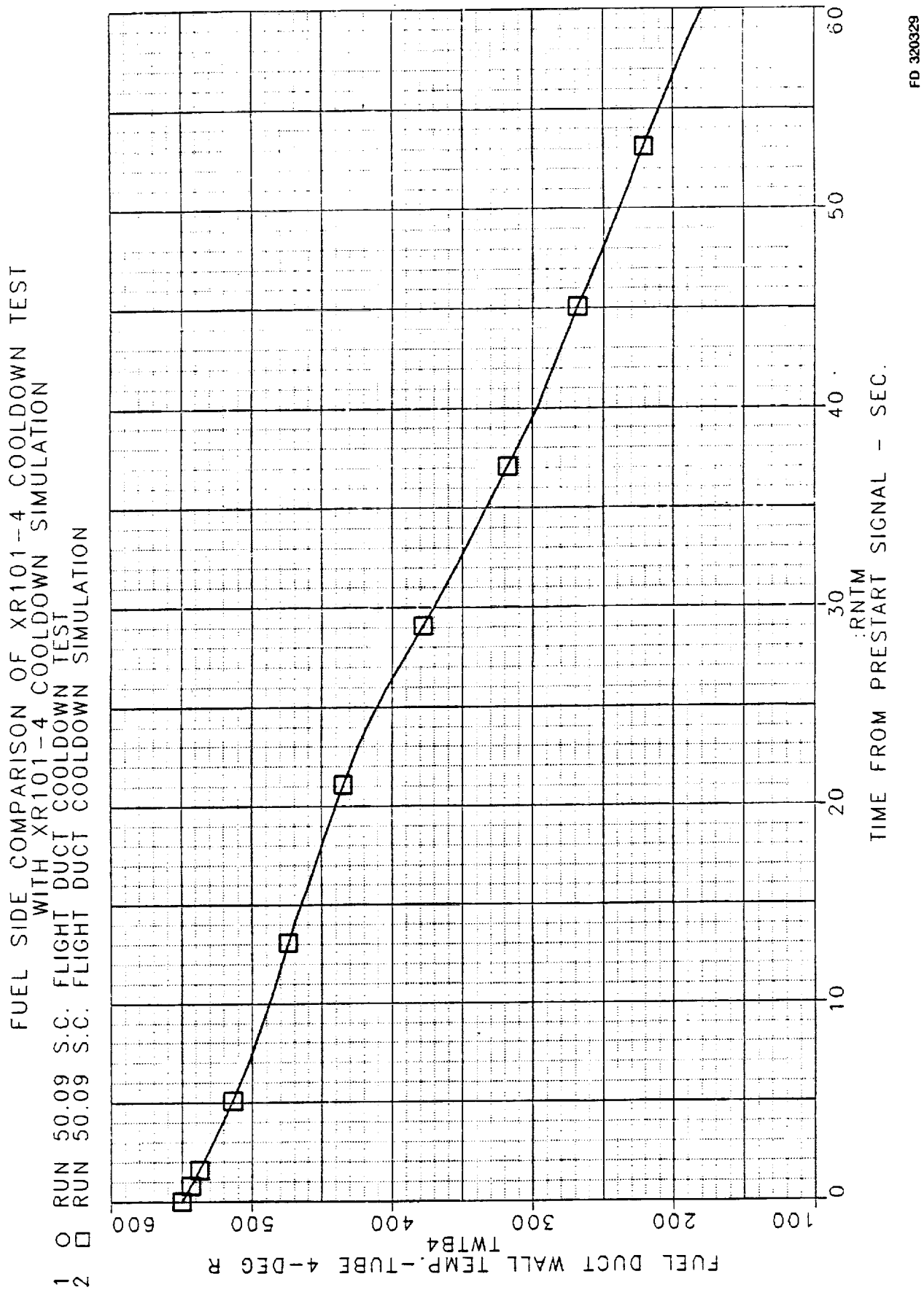

Figure 3-34. Fuel Duct Wall Temperature — Tube 4

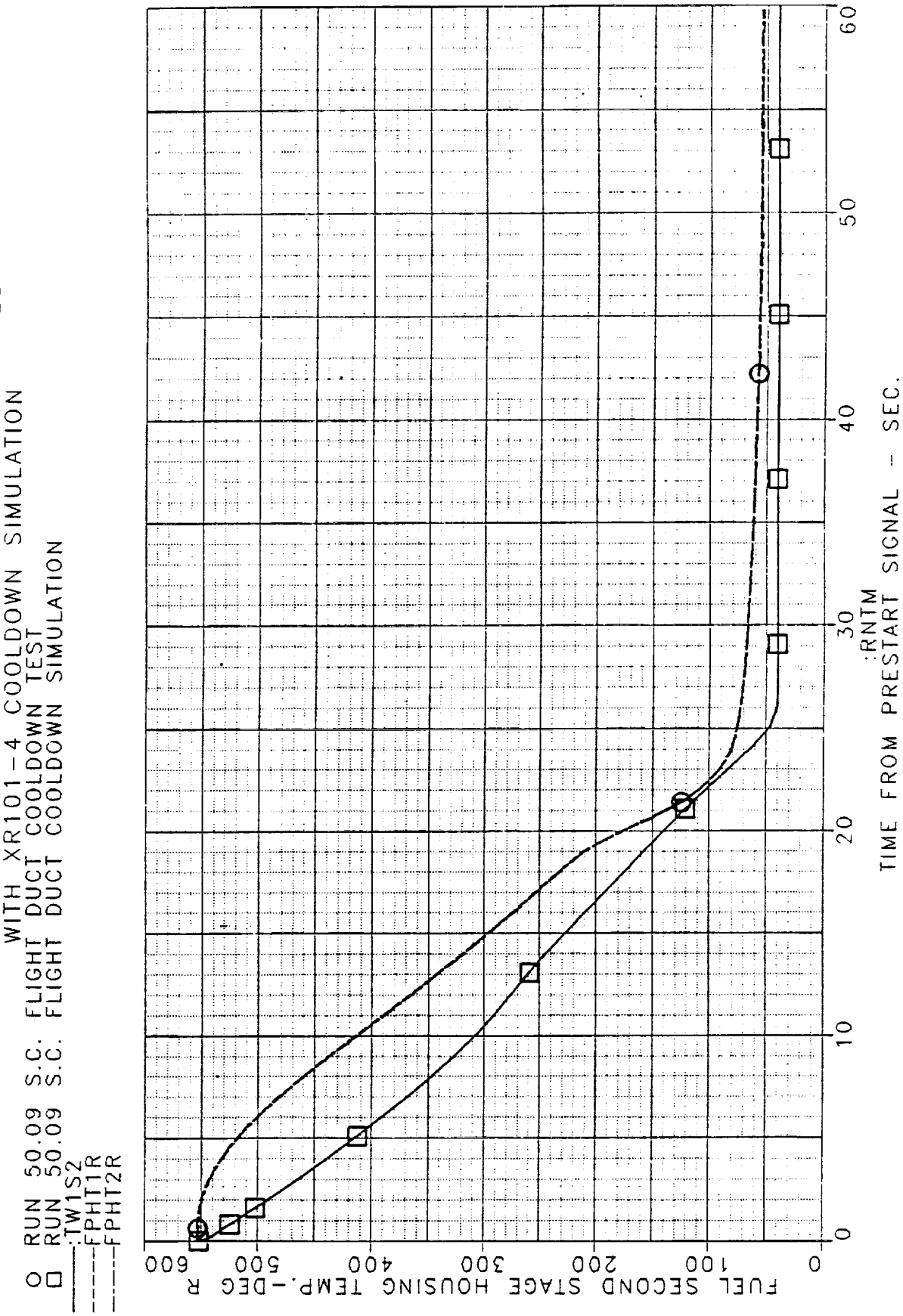

Figure 3-35. Fuel Second Stage Housing Temperature

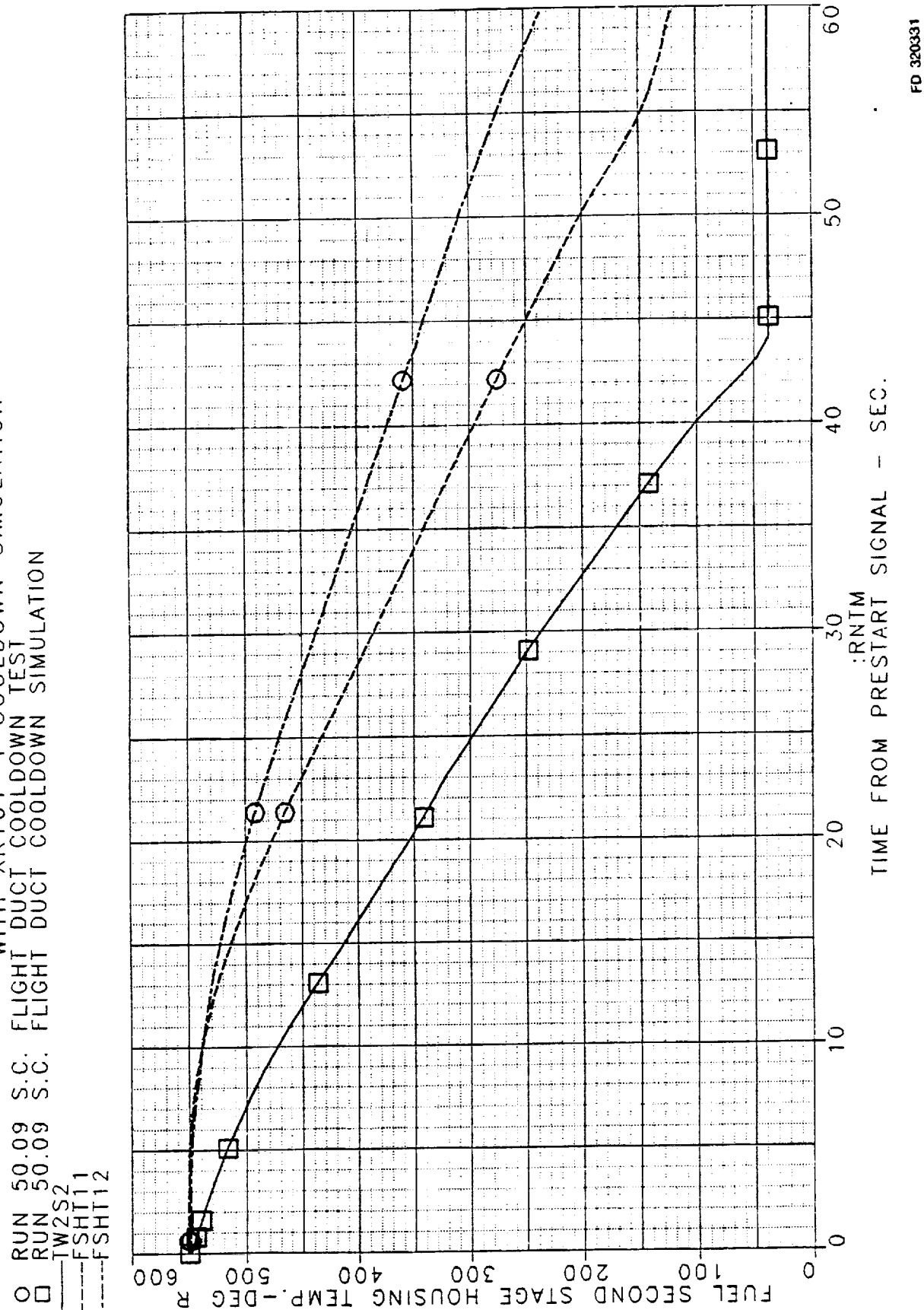

Figure 3-36. Fuel Second Stage Housing Temperature

0632C

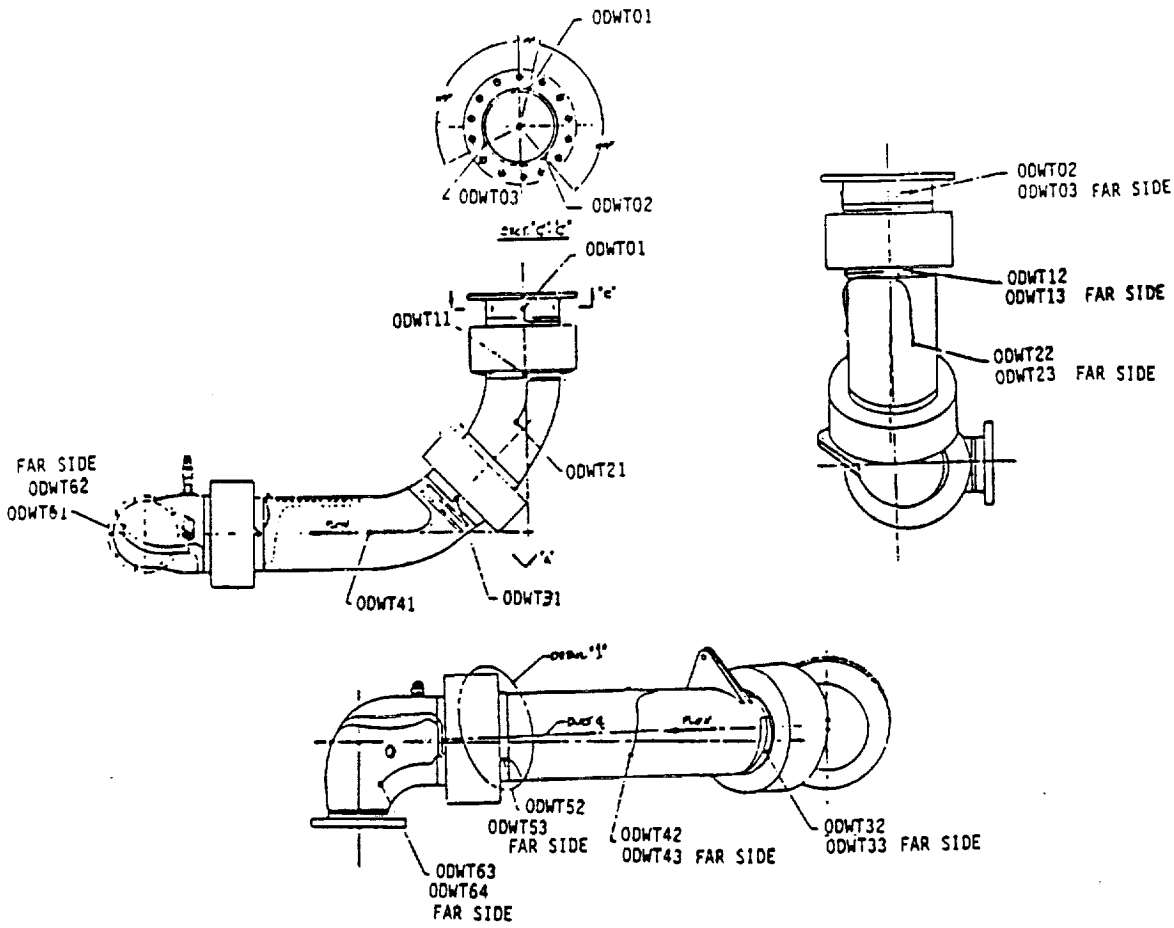

Figure 3-37. Oxidizer Duct Thermocouple Locations

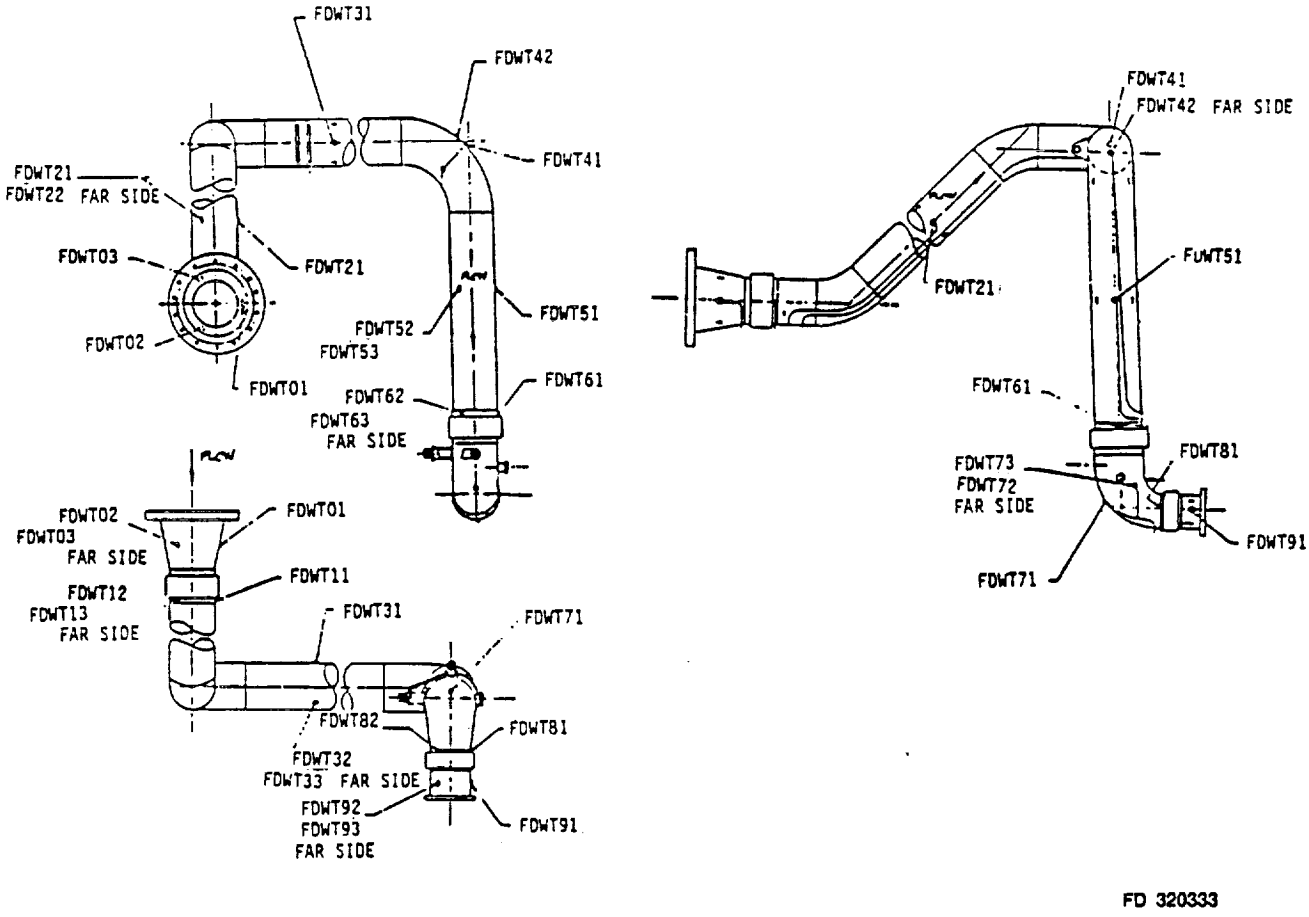

Figure 3-38. Fuel Duct Thermocouple Locations

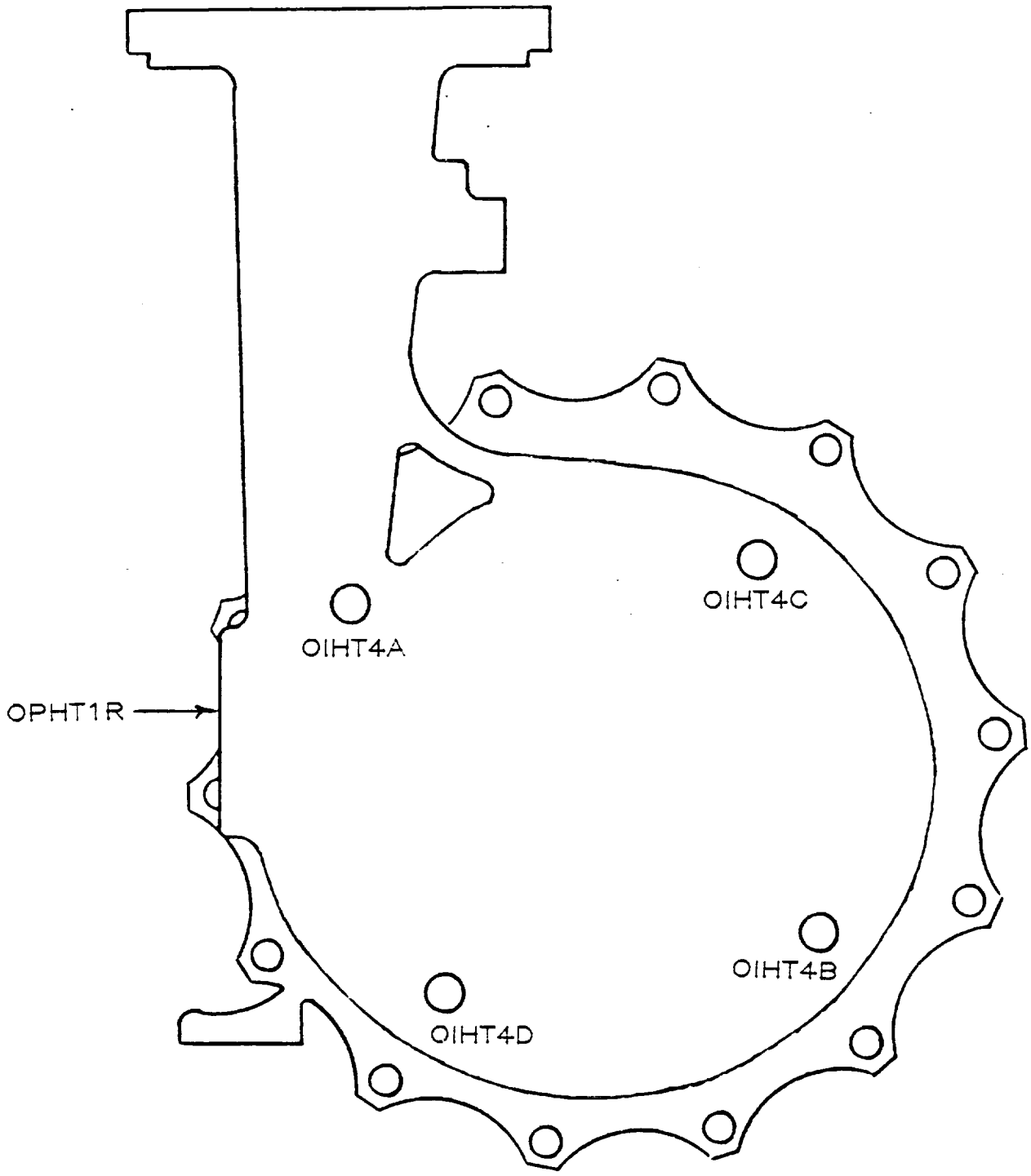

Figure 3-39. LOX Pump Thermocouple Locations

3.3 VERTICAL DUCT TESTS

To determine if the elevated oxidizer inlet temperature characteristic would be present in the Shuttle/Centaur on-orbit environment, a test rig was fabricated consisting of the flight weight inlet ducts installed in a vertical position with an oxidizer pump/oxidizer flow control valve assembly installed on the exit of the duct. By testing the assembly in this position, the majority of the inlet duct was in a vertical orientation instead of the horizontal position present when the ducts are installed on the engine. By installing the ducts in this way, the amount of mixed phase oxidizer traveling back up the inlet duct and the gas trapped in the duct would be reduced. A closer simulation of the on-orbit environment could then be made, determining whether the prevalve inlet temperature profile would exist in flight.

Tests made with the oxidizer rig showed a reduced amount of inlet recirculation due to the complete wetting of the inlet ducts, which resulted in a slightly increased cooling rate for both the oxidizer inlet lines and the oxidizer pump. This implies that the cooldown times determined from the test stand are conservative due to the elevated inlet temperature characteristic and gas trapped in the duct. The propellant recirculation present when cooling the horizontal duct sections will not be present in the zero-G environment due to the lack of a gravity induced pressure gradient.

Comparisons of component cooldown rates and inlet NPSP for tests of engine (horizontal duct) cooldown and LOX pump rig (vertical duct) cooldown are shown in Figures 3-40 through 3-55.

3.4 COOLDOWN CRITERIA

On the oxidizer side, three conditions must be met before the engine is ready to be fired:

1. Engine inlet NPSP must be 3.9 psia or higher.
2. The oxidizer flow control valve must be fully cooled to fluid temperature.
3. The 'C' location on the oxidizer pump inducer housing as shown in Figure 3-39 must be cooled below 290°R.

On the fuel side, two conditions must be met:

1. Engine NPSP must be 1.5 psia or higher.
2. The fuel pump second stage housing temperature (FSHT11) must be cooled below 300°R.

3.5 RECOMMENDED FLIGHT COOLDOWN TEMPERATURE MEASUREMENTS

Oxidizer and fuel pump temperature and oxidizer and fuel inlet NPSP characteristics are shown in Figures 3-56 and 3-57.

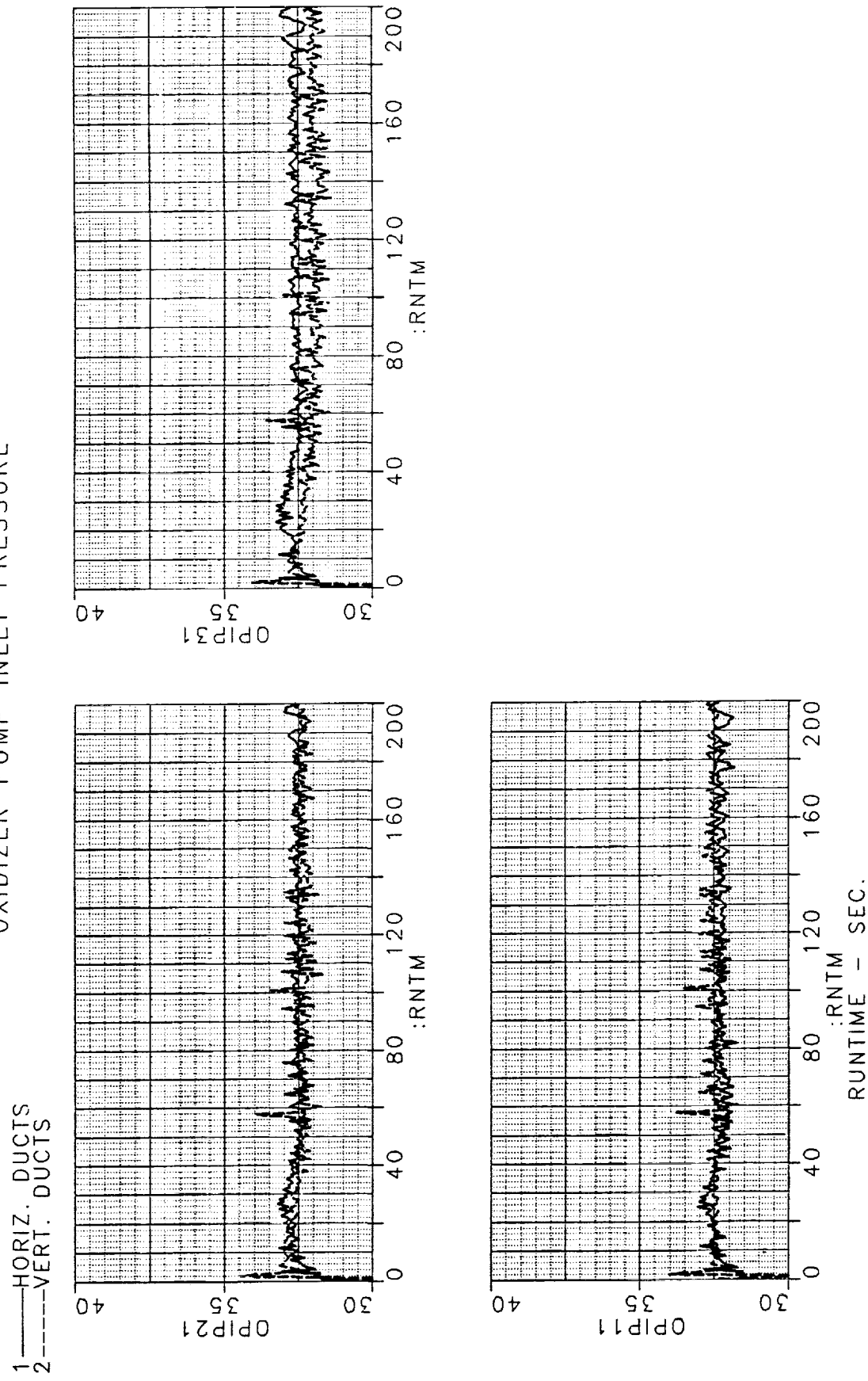

Figure 3-40. Oxidizer Pump Inlet Pressure

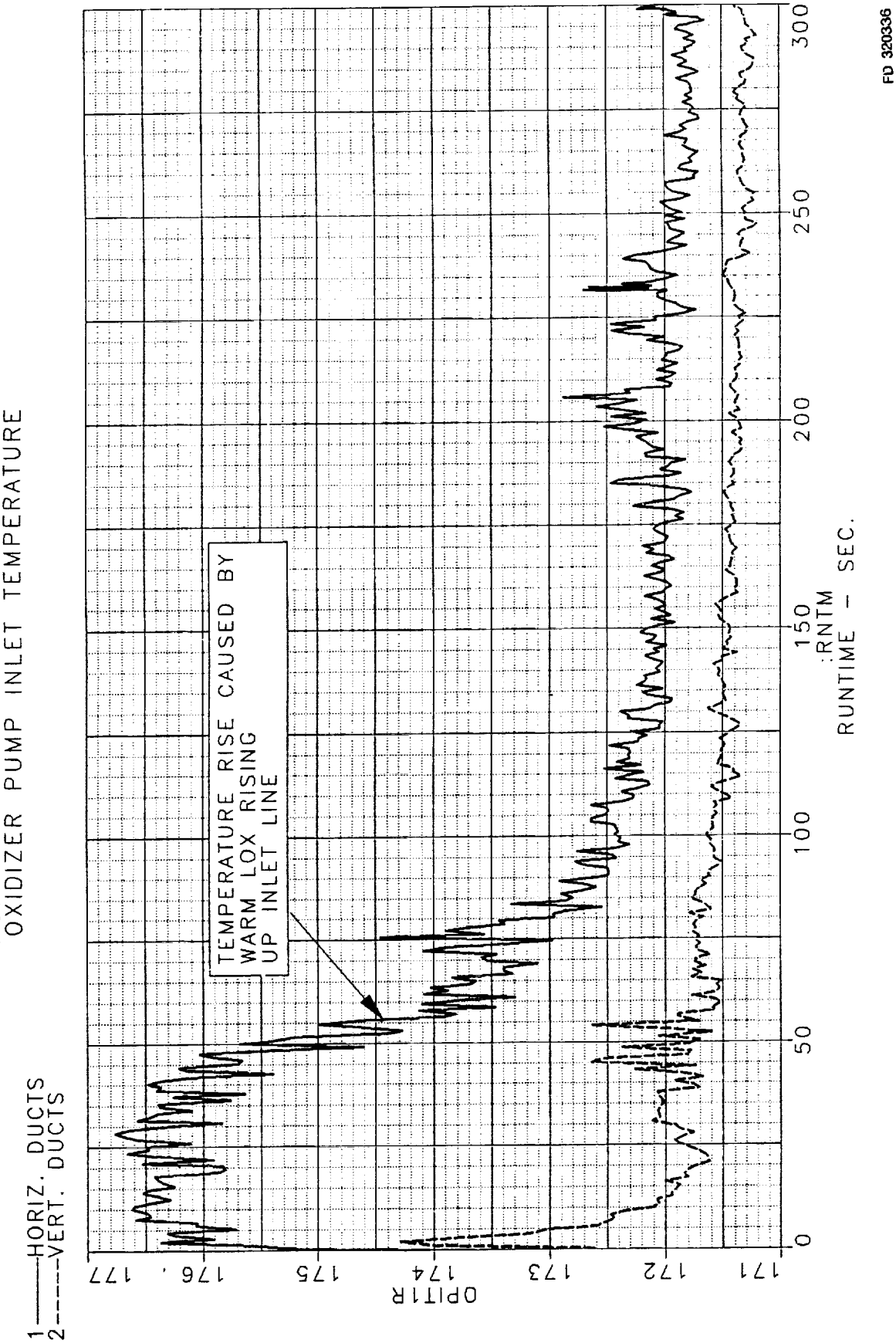

Figure 3-41. Oxidizer Pump Inlet Temperature

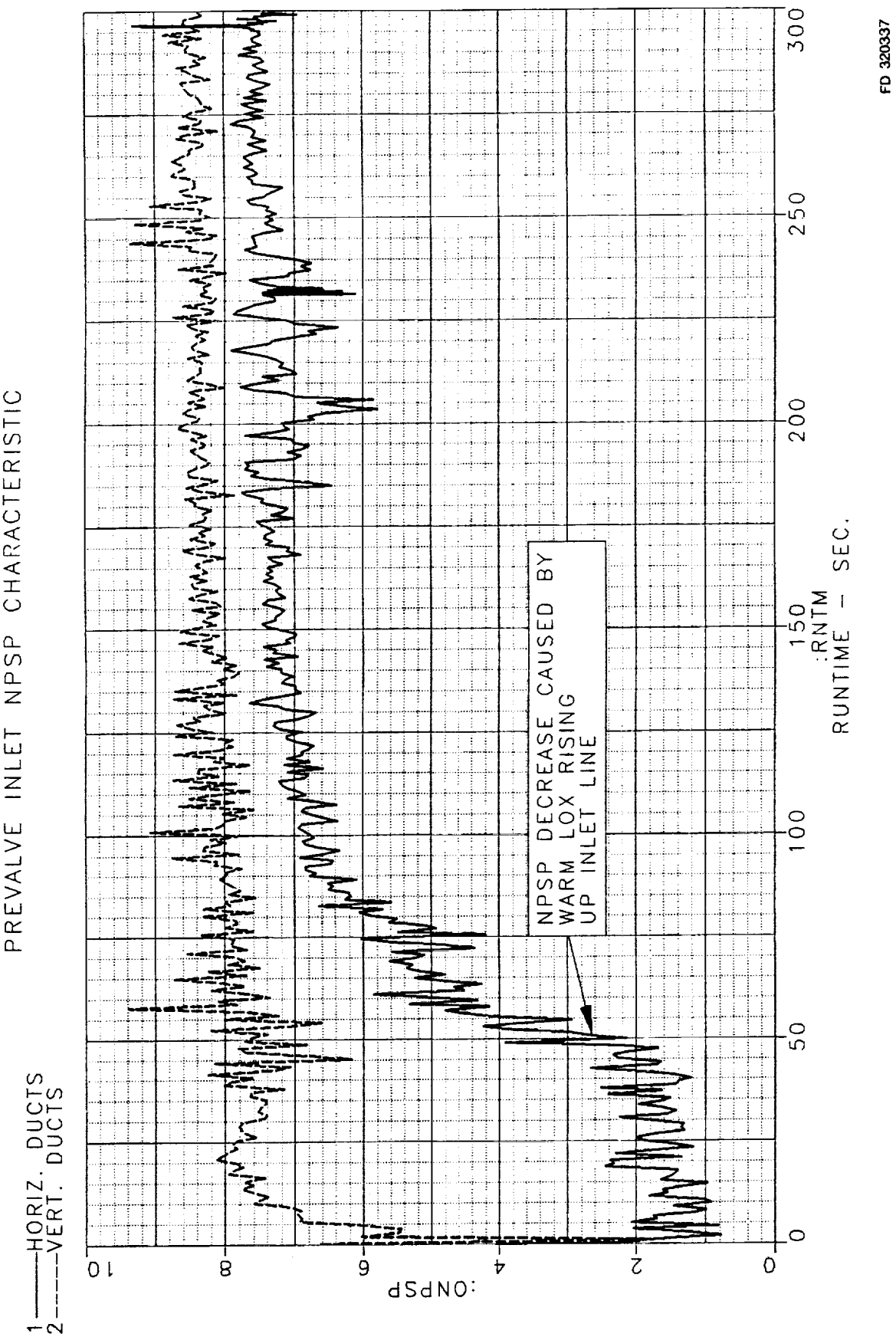

Figure 3-42. Prevalve Inlet NPSP Characteristic

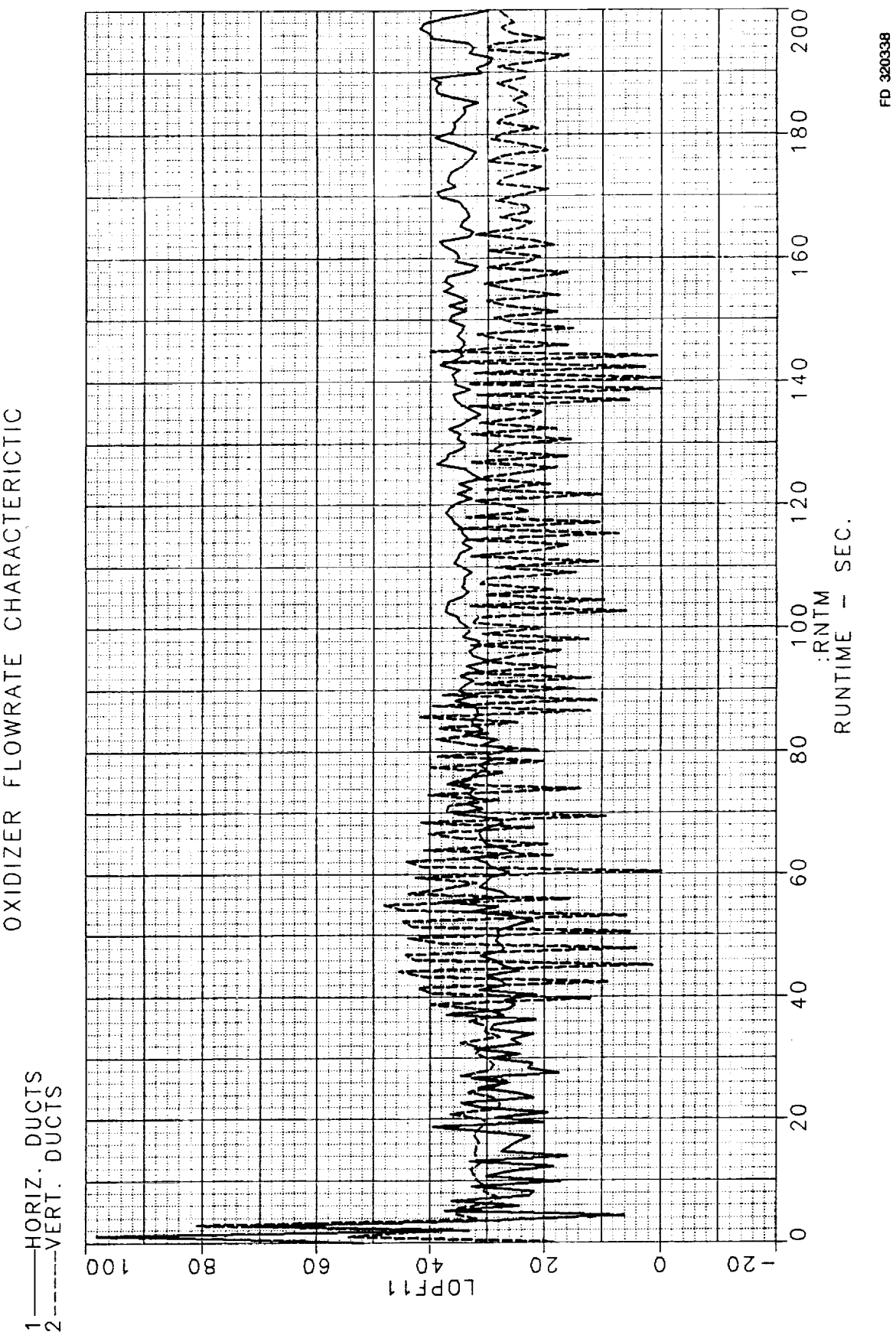

Figure 3-43. Oxidizer Flow Rate Characteristic

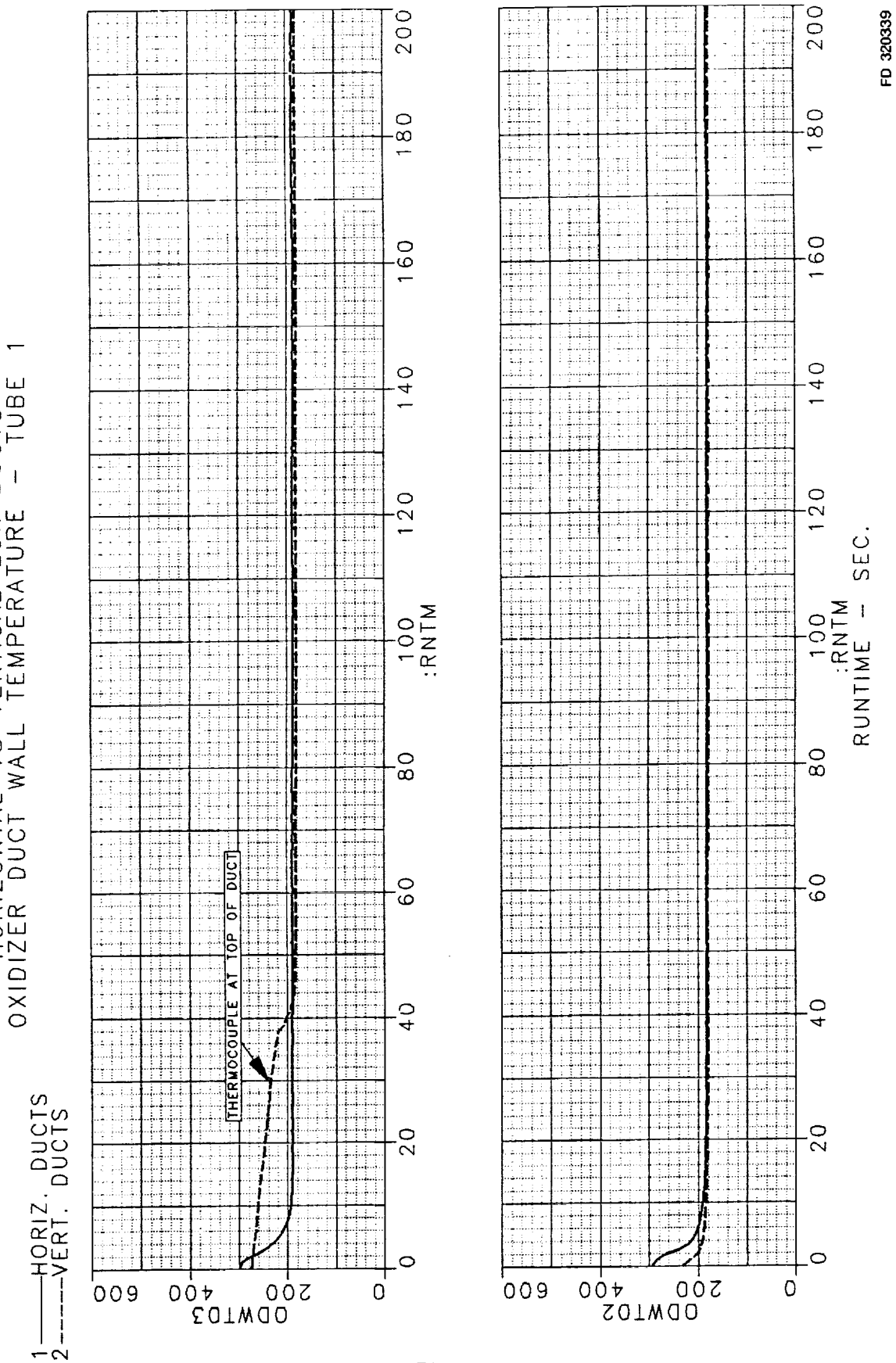

Figure 3-44. Oxidizer Duct Wall Temperature — Tube 1

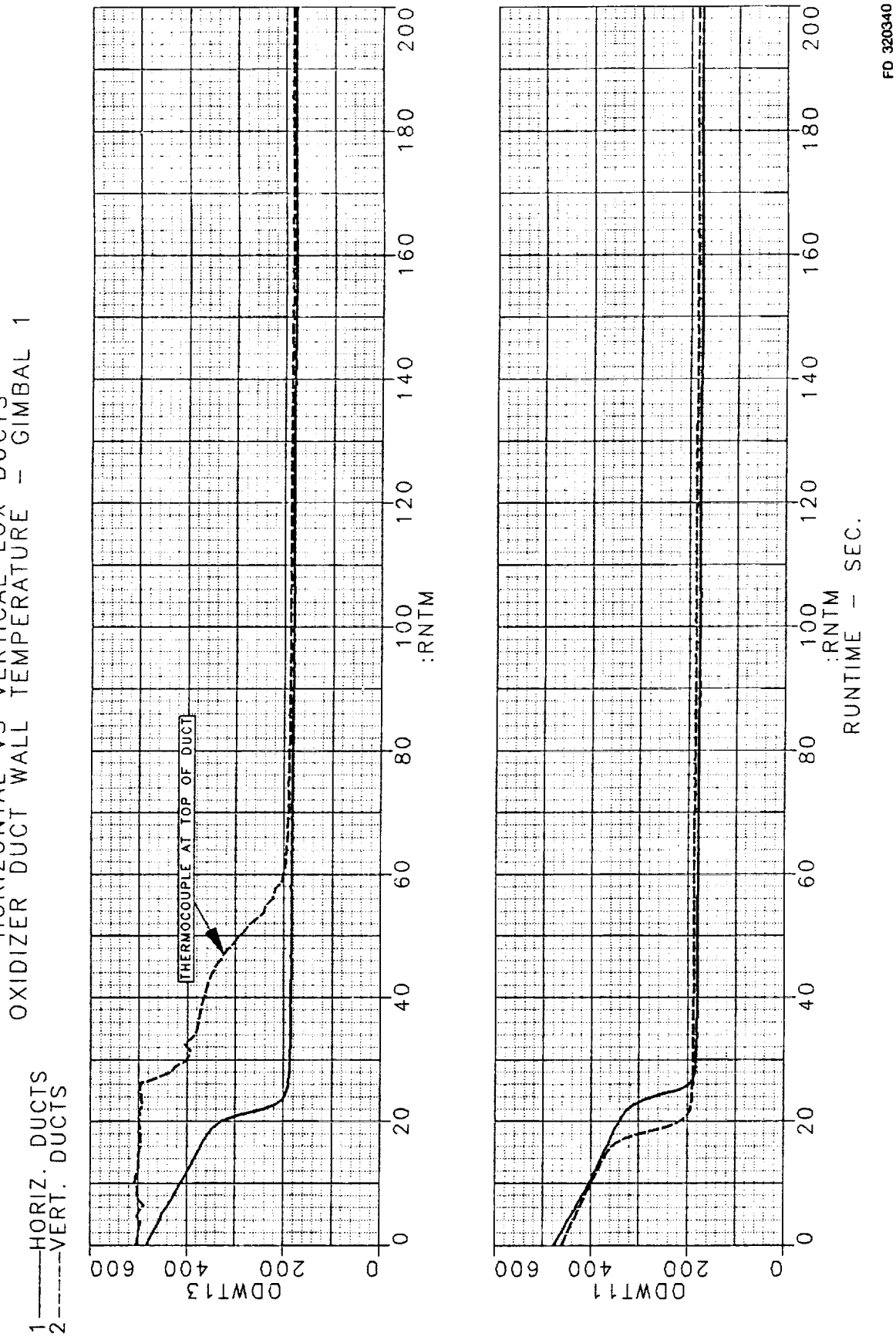

Figure 3-45. Oxidizer Duct Wall Temperature — Gimbal 1

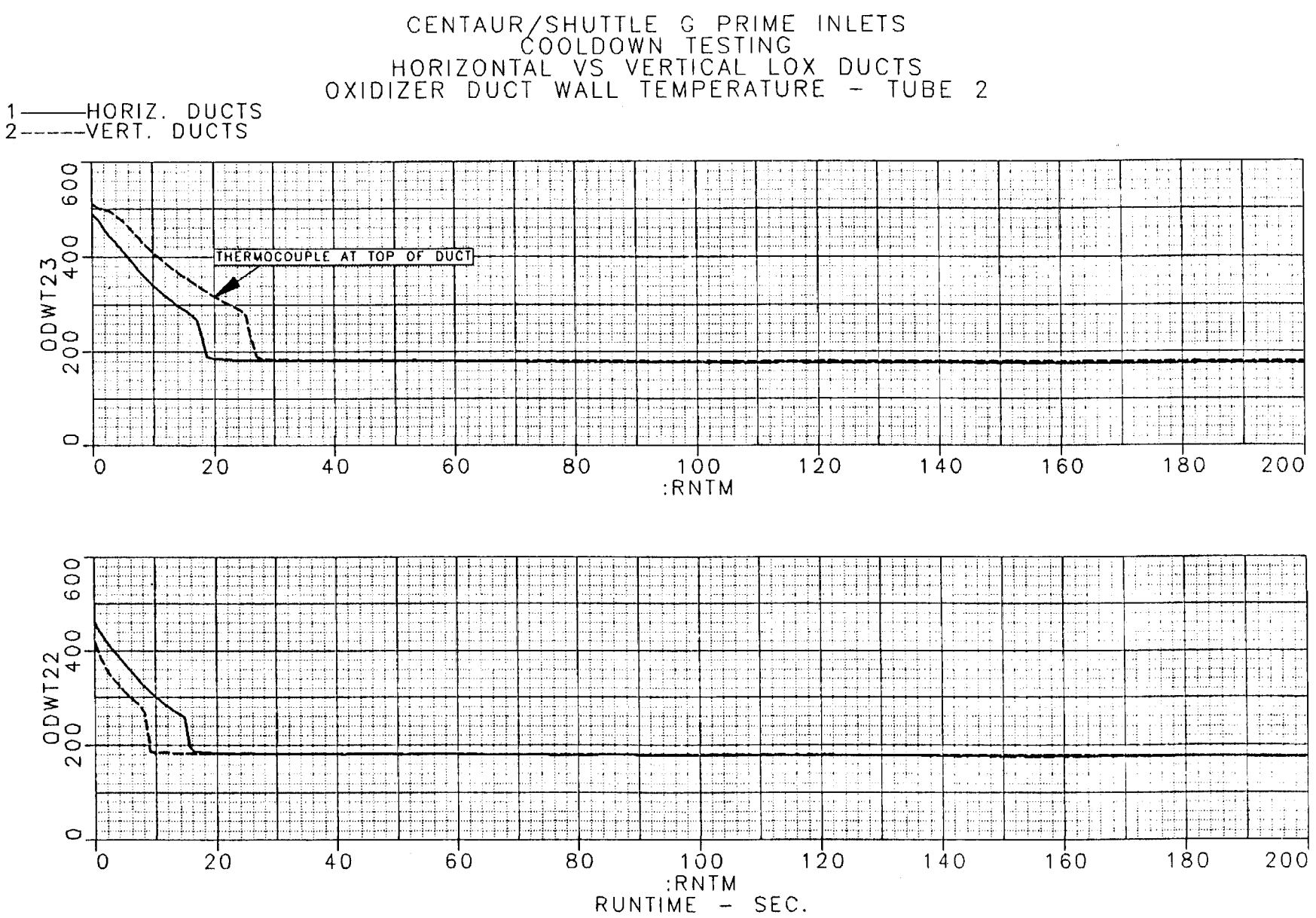

Figure 3-46. Oxidizer Duct Wall Temperature — Tube 2

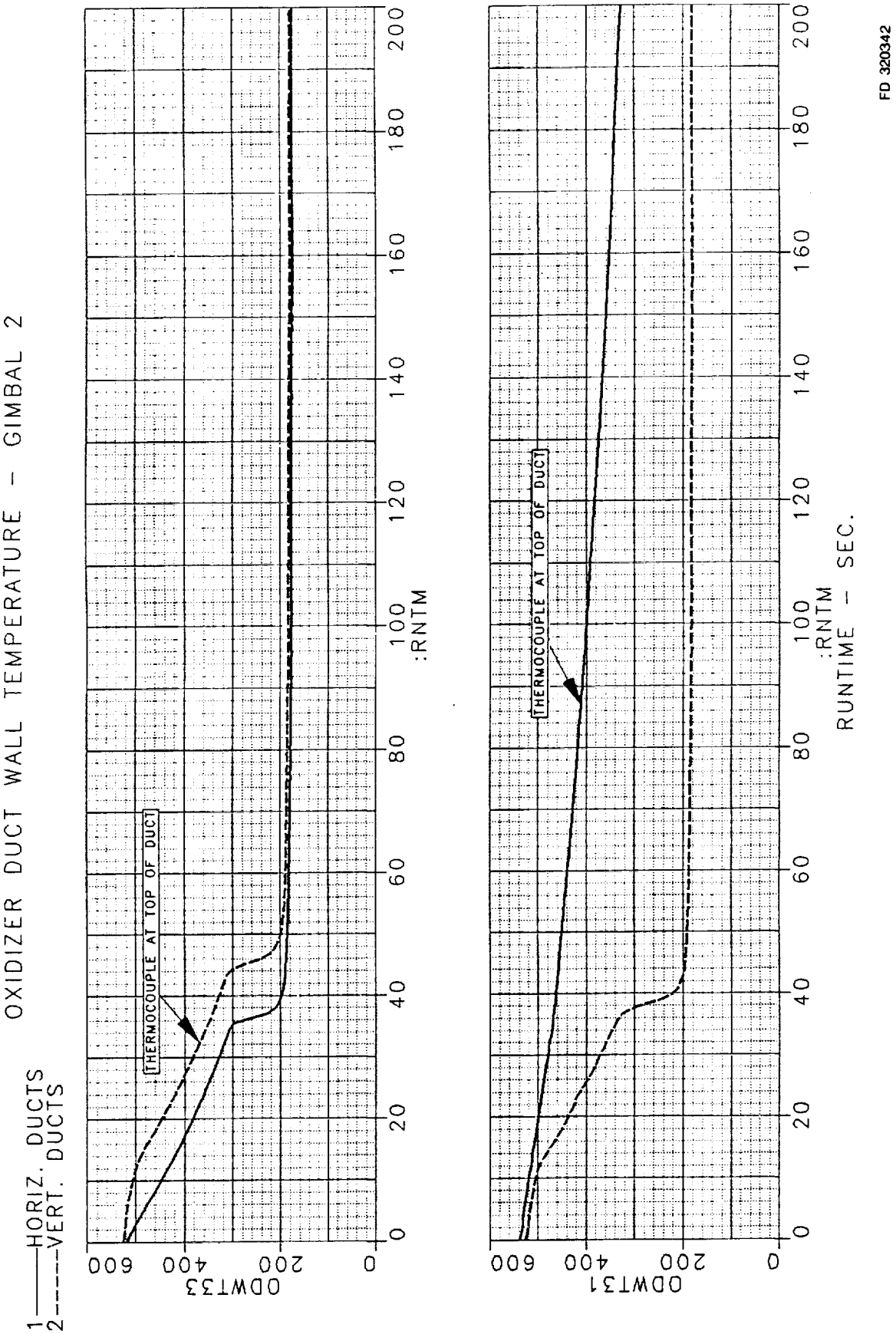

Figure 3-47. Oxidizer Duct Wall Temperature — Gimbal 2

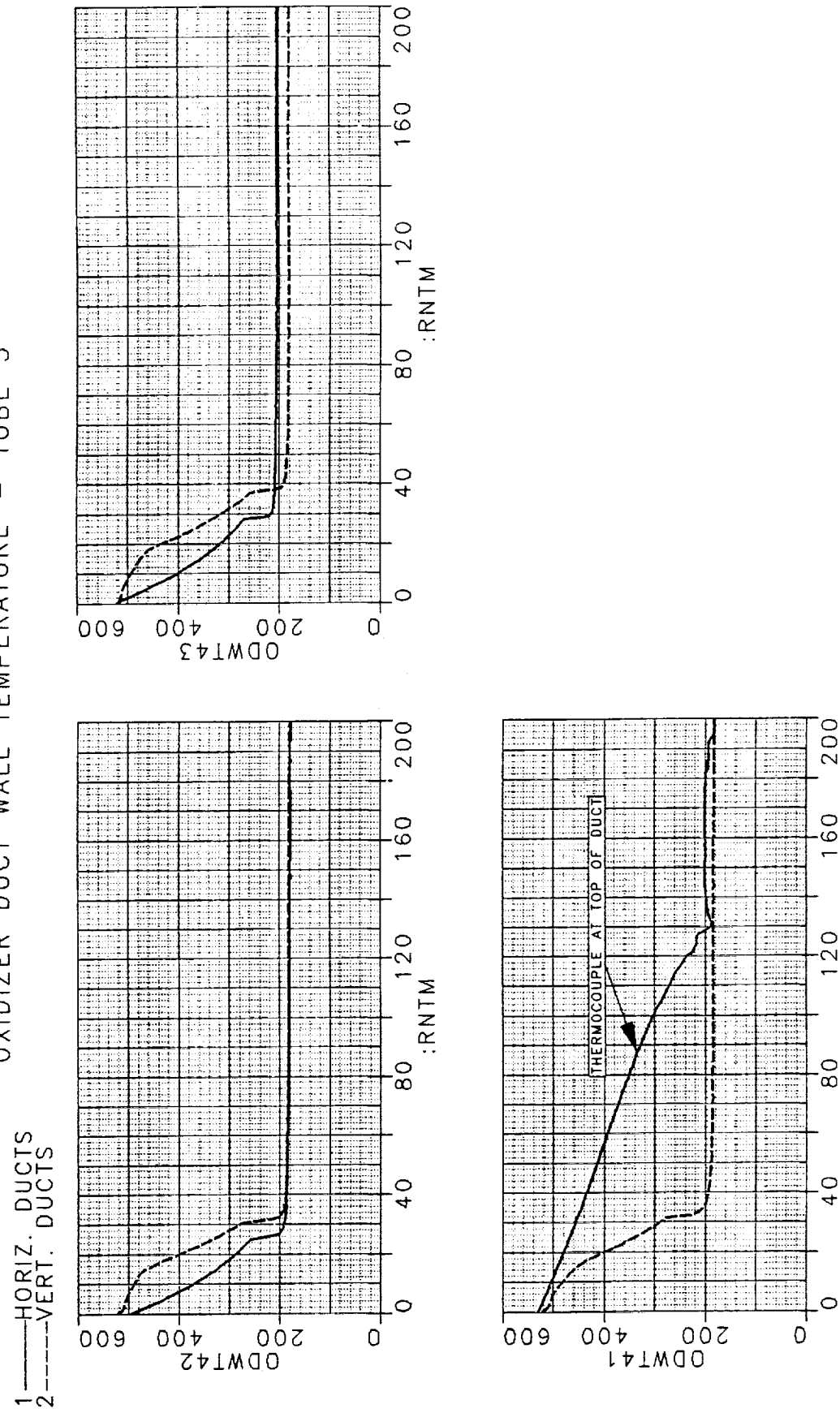

FD 320343

Figure 3-48. Oxidizer Duct Wall Temperature — Tube 3

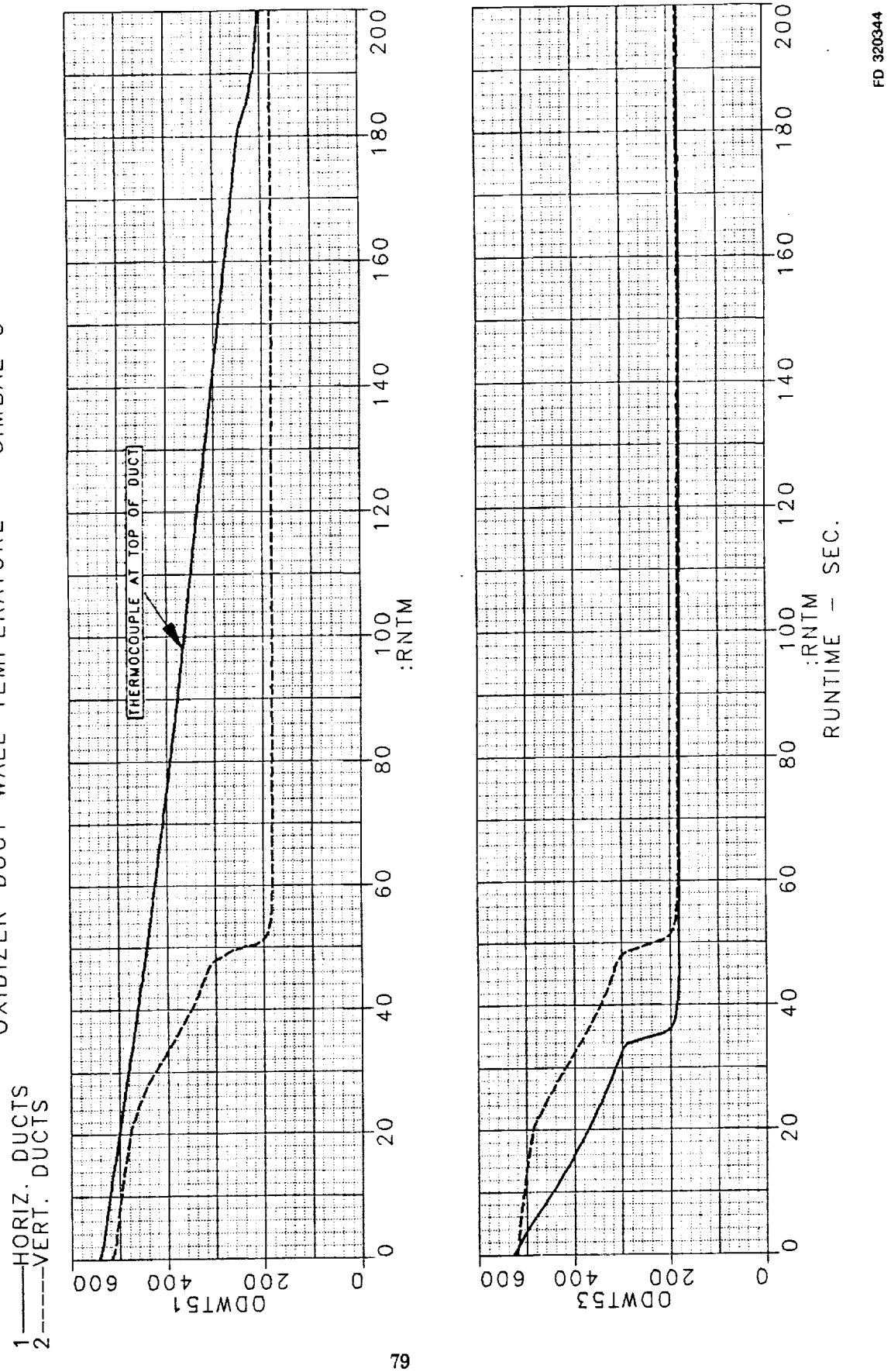

Figure 3-49. Oxidizer Duct Wall Temperature — Gimbal 3

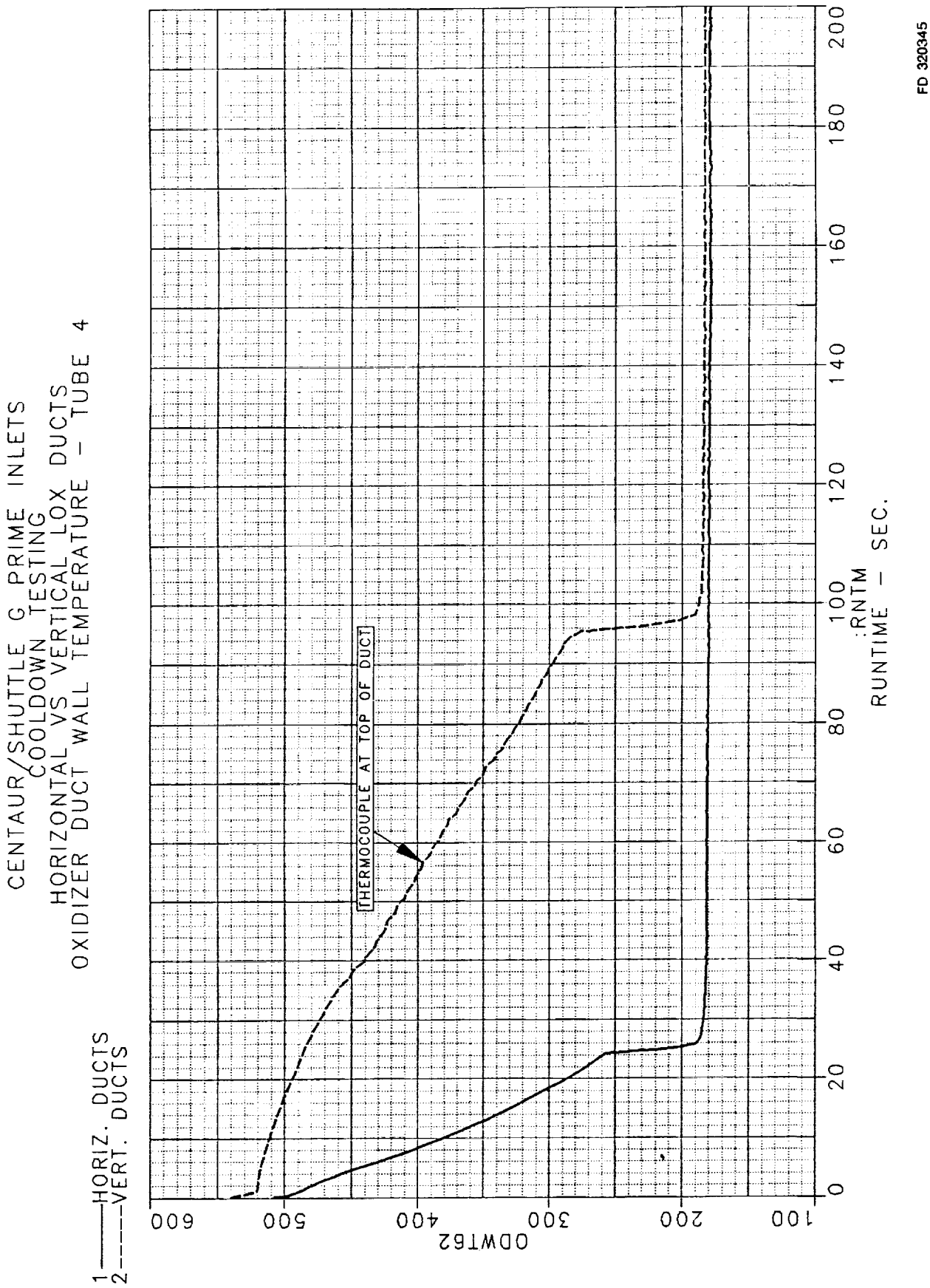

Figure 3-50. Oxidizer Duct Wall Temperature — Tube 4

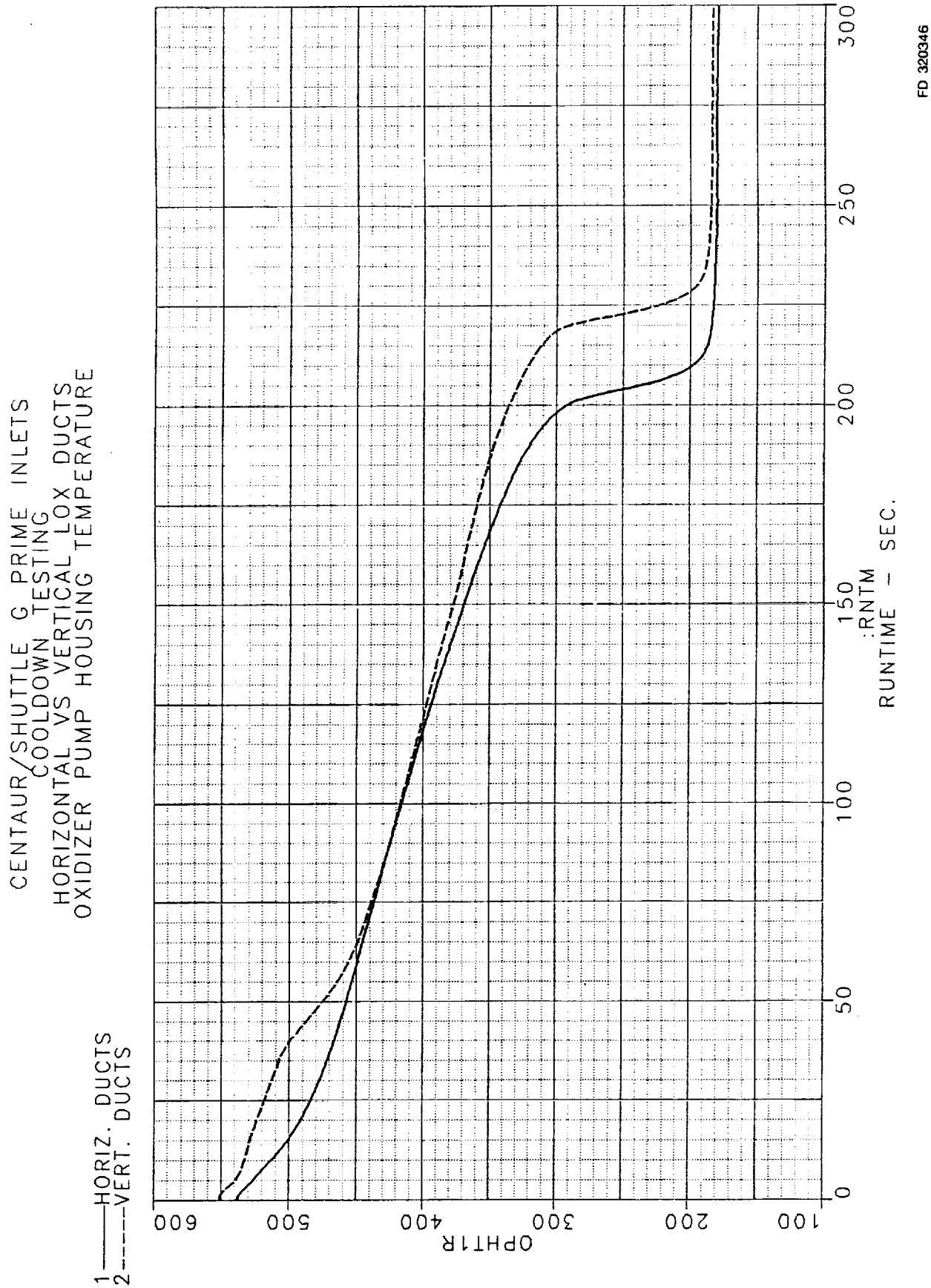

Figure 3-51. Oxidizer Pump Housing Temperature

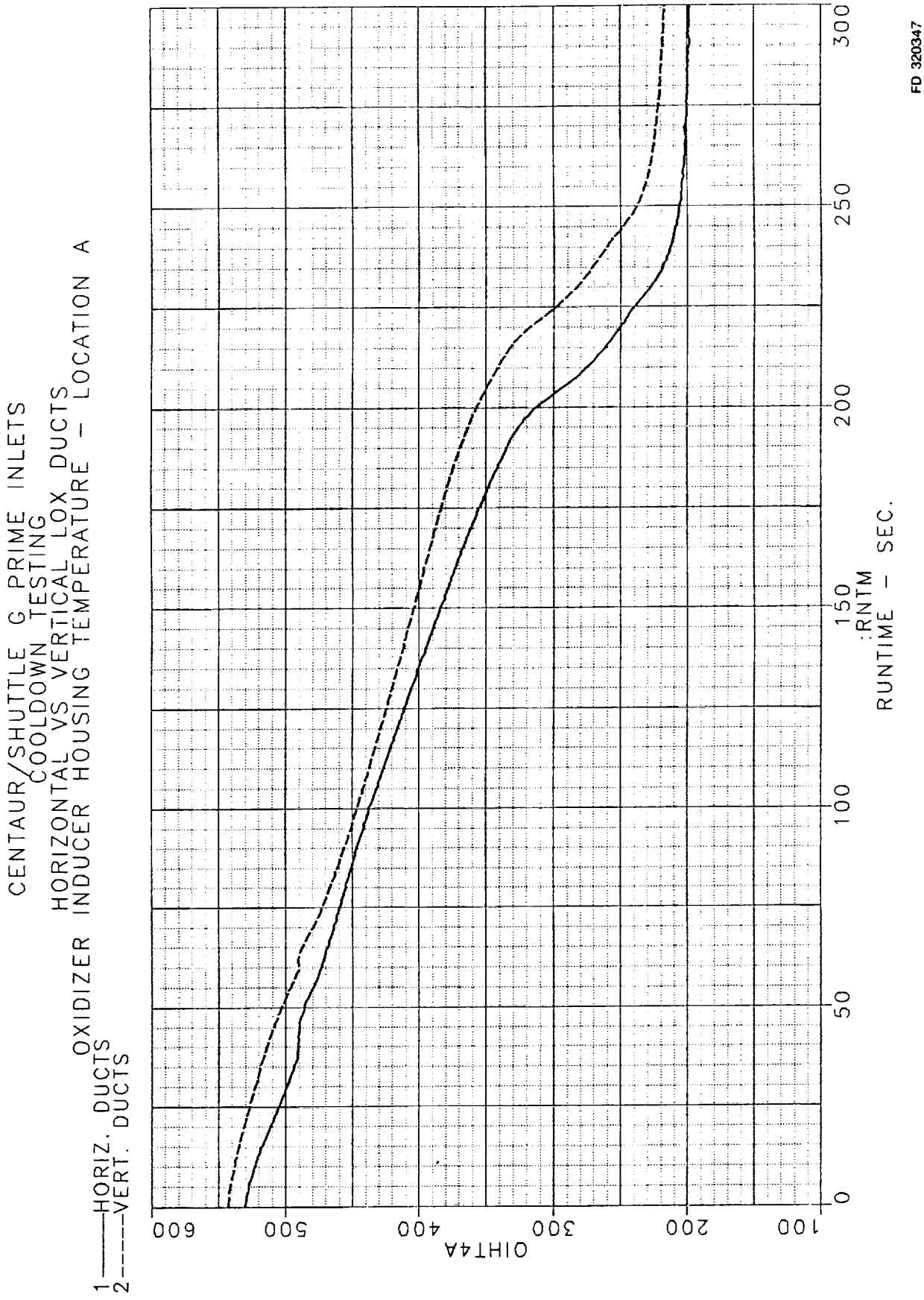

Figure 3-52. Oxidizer Inducer Temperature Housing — Location A

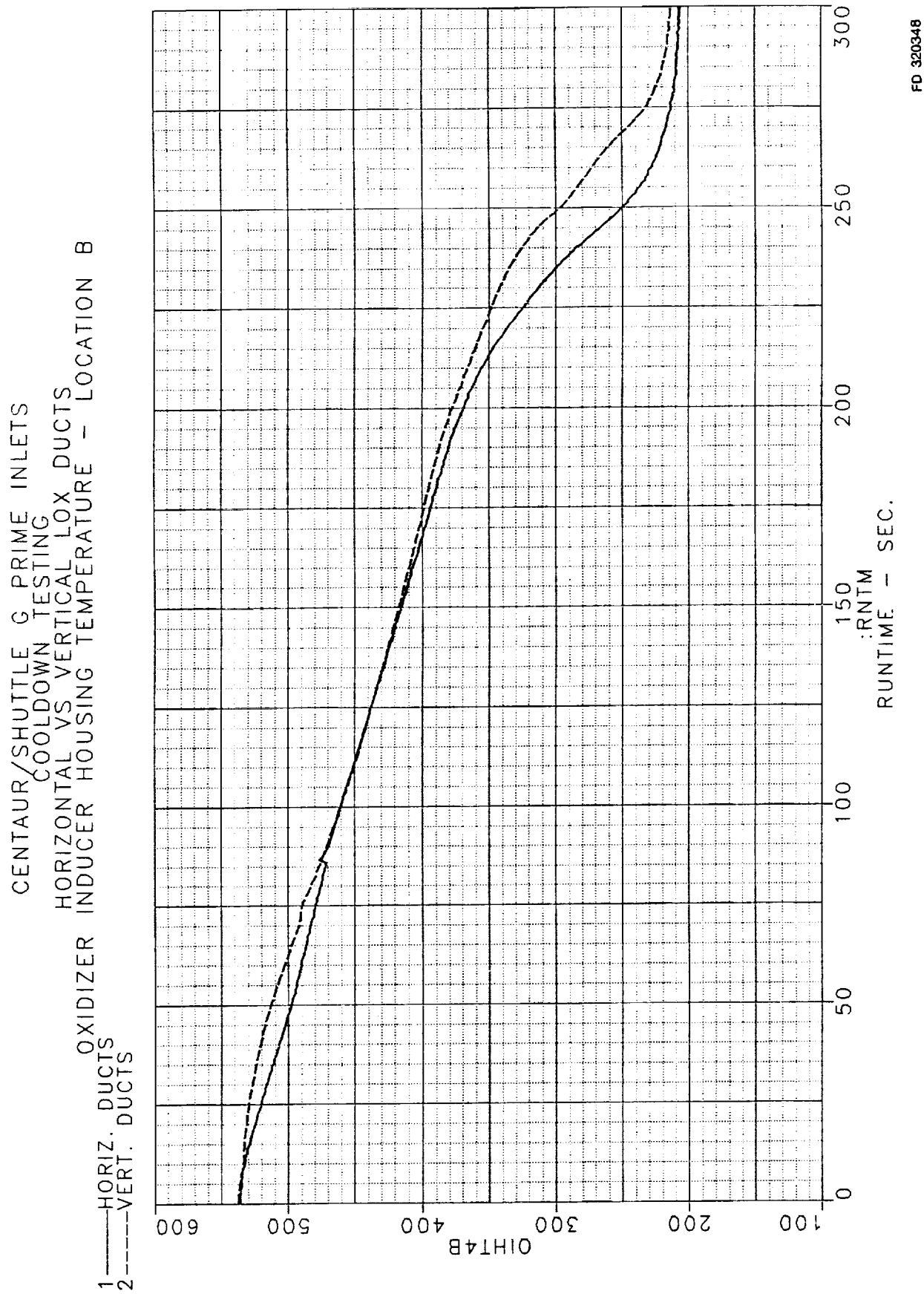

Figure 3-53. Oxidizer Inducer Temperature Housing — Location B

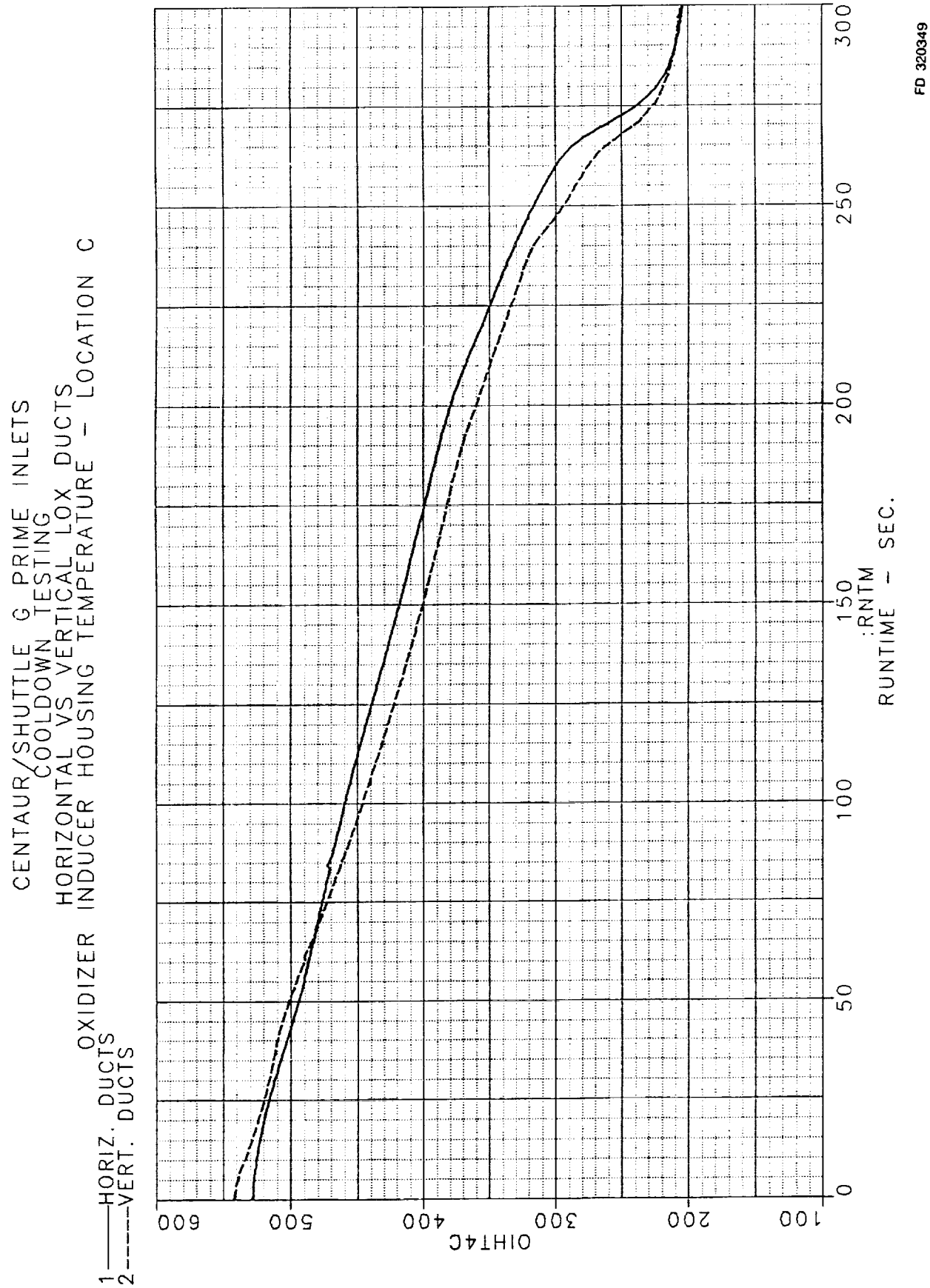

Figure 3-54. Oxidizer Inducer Temperature Housing — Location C

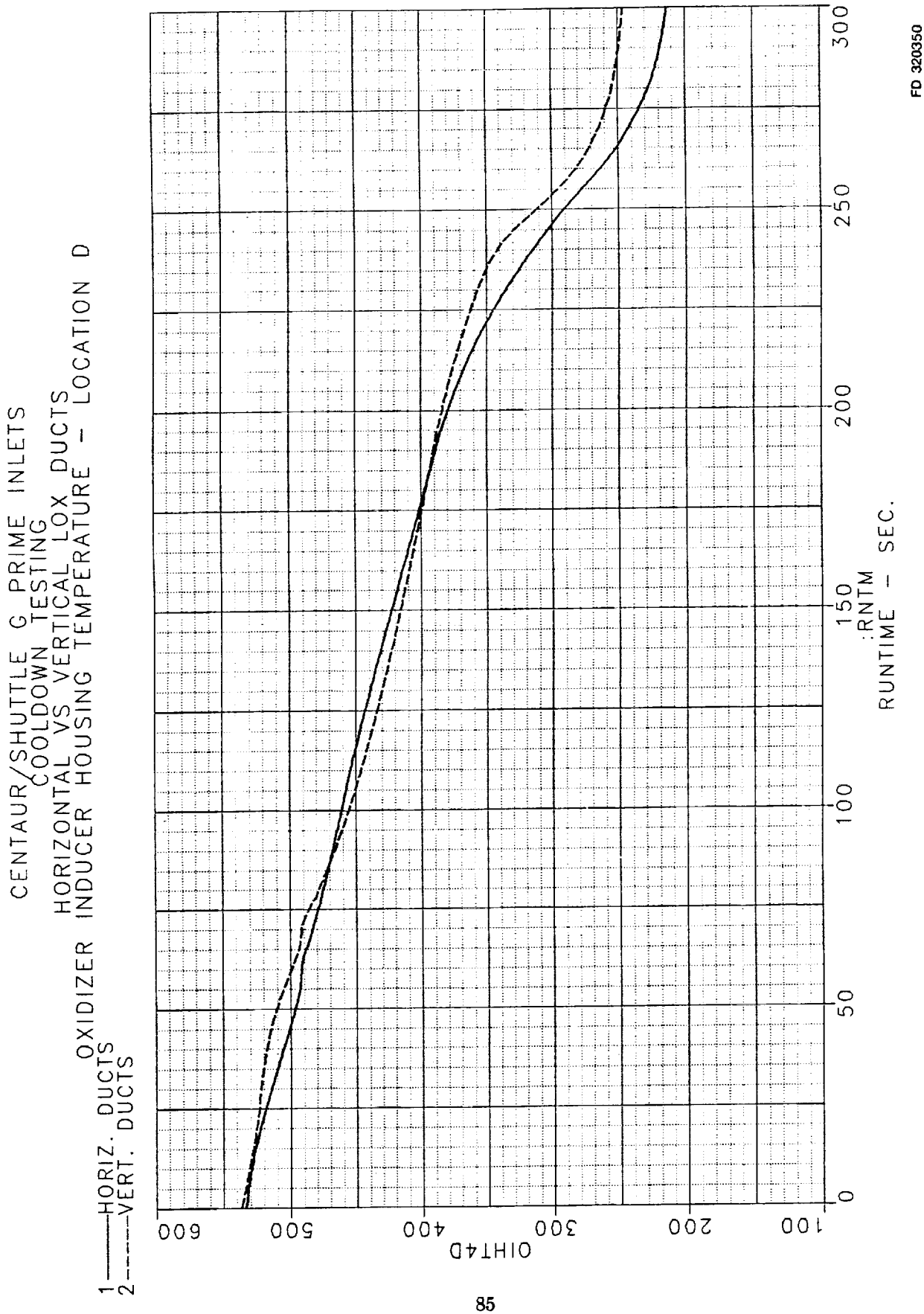

Figure 3-55. Oxidizer Inducer Temperature Housing — Location D

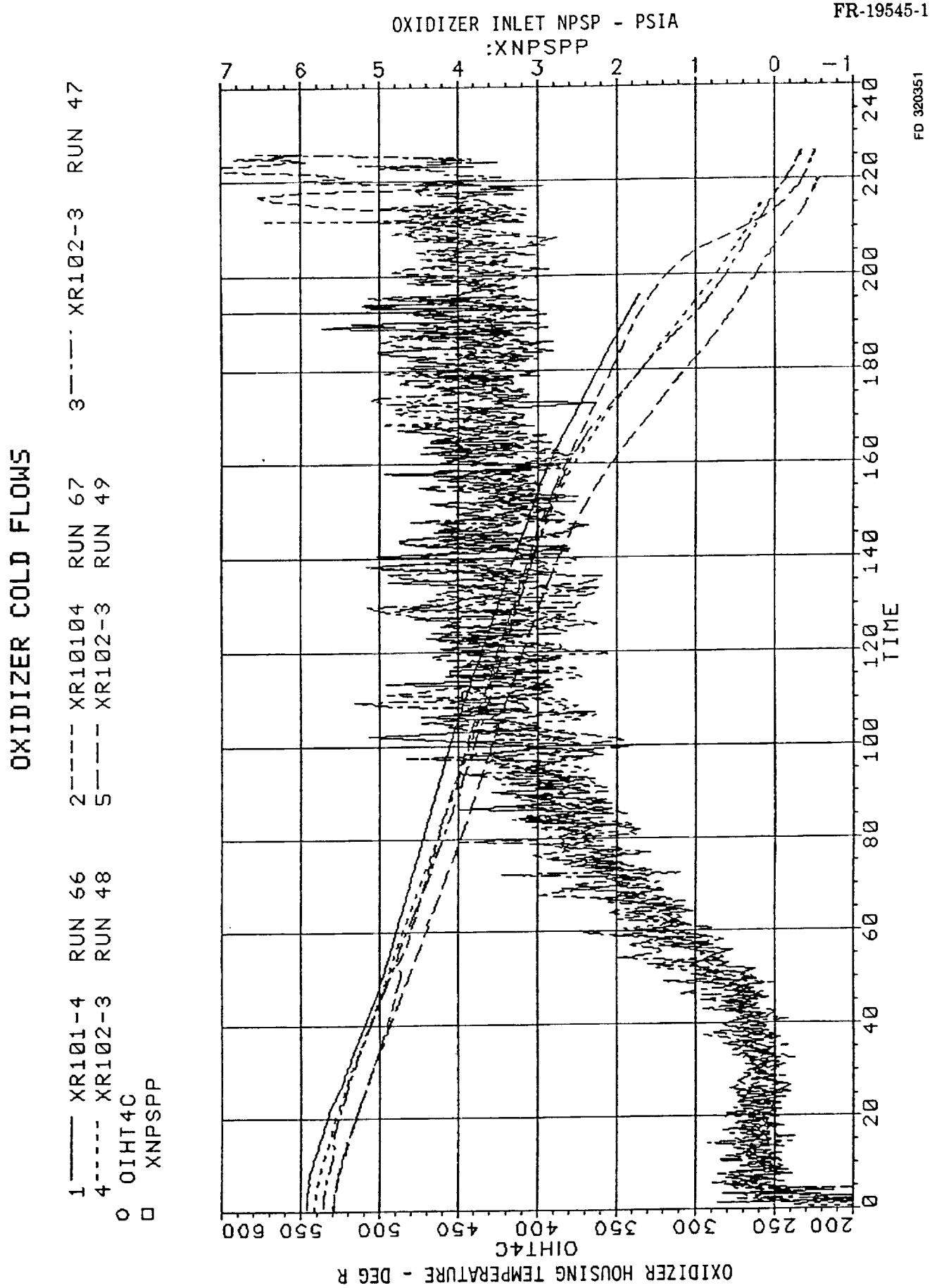

Figure 3-56. Oxidizer Housing Temperature

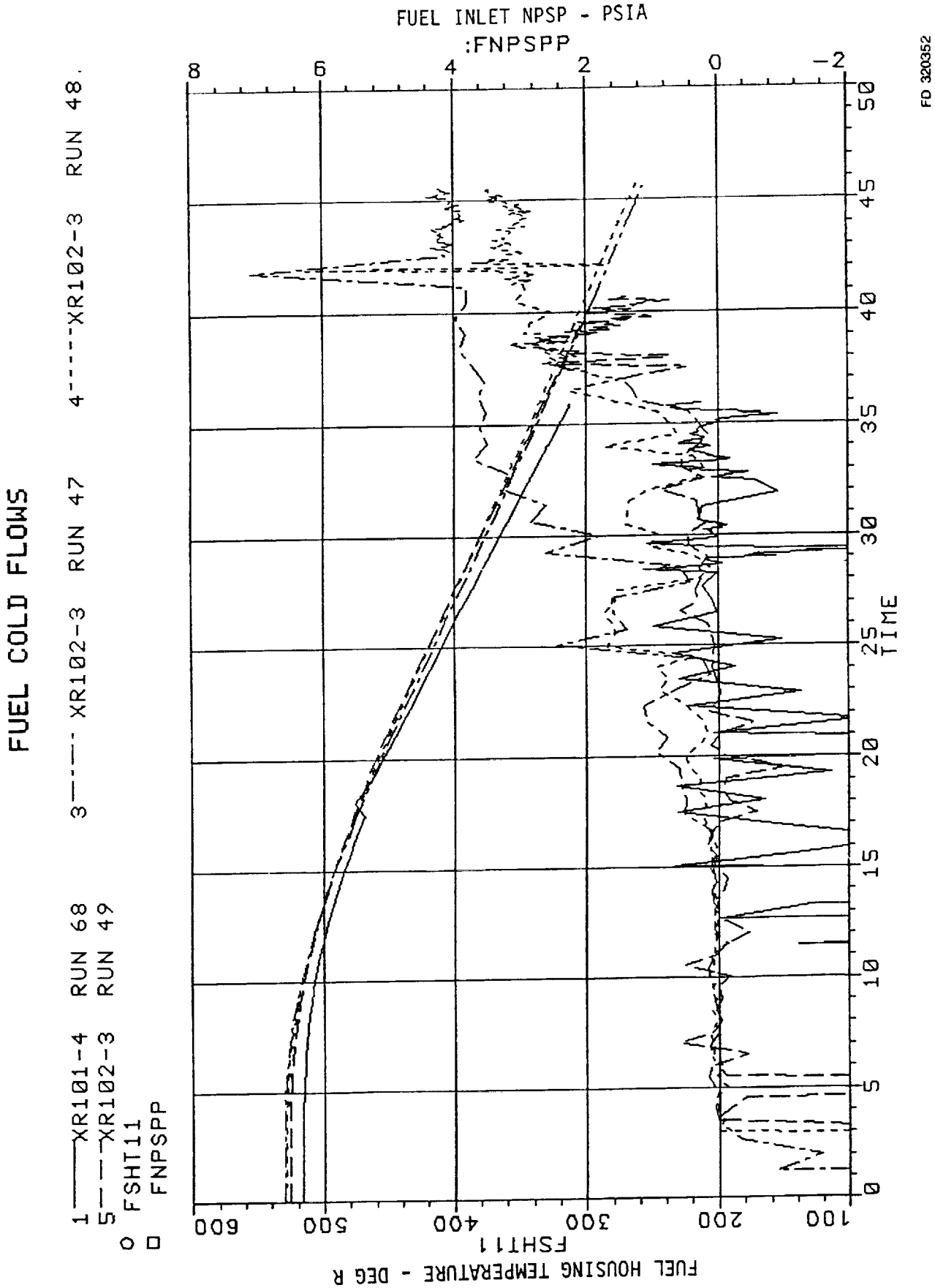

Figure 3-57. Fuel Pump Housing Temperature

C-2

0632C

To insure verification of proper engine component cooldown, it is recommended that temperature transducers be located at the 'C' thermocouple location on the oxidizer pump inducer housing flange, and at the FSHT11 thermocouple location on the fuel pump second stage housing. Figures 3-39 and 3-58 show the locations of the oxidizer and fuel pump temperature transducers.

When engine testing is done, the temperature transducers used are P&W thermocouples, whereas during flights, flight instrumentation temperature transducers will be used. Tests were run comparing the flight instrumentation temperature transducer and the P&W thermocouple used on the oxidizer pump housing. These transducers showed close agreement throughout the operating temperature range.

Comparison of the P&W thermocouple and flight transducer response is made in Figure 3-59.

3.6 WATERHAMMER TESTS

When the Shuttle/Centaur cooldown sequence is initiated, the engine prevalves and LOX inlet valve will be opened simultaneously, with the fuel inlet valve being opened from 200 to 300 seconds later. Because the environment inside the empty inlet ducts will be a near vacuum, it was considered that the propellants could enter the ducts rapidly and, upon reaching the engine inlet, cause an overpressure condition due to waterhammer effects. To determine if this would occur, tests were run with engine inlet valves opened and closed, and using prevalve opening rates from 12 to 0.5 seconds.

The worst case condition used was with engine inlet valves closed, and a prevalve opening time of less than 0.5 second. In this extreme condition, the pressure rise experienced on the LOX side was 3.5 psi, with a fuel side spike of 8.5 psi. These pressure increases were not large enough to be considered hazardous. The fuel and oxidizer worst case inlet pressure characteristics are shown in Figures 3-60 and 3-61.

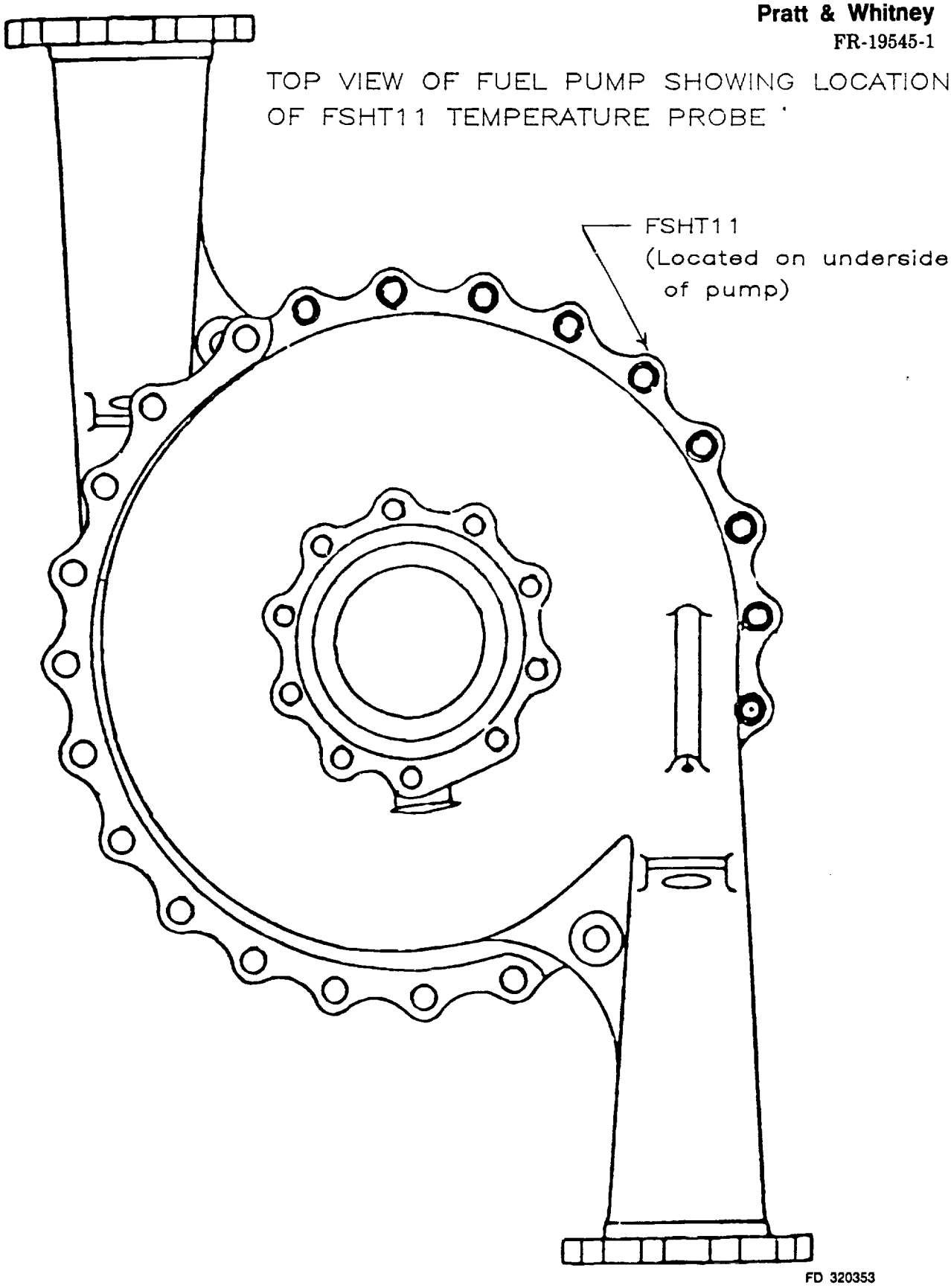

Figure 3-58. Fuel Pump Temperature Probe Location

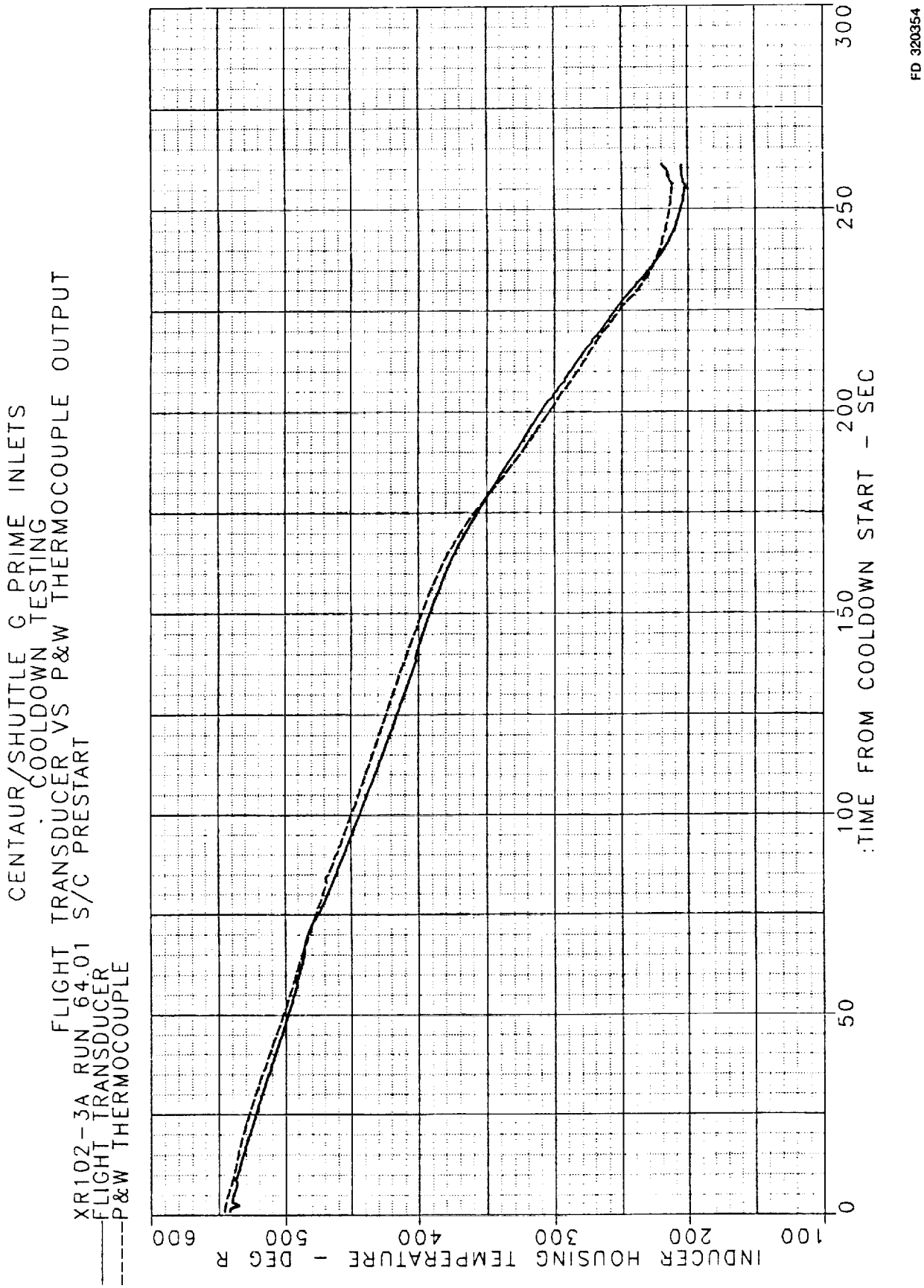

Figure 3-59. Flight Transducer vs P&W Thermocouple Output

0632C

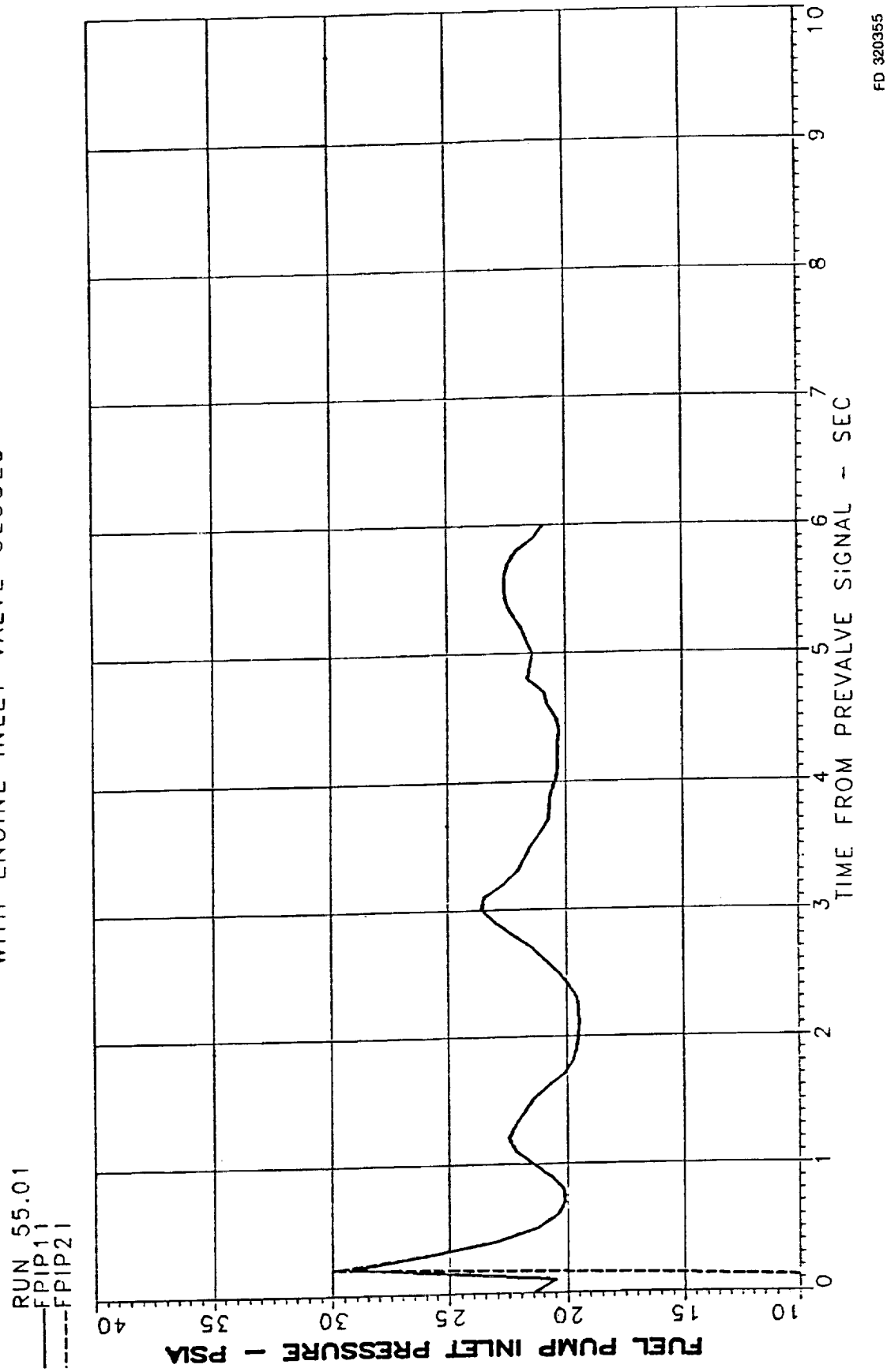

Figure 3-60. Fuel Pump Inlet Pressure Characteristic

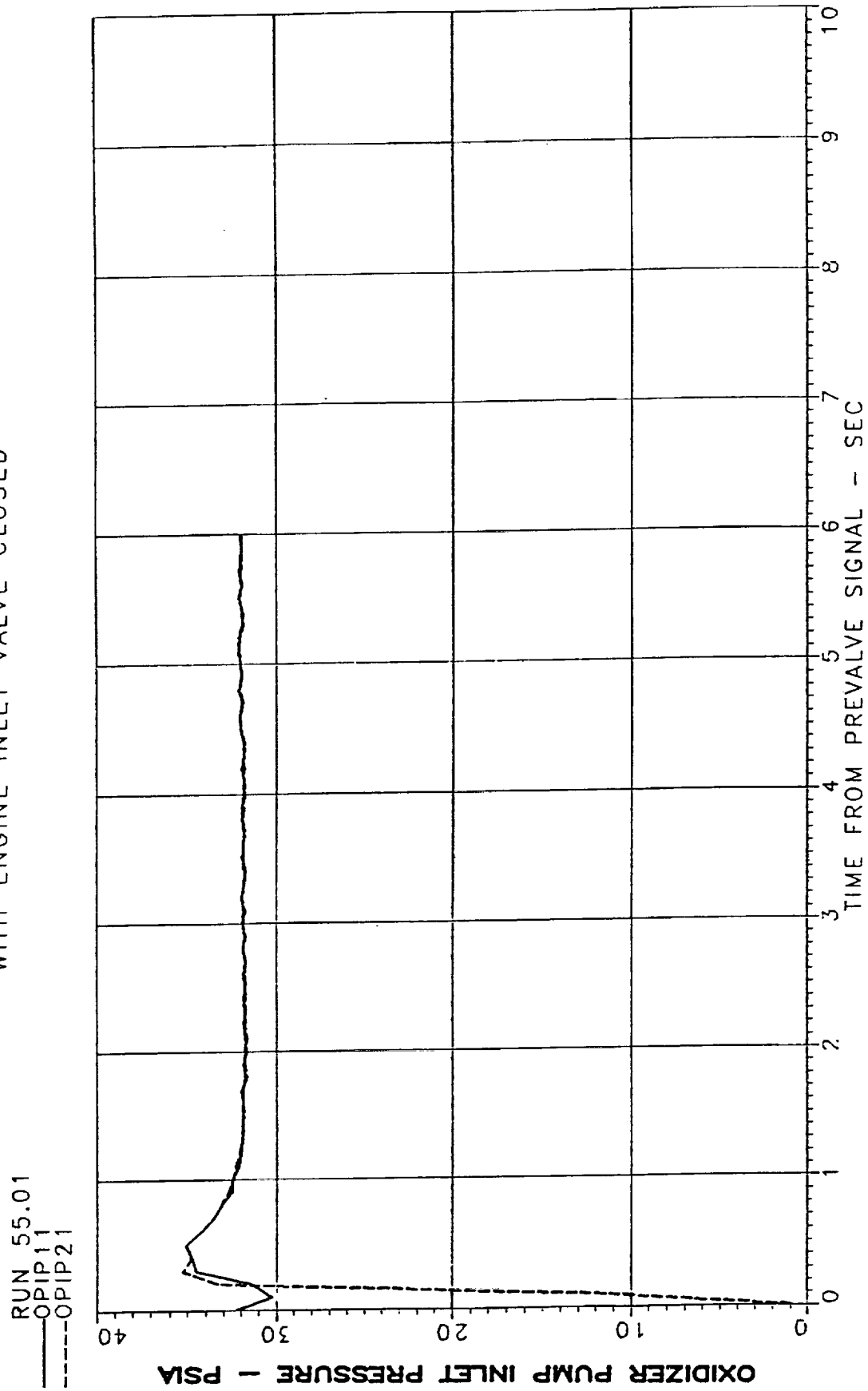

Figure 3-61. Oxidizer Pump Inlet Pressure Characteristic

SECTION 4.0
CENTAUR G-PRIME TESTING

The absolute pressure inlet box had the lowest fuel and oxidizer consumption of the three inlet boxes tested with the G-Prime inlet temperature variation. Because of this, the absolute pressure inlet box was chosen for the G-Prime vehicle. All further analysis regarding the G-Prime vehicle was done with the inlet boxes shown in Figures 1-1 and 1-2 in Section 1.0.

On both the oxidizer and fuel sides, cooling the engine requires the greatest period of time when cooldown is done at point 4 on the inlet box. Cooldown limit tests were done on both the fuel and oxidizer sides, with cooldown performed at point 4 in the inlet box. Cooldown times tested and test results are shown in Tables 4-1 and 4-2.

Table 4-1. *G' Minimum Fuel Inlet Test Summary*

Engine	*Test No.*	*C/D Time (sec)*	*Results*
XR101	68.01	35 sec	No-Go
XR101	70.01	45 sec	Go
XR102	47.03	45 sec	Go
XR102	48.01	40 sec	Go
XR102	49.01	40 sec	Go

0742C

Table 4-2. *G' Minimum LOX Inlet Test Summary*

Engine	*Test No.*	*C/D Time (sec)*	*Results*	*Hsg Temp*	*NPSP*
XR101	66.01	195 sec	No-Go	320	3.80
XR101	67.01	225 sec	Go	225	6.0
XR102	47.03	225 sec	Go	235	4.5
XR102	48.01	215 sec	No-Go	260	3.7
XR102	49.01	220 sec	Go	222	3.9

0742C

Results from cooldown tests including those shown in Tables 4-1 and 4-2 resulted in required test stand cooldown times for the G-Prime inlet boxes of 220 seconds for the LOX side and 40 seconds for the fuel side. These cooldown times allowed proper cooling of the engine components at all locations within the G-Prime inlet boxes. Predicted cooldown times using the cooldown program are 190 seconds for the oxidizer side, and 35 seconds for the fuel side.

The cooldown times recommended for use on the first Shuttle Centaur G-Prime flight are the stand cooldown times plus an additional 10 percent margin. These times are 245 seconds for the LOX side and 45 seconds for the fuel side. After the first flight, it is anticipated the cooldown times can be reduced in response to observed cooling characteristics, which should be close to the predicted values.

The above cooldown times and the resulting consumptions and impulse figures are shown in Table 4-3.

0632C

Table 4-3. *G' Cooldown Consumption and Impulse*

Stand Cooldown Times + 10% Margin		
45 sec Fuel	29.9 lb	1607.5 lb-sec
245 sec Oxidizer	91.6 lb	3947.0 lb-sec
Predicted Cooldown Times + 10% Margin		
40 sec Fuel	24.0 lb	1322.3 lb-sec
210 sec Oxidizer	76.0 lb	3287.3 lb-sec

0742C

0632C

SECTION 5.0
CENTAUR G-TESTING

The delta P pressurization scheme was selected for the G-vehicle. Depending on the mission flown by the Shuttle, the G-mission Centaur vehicle may be in a low earth orbit anywhere from five to approximately seventy hours before the payload can be boosted into geosynchronous orbit. This uncertainty in coast time causes a large range of possible oxidizer inlet temperatures due to the heating effects of the sun, and the cooling effects of the vehicle hydrogen tank and the fact that the oxidizer tank does not have an orbit vent capability. This temperature variation produces the elongated oxidizer inlet boxes shown in Figure 1-3. The fuel inlet box does not suffer as dramatic an effect as seen in Figure 1-4 because it has a controlled vent system.

Because of the large possible variation in inlet temperature, the maximum oxidizer consumption levels are much greater than those associated with the earlier G-Prime inlet boxes. The consumption levels calculated using maximum and minimum conditions were too high for practical vehicle operation.

In an attempt to reduce the quantities of propellants consumed, a new scenario was proposed. Instead of having a single cooldown time for the inlet box determined at the lower left corner, the cooldown time would be dependent on the tank saturation pressure at the time of the start of cooldown. In this way, the cooldown box would be effectively divided into an infinite number of boxes with a width of 5 psia and a temperature variation of approximately 0.1°R. The required cooldown time then decreases as the inlet saturation pressure increases, limiting the amount of time that propellants would be flowed when cooling down at a point on the inlet box with a high vapor pressure.

Depending on the mission the vehicle is required to fly, the oxidizer tank vapor pressure could vary with the number of revolutions over the ranges shown in Figures 5-1, 5-2, and 5-3. Using the worst case pressure variation of Figure 5-2, cooldown times and worst case consumptions were calculated. Required cooldown time is dependent only on saturation pressure, while the worst case propellant consumption is dependent on saturation and length of vehicle coast (duct cooling).

Cooldown time required was determined to be 45 seconds on the fuel side and to range from 210 to 330 seconds on the oxidizer side depending on tank pressure. These times were determined from cooldown testing. A record of cooldown testing is shown in Tables 5-1 and 5-2.

On the oxidizer side, a ten percent margin was added to the cooldown times determined by testing to obtain recommended flight cooldown times. The cooldown deck was used to predict required cooldown time. The predicted time will be used as the vehicle cooldown time if, as anticipated, flight data verifies the cooldown model.

On the fuel side, like the oxidizer side, a ten percent margin was added to the cooldown time determined from test data. This resulted in a recommended cooldown time of 55 seconds on the fuel side for the first Centaur G flight. This cooldown time can then be adjusted downward according to the data received from the flight.

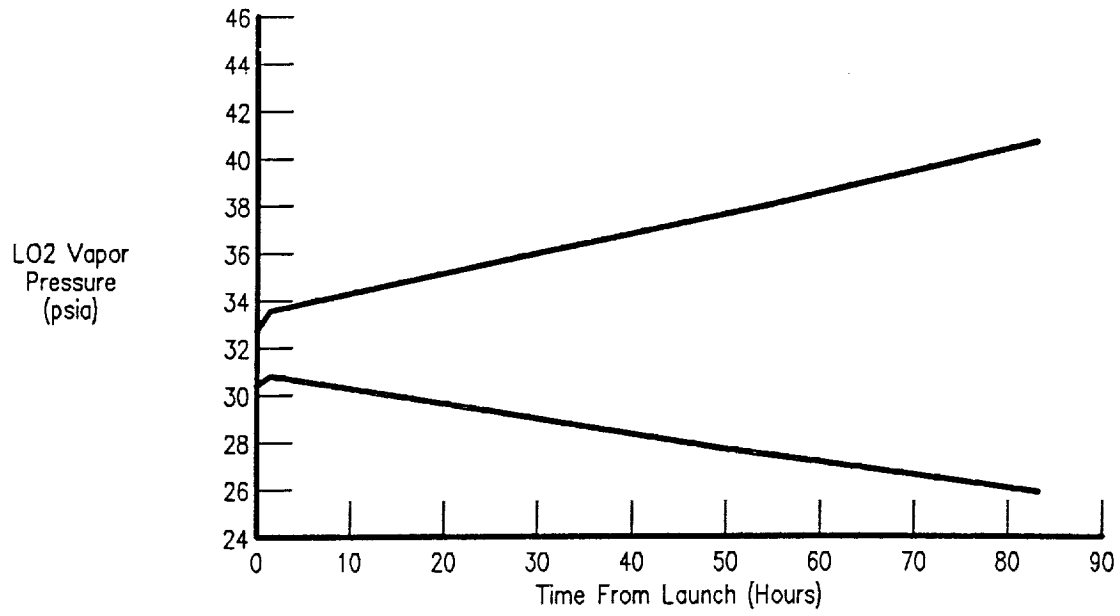

FD 320359

Figure 5-1. LOX Vapor Pressure — Centaur G Mission No. 1

Plots showing oxidizer cooldown times required and oxidizer consumed are shown in Figures 5-4, 5-5, 5-6, and 5-7. The recommended fuel cooldown time and the associated consumption is shown in Table 5-3, along with the worst case oxidizer values.

The component cooldown trends are the same as with the G-Prime cases.

On the oxidizer side, as cooldown proceeds, the oxidizer flow control cools down first, followed by the inlet NPSP increasing to an acceptable level, followed by the oxidizer pump cooling. Cooldown can be monitored using the same thermocouple location on the oxidizer pump inducer housing flange.

The fuel side also behaves in the same manner as with G-Prime cases, allowing the use of the same fuel pump second stage housing temperature probe.

In addition to the first burn engine firing as in the G-Prime vehicles, G-vehicles will also have a short cooldown prior to the second engine firing. The anticipated metal temperatures for the second firing are much lower than first burn predictions. All metal parts will already be near operating temperatures, and propellants will be flowed only long enough to fill the vehicle inlet ducts and assure proper NPSP at the engine inlets. The recommended duration of these flows and the propellants consumed are shown in Table 5-4. Because the cooldown times are so short, there is little variation between best and worst case predicted values. The second burn predictions are within Atlas Centaur experience.

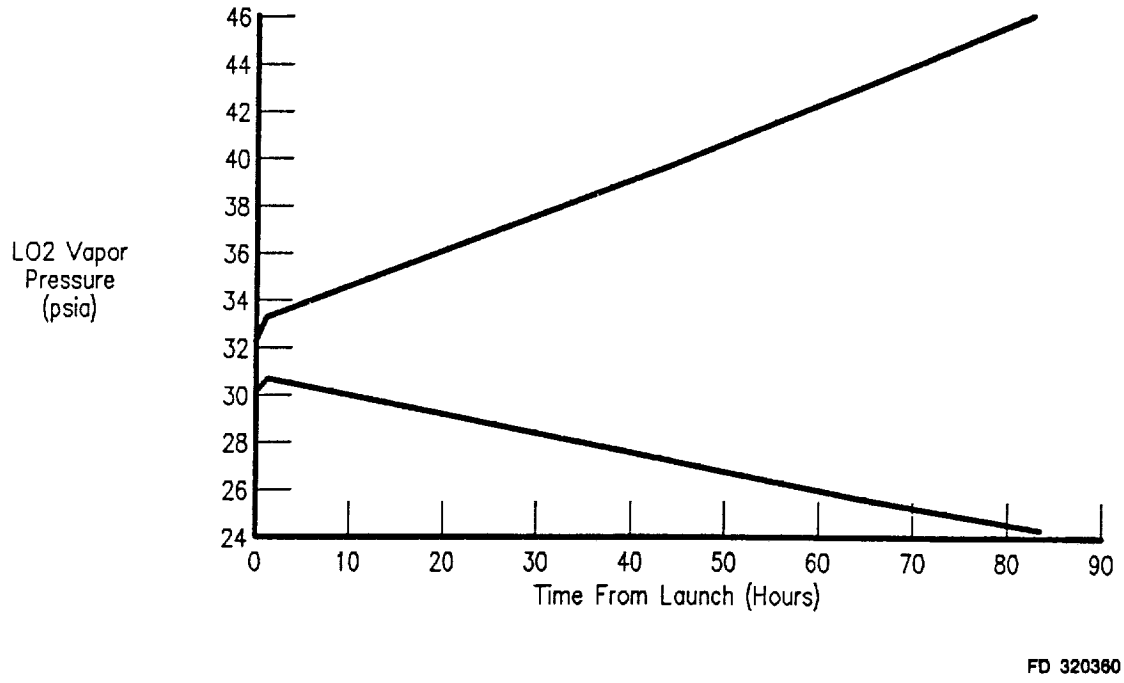

Figure 5-2. LOX Vapor Pressure Centaur G Mission No. 2

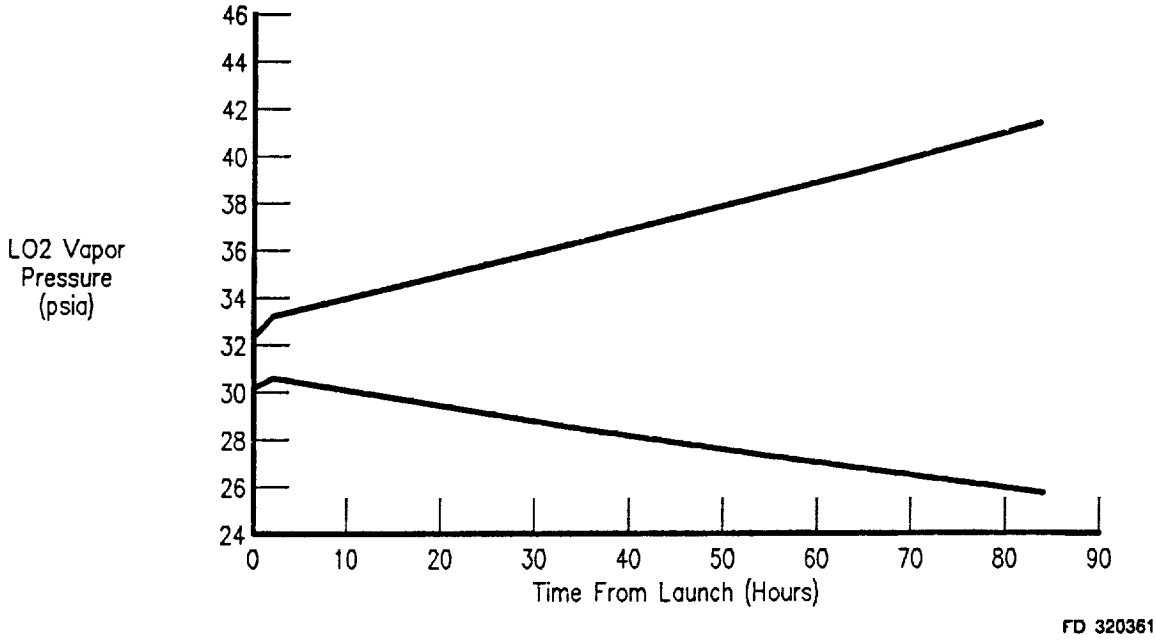

Figure 5-3. LOX Vapor Pressure Centaur G Mission No. 3

Table 5-1. *Centaur G Fuel Cooldown Test Summary*

Engine	*Test No.*	*FPIP11 Pressure*	*C/D Time*	*FPIT1R*	*Results*
XR101-4	74.01	25.8	55	39.1	No-Go
	79.01	25.3	60	39.0	Go
	82.01	25.2	60	38.3	Go
	68.01	29.2	35	39.5	No-Go
	70.01	29.1	45	39.4	Go
XR102	47.03	29.1	40	39.2	Go
	48.01	29.3	40	39.5	Go
	49.01	29.1	40	39.4	Go
	57.01	29.6	40	39.3	Go
	58.01	31.2	40	39.4	Go
	59.01	29.7	40	39.3	Go
	60.01	31.1	40	39.3	Go
	54.01	25.2	60	38.2	Go
	62.01	25.4	60	38.2	Go
	63.01	25.7	60	38.2	Go
	64.01	25.4	60	37.9	Go

0742C

0632C

Table 5-2. *Centaur G LOX Cooldown Test Summary*

Engine	*Test No.*	*Pressure*	*C/D Time*	*Pump Inlet NPSP*	*Results*
XR101-4	77.01	32.3	300	4.2	Go
	79.01	32.4	275	4.1	Go
	80.01	31.9	250	2.9	No-Go
XR102-3A	52.01	32.5	275	2.6	No-Go
	53.01	32.2	275	3.0	No-Go
	54.01	31.9	300	3.4	Go
	61.01	32.5	300	2.6	No-Go (A-3-3 OFC)
	62.01	32.5	330	3.2	Go (A-3-3 OFC)
	63.01	32.4	300	3.4	Go (A-3-3 OFC Start Flow Increased)
	56.01	55.2	190	3.5	No-Go
	57.01	55.2	210	5.4	Go
	59.01	55.0	210	3.0	Go (A-3-3 OFC)
	64.01	43.6	255	3.5	Go (A-3-3 OFC)
XR105-3	33.01	43.7	255	3.7	Go
P642045	01.01	43.8	255	3.6	Go

0742C

0632C

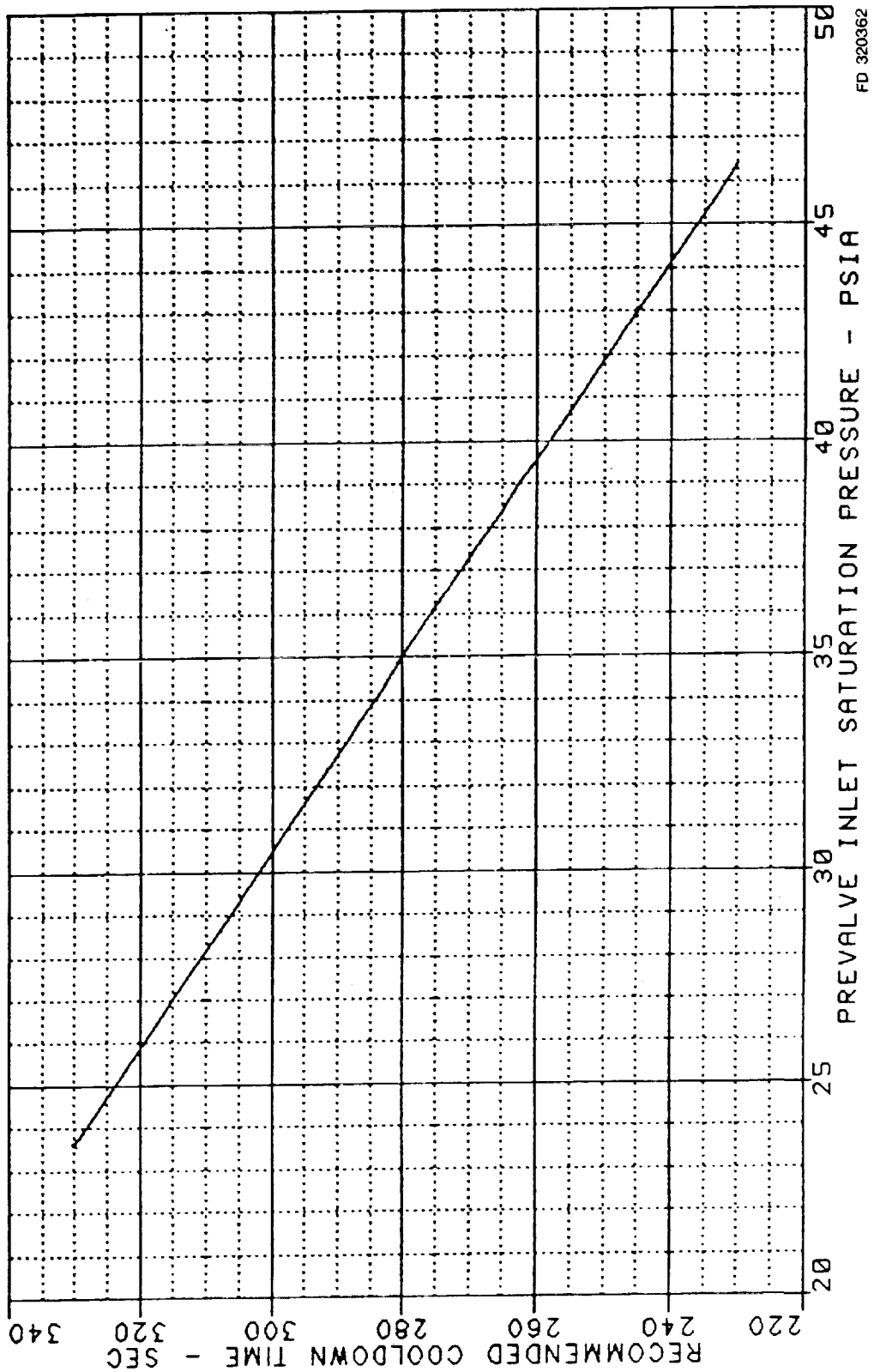

Figure 5-4. Recommended Oxidizer Cooldown Time — 10% Margin

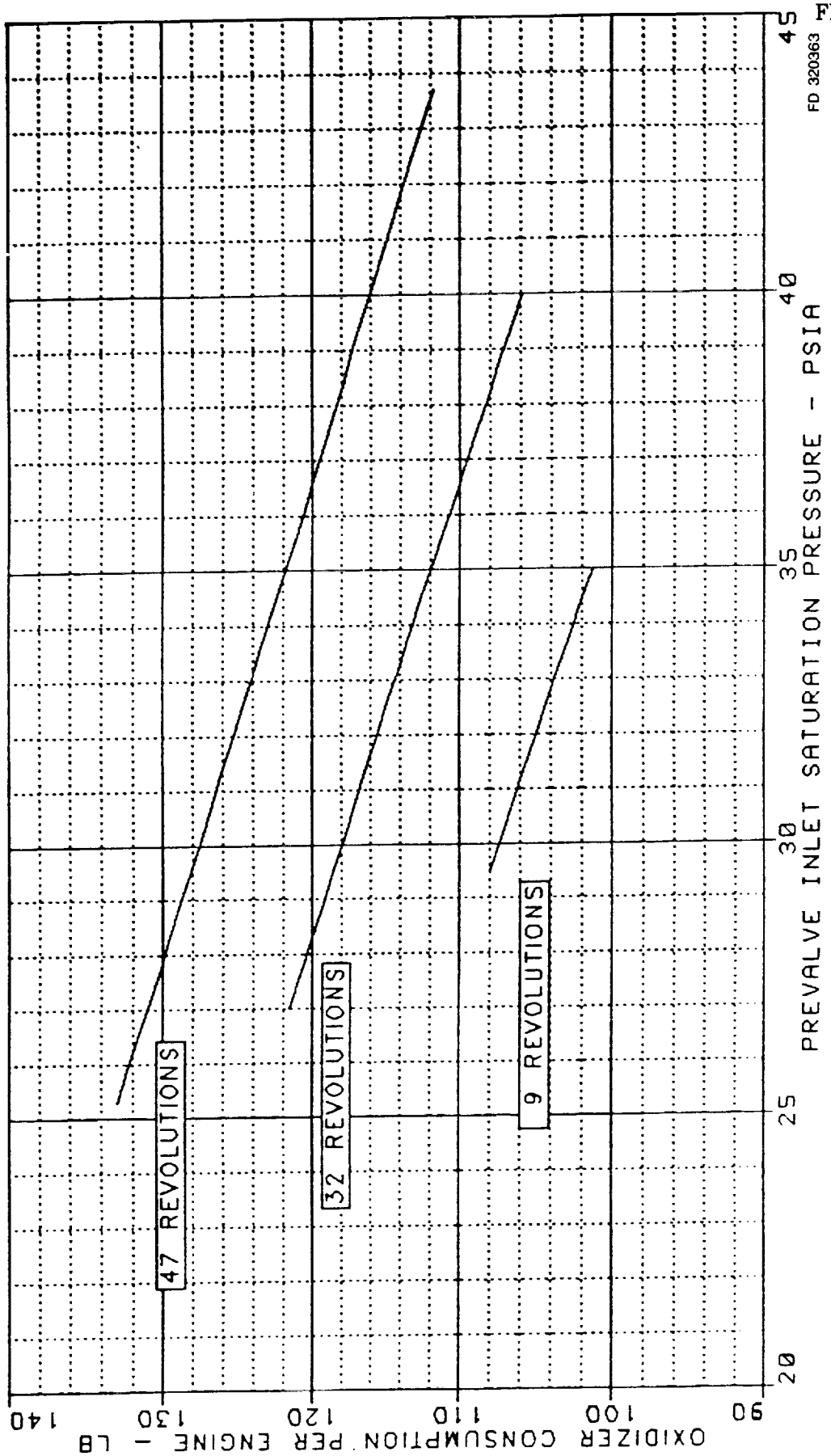

Figure 5-5. Maximum Oxidizer Consumption — 10% Margin

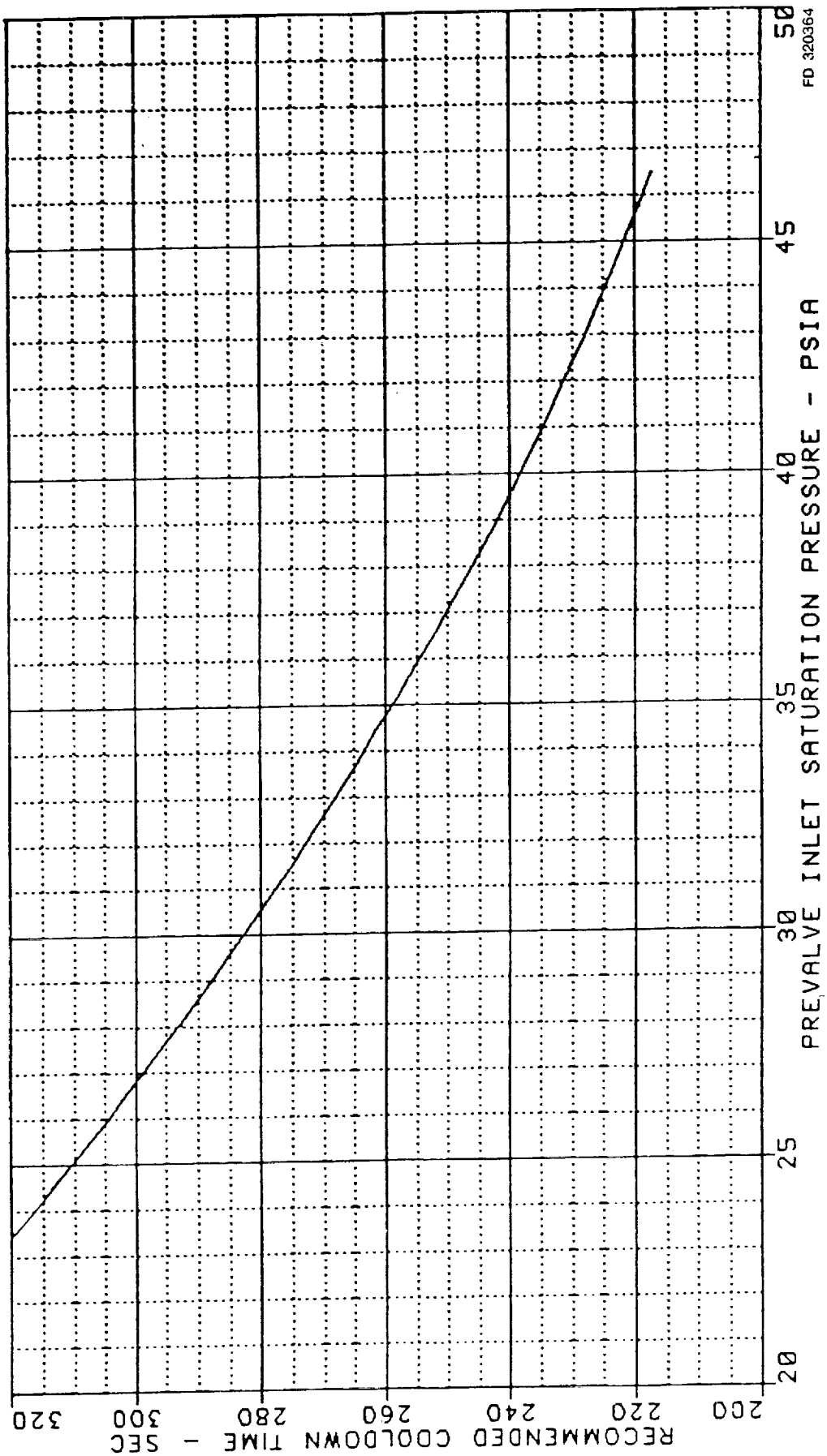

Figure 5-6. Recommended Oxidizer Cooldown Time — 20% Margin

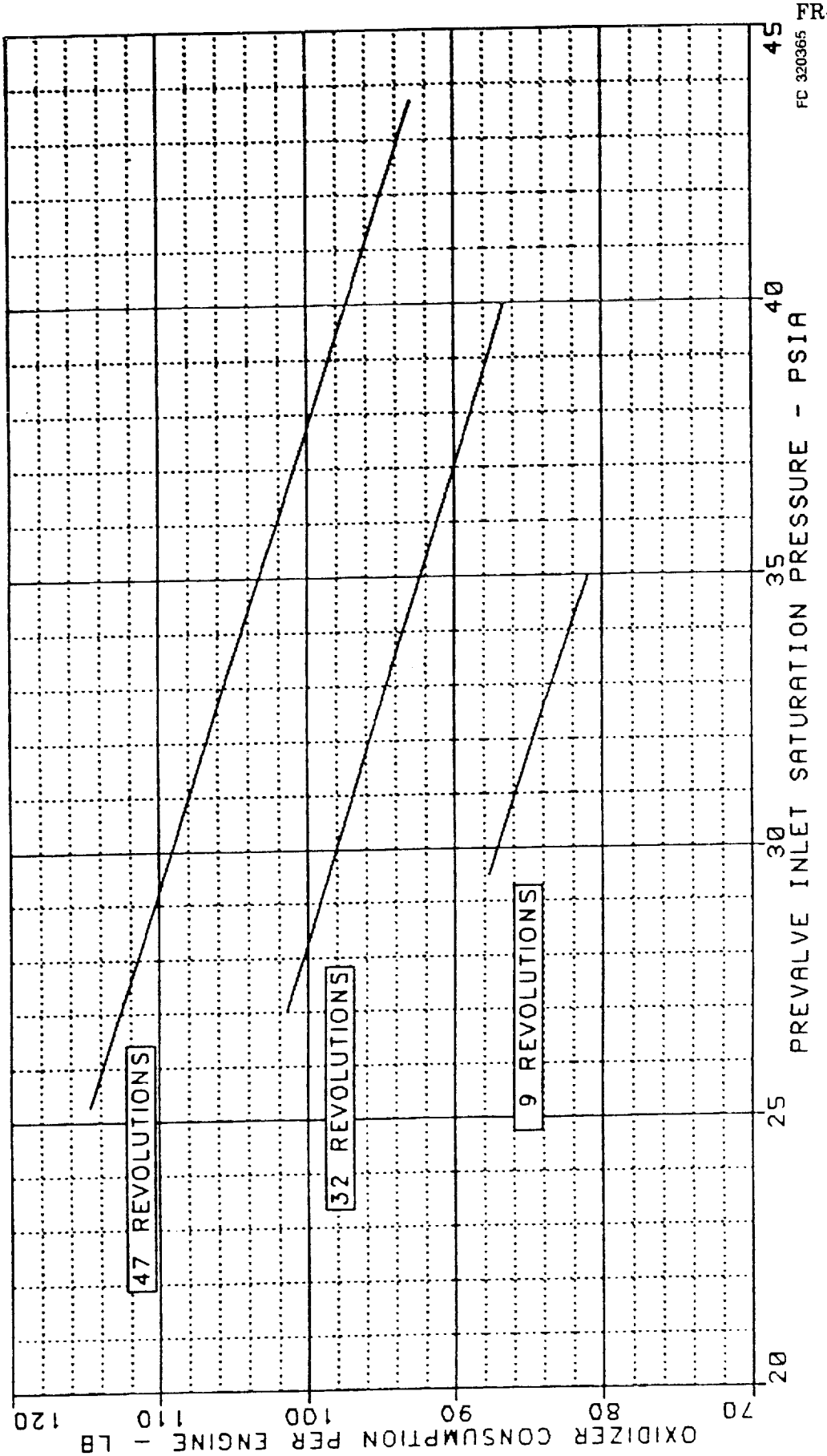

Figure 5-7. Maximum Oxidizer Consumption — 20% Margin

Table 5-3. *Centaur/Shuttle G Vehicle*

Fuel		
Min. Consumption		
Time	Consumption	Impulse
65 sec	44 lb	2266.0 lb-sec
Max. Consumption		
Time	Consumption	Impulse
65 sec	66 lb	3309.0 lb-sec
LOX		
Min. Consumption		
Time	Consumption	Impulse
330 sec	68 lb	2980.0 lb-sec
Max. Consumption		
Time	Consumption	Impulse
330 sec	139 lb	5960.0 lb-sec

0742C

Table 5-4. *G Centaur 2nd-Burn Cooldown Estimates*

Fuel	*NPSP*	*Pump*	*Duct Emptied*	*Impulse*
Time-sec	5	5	9	—
Min. Consumption - lb/engine	—	1	4	205
Max. Consumption - lb/engine	—	2	6	302
Oxidizer				
Time-sec	2	7	43	—
Min. Consumption - lb/engine	—	<1	17	728
Max. Consumption - lb/engine	—	2	20	862

0742C

0632C

SECTION 6.0
EXPANDED INLET TESTING BACKGROUND

The background of the expanded inlet testing is presented as it relates to engine starting. More detail is presented in the "Cooldown Background" section.

For Atlas Centaur application, the pumps are prechilled before launch to provide cold pump housing temperatures at prestart. Large cooldown areas provide high cooldown flows to rapidly complete the conditioning of the pumps during prestart. The prechill allows the high cooldown flows during prestart to provide quick conditioning of the pumps while the vehicle is under low thrust and still within the gravity field.

For Shuttle Centaur (S/C) application, the vehicle is in orbit for an extended time before engine start, and prelaunch prechill of the pumps and ducts would be fruitless. The prestart sequence is the only conditioning provided to the engine. The necessity for rapid conditioning of the pumps and ducts is removed because the vehicle is in orbit and immediate thrust is not needed to resist a gravitational pull. The time spent in orbit prior to the firing may vary significantly. There is heat transfer from the oxidizer to the fuel tank, from the sun into the tanks, and from the tanks to space. Unknowns in these heat transfer relationships result in predictions that the oxidizer tank may cool or heat during the orbit duration. Because the oxidizer tank does not have vent capability while in orbit, the possible range of oxidizer supply temperature and pressure increases with orbit duration. Therefore, the required oxidizer inlet start envelope is a function of the maximum orbit duration for a given mission. Inlet condition ranges were defined by General Dynamics Corp. for two vehicle types, the G and G-Prime Centaurs.

Prior to this testing, the engine was qualified to operate over a limited range of inlet conditions as expected for Atlas Centaur application. The "Expanded Inlet" test program was conducted to define the RL10A-3-3A engine start characteristics over inlet condition ranges defined for the G and G-Prime Shuttle Centaurs, and to define the RL10A-3-3B engine start characteristics over inlet condition ranges defined for the G Shuttle/Centaur. Figure 6-1 shows the previously qualified inlet start envelope along with the requested G and G-Prime Centaur inlet start envelopes.

The engine demonstrated successful start characteristics over the expanded inlet conditions for both mission types, completing the Expanded Inlet test series. A cooldown test series, following the Expanded Inlet testing, revealed that pump conditioning could be accomplished with less propellant consumption if cooldown flows are reduced and cooldown time increased. The Expanded Inlet test series was rerun to define start characteristics of the engine using these reduced cooldown flows and increased cooldown times. Following the rerun of the Expanded Inlet test series, a qualification test series was run using the reduced cooldown flows and increased cooldown time scheme.

For ease of communication, the testing prior to the cooldown series is said to use the "large" cooldown area scheme, and the testing following the cooldown test series is said to use the "small" cooldown area scheme.

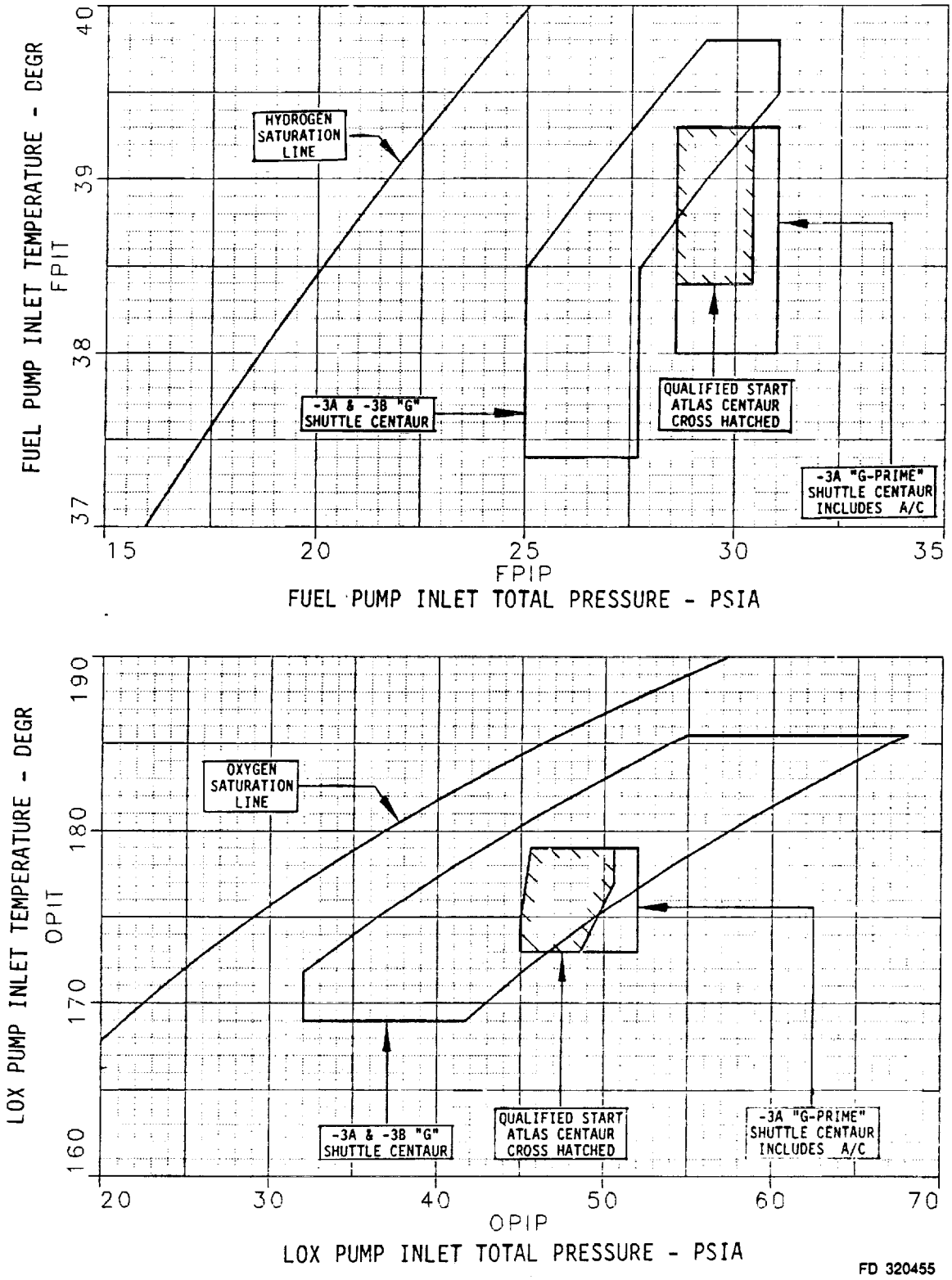

Figure 6-1. Oxidizer and Fuel Pump Inlet Start Envelopes Large or Small Cooldown Areas, No Prechill

The large cooldown area scheme cools the oxidizer pump using a 0.34 $in.^2$ oxidizer flow control valve area during prestart. This area reduces from 0.34 $in.^2$ to a 0.05 $in.^2$ at the start signal. The oxygen flows from the pump, through the oxidizer flow control valve, to the injector and thrust chamber where it is exhausted into space. The fuel pump is cooled using a discharge cooldown valve area of 0.51 $in.^2$ and an interstage cooldown valve area of 0.61 $in.^2$ during prestart. At the start signal the discharge cooldown valve is closed, the interstage cooldown valve area is reduced from 0.61 to 0.37 $in.^2$, and the main fuel valve is opened. The interstage cooldown valve closes completely as fuel pump discharge pressure rises during the start transient. The hydrogen, passing through the two cooldown valves, is exhausted into space.

The small cooldown area scheme cools the oxidizer pump using a 0.050 $in.^2$ oxidizer flow control valve area during prestart which remains unchanged at the start signal. The oxygen passes from the pump and oxidizer flow control valve and continues through the injector and thrust chamber and is exhausted into space. The fuel pump is cooled with a discharge cooldown valve area of 0.51 $in.^2$ and an interstage cooldown valve area of 0.37 $in.^2$ during prestart. At the start signal the discharge cooldown valve closes, the interstage cooldown valve remains at 0.37 $in.^2$, and the main fuel valve is opened. The interstage cooldown valve closes completely as fuel pump discharge pressure rises during the start transient. The hydrogen, passing through the two cooldown valves, is exhausted into space.

The areas quoted above for the fuel pump interstage and discharge valves are geometric areas. The corresponding effective areas, used in the cooldown section, are as follows:

Discharge valve area	0.51 geometric,	0.30 effective	
Interstage valve area	0.61 geometric,	0.36 effective	(full open)
Interstage valve area	0.37 geometric,	0.18 effective	(mid stroke).

Starting impulse has traditionally been defined as the integral of thrust vs time during the first three seconds of the run. However, with expanded inlet start envelopes, the engine occasionally requires more than three seconds to accelerate to 90 percent thrust. In general, conditions conducive to slow acceleration times are low fuel pump inlet pressure (FPIP), high oxidizer pump inlet pressure (OPIP) or high oxidizer net positive suction pressure (ONPSP), and the large cooldown area scheme is slower than the small cooldown area scheme. To accommodate acceleration times greater than 3.0 seconds, starting impulse to 4.0 or 5.0 seconds would have to be quoted. Since the G and G-Prime Centaur inlet start envelopes yield times to accelerate which are less than 3.0 seconds except for a very small corner of the G inlet start envelope when the large cooldown area scheme is used, starting impulse to 3.0 seconds is maintained and acceleration times slower than 3.0 seconds are omitted for the starting impulse correlations.

All tests were conducted with stand inlet ducts, no turbopump blanket, and non-evacuated cooldown valves.

SECTION 7.0
EXPANDED INLET TEST RESULTS AND ANALYSIS

Figure 7-1 shows actual and predicted acceleration times for a S/C engine with the large cooldown (C/D) area scheme, in either the -3A or -3B configuration. The run-to-run and engine-to-engine variations in time-to-accelerate are greater than the engine configuration differences, therefore the predicted acceleration equation applies to either configuration. The actual acceleration times (open symbol) and predicted acceleration times (solid symbol) are plotted as a function of fuel pump inlet total pressure (FPIP), with a background of constant oxidizer net positive suction pressure (ONPSP) curves. The predicted acceleration times and the constant ONPSP curves were determined with the indicated prediction equation. Vertical lines have been drawn from the actual acceleration time symbol to the predicted acceleration time symbol, and the length of the line shows the prediction error. As indicated on the figure the time-to-accelerate equation was generated during fifty-four tests involving three engines. This equation must be incorporated in Specification 2289B, Volume I, after being shifted to account for evacuated cooldown valves and the nominal production acceleration time. Previous testing has indicated that the engine will accelerate 0.095 second slower with the fuel cooldown valves vented to a vacuum compared to their being vented to 14.7 psia.

Figure 7-2 presents starting impulse as a function of time-to-accelerate for a S/C engine using the large cooldown area scheme in both the -3A and -3B configurations. An additional projected impulse was used to anchor each curve at zero time-to-accelerate. If the engine could accelerate instantly, the starting impulse would be its steady-state thrust times 3.0 seconds (49,500 lbf-sec mx for a -3A configuration and 45,000 lbf-sec for a -3B). The equation of the curve through the data is given. The starting impulse correlations reveal that a 0.1 second change in time-to-accelerate will change starting impulse 1491 lbf-sec for a -3A configuration and 1377 lbf-sec for a -3B. The equation for the RL10A-3-3A configuration must be incorporated in Specification 2289B, Volume 1.

Figure 7-3 shows actual and predicted acceleration times for a S/C engine using the small cooldown areas scheme in either -3A or -3B configuration. The run-to-run and engine-to-engine variations in time-to-accelerate are greater than the engine configuration differences, therefore the predicted acceleration equation applies to either configuration. The actual acceleration times (open symbol) and predicted acceleration times (solid symbol) are plotted as a function of FPIP, with a background of constant OPIP curves. Vertical lines have been drawn from the actual acceleration time symbol to the predicted acceleration time symbol, and the length of the line shows the prediction error. As indicated on the figure the time-to-accelerate equation was generated using thirty two tests involving two engines. This equation must be incorporated in Specification 2289B, Volume 2 and Specification 2295 after being shifted to account for evacuated cooldown valves. Previous testing has indicated that the engine will accelerate 0.095 second slower with the fuel cooldown valves vented to a vacuum compared to their being vented to 14.7 psia.

Time-to-accelerate for engines with small cooldown areas correlated with OPIP, rather than ONPSP as it did for the large cooldown area scheme. There are two likely reasons.

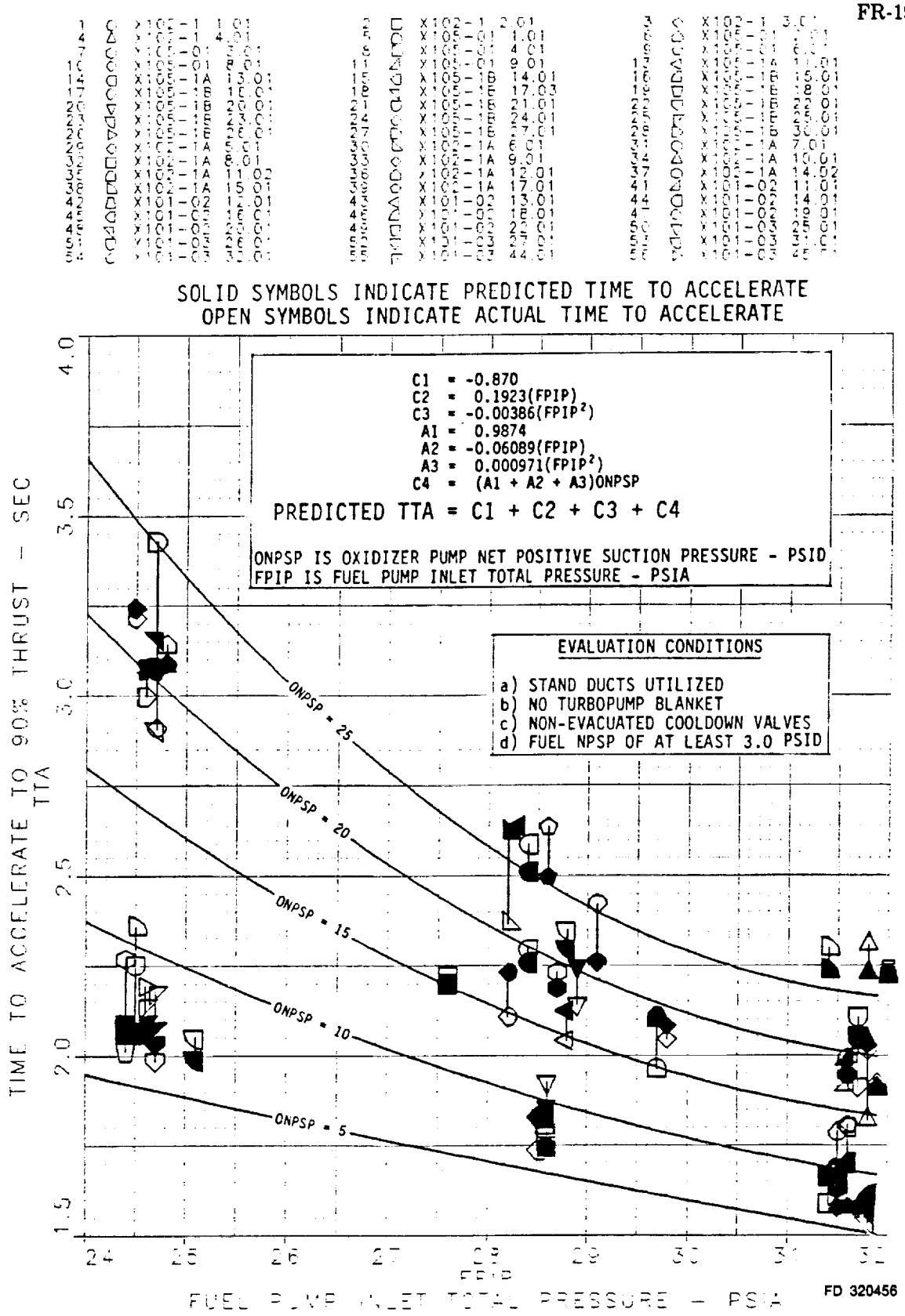

Figure 7-1. -3A and -3B Predicted Acceleration-Shuttle Centaur With Large Cooldown Areas, No Prechill

1	X102-1	1.01	2	X102-1	2.01	3	X102-1	3.01	4	X102-1	4.01
5	X105-01	1.01	6	X105-01	2.01	7	X105-01	3.01	8	X105-01	4.01
9	X105-01	6.01	10	X105-01	8.01	11	X105-01	9.01	12	X105-01	10.01
13	X105-1A	11.01	14	X105-1A	13.01	15	X105-1B	14.01	16	X105-1B	15.01
17	X105-1B	16.01	18	X105-1B	17.03	19	X105-1B	18.01	20	X105-1B	20.01
21	X105-1B	21.01	22	X105-1B	22.01	23	X105-1B	23.01	24	X105-1B	24.01
25	X105-1B	25.01	26	X105-1B	26.01	27	X105-1B	27.01	28	X105-1B	30.01
29	X102-1A	5.01	30	X102-1A	6.01	31	X102-1A	7.01	32	X102-1A	8.01
33	X102-1A	9.01	34	X102-1A	10.01	35	X102-1A	11.02	36	X102-1A	12.01
37	X102-1A	14.02	38	X102-1A	15.01	39	X102-1A	17.01	40	X102-1A	19.01
41	X101-02	11.01	42	X101-02	12.01	43	X101-02	13.01	44	X101-02	14.01
45	X101-02	16.01	46	X101-02	18.01	47	X101-02	19.01	48	X101-02	20.01
49	X101-02	22.01	50	X101-03	25.01	51	X101-03	26.01	52	X101-03	27.01
53	X101-03	31.01	54	X101-03	32.01	55	X101-03	44.01	56	X101-03	45.01
57	X102-02	45.04	58	X102-02	46.01						

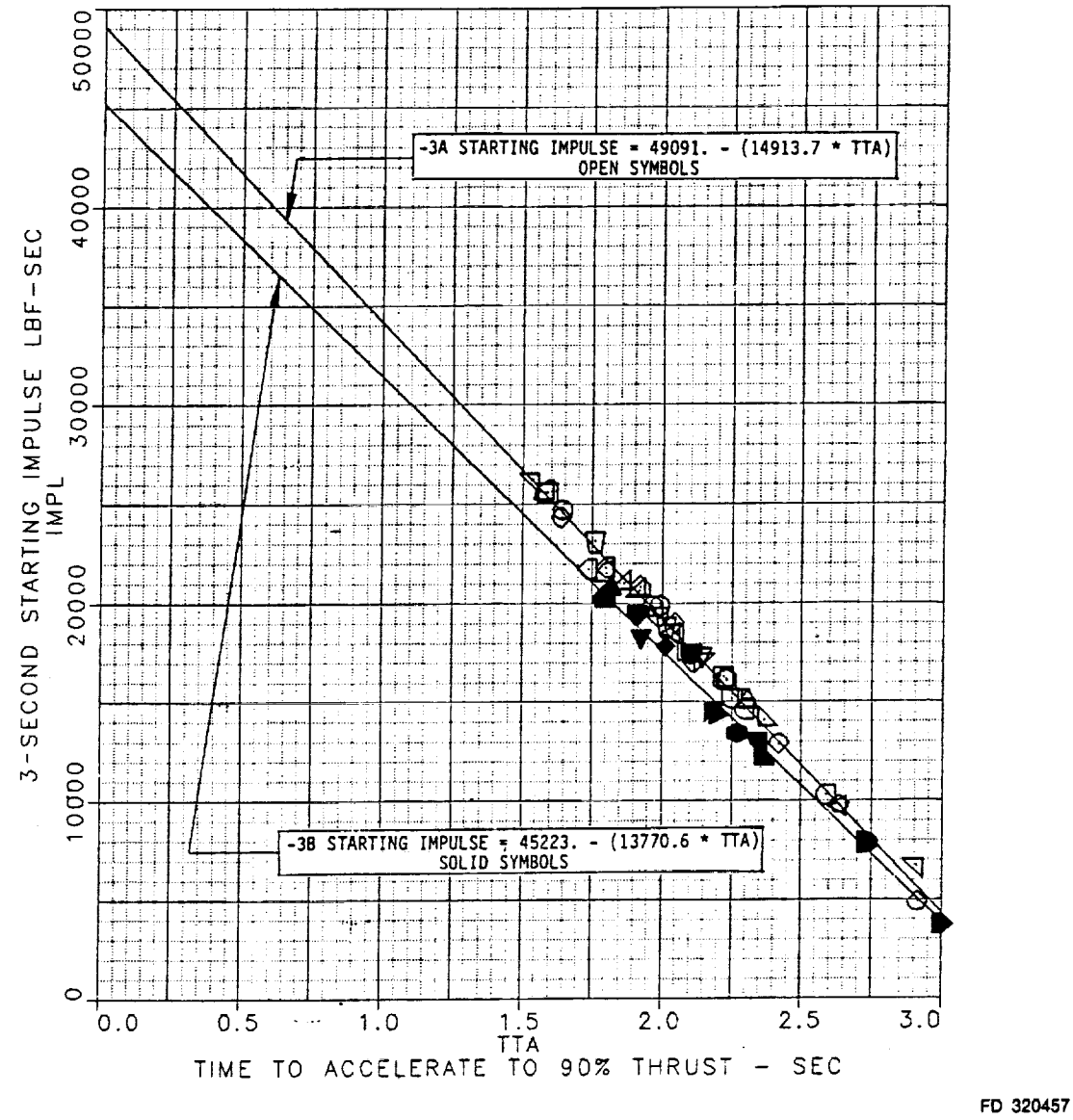

Figure 7-2. -3A and -3B Starting Impulse-Shuttle Centaur With Large Cooldown Areas, No Prechill

1	X101-4A 83.04	2	X101-4A 85.01	3	X101-4A 87.01
4	X101-4A 88.01	5	X101-4A 90.01	6	X101-4A 91.01
7	X101-4A 92.01	8	X101-4A 94.01	9	X101-4A 95.01
10	X101-4A 97.01	11	X101-4A 99.01	12	X101-4A 101.01
13	X101-4A 102.01	14	X101-4A 103.01	15	X101-4A 104.01
16	X101-4A 106.01	17	X101-4A 109.01	18	X103-2 2.01
19	X103-2 3.01	20	X103-2 4.01	21	X103-2 5.01
22	X103-2 6.01	23	X103-2 7.01	24	X103-2 9.01
25	X103-2 11.01	26	X103-2 18.01	27	X103-2 21.01
28	X103-2 24.01	29	X103-2 25.01	30	X103-2 26.01
31	X103-2 27.01	32	X103-2 28.01		

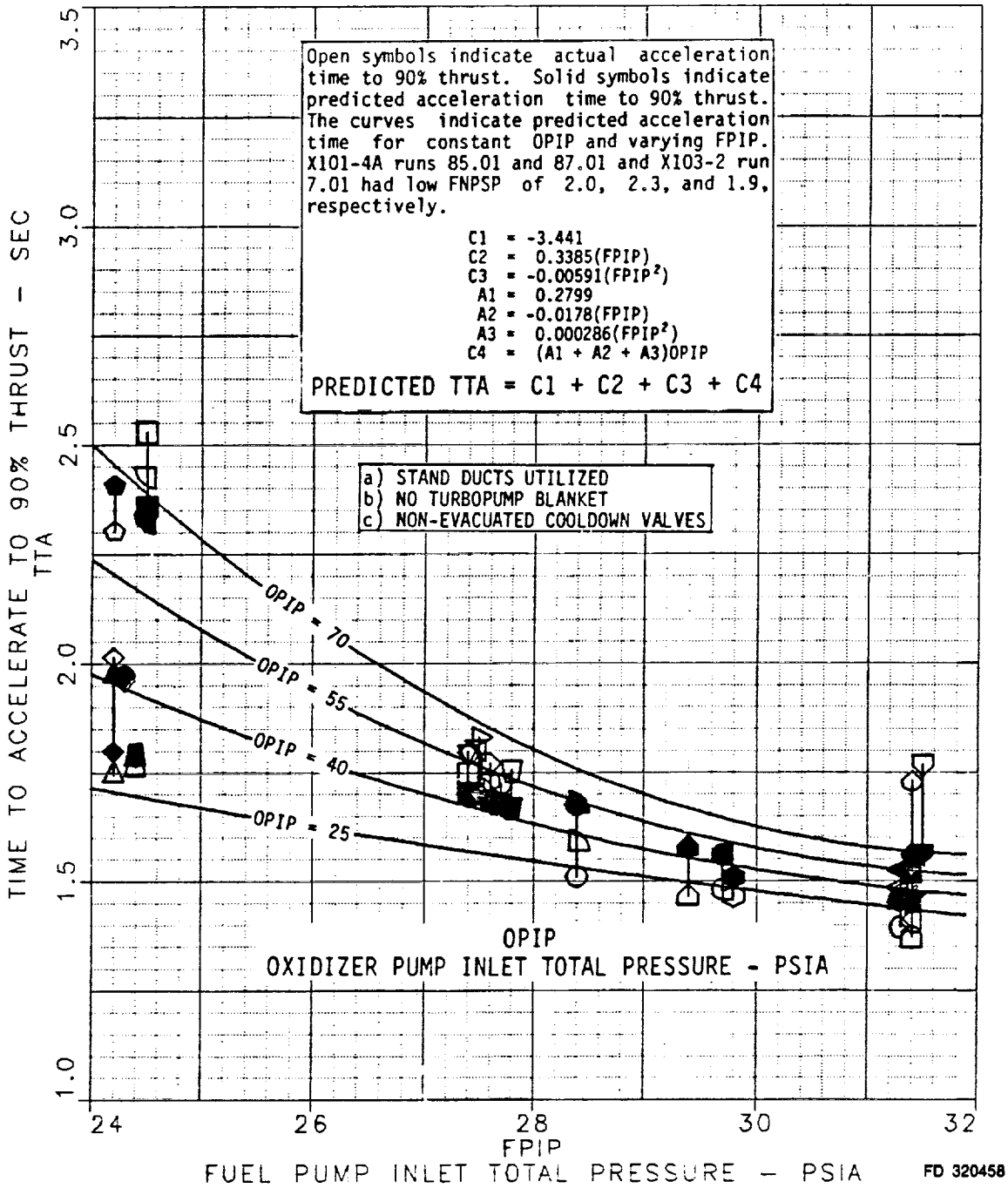

Figure 7-3. -3A and -3B Predicted Acceleration-Shuttle Centaur With Small Cooldown Areas, No Prechill

The dominant reason deals with increased chamber pressure which back-pressures the turbine and increases time-to-accelerate. Chamber pressure early in the transient is largely a function of oxidizer flow. Oxidizer flow is regulated by the oxidizer flow control valve area and the NPSP at the valve. If the NPSP is high at the valve, the flow is a function of NPSP; however if the NPSP is low or two-phase at the valve the flow is a function of pressure.

For a given oxidizer pump inlet pressure and temperature and a given pump housing temperature, a high flow rate would pass through the pump with little heat-per-pound being added. This would yield about the same NPSP at the oxidizer flow control valve as existed at the pump inlet. Therefore for the high cooldown area scheme, the valve NPSP is high and flow is a function of NPSP. In contrast, a low flow rate would pass through the pump with significant heat-per-pound being added and the NPSP at the oxidizer flow control valve would be low or two-phase. Therefore, for the low cooldown area scheme, the valve NPSP is low or two-phase and flow is a function of pressure. In conclusion, the time-to-accelerate for the large cooldown area scheme will correlate with ONPSP and the time-to-accelerate for the small cooldown area scheme will correlate with OPIP.

A secondary reason as to why time-to-accelerate may correlate with OPIP relates to the temperature of the fuel at the turbine inlet early in the start transient. The oxidizer cooldown flow, having cooled the pump, continues through the thrust chamber and is exhausted to space. The oxygen is very cold as it passes through the thrust chamber and cools the chamber tubes. The hydrogen, after start signal and in route to the turbine, passes through the thrust chamber tubes. Cold chamber tubes lead to slow acceleration by reducing heat transfer to the fuel early in the start transient. The small cooldown area scheme used cooldown times which were scheduled as a function of OPIP (165 seconds of cooldown at high OPIP and 250 seconds at low OPIP), see Figure 7-4. Therefore, the influence on time-to-accelerate of cooling the chamber during oxidizer cooldown will appear to correlate with OPIP.

Because both effects correlate with OPIP, it is impossible to separate the dominating effect that backpressuring the turbine has on time-to-accelerate from the secondary effect that cooling the chamber has on time-to-accelerate.

Figure 7-5 presents starting impulse as a function of time-to-accelerate for a S/C engine using the small C/D area scheme in both the -3A and -3B configurations. As before, an additional projected impulse was used to anchor each curve at zero time-to-accelerate. The equation of the curve through the data is given. The correlation reveals that a 0.1 second change in time-to-accelerate will change starting impulse approximately 1540 lbf-sec for a -3A configuration and 1400 lbf-sec for a -3B configuration. The equation for the RL10A-3-3A configuration must be incorporated in Specification 2289B, Volume 2, and the equation for the RL10A-3-3B configuration must be incorporated in Specification 2295.

Figure 7-6 shows the predicted acceleration envelope using the small cooldown area scheme for the G Centaur vehicle utilizing either the RL10A-3-3A or -3B configurations, and for the G-Prime Centaur vehicle utilizing the RL10A-3-3A configuration.

Figure 7-7 shows the three-second starting impulse for Shuttle/Centaur operation, using the small cooldown area scheme, that would result from the predicted acceleration times in Figure 7-6. The G Centaur starting impulse range is indicated by the full length of the -3A and -3B curves, and the G-Prime Centaur range is indicated by symbols.

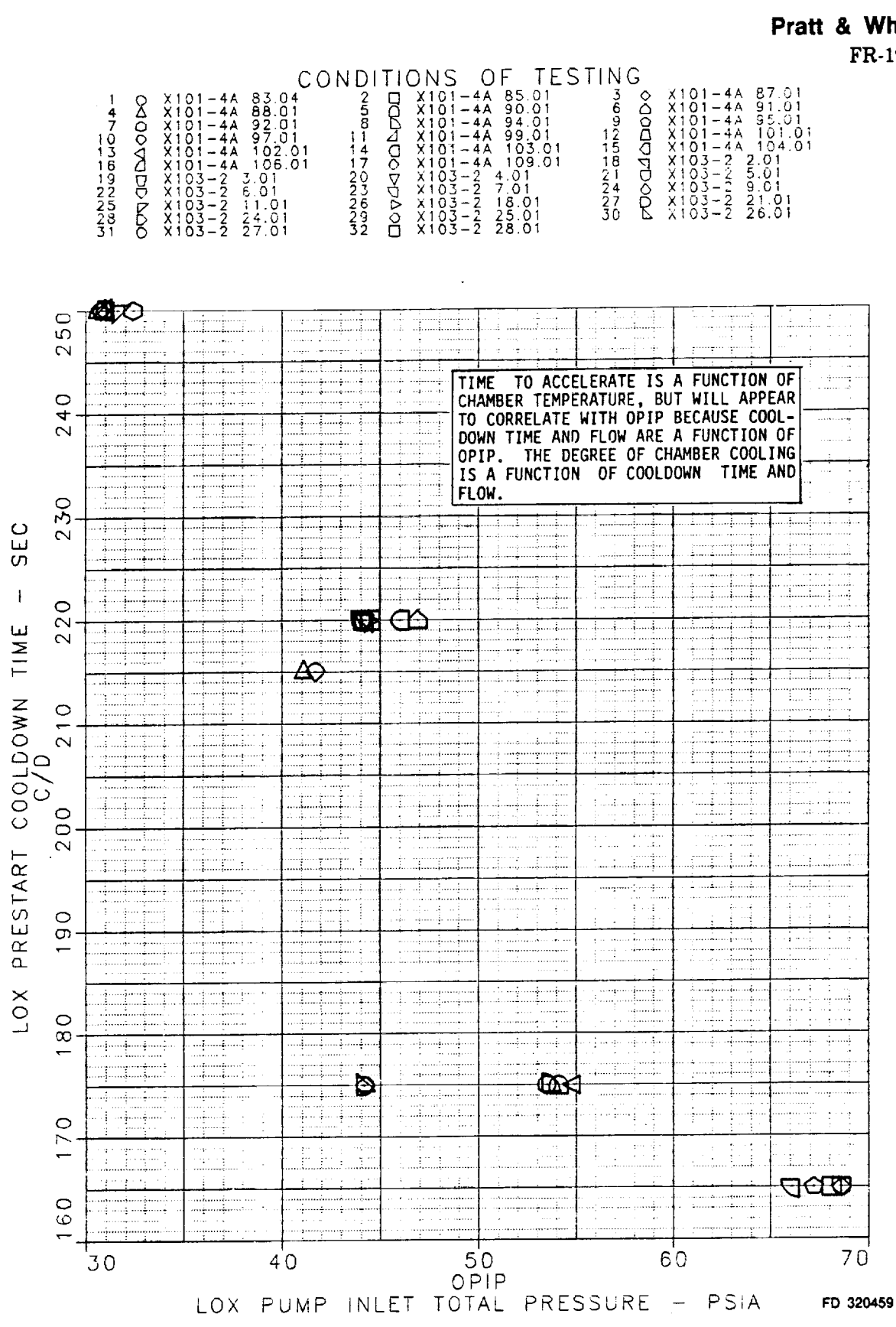

Figure 7-4. Oxidizer Cooldown Time vs Oxidizer Pump Inlet Pressure-Shuttle Centaur With Small Cooldown Areas, No Prechill

1	X101-4A 83.04	2	X101-4A 85.01	3	X101-4A 87.01
4	X101-4A 88.01	5	X101-4A 90.01	6	X101-4A 91.01
7	X101-4A 92.01	8	X101-4A 94.01	9	X101-4A 95.01
10	X101-4A 97.01	11	X101-4A 99.01	12	X101-4A 101.01
13	X101-4A 102.01	14	X101-4A 103.01	15	X101-4A 104.01
16	X101-4A 106.01	17	X101-4A 109.01	18	X103-2 2.01
19	X103-2 3.01	20	X103-2 4.01	21	X103-2 5.01
22	X103-2 6.01	23	X103-2 7.01	24	X103-2 9.01
25	X103-2 11.01	26	X103-2 18.01	27	X103-2 21.01
28	X103-2 24.01	29	X103-2 25.01	30	X103-2 26.01
31	X103-2 27.01	32	X103-2 28.01		

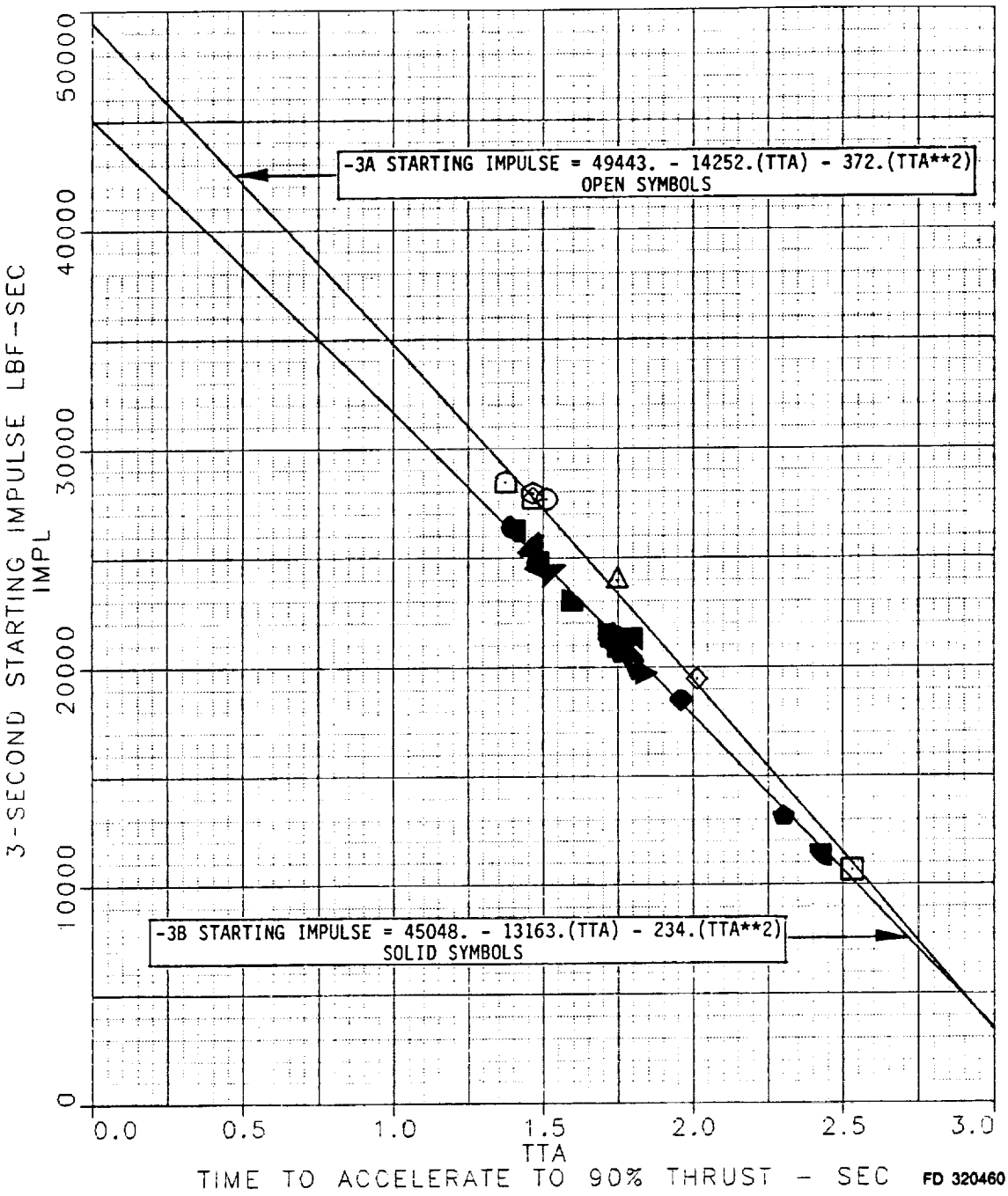

Figure 7-5. -3A and -3B Starting Impulse-Shuttle Centaur With Small Cooldown Areas, No Prechill

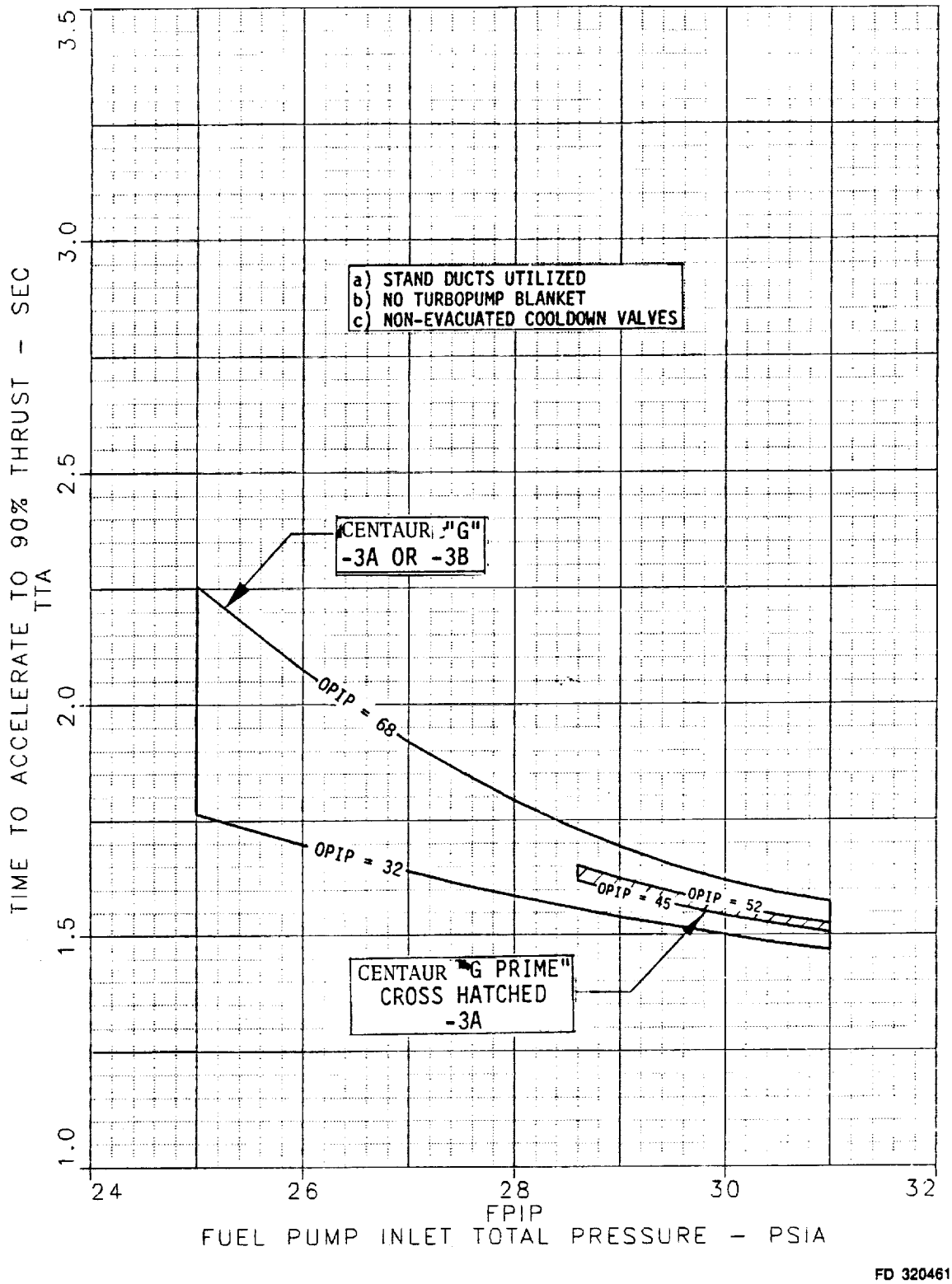

Figure 7-6. Predicted Acceleration Envelope-Shuttle Centaur With Small Cooldown Areas, No Prechill

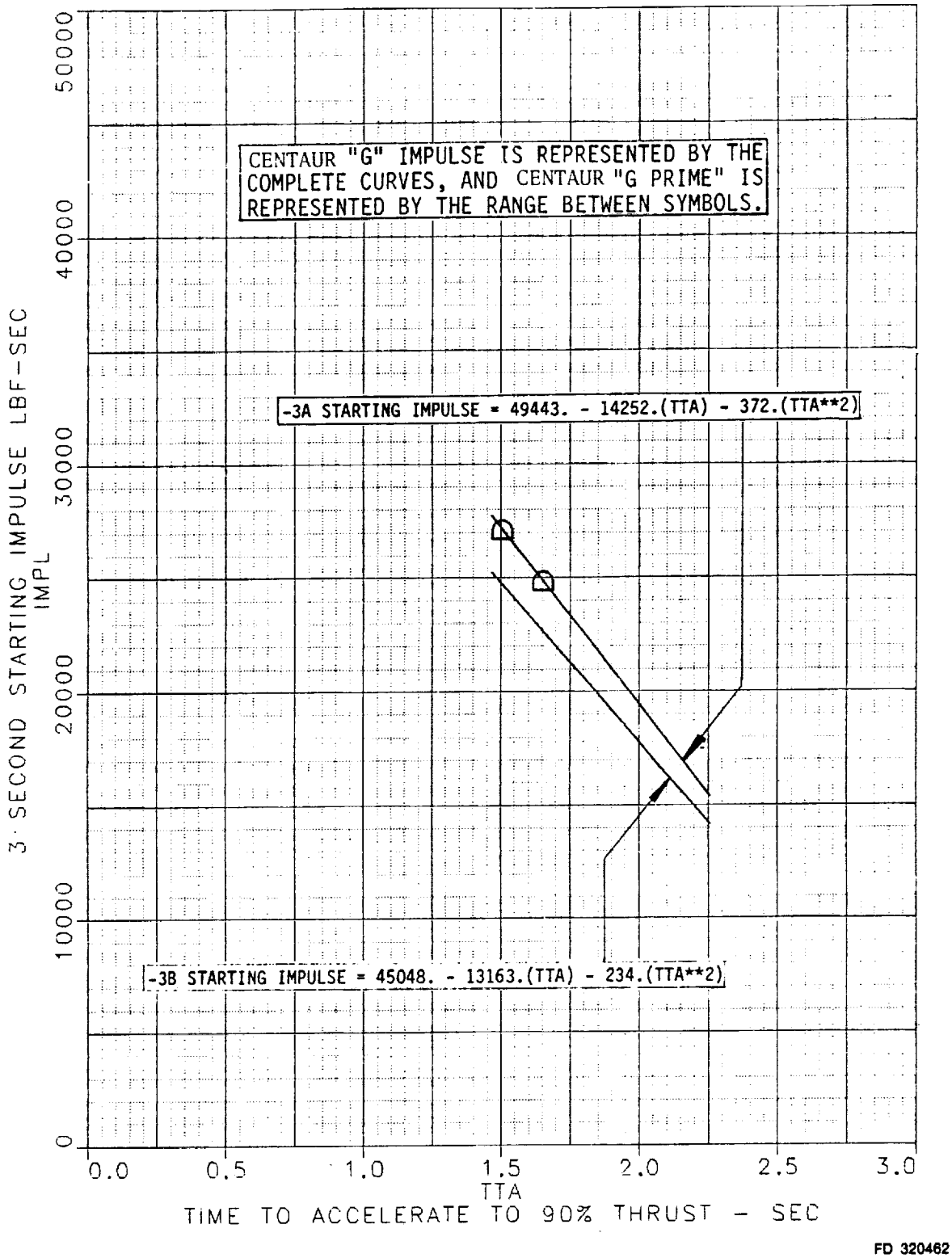

Figure 7-7. Three-Second Starting Impulse-Shuttle Centaur With Small Cooldown Areas, No Prechill

Figure 7-8 shows the predicted acceleration envelope using the large cooldown area scheme for the G Centaur vehicle utilizing either the RL10A-3-3A or -3B configurations, and for the G-Prime Centaur vehicle utilizing the RL10A-3-3A configuration.

Figure 7-9 shows the three-second starting impulse for Shuttle/Centaur operation, using the large cooldown area scheme, that would result from the predicted acceleration times in Figure 7-8. The G Centaur range is indicated by the full length of the -3A and -3B curves, and the G-Prime Centaur range is indicated by symbols.

The test data used in defining the starting characteristics of the engines is presented in Table 7-1, large cooldown area scheme, and Table 7-2, small cooldown area scheme.

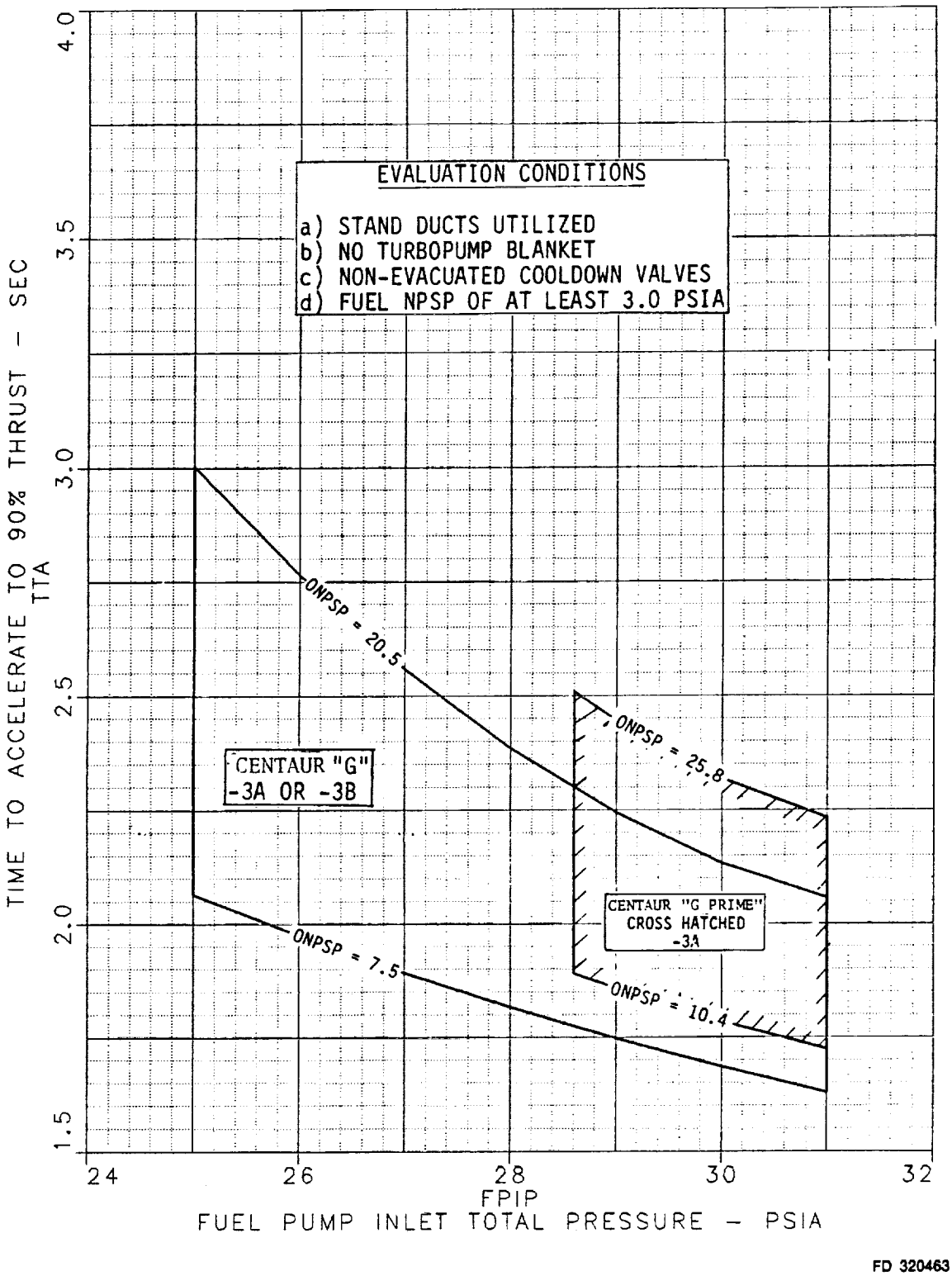

Figure 7-8. Predicted Acceleration Envelope-Shuttle Centaur With Large Cooldown Areas, No Prechill

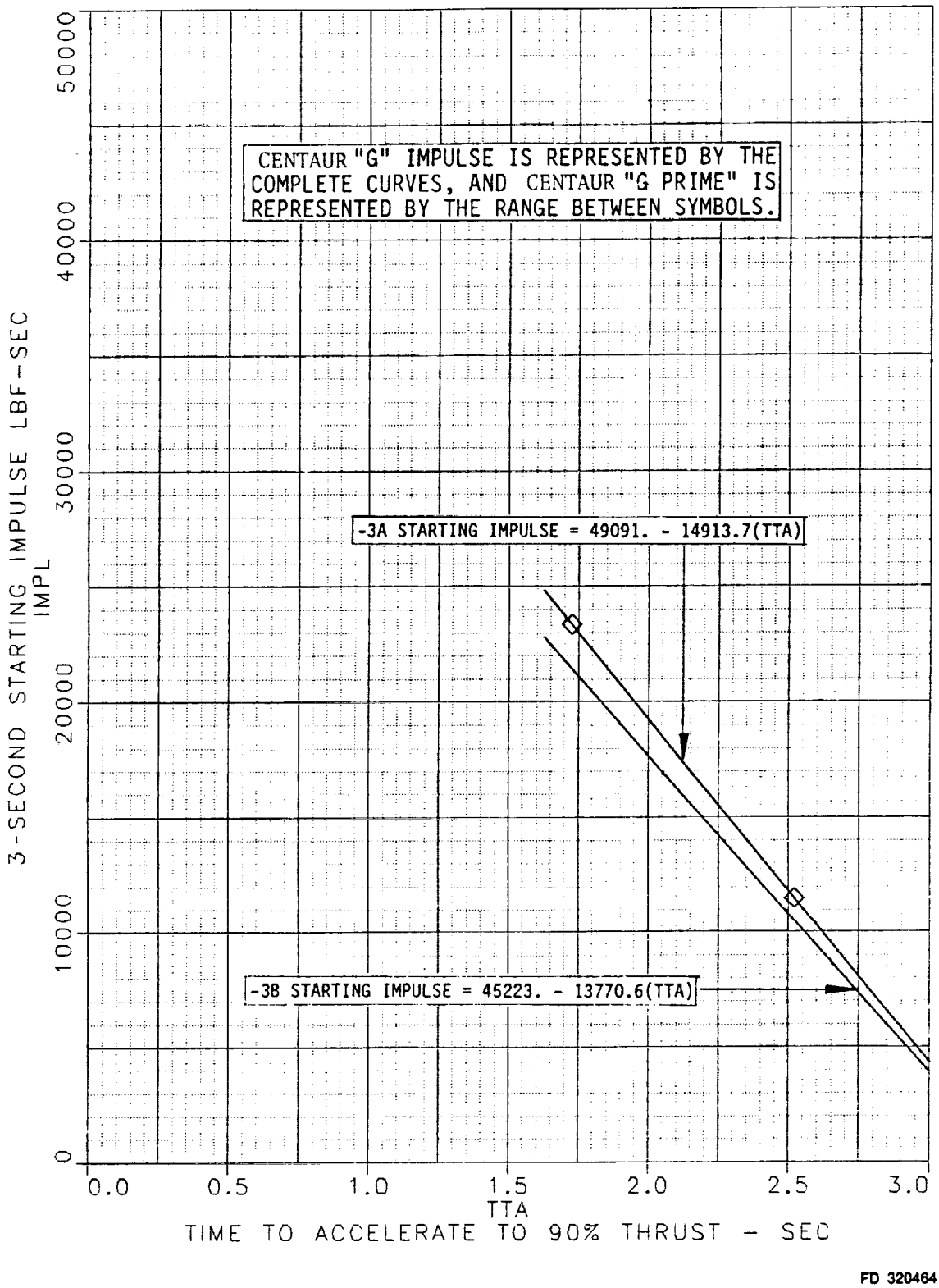

Figure 7-9. Three-Second Starting Impulse-Shuttle Centaur With Large Cooldown Areas, No Prechill

Table 7-1. *Engine Test Data-Large Cooldown Area Scheme-RL10A-3-3A and RL10A-3-3B*

Engine	Run No.	FPIP (psia)	FPIT (°R)	FNPSP at Start (psid)	OPIP at Start (psia)	OPIT (°R)	ONPSP (psid)	LOX C/D Time (sec)	TTA (sec)	Start Impulse (lbf-sec)	Config
XR101-2	11.01	32.2	39.6	8.5	53.5	179.3	17.9	50	1.866	21039	-3A
	12.01	32.0	38.1	13.1	52.4	172.5	26.9	50	2.233	16114	-3A
	13.01	28.3	39.5	5.0	53.0	172.4	27.6	50	2.639	9712	-3A
	14.01	28.4	37.9	10.0	44.1	172.2	18.9	50	2.296	14638	-3A
	16.01	31.6	37.9	13.2	46.4	179.4	10.6	50	1.800	21826	-3A
	18.01	31.8	37.9	13.4	27.1	167.0	8.0	50	1.583	25618	-3A
	19.01	24.5	38.5	4.4	41.4	167.4	21.9	50	3.216	1755	-3A
	20.01	24.7	38.8	3.6	41.0	167.3	21.6	50	2.909	6731	-3A
	22.01	24.4	38.2	5.2	27.2	167.9	7.1	50	2.015	18851	-3A
XR101-3	25.01	28.9	38.1	10.0	39.9	167.5	20.3	50	2.143	17420	-3A
	26.01	24.5	37.7	6.8	26.8	167.9	6.8	80	2.251	15156	-3A
	27.01	24.7	38.0	6.2	26.7	167.8	6.8	50	1.986	19333	-3A
	32.01	24.7	38.8	3.6	69.1	186.2	20.4	50	2.913	4937	-3A
	33.01	24.7	38.7	4.1	69.2	185.9	21.1	5	2.495	13696	-3A
	41.01	24.6	38.8	3.4	26.8	167.7	6.9	6	1.872	22040	-3A
	43.01	24.5	38.6	4.0	26.7	168.1	6.4	6	1.958	20917	-3A
	44.01	24.6	37.8	6.3	27.0	167.5	7.3	80	2.140	17166	-3A
	45.01	24.4	38.3	4.9	31.6	171.7	7.1	50	2.079	17564	-3A
XR102-1	1.02	31.6	40.0	6.5	53.4	179.1	8.1	40	1.992	19900	-3A
	2.01	27.6	38.8	6.5	47.2	177.1	15.1	40	2.220	16313	-3A
	3.01	29.8	38.9	8.4	48.9	176.0	18.5	35	2.046	19047	-3A
	4.01	31.8	38.2	12.6	52.3	172.4	26.9	35	2.308	15014	-3A
XR102-1A	5.01	28.2	37.7	10.4	43.8	173.0	17.6	50	2.108	17045	-3A
	6.01	28.2	39.6	4.5	52.9	172.9	26.8	50	2.368	14103	-3A
	7.01	31.5	37.7	14.0	46.2	180.6	8.3	50	1.648	24709	-3A
	8.01	31.4	37.6	13.9	45.9	179.9	9.2	50	1.588	25593	-3A
	9.01	31.8	38.8	10.7	69.4	186.1	20.9	50	2.013	17847	-3B
	10.01	31.8	39.8	7.4	69.7	186.1	21.2	50	1.820	20787	-3B
	11.02	28.6	40.1	3.2	55.7	186.3	6.8	50	1.797	20333	-3B
	12.01	24.8	38.9	3.4	69.1	185.9	21.0	50	3.143	1979	-3B
	14.02	24.4	37.5	7.1	27.2	168.3	6.7	50	2.270	13421	-3B
	15.01	24.5	38.8	3.3	27.2	168.0	7.0	50	2.358	12149	-3B
	17.01	31.6	38.6	11.2	27.5	168.4	6.9	50	1.806	20557	-3B
	19.01	24.6	39.0	2.9	41.2	167.9	21.1	50	3.730	1644	-3B
XR102-2	45.04	24.5	39.1	2.5	31.9	171.2	8.0	50	2.734	7882	-3B
	46.01	24.7	39.3	2.0	31.9	171.2	8.0	50	3.287	1566	-3B

Table 7-1. *Engine Test Data-Large Cooldown Area Scheme-RL10A-3-3A and RL10A-3-3B (Continued)*

Engine	Run No.	FPIP (psia)	FPIT (°R)	FNPSP at Start (psid)	OPIP at Start (psia)	OPIT (°R)	ONPSP (psid)	LOX C/D Time (sec)	TTA (sec)	Start Impulse (lbf-sec)	Config
XR105-1	1.01	29.7	38.6	9.3	49.2	175.9	18.9	40	1.996	19874	-3A
	2.01	31.9	39.3	9.2	52.5	179.0	17.4	40	1.922	20865	-3A
	4.01	31.4	37.6	13.9	52.8	173.0	26.6	40	2.298	15079	-3A
	6.01	28.6	39.7	4.6	52.4	173.5	25.5	40	2.636	9768	-3A
	8.01	29.1	37.7	11.3	42.7	169.2	21.2	40	2.420	12866	-3A
	9.01	31.6	40.0	6.5	68.7	186.5	19.4	45	1.918	20660	-3A
	10.01	24.7	39.1	2.7	42.8	170.5	20.4	40	3.229	1739	-3A
XR105-1A	11.01	28.8	39.0	7.1	46.5	175.5	16.8	40	2.042	18527	-3A
	13.01	28.4	39.8	4.0	52.9	173.5	26.0	40	2.588	10282	-3A
XR105-1B	14.01	28.5	40.0	3.4	54.9	185.0	8.7	40	1.737	21764	-3A
	15.01	28.6	40.0	3.5	56.9	186.0	8.6	40	1.802	21522	-3A
	16.01	31.5	37.5	14.2	44.9	178.8	10.1	40	1.641	24337	-3A
	17.03	31.8	37.5	14.5	28.4	169.4	6.7	50	1.535	26258	-3A
	18.01	32.1	37.4	15.1	45.4	179.2	9.9	50	1.761	23140	-3A
	20.01	28.6	39.7	4.6	57.0	185.6	9.6	50	1.926	18367	-3B
	21.01	31.7	39.7	7.7	70.1	186.3	21.2	50	2.104	17445	-3B
	23.01	28.8	37.3	12.1	40.7	167.3	21.3	50	2.350	13057	-3B
	24.01	31.5	38.5	11.4	27.5	168.5	6.8	50	1.789	20344	-3B
	25.01	24.7	39.0	3.0	27.7	168.2	7.3	50	2.178	14689	-3B
	26.01	24.6	37.4	7.6	27.4	168.3	6.9	50	2.193	14372	-3B
	27.01	24.7	38.7	20.7	40.8	168.1	20.5	50	3.428	1613	-3B
	30.01	24.6	38.8	3.5	40.5	168.2	20.1	50	2.998	3755	-3B

0818C

Table 7-2. *Engine Test Data-Small Cooldown Area Scheme-RL10A-3-3A and RL10A-3-3B*

Engine	Run No.	FPIP (psia)	FPIT (°R)	FNPSP at Start (psid)	OPIP at Start (psia)	OPIT (°R)	ONPSP (psid)	LOX C/D Time (sec)	TTA (sec)	Start Impulse (lbf-sec)	Config
XR101-4A	83.04	28.4	39.6	4.6	53.5	186.4	4.4	175	1.511	27680	3A
	85.01	24.5	39.2	2.0	68.1	186.3	19.1	165	2.529	10670	3A
	87.01	24.2	39.0	2.3	30.7	172.4	5.3	250	2.014	19478	3A
	88.01	24.2	38.2	4.8	41.1	168.4	20.5	215	1.747	23945	3A
	90.01	31.4	38.6	11.0	54.1	186.5	4.8	175	1.373	28479	3A
	91.01	29.4	38.5	9.0	46.9	178.4	12.7	220	1.466	27696	3A
	92.01	29.8	38.3	10.2	32.4	172.6	6.8	250	1.465	27954	3A
	94.01	28.4	39.2	5.7	53.6	185.6	6.2	175	1.589	22952	3B
	95.01	24.2	38.3	4.7	67.2	185.1	20.6	165	2.302	13159	3B
	97.01	24.3	38.1	5.3	41.7	168.4	21.1	215	1.960	18462	3B
	99.01	31.4	38.7	10.5	31.0	171.6	6.6	250	1.462	25555	3B
	101.01	24.4	38.6	3.9	30.9	171.6	6.5	250	1.765	21075	3B
	102.01	31.3	38.8	10.2	54.9	185.5	7.6	175	1.485	24550	3B
	103.01	29.7	38.5	9.6	46.0	177.9	12.5	220	1.481	24796	3B
	104.01	31.4	38.8	10.2	31.0	171.8	6.3	250	1.407	26247	3B
	106.01	31.3	38.7	10.6	30.7	171.6	6.2	250	1.467	25444	3B
	109.01	31.3	38.7	10.6	30.8	171.6	6.4	250	1.395	26430	3B

0632C

Table 7-2. *Engine Test Data-Small Cooldown Area Scheme-RL10A-3-3A and RL10A-3-3B (Continued)*

Engine	Run No.	FPIP (psia)	FPIT (°R)	FNPSP at Start (psid)	OPIP at Start (psia)	OPIT (°R)	ONPSP (psid)	LOX C/D Time (sec)	TTA (sec)	Start Impulse (lbf-sec)	Config
XR103-2	2.01	27.5	38.8	6.5	44.3	175.9	14.0	220	1.809	19790	3B
	3.01	27.8	38.7	6.9	44.1	175.8	13.9	220	1.757	20788	3B
	4.01	27.4	38.7	6.6	44.2	175.8	14.1	220	1.799	20066	3B
	5.01	27.7	38.9	6.2	44.0	175.8	13.9	220	1.722	21365	3B
	6.01	31.5	39.4	8.4	68.6	185.3	21.8	165	1.768	20984	3B
	7.01	24.5	39.2	1.9	66.1	184.7	20.3	165	2.432	11438	3B
	9.01	31.4	39.2	9.1	68.6	185.3	21.6	165	1.731	21562	3B
	11.01	31.4	39.4	8.4	31.6	171.3	7.5	250	1.523	24356	3B
	18.01	27.5	38.7	6.7	44.3	176.3	13.4	220	1.832	19731	3B
	21.01	27.7	39.0	6.0	44.1	176.0	13.6	220	1.724	21450	3B
	24.01	27.6	38.8	6.3	44.2	175.9	13.9	220	1.772	20761	3B
	25.01	27.4	38.7	6.6	44.2	175.8	14.0	220	1.797	20284	3B
	26.01	27.6	38.9	6.2	44.1	175.8	13.9	220	1.707	21534	3B
	27.01	27.6	38.7	6.8	44.1	175.7	14.1	220	1.731	21274	3B
	28.01	27.4	38.9	5.9	44.5	175.6	14.6	220	1.749	20959	3B

0818C

0632C

APPENDIX A

To perform accurate cooldown predictions of the RL10 Shuttle Centaur inlet ducts, the RL10 Atlas Centaur cooldown prediction deck was modified. The inlet duct portion of the deck was altered to reflect the differing dimensions of the ducts and gimbals. Fuel and oxidizer prevalves, which are not present in the Atlas Centaur configuration, were added upstream of the inlet lines. Two prediction models were configured, one that represented the ducts and valves of the ground test configuration and another that represented the flight configuration. The ground test configuration was used to check the formulation of the prediction program, and the flight configuration was used to make predicted cooldown times and consumptions for flight.

The oxidizer pump section of the deck was modified to allow calculation of metal temperatures at various locations throughout the oxidizer pump housing. Previously, the housing was treated as a single mass with one bulk metal temperature, which was adequate for the Atlas Centaur configuration where the bulk metal temperature of the oxidizer pump was below 400°R. This configuration proved to be inadequate in predicting the oxidizer pump metal temperatures for Shuttle Centaur cases where the bulk metal temperatures are approximately 500°R at the start of cooldown and where different areas of the pump do not experience the same flowrate as the average pump flowrate. The revised oxidizer pump model includes convective heat transfer to five portions of the pump. The pump was divided circumferentially into four quarters plus the diffuser. Each of the four quarters includes conductive heat transfer from the pump flow surfaces to the pump external surface where the flight temperature probe will be located. A cross section showing the five axial nodes is shown in Figure A-1. Convective heat transfer from metal to fluid occurs at node 2. Conductive heat transfer occurs between nodes 1 and 2, 2 and 3, etc.

On the fuel side, changes included adding a prevalve at the entrance to the inlet duct, updating the masses and surface areas of the inlet ducts to those of the Shuttle Centaur configuration, and adding conduction between the gimbals and tubes that make up the duct.

Adjustments were made to both the fuel and oxidizer sides of the ground test prediction deck to compensate for peculiarities in propellant flow due to the low flowrates and one-G gravity field of these tests.

In the horizontal sections of the oxidizer ducts, fluid did not completely wet the surface of the inlet duct. This caused the bottom of the oxidizer ducts to cool faster than the upper surfaces, which were exposed only to oxygen vapor. This can be seen in Figure A-2. To model this, the surface areas of the horizontal duct surfaces in the prediction deck were reduced by half when the reduced GMRV flow area was being used. During the testing with LOX pump rig B50C041, the duct section which was previously in a horizontal position was in a vertical orientation, and did not display the same characteristics (Figure A-3).

On the fuel side, when using the small interstage cooldown area, the fuel in the inlet ducts showed circulating flow, with warm fuel from the bottom of the duct travelling upward against the flow and exiting through the facility dumpline located just upstream of the prevalve. This caused the duct to cool faster than expected because of the additional heat the fluid picked up as it travelled up the duct, and because of the greater amount of cool fluid drawn into the duct. This was adjusted for in the simulation by allowing 0.4 pound per second of additional flow to pass through the inlet duct. This additional flow was allowed when the prevalve was opened at the same time as the inlet valve, and the small interstage cooldown area was being used.

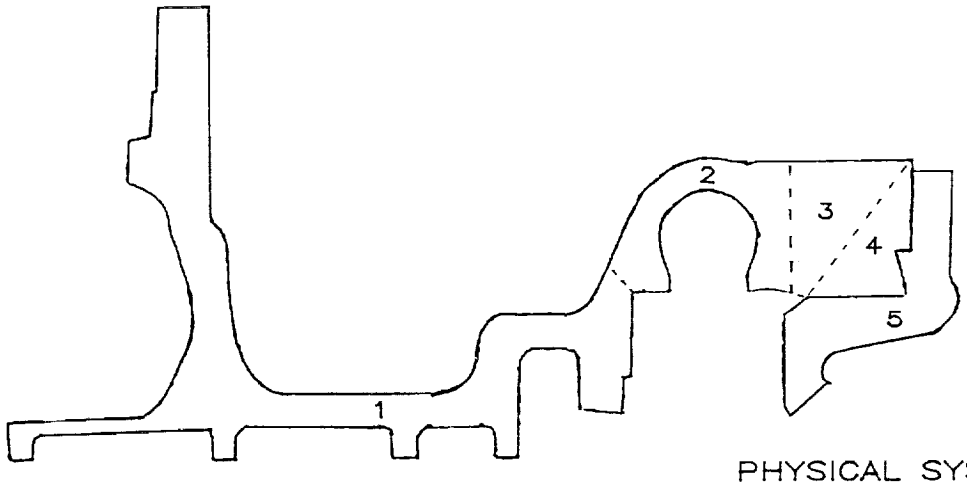

PHYSICAL SYSTEM

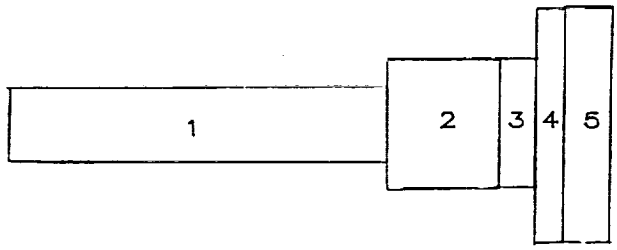

CONDUCTION MODEL

The amount of conduction between the various pump components is calculated by equating the heat contained within each component with the amount of heat transferred across each boundary between parts. A differential equation is written for each part interface, and they are solved simultaneously to determine the quantity of heat transferred between each part and the resulting temperature for each part.

FD 320366

Figure A-1. Revised Oxidizer Pump Model

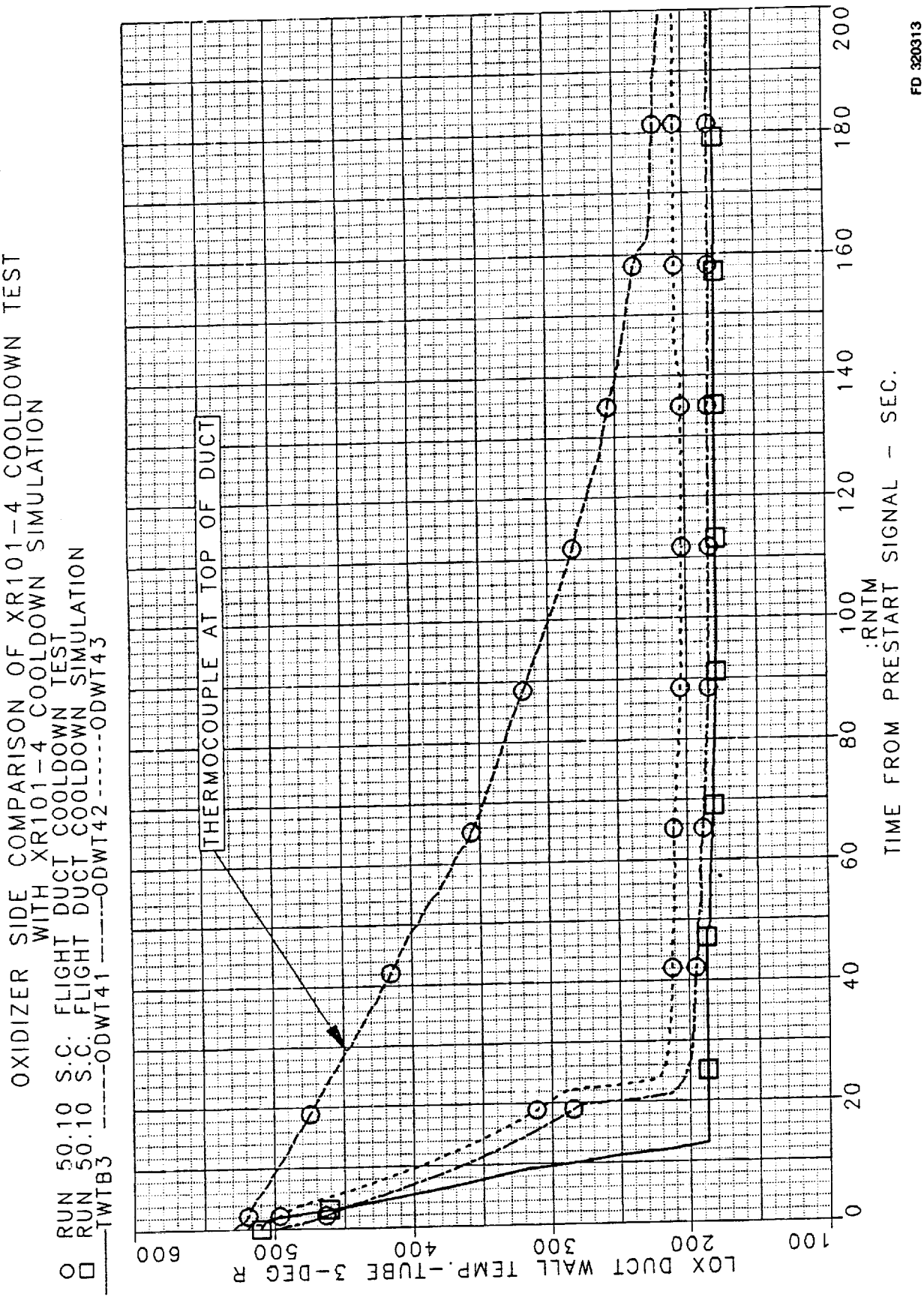

Figure A-2. LOX Duct Wall Temperature — Tube 3

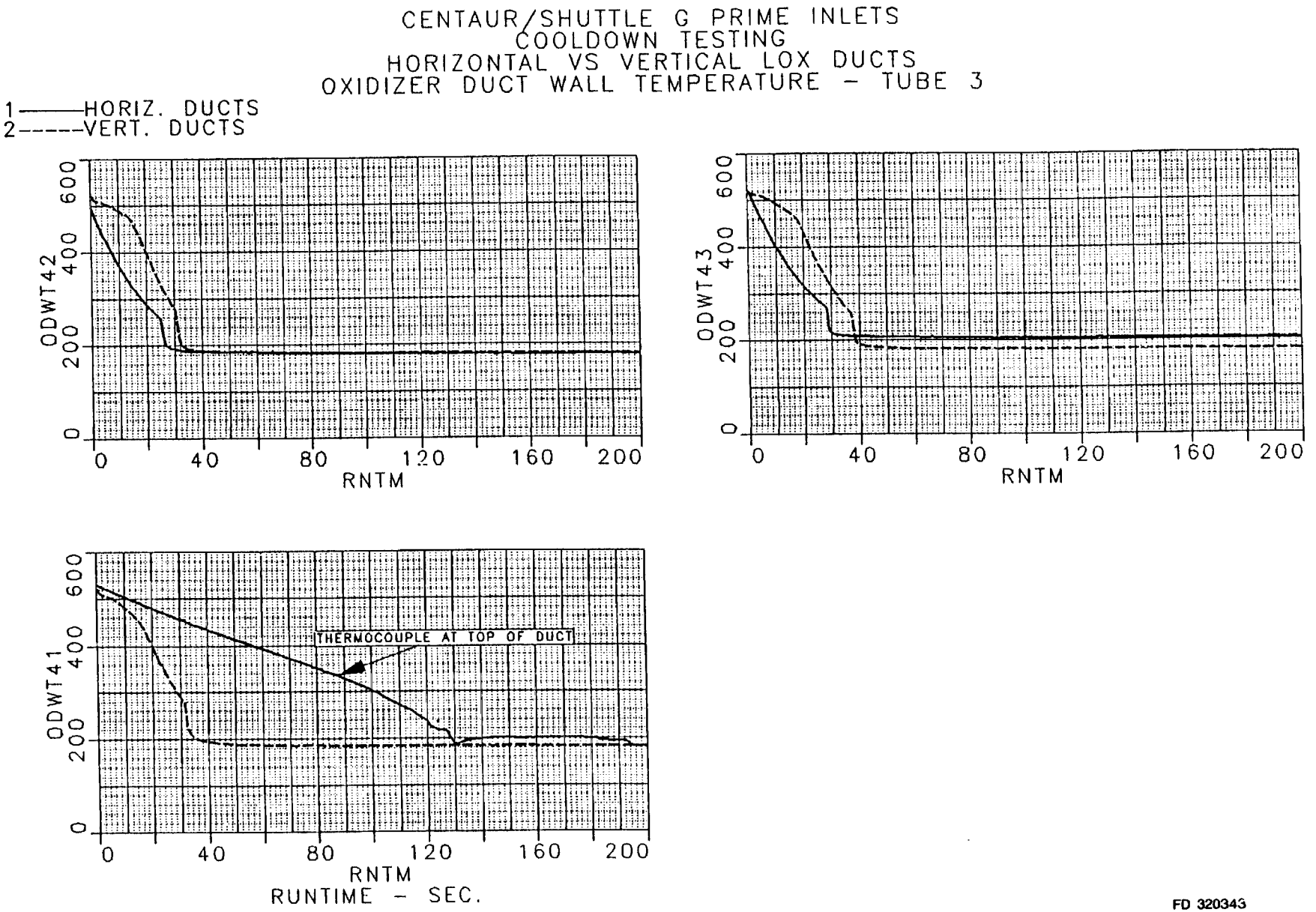

FD 320343

Figure A-3. Oxidizer Duct Wall Temperature — Tube 3

The oxidizer and fuel flows calculated by the RL10 cooldown deck were compared to actual flow rates and consumptions for both the oxidizer and fuel sides. Calculated flowrates compared well with the actual measured rates (Figures A-4 and A-5).

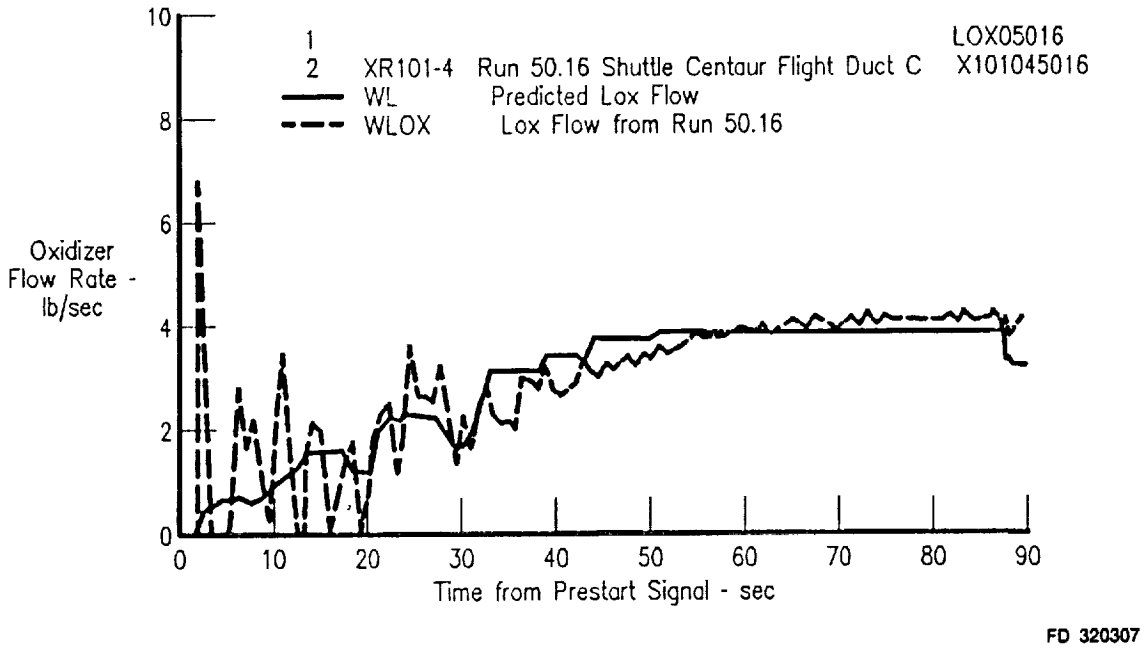

Figure A-4. Comparison of Predicted and Test Run LOX Flow Rate

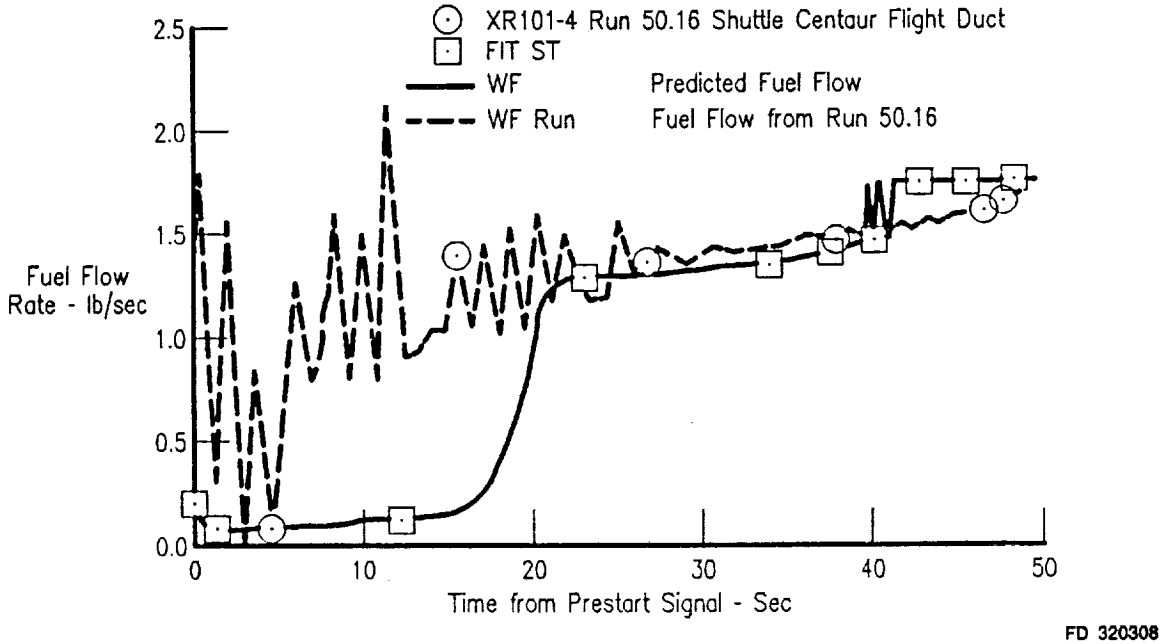

Figure A-5. Comparison of Predicted and Test Run Fuel Flow Rate

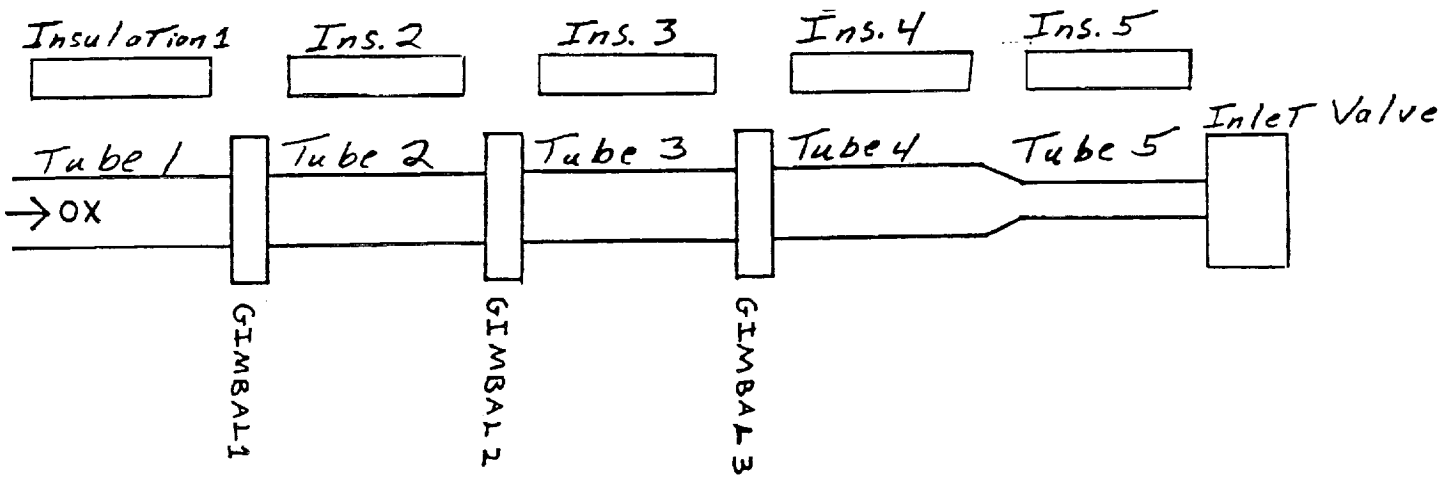

The oxidizer flow ducts bringing oxidizer to the engine have been broken into four tubes, three gimbals, an inlet valve, and the tube insulation. The mass of flanges, bolts and similar hardware have been included in the mass of the tubes or gimbals.

Calculations of convective and conductive heat transfer, fluid flow, temperature and pressure are made at each station for every time increment.

FD 320367

Figure A-6. Oxidizer Side Ducts

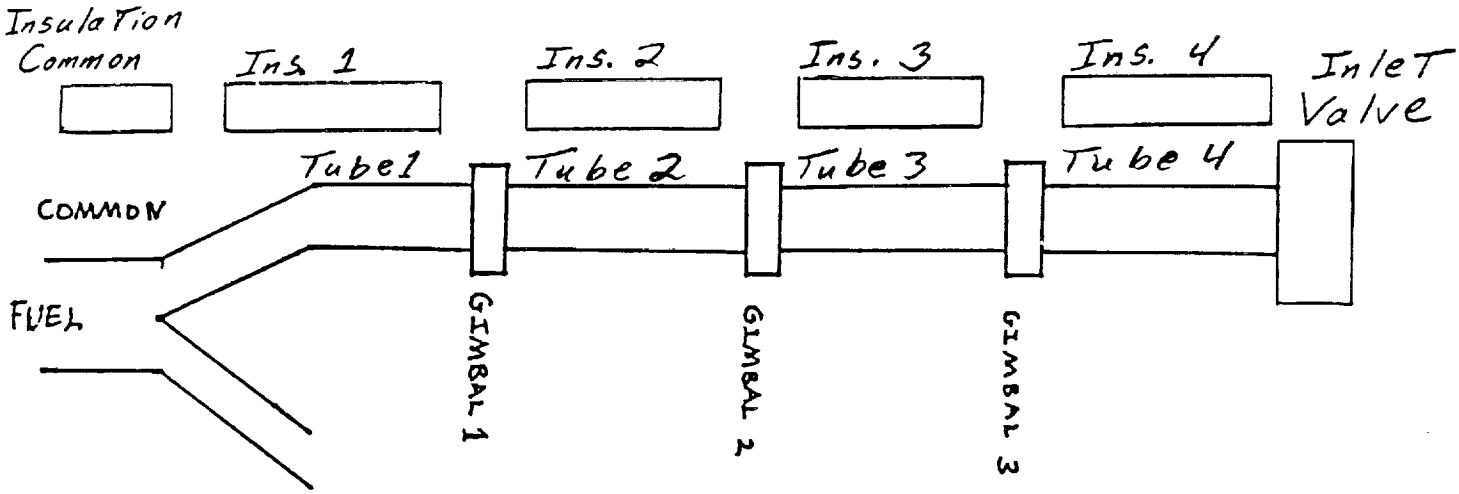

The fuel side has been divided into four tubes, three gimbals, an inlet valve, and tube insulation, with the initial tube having a common leg. The masses of the flanges, bolts, etc. have been included in the mass of the tubes and gimbals.

Like the oxidizer side, conductive and convective heat transfer, fluid flow, temperature and pressure calculations were performed at each station.

FD 320368

Figure A-7. Fuel Side Ducts

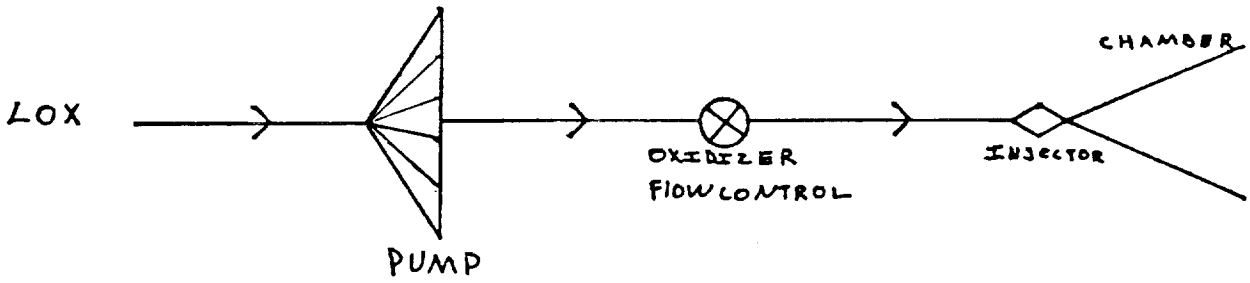

1. The oxidizer enters the segmented pump with known temperature and pressure. Conductive and convective heat transfer, pressure, temperature, and fluid flow are calculated.

2. After leaving the pump, the flow enters the oxidizer flow control valve(made up of the GMRV and PU valves) where once again heat transfer, fluid flow, pressure and temperature calculations are performed.

3. When the oxidizer leaves the oxidizer flow control, it enters the oxidizer line between the oxidizer flow control and the injector. Here, another set of heat transfer, fluid flow, pressure and temperature calculations are done.

4. The fluid enters the injector where the same heat transfer, fluid flow, pressure and temperature calculations are performed.

FD 320369

Figure A-8. Oxidizer Flow Schematic

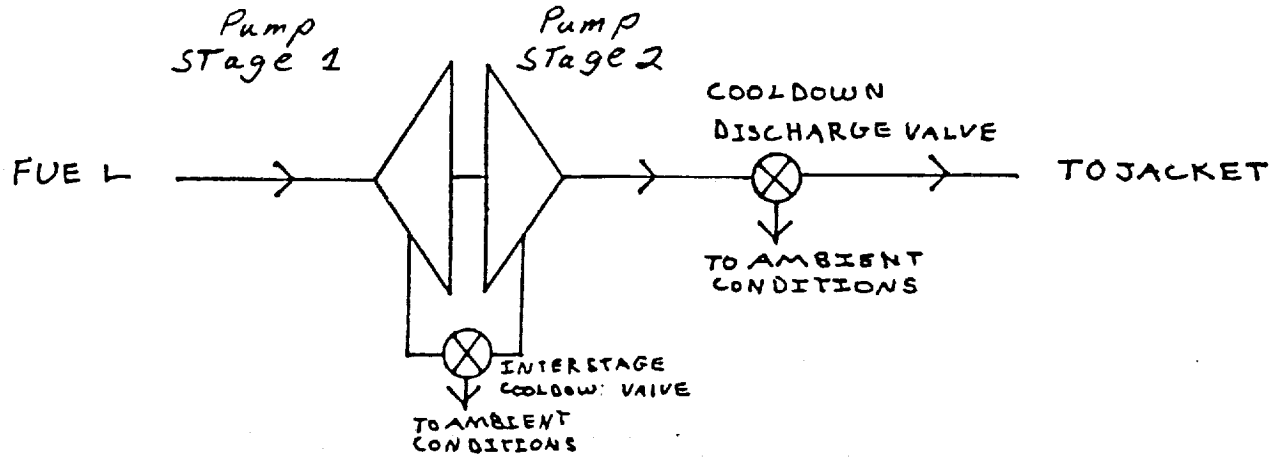

1. The pressure and temperature of the fuel entering the first stage pump are known. Heat transfer from this first stage pump to the fluid is calculated as well as the flow, pressure, and temperature. The fluid now moves to the interstage cooldown valve and the second stage pump.

2. As the fuel leaves the first stage pump, some flow enters the interstage cooldown valve and is exhausted to ambient conditions. The remainder of the fuel enters the second stage pump where heat transfer, pressure, temperature, and fluid flow are calculated.

3. During the cooldown process, all of the fuel is diverted to ambient conditions. A flow calculation across the cooldown discharge valve is done.

FD 320370

Figure A-9. Fuel Flow Schematic

BASIC ASSUMPTIONS

1. 1-D QUASI-STEADY STATE FLOW
2. EACH COMPONENT INFINITELY CONDUCTIVE
3. NO WORK OR GRAVITY EFFECTS
4. INSTANTANEOUS COMPONENT FILLING
5. EACH COMPONENT HAS A CONSTANT EFFECTIVE FLOW AREA
6. HEAT REJECTED FROM COMPONENTS = ENERGY INCREASE OF FLUID
7. COMPONENT AVERAGE AREA USED TO CALCULATE FORCED CONVECTION HEAT TRANSFER COEFFICIENT

FD 320371

Figure A-10. Base Assumptions

HEAT TRANSFER MODEL SIMULATES THERMAL CONDITIONS OF COMPONENTS AND FLUIDS

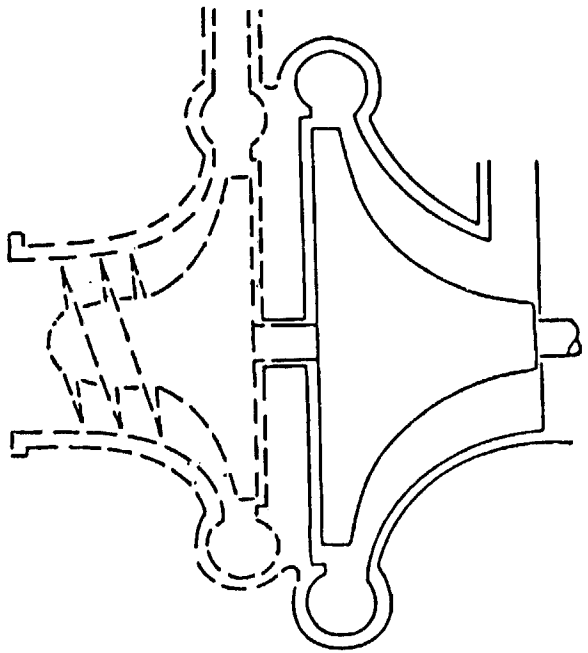

HIGH PRESSURE FUEL PUMP
PLAN VIEW

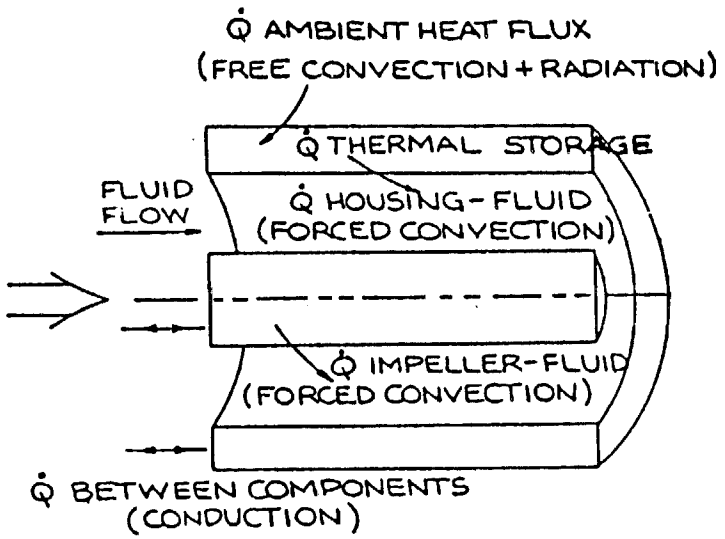

AXISYMMETRIC THERMAL
MODEL ANALOG

FD 320372

Figure A-11. Heat Transfer Model Simulates Thermal Conditions of Components and Fluids

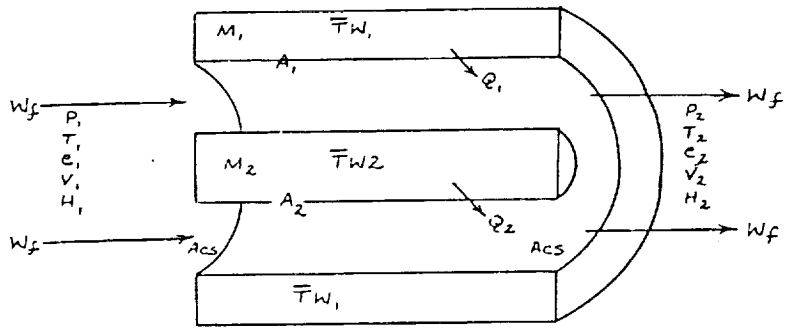

BASIC EQUATIONS:

$$T_B = (\bar{T}_1 + T_2)/2$$

$$Q = h A (\bar{T}_W - \bar{T}_B)\, dt$$

$$Q = MC_p (T_{W_{PREVIOUS}} - T_W)$$

$$Q_{TOTAL} = Q_1 + Q_2$$

$$Q_{TOTAL} = H_2 - H_1 + \frac{V_2^2}{2} - \frac{V_1^2}{2}$$

$$\rho_1 V_1 = \rho_2 V_2$$

$$\bar{T}_W = (T_{W_n} + T_{W_{n+1}})/2$$

The cooldown prediction deck determines the magnitude of convective heat transfer by utilizing the component surface areas, masses, flow areas, average bulk metal temperature, as well as the fluid flowrate and average bulk temperature to determine a film coefficient for convective heat transfer.

The heat transfer process is as follows:

1. The fluid properties are used along with the present metal temperature and a predicted metal temperature to determine a heat transfer coefficient.

2. The coefficient is used to calculate the quantity of heat removed from the metal part using the part surface area, fluid temperature, and time duration.

3. The calculated heat loss is used with the part's specific heat and starting temperature to determine the temperature decrease which would occur, and the part's average temperature for the time period.

4. The calculated average temperature is compared to the average temperature used to calculate the heat transfer coefficient. If the two differ, a new predicted temperature is used to calculate a new coefficient, and the process is repeated until the predicted heat transferred results in the same average metal temperature as that used to find the coefficient.

FD 320373

Figure A-12. Convective Heat Transfer Model

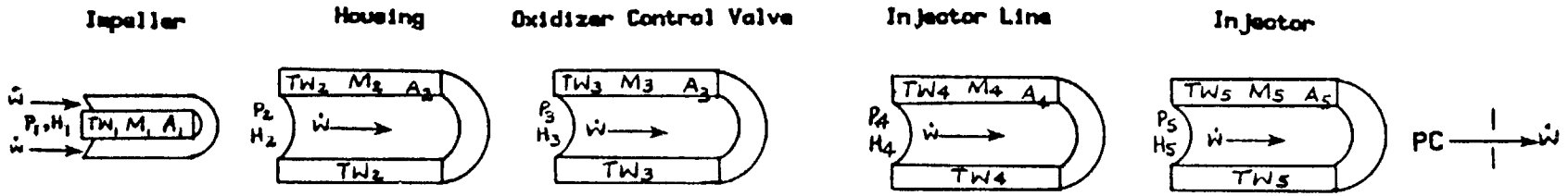

PROGRAM CALCULATES HEAT TRANSFER BASED ON PREVIOUS TIME INCREMENT FLOW - THEN CALCULATES FLOW FOR NEXT TIME WITH SMITE BALANCE ON PRESSURES. VARIES PRESSURES UNTIL FLOWS ACROSS ALL COMPONENTS ARE THE SAME.

FD 320374

Figure A-13. RL10 Cooldown Deck Oxidizer Side Arrangement

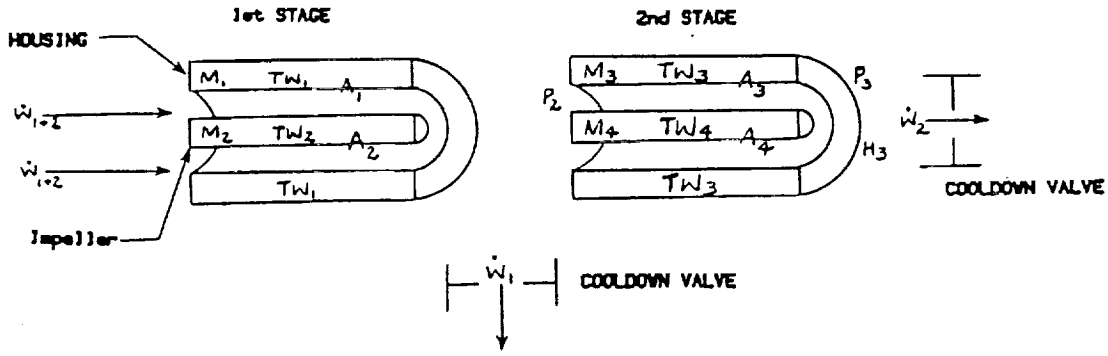

FLOWS CALCULATED BY VARYING PRESSURES UNTIL TOTALS MATCH

The fluid flowrates are balanced by varying all component upstream and downstream pressures until the flowrates calculated are either equal to one another as on the oxidizer side, or the sum of the exit flows are equal to the inlet flow as on the fuel side. The fluid temperatures and enthalpies used for the flow calculations are determined by the heat transfer calculations for the system.

FD 320375

Figure A-14. RL10 Cooldown Deck Fuel Side Arrangement

REPORT DISTRIBUTION LIST

NASA Lewis Research Center
21000 Brookpark Road
Cleveland, OH 44135

Attn: J. A. Burkhart/MS 500/120
T. P. Burke/MS 500-319
R. C. Oeftering/MS 500-107
S. R. Graham/MS 500-107 (3 copies)
A. J. Willoughby/Analex/MS 500-105
Library

NASA Headquarters
Washington, D.C. 20546

Attn: MSD/S. J. Cristofano
MSD/J. R. Lease
MS/J. B. Mahon
MTT/L. K. Edwards
RST/F. W. Stephenson
Library

General Dynamics Space Systems Division
P. O. Box 80847
San Diego, CA 92138

Attn: W. J. Ketchum
J. Rager
K. Allen
R. Beach
J. Cimenski
Library

Martin Marietta Corp.
P. O. Box 179
Denver, CO 80201

Attn: J. Bunting
Library

USAF Space Division
P. O. Box 92960
Worldway Postal Center
Los Angeles, CA 90009-2960

Attn: CLVD/Col. W. Anders
CL/Col. Hard
YXD/Maj. R. Proctor
YXD/Lt. J. Creamer
YXD/Capt. R. Soland
CLVD/Lt. Col. J. Rogers